CHARACTERIZATION OF GROUNDWATER IN JOHNS AND EMERY VALLEYS, GARFIELD AND KANE COUNTY, UTAH, WITH EMPHASIS ON THE GROUNDWATER BUDGET AND GROUNDWATER–SURFACE-WATER INTERACTION

by Janae Wallace, Trevor H. Schlossnagle, Kathryn Ladig, Paul C. Inkenbrandt, Hugh Hurlow, and Christian Hardwick

SPECIAL STUDY 172
UTAH GEOLOGICAL SURVEY
UTAH DEPARTMENT OF NATURAL RESOURCES
2024

Blank pages are intentional for printing purposes.

CHARACTERIZATION OF GROUNDWATER IN JOHNS AND EMERY VALLEYS, GARFIELD AND KANE COUNTY, UTAH, WITH EMPHASIS ON THE GROUNDWATER BUDGET AND GROUNDWATER–SURFACE-WATER INTERACTION

by
Janae Wallace, Trevor H. Schlossnagle, Kathryn Ladig, Paul C. Inkenbrandt, Hugh Hurlow, and Christian Hardwick

Cover photo: *Emery Valley and southern Johns Valley view looking west from Henderson Point. The Claron Formation of Bryce Canyon National Park is visible to the left. Photo by Trevor H. Schlossnagle.*

Suggested citation:

Wallace, J., Schlossnagle, T.H., Ladig, K., Inkenbrandt, P.C., Hurlow, H., and Hardwick, C., 2024, Characterization of groundwater in Johns and Emery Valleys, Garfield and Kane County, Utah, with emphasis on the groundwater budget and groundwater–surface-water interaction: Utah Geological Survey Special Study 172, 76 p., 7 appendices, https://doi.org/10.34191/SS-172.

SPECIAL STUDY 172
UTAH GEOLOGICAL SURVEY
UTAH DEPARTMENT OF NATURAL RESOURCES
2024

STATE OF UTAH
Spencer J. Cox, Governor

DEPARTMENT OF NATURAL RESOURCES
Joel Ferry, Executive Director

UTAH GEOLOGICAL SURVEY
R. William Keach II, Director

PUBLICATIONS
contact
Natural Resources Map & Bookstore
1594 W. North Temple
Salt Lake City, UT 84116
telephone: 801-537-3320
toll-free: 1-888-UTAH MAP
website: utahmapstore.com
email: geostore@utah.gov

UTAH GEOLOGICAL SURVEY
contact
1594 W. North Temple, Suite 3110
Salt Lake City, UT 84116
telephone: 801-537-3300
website: geology.utah.gov

CONTENTS

FIGURES

TABLES

CHARACTERIZATION OF GROUNDWATER IN JOHNS AND EMERY VALLEYS, GARFIELD AND KANE COUNTY, UTAH, WITH EMPHASIS ON THE GROUNDWATER BUDGET AND GROUNDWATER–SURFACE-WATER INTERACTION

by Janae Wallace, Trevor H. Schlossnagle, Kathryn Ladig, Paul C. Inkenbrandt, Hugh Hurlow, and Christian Hardwick

ABSTRACT

Johns and Emery Valleys are in south-central Utah, about 20 miles (32 km) southeast of Panguitch in Garfield and Kane Counties, and have a population of about 360 residents. However, Bryce Canyon National Park forms the southeastern boundary of the study area and tourist visitation to the park and the valleys reaches the millions annually. Water resource development and water quality concerns in this seasonally overpopulated area have prompted our comprehensive study of groundwater in Johns and Emery Valleys.

This report presents a new estimate of valley-fill thickness; six valley-fill cross sections; potentiometric surfaces and water-level change maps; a water-level trend analysis; a comprehensive analysis of the stable isotope signatures of surface water and groundwater; a groundwater age analysis; a water balance of Johns and Emery Valleys and of Tropic Reservoir, all backed by gross estimates of water-budget components; a groundwater quality classification; and an evaluation of predicted water-quality degradation by future septic tanks.

We completed fieldwork for this study from 2018 to 2022, which included collecting new gravity measurements to understand basin geometry. We sampled wells, springs, surface water, and precipitation for general chemistry and stable and radioactive isotopes. We also conducted seepage runs on the East Fork Sevier River and its tributaries as well as the Tropic Ditch. We measured streamflow of the East Fork Sevier River periodically by monitoring the water level in the stream channel at key locations to create a stage-discharge relationship for each location for the 2022 water year.

Groundwater quality in the principal valley-fill aquifer in Johns and Emery Valleys is excellent and was deemed Pristine by the Utah Division of Water Quality Board's groundwater quality classification designation. The average total-dissolved-solids (TDS) concentration in the study area is 295 milligrams per liter (mg/L), with the valley-fill aquifer and Claron Formation yielding higher quality water than the Cretaceous sandstone aquifers. Our report provides an evaluation of predicted water-quality degradation by future increased septic tanks, including large underground wastewater disposal systems.

This study uses a soil-water-balance (SWB) model to understand the interaction between surface water, the unconsolidated valley-fill aquifer, and Tropic Reservoir. SWB-modeled precipitation averaged approximately 383,000 acre-feet/yr and evapotranspiration averaged 372,000 acre-feet/yr over the entire study area for the years 2017 through 2021. The SWB model indicated an average recharge to the valley-fill aquifer of 9400 acre-feet/yr and average gross loss of 11,000 acre-feet/yr. These data indicate that the valley-fill aquifer had a net loss of water from 2017 to 2021.

The major findings of this study are: (1) the valley-fill aquifer is relatively thin (less than 250 feet thick in most places) with low storativity and high transmissivity; (2) water levels in wells in most of the valley-fill aquifer increase directly in response to high precipitation years and decrease in low precipitation years relative to bedrock wells, which show little response to seasonal fluctuations in precipitation; (3) the East Fork Sevier River in Emery Valley is strongly controlled by releases from Tropic Reservoir and the Tropic Ditch diversion, and is regularly completely diverted from April to October; the river begins to become perennial and reappear in northern Johns Valley where it encounters groundwater discharge from the valley-fill aquifer, where the water table intersects the land surface and supports extensive wetlands; (4) the East Fork Sevier River is both a net losing and net gaining stream depending on timing and location in the watershed; (5) the valley-fill aquifer receives recharge primarily from mountain-block recharge (approximately 4390 acre-feet/yr) and from precipitation (940 acre-feet/yr); (6) groundwater loss from the valley-fill aquifer is from evapotranspiration and well water withdrawal (averaging approximately 5400 acre-feet/yr) and to the East Fork Sevier River in the northernmost part of Johns Valley (approximately 5600 acre-feet per/yr on average); (7) Tropic Reservoir loses water each year to the groundwater system; (8) based on a nitrate mass balance model, we project that adding the equivalent nitrate loading of 124 septic tanks in the form of large underground wastewater disposal systems to the aquifer in Emery Valley could result in a septic tank density of 57 acres per system and 14 acres per system if allowable nitrate concentration is increased to 5 mg/L, and (9) water quality in the valley-fill aquifer is Pristine, having TDS concentrations less than 500 mg/L.

INTRODUCTION

Purpose and Scope

The primary goals of this study are to (1) characterize the hydrogeology of the Johns and Emery Valley drainage basin as it pertains to the occurrence and flow of groundwater, with emphasis on delineating the valley-fill aquifer thickness and lithology and determining the water-yielding characteristics of unconsolidated and fractured-rock aquifers in the study area; (2) characterize groundwater levels, chemistry, flow paths, and connection to surface water; (3) develop a water budget for the drainage basin; and (4) develop septic-system density recommendations and an aquifer classification map. To accomplish these goals, we:

- Compiled a geologic map of the Johns and Emery Valley study area, with accompanying stratigraphic columns.
- Assembled existing well data, including specific capacity and aquifer test data.
- Estimated aquifer characteristics and produced a map showing the transmissivity for the valley-fill aquifer and bedrock aquifers.
- Measured water levels in wells and constructed potentiometric surface maps for the valley-fill aquifer, from which change-over-time maps were created.
- Delineated the hydrostratigraphy of valley-fill and fractured-rock units and produced six valley-fill cross sections.
- Produced an isopach map for the valley fill using new and existing gravity data.
- Collected groundwater and surface water samples and analyzed for environmental tracers and geochemistry.
- Determined groundwater–surface-water connection based on water chemistry type, age of groundwater, and the isotopic signature of stream water compared to groundwater.
- Developed a hydrologic water budget for the Johns and Emery Valley drainage basin, with a focus on the valley-fill aquifer system.
- Calculated expected water-quality degradation based on septic-tank density.
- Performed a potential contaminant inventory to document potential threats to groundwater quality.
- Classified groundwater quality of the principal valley-fill aquifer to formally document the area's groundwater resources.

Some of the data and interpretations in this report were previously published in Utah Geological Survey Open-File Report 733 (Wallace et al., 2021), which describes the hydrogeology and connection between surface water and groundwater in the upper East Fork Sevier watershed, focusing on Emery Valley and the southern end of Johns Valley. This report supersedes any information found in that publication. We expanded the study area in this report to include the entire watershed extending to northern Johns Valley where the East Fork Sevier River exits through Black Canyon.

Background Information

Location and Geography

The study area encompasses Johns and Emery Valleys in eastern Garfield and northern Kane Counties, south-central Utah. The study area includes Bryce Canyon City and the gently rolling, forested slope to the north and northwest; the East Fork Sevier River below Tropic Reservoir and associated side drainages, particularly East Creek; and Johnson Bench, Emery Valley, and Johns Valley (Figure 1). Bryce Canyon City is about 20 miles (32 km) southeast of Panguitch, the Garfield County seat. The eastern administrative boundary of Bryce Canyon National Park forms the southeastern boundary of the study area in northern Kane County. Emery Valley is an intermontane basin that is bounded by the Sevier Plateau on the north and the Paunsaugunt Plateau on the southwest, and opens to Johns Valley to the northeast. Johns Valley is also an intermontane basin bounded by the Sevier Plateau to the west and Escalante Mountains to the east. The East Fork Sevier River flows through Emery Valley from southwest to northeast and continues northeast through Johns Valley, exiting through Black Canyon. The hand-dug Tropic Ditch, an irrigation canal listed on the National Register of Historic Places dating back to 1892, taps into the East Fork Sevier River south of Emery Valley and transports water east across the Great Basin Divide (Davis and Pollock, 2010).

Climate

Johns and Emery Valleys are in a high-altitude, semi-arid environment. Weather conditions are variable throughout the year, with an average of 69 freeze-free days per year at the Bryce Canyon Airport weather station (years 1949 to 2022; data were retrieved from https://climate.usu.edu/mapServer/mapGUI/index.php). Monsoon season is common in July and August, with heavy, short-lived downpours. SNOTEL data (Widtsoe #3 station in the Escalante Mountains and Agua Canyon station on the Paunsaugunt Plateau; Natural Resources Conservation Service, 2021) indicate an average of about 25 inches of precipitation per year (1981–2020). The Bryce Canyon Airport weather station recorded a maximum temperature of 95°F (35°C) and a minimum temperature of -32°F (-35°C) between 1948 and 2023.

Population and Land Use

Johns and Emery Valleys, having a total permanent population of 363, are sparsely populated rural areas that have had

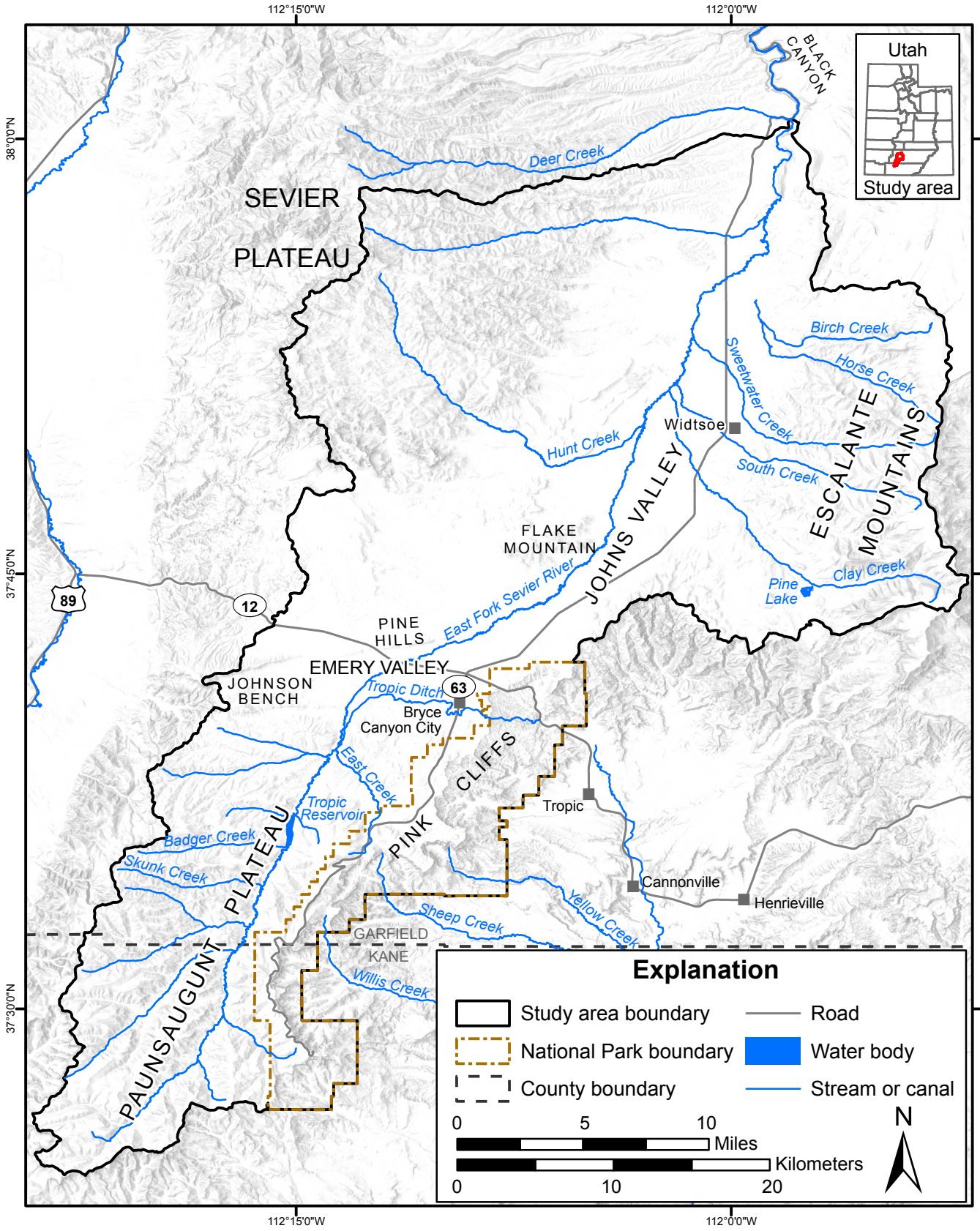

Figure 1. *Johns and Emery Valleys study area and geographic setting.*

little to moderate population growth, but rapid growth in tourism (U.S. Census Bureau, 2021). Although the population of Bryce Canyon City has grown from 138 at its incorporation in 2007 to 336 in 2020 (U.S. Census Bureau, 2021) and swells with seasonal employment, visitation to Bryce Canyon National Park increased from one million in 2008 to 2.7 million in 2018 (National Park Service, 2020).

Although land use and development in the study area is centered around tourism, agriculture remains an important land use in Johns and Emery Valleys. In 2021, over 7700 acres of land were designated as irrigated, sub-irrigated, or non-irrigated agricultural use (Utah Division of Water Resources, 2022). Irrigation in the study area is typically from surface water sources such as the Tropic Ditch in Emery Valley and drainages in the Escalante Mountains bordering Johns Valley, including Horse Creek, Sweetwater Creek, Birch Creek, and South Creek. Non-irrigated agriculture use includes fallow and idle croplands as well as dry land. Urban areas comprise 1200 acres of the study area.

Wastewater disposal in Johns and Emery Valleys is a mix of sewage lagoon systems and underground wastewater disposal systems. Bryce Canyon National Park and Bryce Canyon City have their own sewage lagoons, and outside of these areas, hotels currently use three large underground wastewater disposal systems (LUWDS) and 36 homes or other structures use septic tank soil-absorption systems.

Previous Work

Dutton (1880) described the geology of the High Plateaus of Utah, including the Sevier and Paunsaugunt Plateaus and associated valleys. Gregory (1944) described the geology of the East Fork Sevier River valley, focusing on the Tertiary Claron Formation (then called the Wasatch Formation) and Brian Head Formation. Marine (1963) appraised the groundwater resources of Bryce Canyon National Park, focusing on shallow alluvial drainages, springs, and potential development of the Claron Formation and Cretaceous bedrock.

Carpenter et al. (1967) investigated groundwater conditions of the Upper Sevier River Basin, emphasizing the interrelation of groundwater and surface water, the effects of increased groundwater pumping, and the amount of groundwater storage. They divided the East Fork Valley into three sub-basins: Emery Valley, Johns Valley, and Antimony, and noted that Johns and Emery Valleys exhibited no confined groundwater conditions. They reported 6000 and 90,000 acre-feet of groundwater storage in Emery Valley and Johns Valley, respectively.

Thiros and Brothers (1993) summarized the water-yielding characteristics of the East Fork Valley that includes Johns and Emery Valleys. In Emery Valley, they identified the sand and gravel deposits of the valley-fill aquifer as having the highest hydraulic conductivity. They estimated transmissivity, based on an aquifer test in Emery Valley, at 6 square feet per day (ft^2/day) (0.56 m^2/day). Aquifer tests yielded hydraulic conductivity values of 0.2 feet per day (ft/day) (0.06 m/day) from an alluvial fan in Johns Valley and 1500 ft/day (457 m/day) for a well in Emery Valley completed in gravel and sand. Hydraulic conductivity values were estimated from specific capacity data from 21 well logs and ranged from 6 to 20 ft/day (1.8 to 6 m/day), and specific yield was estimated to be 0.13 (Thiros and Brothers, 1993).

Ott (1999) surveyed springs and surface water within Bryce Canyon National Park with an emphasis on water quality. Doremus and Kreamer (2000) studied water quality and quantity in Bryce Canyon National Park, focusing on Mossy Cave Spring and Water Canyon, and produced a simple hydrologic budget for the park. Loughlin Water Associates (2022) performed a hydrogeologic assessment of several wells in Emery Valley located along Highway 12. They concluded that the valley-fill aquifer there locally has transmissivities as high as 59,000 ft^2/day (5500 m^2/day) and that pumping wells completed in the valley-fill aquifer have no or negligible effect on nearby wells completed in Cretaceous sandstone bedrock.

Geologic Setting

The study area falls within three 30′ x 60′ quadrangles: Panguitch, Escalante, and Kanab. The primary sources for the geologic summary below are the geologic maps of these quadrangles produced by Biek et al. (2015), Doelling and Willis (2018), and Doelling (2008), respectively. Johns and Emery Valleys are in the Colorado Plateau physiographic province. Johns Valley, situated between the Escalante Mountains and Sevier Plateau, is a topographic depression in which valley-fill sediment has accumulated from the East Fork Sevier River and alluvial fans and side drainages emanating from the surrounding hills. Emery Valley extends southwest from Johns Valley and is situated between the Sevier and Paunsaugunt Plateaus. The valley fill forms the principal aquifer of both valleys. Bryce Canyon is a major geologic feature to the south of these valleys.

Geologic units in the study area are Quaternary unconsolidated deposits, Tertiary volcanic and sedimentary rocks, and Cretaceous sedimentary rocks. The predominant geologic units are Quaternary valley fill, the Tertiary Osiris Tuff, and the Tertiary Mount Dutton, Brian Head, Claron, Pine Hollow, and Grand Castle Formations, as well as the Cretaceous Kaiparowits, Wahweap, and Straight Cliffs Formations.

The Quaternary unconsolidated deposits include gravel, sand, and clay derived from adjacent hills and mountains that were deposited in alluvial-fan, fluvial, and mass-movement environments.

The early Miocene to late Oligocene Osiris Tuff is mapped as the outflow facies of the Marysvale volcanic field (Biek et

al., 2015). It consists of resistant, light-gray and brown, rhyodacitic ash-flow tuff (Williams and Hackman, 1971).

The Oligocene-Miocene Mount Dutton Formation is volcanic mudflow breccia consisting of angular to subrounded, pebble- to boulder-size clasts in a muddy to sandy matrix (Mackin and Rowley, 1976; Maldonado and Williams, 1993a, 1993b; Rowley et al., 1994). In the northwestern part of Johns Valley in the Sevier Plateau, the Mount Dutton Formation is light- to dark-gray and brown volcanic mudflow breccia and lesser interbedded volcaniclastic conglomerate and tuffaceous sandstone (Biek et al., 2015). Exposures in the plateau are the alluvial facies of the Mount Dutton Formation, are part of the Markagunt gravity slide, and are about 2000 feet (600 m) thick at the southern end of the plateau (Rowley et al., 2013; Biek et al., 2015).

The Eocene-Oligocene Brian Head Formation is composed of non-tuffaceous sandstone and conglomerate, volcanic mudflow breccia, mafic lava flows, volcaniclastic sandstone with minor limestone and chalcedony, and ash-flow tuff (Biek et al., 2015). The unit consists dominantly of yellowish-gray and light-gray tuffaceous sandstone with interbedded pebble- to boulder-size conglomerate, sandstone, and minor limestone and mudflow breccia (Maldonado and Moore, 1995).

The Eocene-Paleocene Claron Formation in the study area consists of mudstone, siltstone, sandstone, limestone, and minor conglomerate deposited in fluvial, floodplain, and lacustrine environments of an intermontane basin (Mullet, 1989; Ott, 1999; Biek et al., 2015).

The Claron Formation is divided into the younger white member that was deposited in both fluvial and lacustrine environments and the older pink member that is dominantly fluvial (Goldstrand,1994; Bown et al., 1997). The upper limestone unit of the white member is white, pale-yellowish-gray, pinkish-gray, and very pale-orange micritic limestone, and is typically about 80 to 100 feet (24–30 m) thick on the southern flank of the Sevier Plateau (Biek et al., 2015). The lower part of the white member consists of micritic limestone similar to the upper white limestone interval and forms a cliff or steep, ledgy, white slope. The lower limestone unit has a maximum thickness of about 300 feet (91 m) at Bryce Point in Bryce Canyon National Park (Bowers, 1991), and is about 160 feet (49 m) thick to the north on the southwestern flank of the Sevier Plateau (Biek et al., 2015). Within Bryce Canyon National Park at Inspiration Point, the lower limestone unit of the White Member is mostly white, pink, and pale-orange, slope-forming mudstone and siltstone with only minor limestone (Knudsen et al., in preparation).

The pink member of the Claron Formation consists of micritic limestone, calcite-cemented sandstone, calcareous mudstone, and minor pebbly conglomerate that weather to colluvium-covered ledgy slopes. The unit is about 600 feet (183 m) thick at Bryce Canyon National Park (Biek et al., 2015).

The early Paleocene to middle Eocene Pine Hollow Formation consists of purple-gray to red-brown conglomerate, mudstone, siltstone, and claystone. The claystone is commonly smectitic, particularly near the middle of the formation. The unit contains interbeds of gray, tan, or red, fine- to coarse-grained sandstone in the lower part and has thin conglomerate lenses mostly near the base (Goldstrand and Mullet, 1997). The unit thins to the north and has a thickness of 0 to 450 feet (0–137 m) (Doelling and Willis, 2018).

The Cretaceous Grand Castle Formation is light-gray and light-red massive conglomerate. Clasts are well-rounded, pebble- to boulder-size quartzite, limestone, sandstone, and chert. The formation is locally mapped on the Paunsaugunt Plateau where it is typically thin and poorly exposed at the base of the Claron Formation (Bowers, 1972).

The Kaiparowits Formation is a light-brown, very fine grained sandstone and gray sandy mudstone that crops out above the capping sandstone member of the Wahweap Formation southwest of Tropic Reservoir (Bowers, 1991). The Kaiparowits Formation was deposited in a relatively wet, subhumid alluvial plain that had periodic to seasonal aridity near the western margin of the Late Cretaceous Western Interior Seaway (Roberts, 2007).

The Late Cretaceous Wahweap Formation overlies the Straight Cliffs Formation in the East Fork Sevier River drainage basin. These two units are very similar, especially near their contact, and are commonly lumped together as an undivided map unit. The Wahweap Formation is mostly fine-grained sandstone, siltstone, and mudstone deposited in braided and meandering river and floodplain environments of a coastal plain (Lawton et al., 2003). Around Tropic Reservoir, because of extensive vegetative cover and poor geomorphic expression, three members of the Wahweap Formation are mapped as undivided, except for the distinctive capping sandstone (Knudsen et al., in preparation).

The Late Cretaceous Straight Cliffs Formation consists of the Drip Tank and John Henry Members in the study area. On the Paunsaugunt Plateau, the Drip Tank Member is white to light-gray, fine- to medium-grained quartzose sandstone, and, in the upper part of the unit, it has pebbly sandstone and pebbly conglomerate (Biek et al., 2015). The John Henry Member consists of gray, brown, and reddish-brown mudstone and thin- to thick-bedded, grayish-orange to yellowish-brown, fine-grained sandstone and forms ledgy slopes on the eastern margin of the Bryce Canyon National Park boundary. In the area around Bulldog Hollow near the town of Tropic, the John Henry Member is stacked or amalgamated sandstone in the upper part of the unit. North of Tropic, a prominent 20- to 40-foot-thick (6–12 m) coal-rich interval is mapped as a marker bed (Knudsen et al., in preparation).

The principal structural elements of the study area (Biek et al., 2015) include the Paunsaugunt fault zone, a northwest-side-down Quaternary normal fault that strikes northeast through Johns Valley along the eastern margin of the study area; the Pine Hills and Rubys Inn thrust faults, which strike east-west and form the northern and southern boundaries, respectively, of Emery Valley; the Johns Valley thrust fault northwest of Flake Mountain, which strikes northeast through the central part of Johns Valley in the northern part of the study area; and the Hunt Creek thrust fault, which strikes northeast parallel to the Johns Valley thrust fault. The thrust faults are interpreted as resulting from the Markagunt gravity slide (Biek et al., 2015).

HYDROSTRATIGRAPHY AND AQUIFER PROPERTIES

Delineation of Hydrostratigraphy

We derived hydrostratigraphy for the geologic units in our project area based on geologic maps, water-well data, and limited field observations. Defining hydrostratigraphic units involves grouping or splitting geologic formations based on their known or inferred water-yielding characteristics. The scheme used here includes aquifer, heterogeneous unit (mixed confined/unconfined or interbedded fine and coarse sedimentary layers), and confining unit. Hydrostratigraphic units were delineated for the valley fill, Claron Formation, and Cretaceous formations (Kaiparowits, Wahweap, and Straight Cliffs), all of which yield water to wells and springs in the study area (Figures 2–4).

Quaternary and late Tertiary deposits are primarily alluvial and coarse- to medium- grained, include comparatively thin and laterally discontinuous fine-grained layers, and are classified as aquifer units. The next section provides more detail about the lithology and stratigraphy of the Quaternary-Tertiary valley-fill deposits. Quaternary mass-movement deposits are prominent in the northeast and are primarily composed of slump blocks and debris slides of volcanic rock. These deposits are classified as heterogeneous units. The Sevier River Formation is a crudely stratified conglomerate, sandstone, and siltstone derived from volcanic sources and is classified as a heterogeneous unit. The Mount Dutton Formation, predominantly volcaniclastic mudflow breccia, is classified as a heterogeneous unit due to lateral and vertical variations in texture and fracturing. This unit's water-yielding characteristics are expected to vary with location, and individual aquifers within the unit are not expected to be connected at a regional scale. The Osiris Tuff is a densely welded ash-flow tuff that is classified as a heterogeneous unit due to the presence of extensive fracturing and at least one spring that appears to source from an outcrop. The Brian Head Formation is classified as a confining unit based on its composition of volcanogenic mudstone and localization of springs at its top in the northern part of the study area. The Claron Formation is split into two heterogeneous units; the upper unit is composed predominantly of carbonate rocks and the lower unit is composed predominantly of siliciclastic rocks (Figure 2). Both units yield water to wells. The carbonate heterogeneous unit is karstic on the Markagunt Plateau about 35 miles (56 km) to the west (Biek et al., 2015). Karst features were not observed in outcrop in this study area but may be present in the subsurface and control the locations of springs. Late Cretaceous formations are composed of alternating predominantly coarse-grained and predominantly fine-grained intervals that are classified as aquifer units and heterogeneous units, respectively (Figure 3). The heterogeneous units are mostly fine-grained sandstone grading to conglomerate having a coarse-grained sandy matrix and include shale interbeds. These units yield water to wells and springs.

Valley-fill Aquifer

Lithology

We entered lithology data from well logs (Utah Division of Water Rights, 2018) into a well management program, constructed cross sections through the valley fill, and identified laterally continuous lithologic units. We chose cross-section lines based on the distribution of well logs within the study area (Figure 5). We used 48 well logs to interpret subsurface geology on the cross sections based on their proximity to the section lines. Wells used in cross sections (Figure 6) are labeled by HydroID, a unique identifier assigned by the well management program. The cross sections assist in interpreting valley-fill stratigraphy and thickness, water levels, flow paths, groundwater–surface-water interactions, and constructing the conceptual flow model. The valley fill in Johns and Emery Valleys is divided into predominantly coarse (sands and gravels), predominantly fine (clay, silt, and fine sand), and mixed-grain-size units. Some well borehole lithologies are mismatched with adjacent interpolations in the cross sections. Borehole lithologies are based on recorded drilling observations, and some well logs include inaccurate lithologic information (e.g., unconsolidated material overlain by bedrock). The potentiometric surface from spring 2022 is projected onto cross sections in Figure 6 (discussed in Groundwater Levels and Streamflow section below).

Cross section A-A′ trends northwest-southeast through central Emery Valley and includes the area of greatest groundwater development in the study area, along highway 12 (Figures 5 and 6A). Within 25 to 30 feet (8–9 m) of land surface, unconsolidated deposits are predominantly coarse grained near the valley margins and predominantly mixed grain size in the valley center. In the middle to lower parts of the valley fill, predominantly fine-grained deposits exist near both ends of the cross section. The valley-fill deposits are over 100 feet (30 m) thick in the center of the valley and overlie Cretaceous (undivided) rocks below the valley floor and the Claron Formation (undivided) near the valley margins. Well logs are insufficiently detailed to identify hydrostratigraphic units within the Claron Formation and

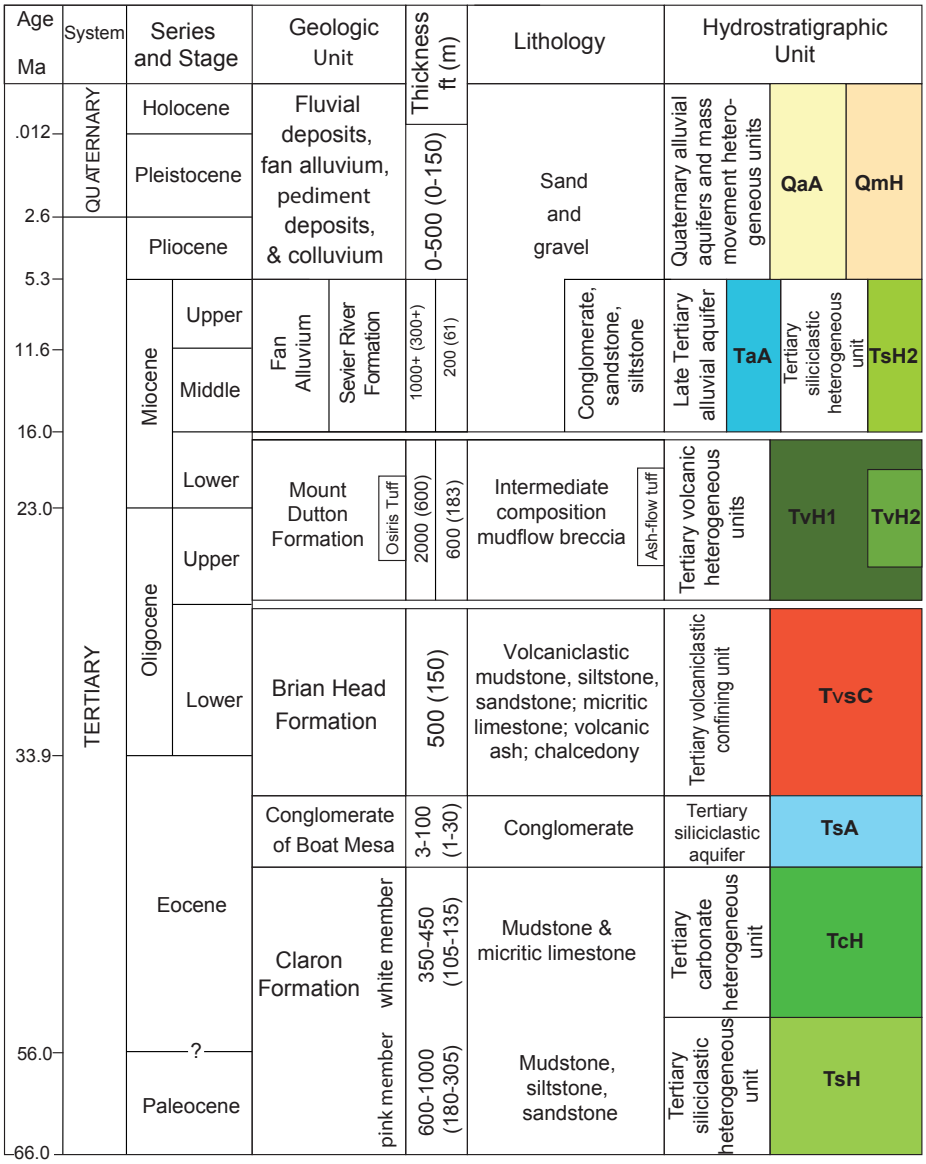

Figure 2. *Hydrostratigraphy of Quaternary and Tertiary sedimentary deposits and rock units in the study area. Modified from Biek et al. (2015) and Doelling and Willis (2008).*

Cretaceous rocks; however, several wells along the cross section are completed in each, suggesting they yield at least moderate amounts of groundwater.

Cross section B-B′ trends north-south through the west end of Emery Valley (Figures 5 and 6B). Valley-fill deposits are primarily fine grained and mixed grain size, are as much as 200 feet (61 m) thick, and overlie Cretaceous bedrock. Cuttings (housed at the Utah Geological Survey [UGS] Utah Core Research Center) from a petroleum exploration well located north of the section line were examined for this study and indicated about 200 feet (61 m) of pebbly valley-fill deposits lie above medium-grained, well-sorted sandstone (Appendix A). The pebbly deposits are Quaternary alluvial pediment deposits (unit Qap from Biek et al., 2015). Well 1035 is a water supply well for the petroleum exploration well, but its log indicates only bedrock. Valley-fill deposits in this area evidently vary in thickness substantially over short distances. The line of cross section B-B′ is south of a limited exposure of the John Henry Member of the Straight Cliffs Formation along the north wall of a modern dry wash. The valley fill–bedrock contact, therefore, rises steeply south to intersect the land surface on the north side of the dry wash.

Cross section C-C′ trends north-south across central Emery Valley (Figures 5 and 6C). Moderately continuous fine-grained deposits overlie mixed- and coarse-grained deposits in the valley margins, which may indicate locally confining conditions. Wells completed in the northern valley margin are primarily completed across or below the alluvium-bedrock interface.

Cross section D-D′ trends north-south across eastern Emery Valley (Figures 5 and 6D). Mixed-grain-size deposits overlie coarse-grained deposits in the valley margins. Wells at the south end of the cross section are primarily completed in

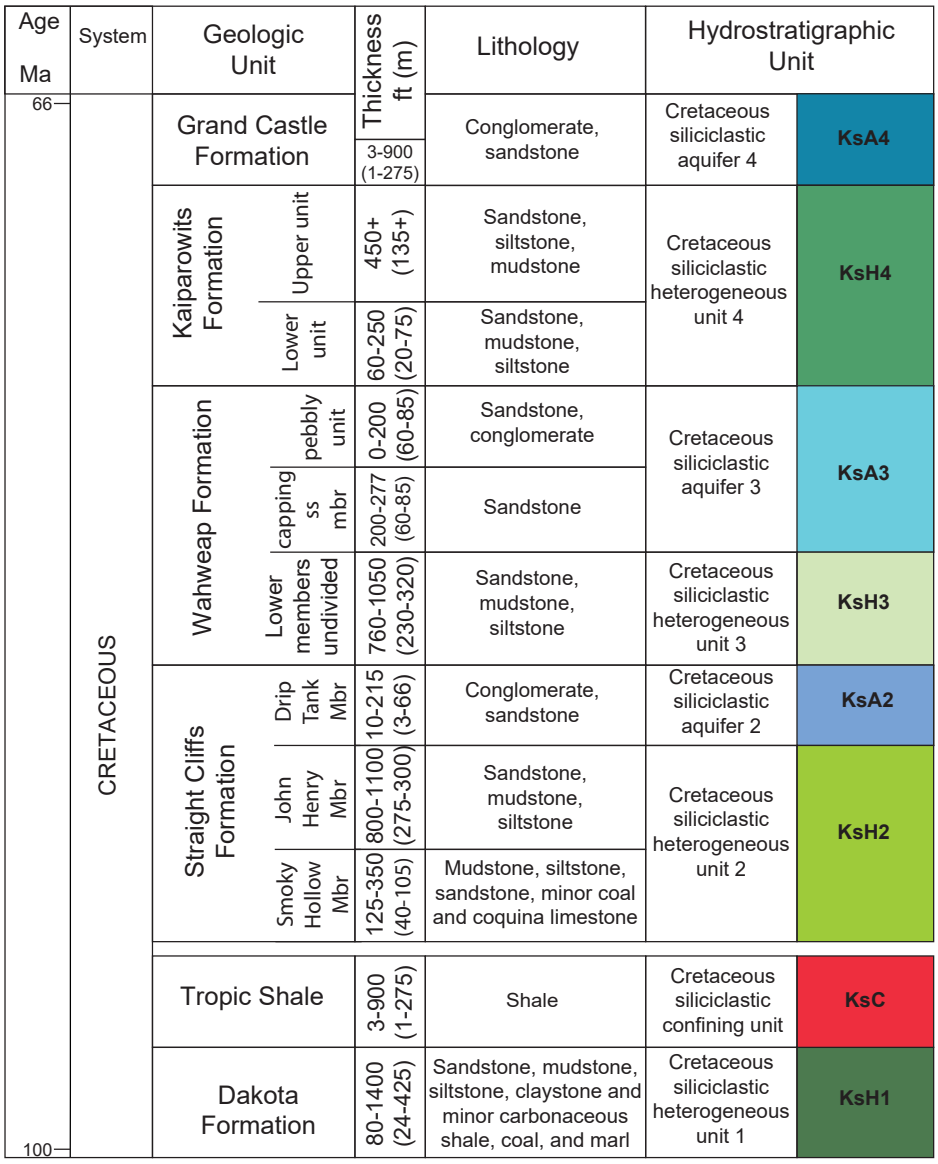

Figure 3. *Hydrostratigraphy of Cretaceous rock units in the study area. Modified from Biek et al. (2015) and Doelling and Willis (2008).*

Cretaceous rocks. In the valley center, mixed-grained alluvial-fan deposits overlie a substantial lens of predominantly fine-grained deposits.

Cross section E-E′ trends east-northeast across southern Johns Valley (Figures 5 and 6E). Valley-fill deposits are predominantly coarse grained in the west-southwest part of the section, and predominantly mixed grain size in the northeast part of the section. A fine-grained layer exists at about 120 to 180 feet (37–55 m) below the land surface in the central part of the section. Most wells in the northeast part of the section are drilled into and likely completed in Cretaceous bedrock. The cross section intersects the Johns Valley thrust fault in the southwest and the Paunsaugunt normal fault in the northeast. We do not know the age of the deepest coarse-grained deposits in the central part of the section; they could be cut by either or both faults. Younger valley-fill deposits onlap the fault surfaces.

Cross section F-F′ trends north-south along the axis of northern Johns Valley (Figures 5 and 6F). Valley-fill deposits are predominantly coarse grained in the northern and central parts of the section and transition to predominantly mixed grain size in the southern part of the section. These deposits are overlain by a fine-grained deposit at the surface in the center of the section. The section also intersects a fine-grained layer described in section E-E′ above. The cross section intersects the Hunt Creek thrust fault in the center and the Johns Valley thrust fault in the south. Well 1089 at the northern end of the section is drilled through the Osiris Tuff, which likely pinches out to the south.

The cross sections collectively indicate that the valley-fill deposits of Emery Valley and Johns Valley are predominantly coarse grained to mixed grain size and are less than about 200 feet (61 m) thick in most places. Coarse-grained deposits are prevalent near the mountain fronts and are interbedded with

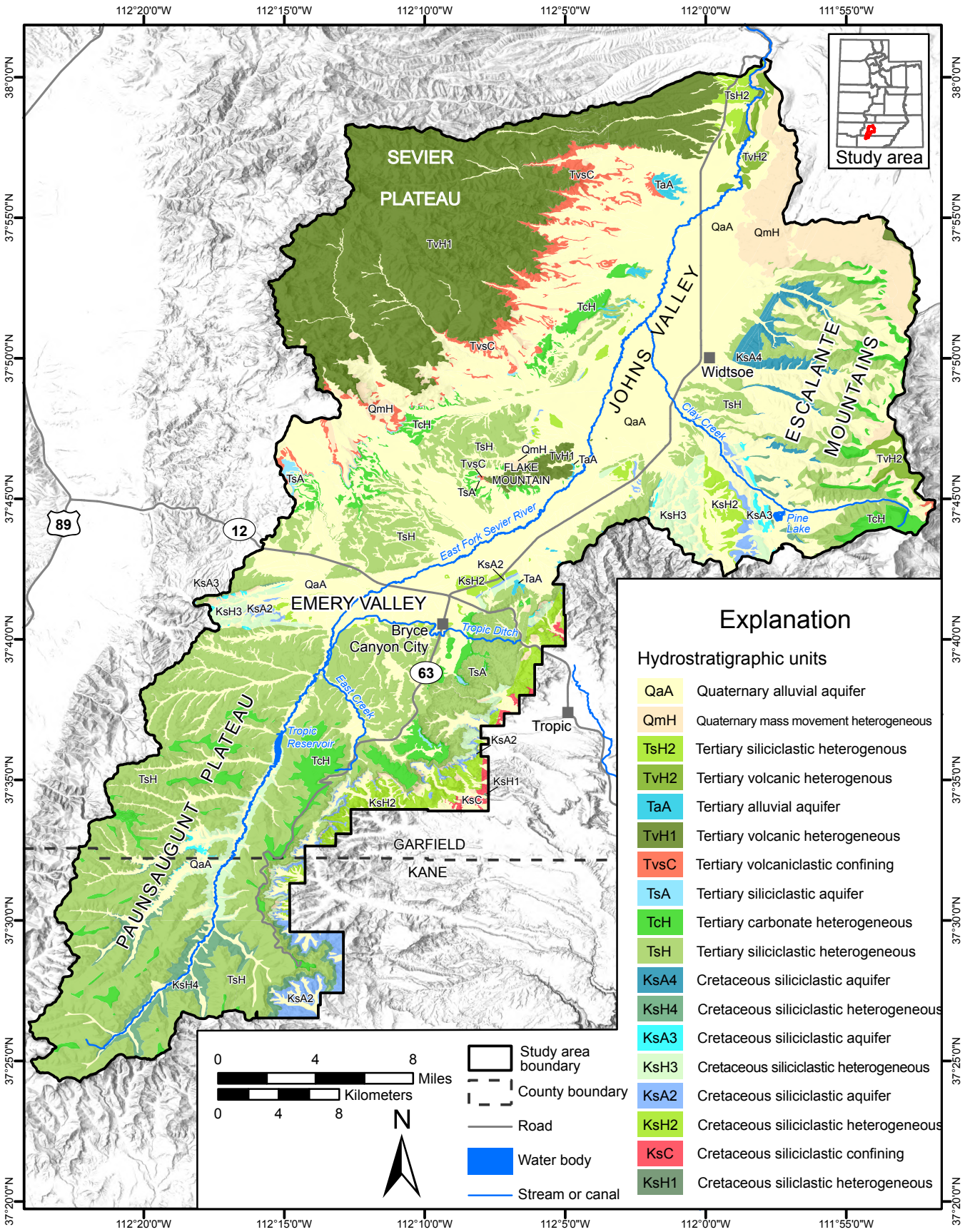

Figure 4. *Distribution of hydrostratigraphic units in Emery and Johns Valleys. Quaternary units are depicted in shades of tan, other aquifer units in shades of blue, heterogeneous units in shades of green, and confining units in shades of red.*

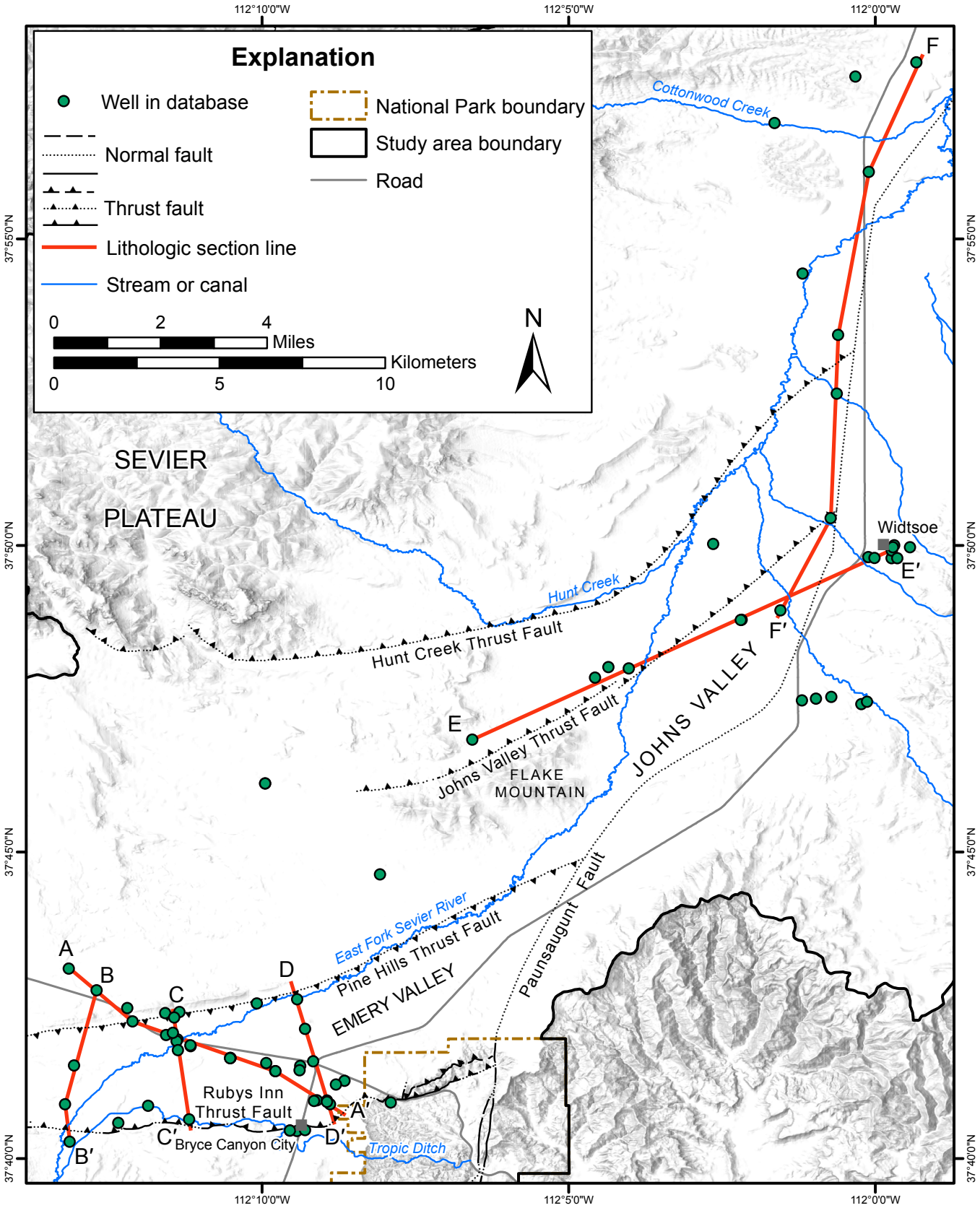

Figure 5. *Location of cross sections shown on Figure 6.*

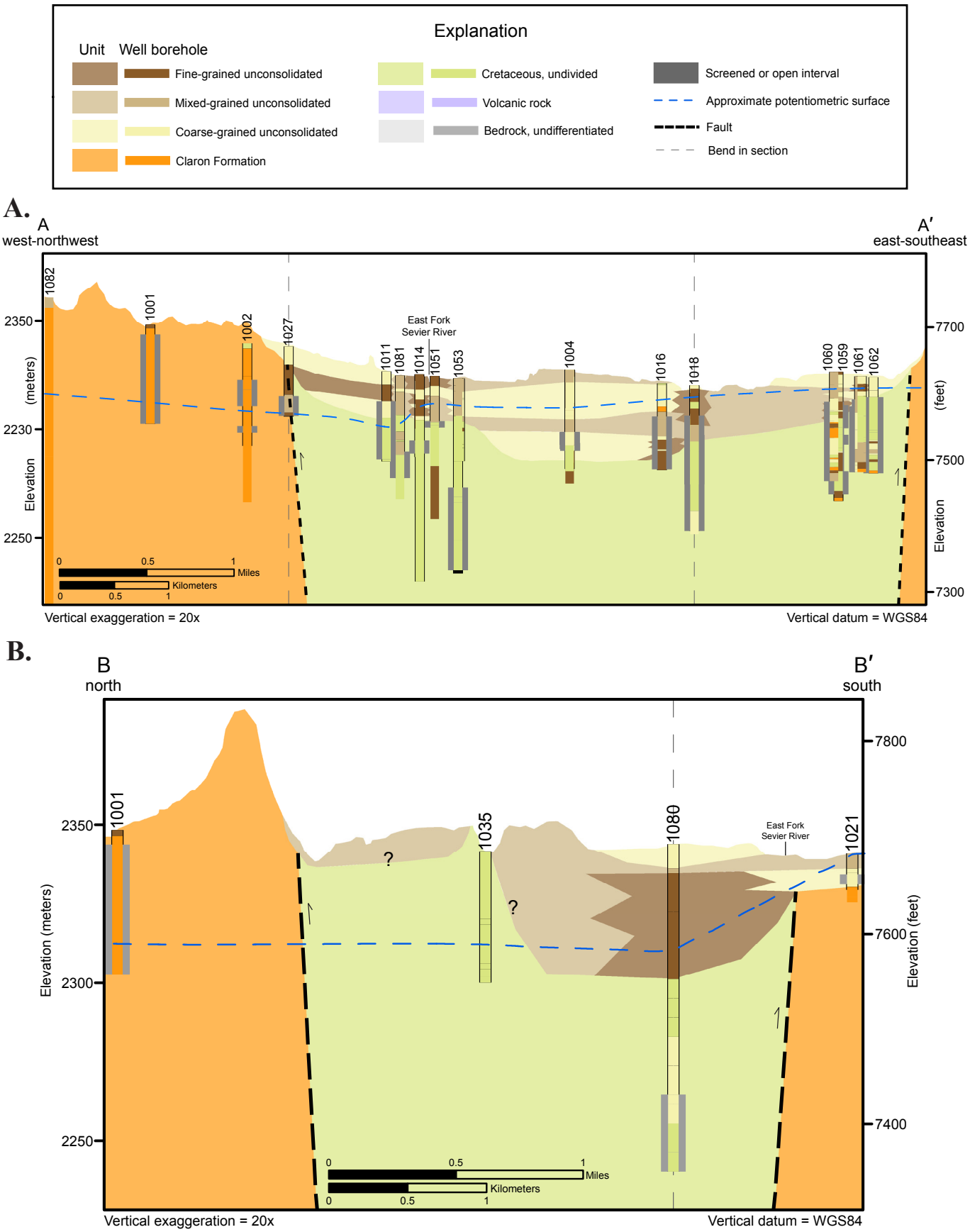

Figure 6. *Schematic geologic cross sections. See Figure 5 for cross section location. Cross-section well HydroIDs keyed to Appendix E. Potentiometric surface from spring 2022. Lateral changes in the potentiometric surface that appear abrupt (e.g., from pumping influence) are amplified visually by the vertical exaggeration of the cross sections.* ***A)*** *Cross section A-A'.* ***B)*** *Cross section B-B'.*

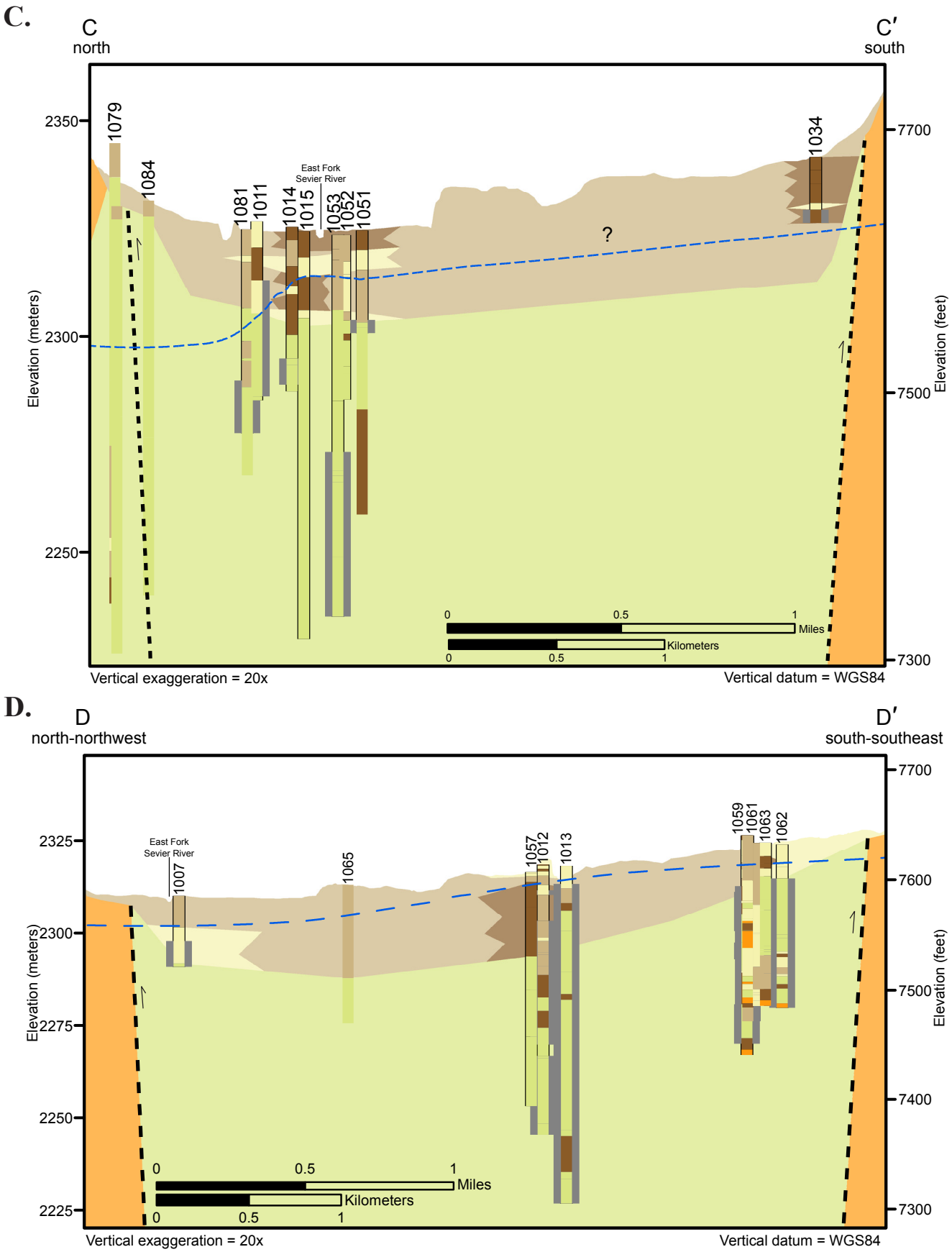

Figure 6. Continued. *Schematic geologic cross sections. See Figure 5 for cross section location. Cross-section well HydroIDs keyed to Appendix E. Potentiometric surface from spring 2022. Lateral changes in the potentiometric surface that appear abrupt (e.g., from pumping influence) are amplified visually by the vertical exaggeration of the cross sections.* ***C)*** *Cross section C-C'.* ***D)*** *Cross section D-D'.*

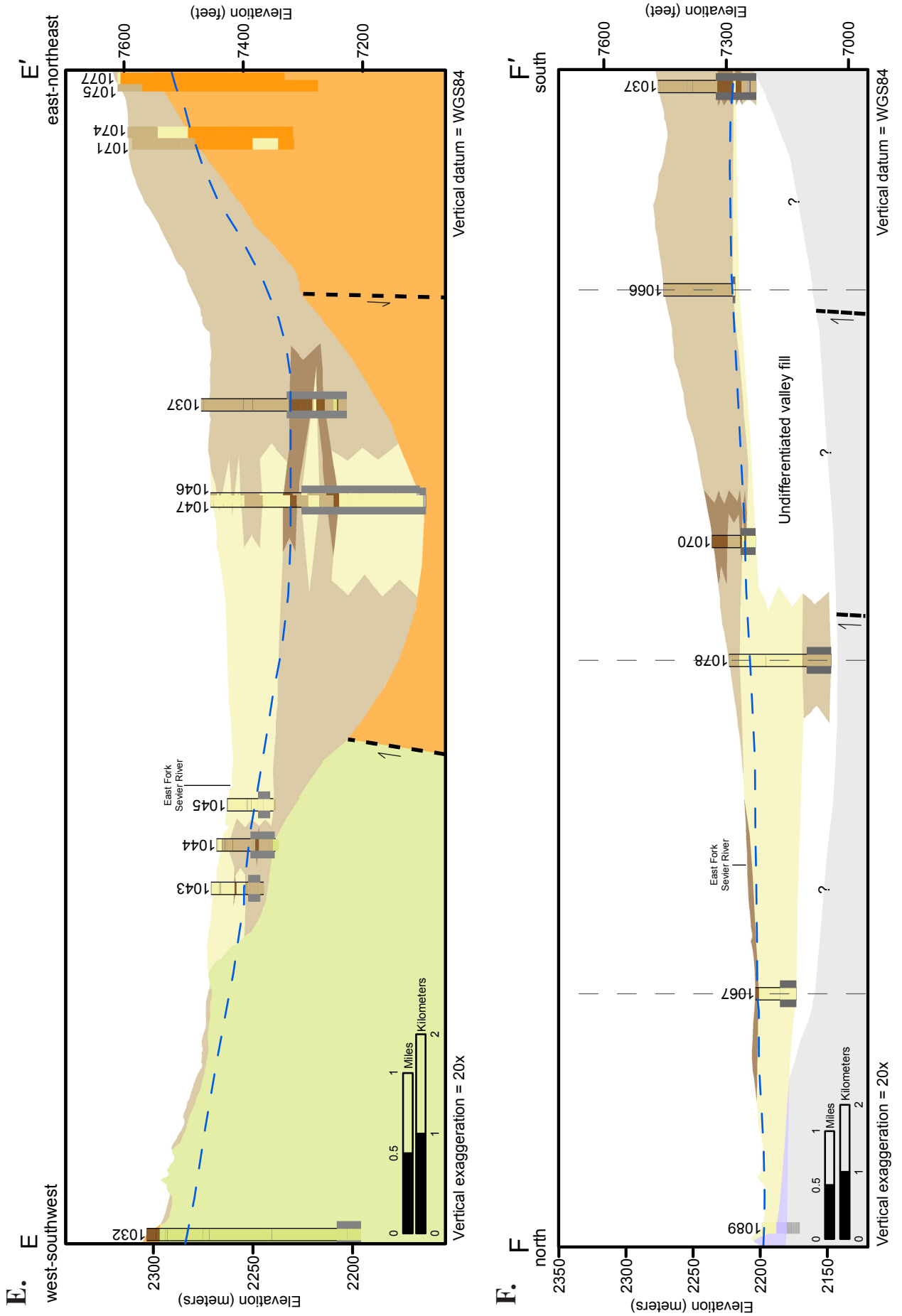

Figure 6. Continued. *Schematic geologic cross sections. See Figure 5 for cross section location. Cross-section well HydroIDs keyed to Appendix E. Potentiometric surface from spring 2022. Lateral changes in the potentiometric surface that appear abrupt (e.g., from pumping influence) are amplified visually by the vertical exaggeration of the cross sections.* ***E)*** *Cross section E-E'.* ***F)*** *Cross section F-F'.*

heterogeneous deposits below the valley floor. Fine-grained layers are rare and generally laterally discontinuous, suggesting unconfined groundwater conditions exist in most areas. We are uncertain whether the mixed-grain-size deposits consist of poorly sorted deposits or interlayered fine- and coarse-grained deposits.

Thickness

Wells: We interpreted depth to bedrock using well logs. Locating the valley fill–bedrock contact from well logs can be straightforward or ambiguous, depending on the level of detail of the log and on the lithologic contrast between valley fill and bedrock. For example, cuttings from the Lion/Monsanto 1 Bryce well (Appendix A) include a wide variety of rock types having rounded edges (i.e., pebbles) in the upper 200 feet (61 m), and exclusively medium- to fine-grained, angular sandstone fragments below 270 feet (82 m); the exact contact is, unfortunately, missing. The contact between multi-lithologic gravel and uniform sandstone would be evident to most well drillers. Where fine-grained valley-fill deposits overlie Cretaceous shale (e.g., one of the confining hydrostratigraphic units shown on Figure 3), the change in lithology and drilling characteristics between valley fill and bedrock is more difficult to discern. We subjectively chose the most reliable well logs to estimate valley-fill thickness.

Gravity study: We conducted a gravity survey in the study area to delineate valley-fill thickness and subsurface structures, acquiring 124 new gravity stations during the 2019 field season (Figure 7). In gravity surveys, the working unit Gal is defined as 1 centimeter per second squared (cm/s^2) making, for example, the commonly stated acceleration due to gravity at the Earth's surface 980 Gal (9.8 m/s^2). Observed changes in the Earth's local gravity field are most sensitive to elevation (vertical changes) which makes elevation control a critical parameter in gravity surveys.

We used two Scintrex CG-5 Autogravs (precision of 1 μGal, accuracy of 5 μGal) to make field measurements of the vertical component of the gravity field, following the methods of Gettings et al. (2008) and utilizing an absolute gravity base station located near the Utah Department of Natural Resources building in Salt Lake City. We established elevation control through post-processing of data collected by high-precision Global Positioning System (GPS) survey equipment. When logging for a minimum of 10 minutes, we observed better than 3 cm (1 inch) vertical precision for 114 stations, 20 cm (8 inches) or better for 5 stations, and the remaining 5 stations were submeter (39 inches). The vertical absolute accuracy depends on the local base station absolute coordinates which are within the range of 1 to 3 cm (0.4 –1.2 inches). From calculations based on the vertical gravity gradient (0.309 mGal/m), the GPS surveying procedure would result in a vertical gravity accuracy of better than 0.001 mGal (1 μGal) for 90% of the stations, which is acceptable because 1 μGal exceeds the gravimeter's sensor accuracy of 5 μGal. We applied terrain corrections to the processed gravity data and calculated the Complete Bouguer Gravity Anomaly (CBGA) for each station using the methods outlined in Hintze et al. (2005) with a reduction density of 2.67 grams per cubic centimeter (g/cm^3). UGS gravity data were merged with 749 legacy gravity stations from PACES (Pan-American Center for Earth & Environmental Studies [PACES], 2012), a national gravity and magnetics data repository, to improve data coverage in the study area.

Gravity data are tabulated in Appendix B. The map of the CBGA field (Figure 7) illustrates broad downward steps in a northwestward direction in the gravity anomaly signal that are on the order of 30 mGal in the southeast to 15 mGal in the northwest. These broad, sequential steps in the gravity anomaly are a result of density contrasts between the local geology bounding Emery and Johns Valleys. The shape of the anomaly is elongated and shelf-like, the main axis trending south-southwest to north-northeast along the Sevier and Paunsaugunt Plateaus, and the steepest gradients in the gravity field are on the southeastern margins. We interpret the areas having the most widely spaced CBGA contours—central Emery Valley, southwestern Johns Valley, and northeastern Johns Valley—as the thickest parts of the valley fill.

Valley-fill isopach map: We constructed an isopach map (Figure 8) of the unconsolidated valley-fill deposits in Emery and Johns Valleys based on information from well logs and the CBGA map. Uncertainty in interpretation of the well logs for this purpose is discussed above. The shape and gradient of the CBGA field was used to guide the location and spacing of thickness isolines; however, as discussed in the previous section, the contours reflect both lateral gradients in pre-Quaternary geologic units and the thickness of the valley-fill aquifer. Interpretation of valley-fill thickness beneath southwestern Johns Valley south of Flake Mountain and northeastern Johns Valley northeast of Widtsoe is based solely on the CBGA anomaly and is highly speculative because no local well data exist (Figure 8). As drawn, the isopach contours indicate: (1) mostly shallow and highly variable valley-fill thickness in western Emery Valley, (2) an elongate, northeast-trending, oval-shaped depositional center in eastern Emery Valley and southeastern Johns Valley, and (3) an oval-shaped, north-northeast-trending depositional center in central Johns Valley. The isopach contours have high uncertainty and could be modified based on new well data or additional analysis of the gravity data. These isopach contours should not be used to estimate depth to bedrock for potential new wells, except in a very general way, or to interpret the depositional or structural evolution of the basin.

Aquifer Properties Estimates

Aquifer properties describe how well an aquifer will yield water to wells and springs. Aquifer tests, which involve

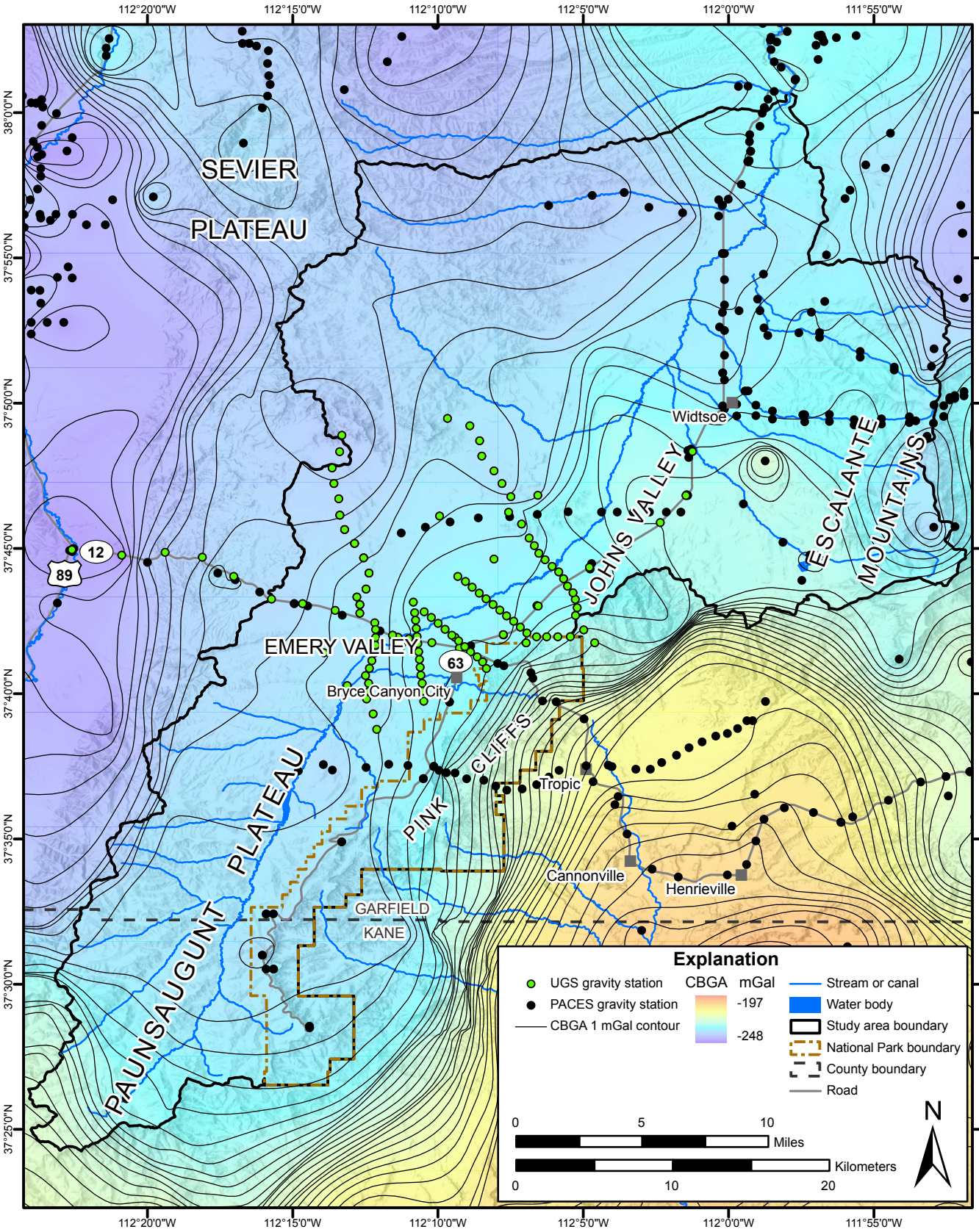

Figure 7. *Complete Bouguer Gravity Anomaly map for the study area.*

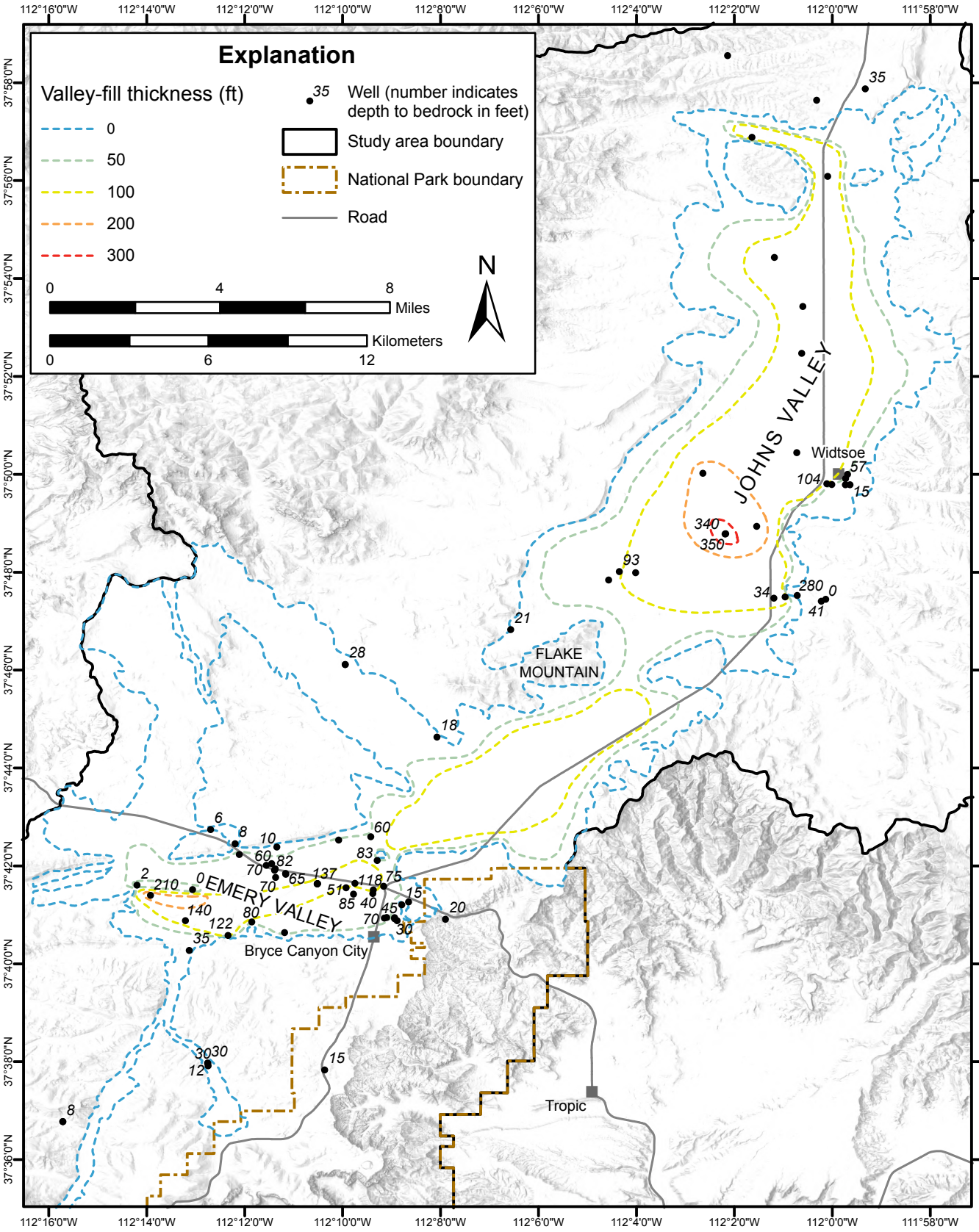

Figure 8. *Isopach map for the valley fill based on well logs and gravity data.*

pumping a well while monitoring the water-level response in the pumping well and/or nearby wells, provide good estimates of aquifer properties. We compiled data from aquifer tests performed on public drinking water sources for the Utah Division of Drinking Water, which provide good estimates of aquifer properties (Appendix C and Appendix D Table D-1). Aquifer test data for most domestic wells are not readily available, so we estimated aquifer properties from information obtained from water well logs.

Eight aquifer tests were conducted in the study area for public water supply wells (Appendix C). Three of the tests were conducted on wells in the valley-fill aquifer or alluvial sediments: two in Emery Valley and one in the East Creek drainage for a Bryce Canyon National Park public supply well. One test was conducted in the Claron Formation and the remaining four were conducted in various formations within the Cretaceous bedrock. Transmissivities derived from aquifer tests in the valley-fill aquifer ranged from 8900 to 60,700 ft^2/day (827–5640 m^2/day). Transmissivities from bedrock aquifer tests ranged from 65 to 1350 ft^2/day (6–125 m^2/day). These data were not included with summary statistics of transmissivity values estimated from specific capacity data, but are shown on Figure 9.

We estimated storativity using the equation S=Sy + (Ss*b), where S is storativity, Sy is specific yield, Ss is specific storage, and b is aquifer thickness. We based Sy and Ss on published values for aquifer materials from Johnson (1967) and Domenico (1972) and based b on well logs. We derived specific capacity estimates using drawdown data from well logs where specific capacity is the pumping rate divided by drawdown. We estimated transmissivity using specific capacity data from well logs using the TGUESS algorithm of Bradbury and Rothschild (1985), which utilizes the Cooper and Jacob (1946) solution of the Theis (1935) equation. We estimated hydraulic conductivity by dividing transmissivity by saturated aquifer thickness. Aquifer thickness was assumed to be the length of the screened or perforated interval.

We estimated transmissivity for the principal valley-fill aquifer (n = 19) and grouped the Tertiary Claron Formation and Cretaceous sandstone aquifers together as bedrock aquifers (n = 28) (Figure 9). We used a storativity of 0.3 for the valley-fill aquifer and a range of 0.005 to 0.0005 for the bedrock aquifers. The valley-fill aquifer had the highest estimated transmissivities, ranging from 10 to 10,680 ft^2/day (0.9–992 m^2/day). The geometric mean for this aquifer was 316 ft^2/day (29 m^2/day). Transmissivities in the bedrock aquifers ranged from 8 to 1252 ft^2/day (0.7–116 m^2/day), with a geometric mean of 69 ft^2/day (7 m^2/day). The range of transmissivity data from specific capacity data is shown on Figure 10.

In Emery Valley, valley-fill aquifer transmissivities appear to correlate with valley-fill thickness, with lower values on the valley margins and higher values toward the valley center. South of Emery Valley on the Paunsaugunt Plateau, several wells are completed in young alluvium in the East Creek and East Fork Sevier River drainages that have high transmissivities despite limited aquifer thickness. To the north in Johns Valley, valley-fill aquifer transmissivities are low despite having the greatest aquifer thicknesses in the study area. However, the sparse wells of Johns Valley are used for domestic and stock watering and have no associated aquifer test data, so the existing data may not reflect the potential transmissivity of the aquifer. Transmissivities from aquifer test data are higher than transmissivities derived from specific capacity data, but generally correlate.

GROUNDWATER LEVELS AND STREAMFLOW

Water Levels and Potentiometric Surfaces

Methods

To construct potentiometric surface maps, we measured water levels in a total of 45 wells from September 2018 to May 2022 (Figure 11). We measured water levels biannually, in approximately spring and autumn of each year. Our water level measurements were focused on southern Johns Valley, Emery Valley, and the Paunsaugunt Plateau from 2018 to 2020 and expanded to include the rest of Johns Valley in 2021 and 2022 (Figure 12, Appendix D Table D-2). We calculated the water-level elevation at each well by subtracting the measured depth to water referenced to land surface from the land surface elevation (Appendix D Tables D-1 and D-2), which was measured using a Trimble high-precision GPS instrument having vertical accuracy of 10 centimeters or better. We constructed potentiometric surface maps for each season of measurement; May 2021, October 2021, and May 2022 are presented on Figure 12 and discussed below, whereas potentiometric surface maps from 2018 to 2020 are in Appendix D.

Potentiometric Surfaces

We used wells completed in only the valley-fill aquifer, screened in both alluvium and bedrock, or screened in bedrock having water levels consistent with nearby valley-fill wells to generate potentiometric surface maps (Figure 12). Due to the paucity of wells in the study area, we included water-level data regardless of well pumping activity.

Potentiometric surfaces from all seasons show that valley-fill water-level elevations are highest in the East Creek drainage where the National Park Service well field is located, and lowest at the northern end of Johns Valley. Because most of the wells in Emery Valley provide water to hotels and businesses centered around the high tourism season from May to September, we expected to see water level measurements reflecting pumping and localized cones of depression, evident

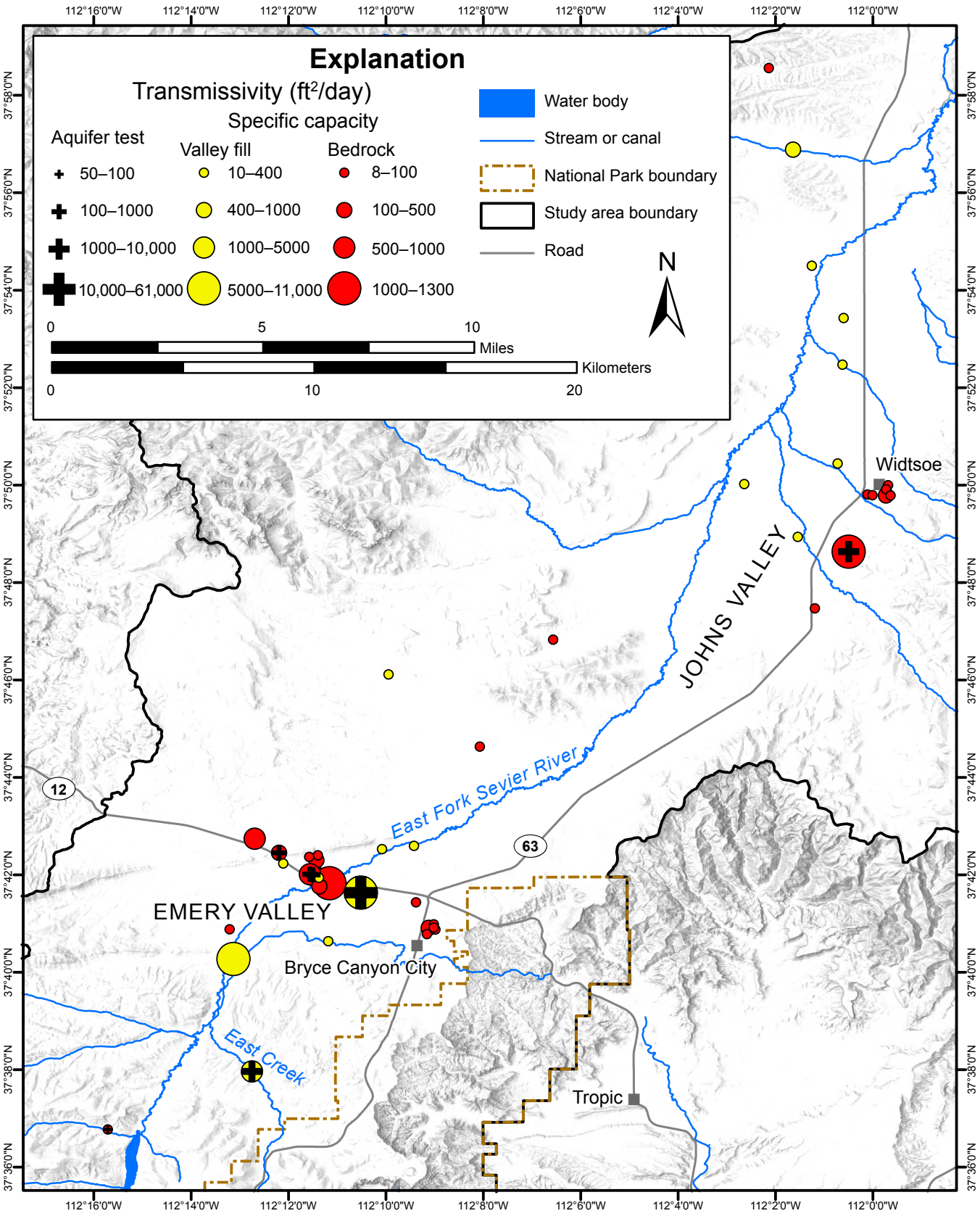

Figure 9. *Transmissivity map compiled from public supply well data and well logs. Note that the ranges of transmissivity values represented by circle diameter are different for the valley-fill aquifer and the bedrock aquifers.*

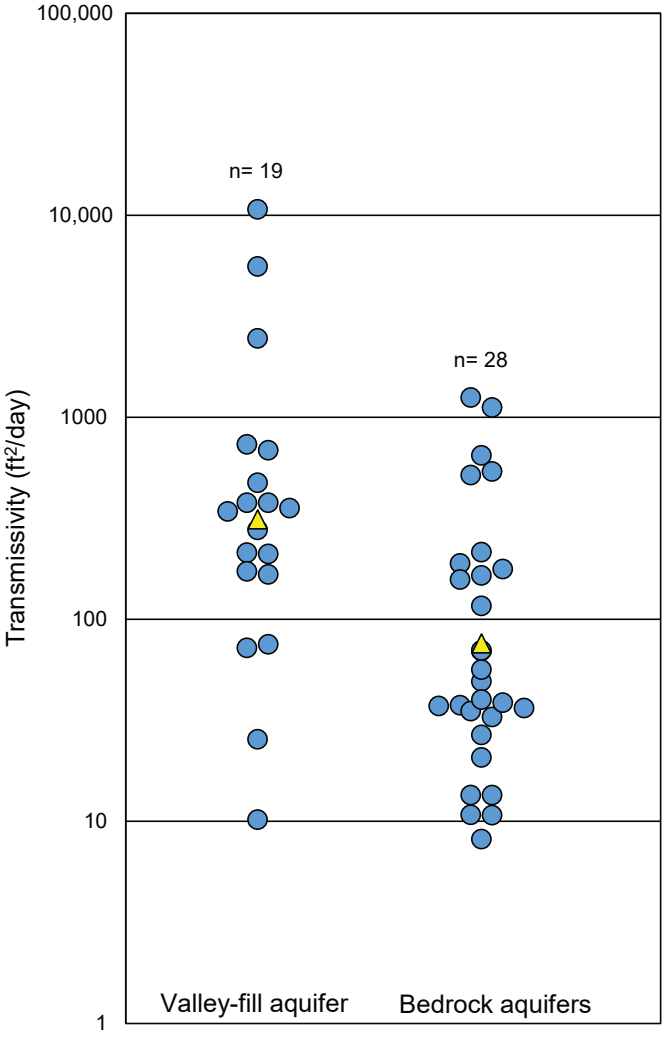

Figure 10. *Transmissivity values for study area aquifers. Geometric mean shown as yellow triangle.*

in all measuring campaigns (Figure 12, Appendix D Figure D-1). However, water level measurements in Johns Valley are mostly from stock watering wells used less frequently relative to the commercial wells in Emery Valley, and from landfill monitoring wells that are pumped infrequently, if at all. Water levels in the Cretaceous bedrock aquifer fluctuate less than in the valley-fill aquifer. Hydraulic gradients are generally steeper in Emery Valley than in Johns Valley, although data are sparse in most of Johns Valley.

The potentiometric surface for the spring 2021 season (Figure 12A) shows conditions that reflect the poor snowpack of that year but shows the highest water-level measurements for most wells of the 2021 to 2022 measurement period, due to another below-median snowpack in 2022. Although the shape of groundwater contours on Figures 12A–C suggest possible groundwater discharge in Emery and southern Johns Valley to the East Fork Sevier River, the contours are poorly constrained near the stream and groundwater levels in wells nearest to the stream are as much as 50 feet (15 m) deep. Where the streambed is permeable, streamflow may infiltrate to recharge the local valley fill, but the regional groundwater table is too deep to likely provide discharge to the stream. However, in northern Johns Valley, the potentiometric surface essentially intersects the land surface, coinciding with an extensive wetland (~100 acres) and conspicuous spring system. The spring 2022 potentiometric surface is projected approximately onto the cross sections on Figure 6.

Depth to water in valley-fill aquifer wells generally ranges from 1 to 175 feet (0.3–53 m) below ground surface (bgs). In the shallow drainages upgradient from Emery Valley, depth to water in valley-fill aquifer wells is generally between 1 and 15 feet (0.3–4.6 m) bgs. Along the Highway 12 corridor within Emery Valley, depth to water in the valley fill is typically 20 to 70 feet (6–21 m) bgs. In northern Johns Valley, depth to water in wells near the valley margin generally ranges from 6 to 27 feet (2–8 m) bgs, whereas in the center of the valley depth to water is typically 75 to 160 feet (23–49 m) bgs. Depth to water in the Cretaceous bedrock aquifer wells ranges from 24 to 247 feet (7–75 m) bgs.

Water-Level Trends

We measured the generally lowest and highest water levels during our study in valley-fill wells in autumn 2018 and spring 2020, respectively. Figure 13 shows water-level changes for autumn 2019 to spring 2020, spring 2020 to autumn 2020, autumn 2020 to spring 2021, spring 2021 to autumn 2021, and autumn 2021 to spring 2022. Except for the water-level-change map for autumn 2020 to spring 2021 (Figure 13C), which shows some water-level rises in wells north and south of Highway 12, the remaining maps show that most wells have water-level declines independent of season or year. This decline is likely due to the below-average snowpack recorded during winter 2020, 2021, and 2022 (Appendix D Figure D-1). Water levels in wells completed in bedrock generally were less variable than valley-fill wells, with some water levels declining and others rising during different seasons and years, independent of weather and snowpack.

The 2023 water year was a banner year in terms of record-breaking precipitation throughout the state of Utah, including the study area. Although this report focuses on data collected from 2018 through 2022, we took water-level measurements from five wells situated near the densest development in Emery Valley on May 17, 2023; three measurements were in bedrock wells and two in valley-fill wells. Water levels, as expected, rose in the valley-fill wells, and either dropped or maintained similar levels in bedrock wells (Figure 14, Table 1).

Water levels have been monitored long-term in only two wells: one in Emery Valley and one in Johns Valley. We analyzed long-term trends in water levels using data from these two wells. To consistently interpret the year-to-year changes in water table depth, we used only measurements from March and April for analysis due to availability of data.

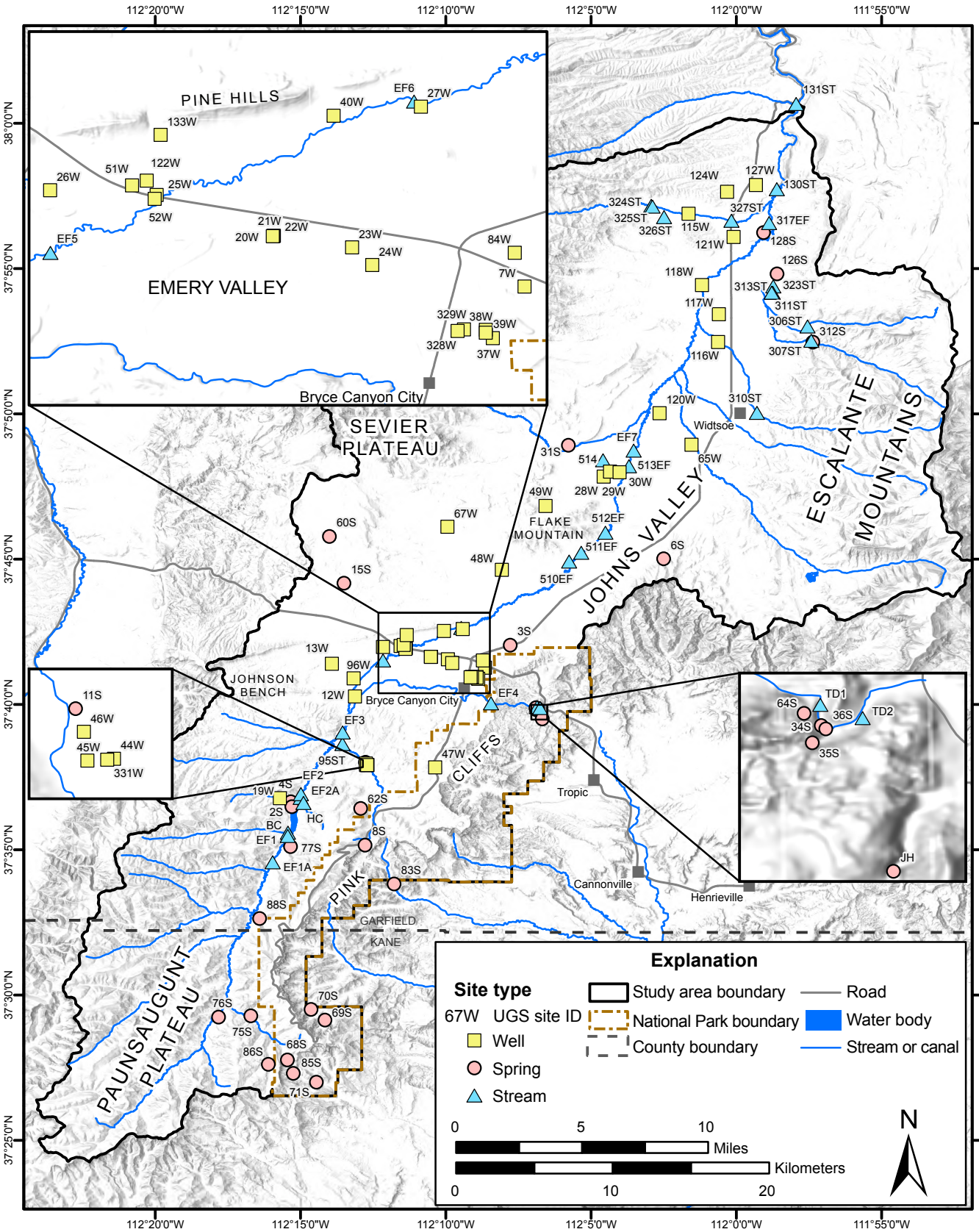

Figure 11. *Well, spring, and stream water-level and discharge measurement locations.*

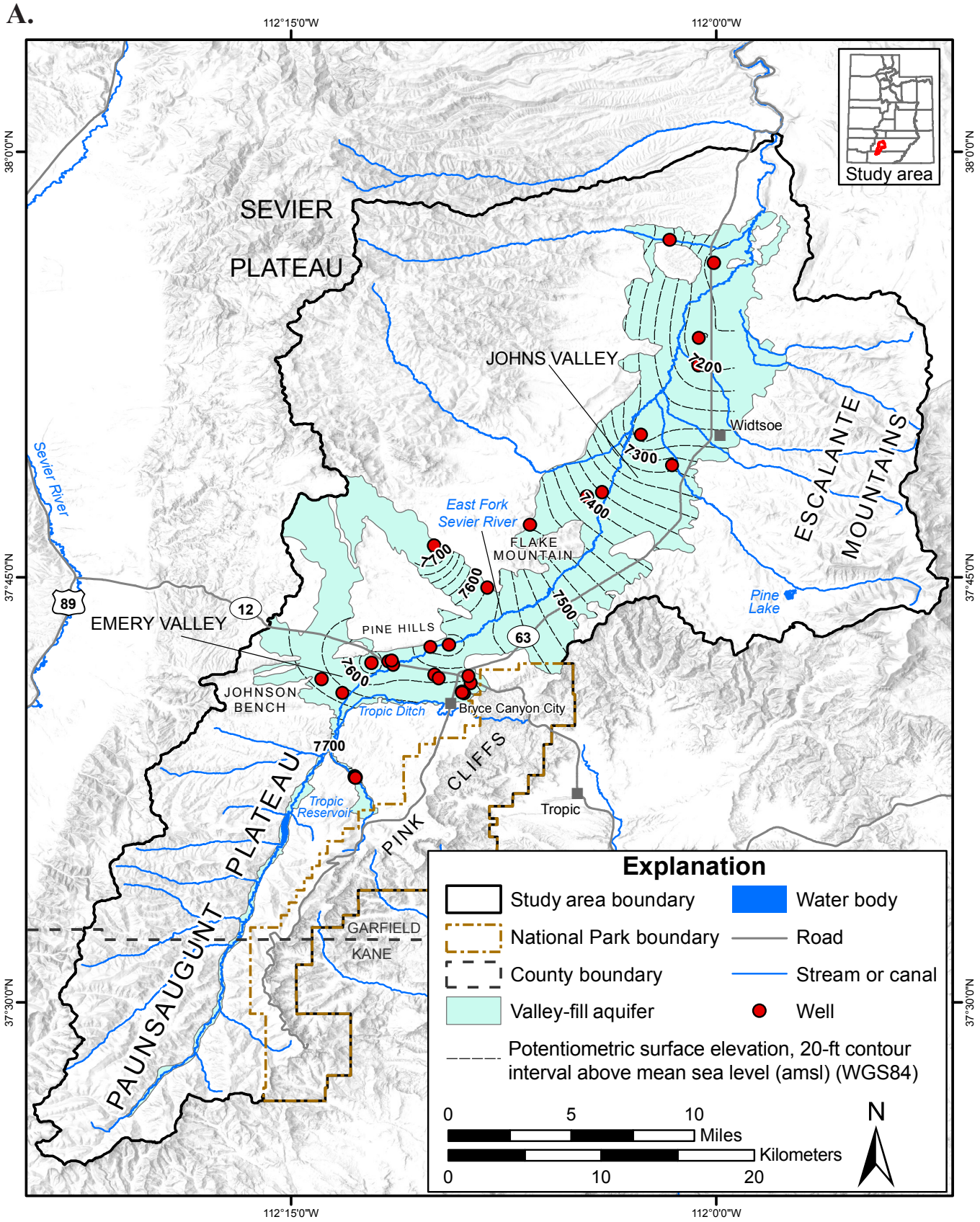

Figure 12. *Potentiometric surface maps of water levels from wells. Overall direction of groundwater flow is north-northeast.* ***A)*** *Spring 2021 water levels.*

B.

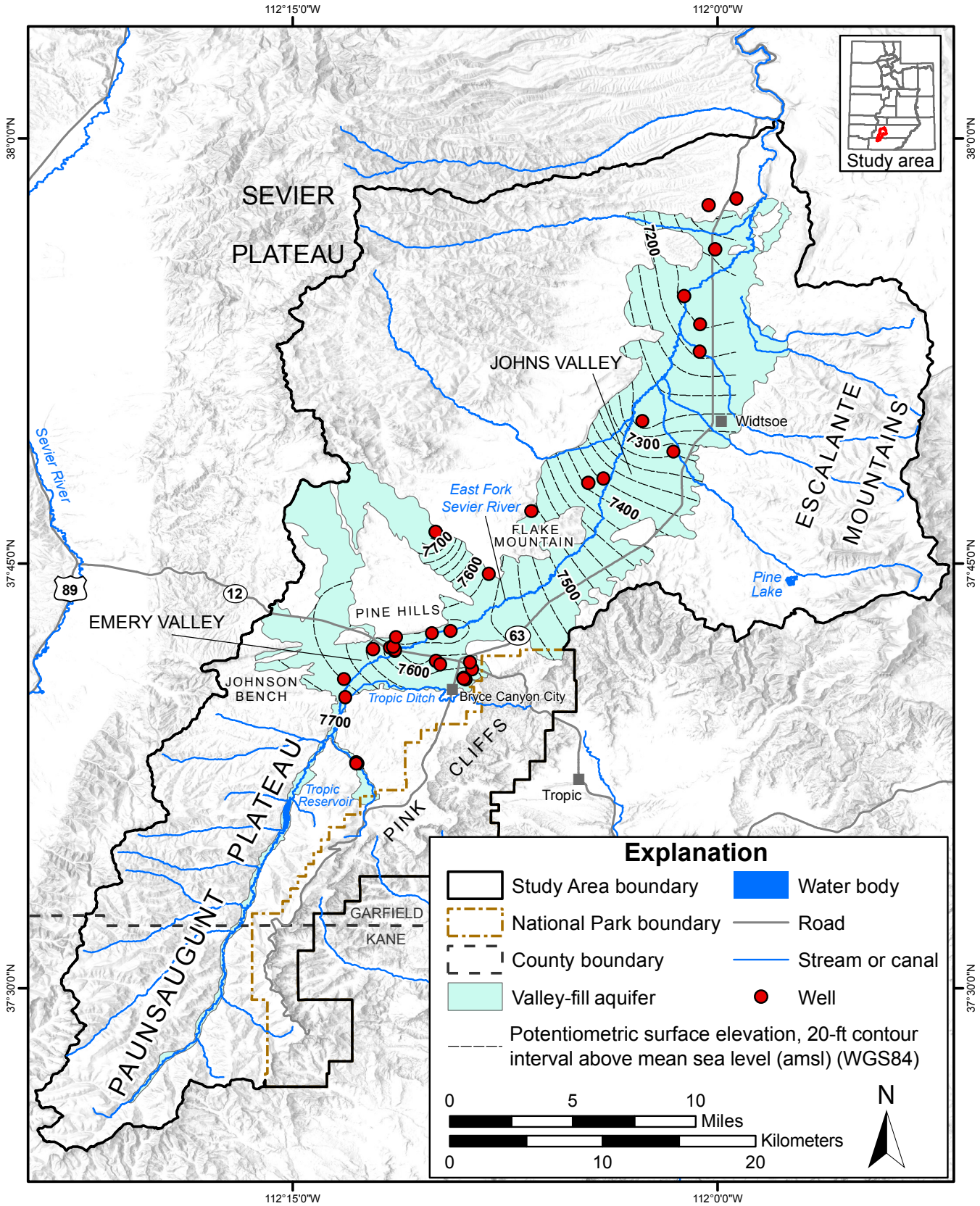

Figure 12. Continued. *Potentiometric surface maps of water levels from wells. Overall direction of groundwater flow is north-northeast.* ***B)*** *Autumn 2021 water levels.*

C.

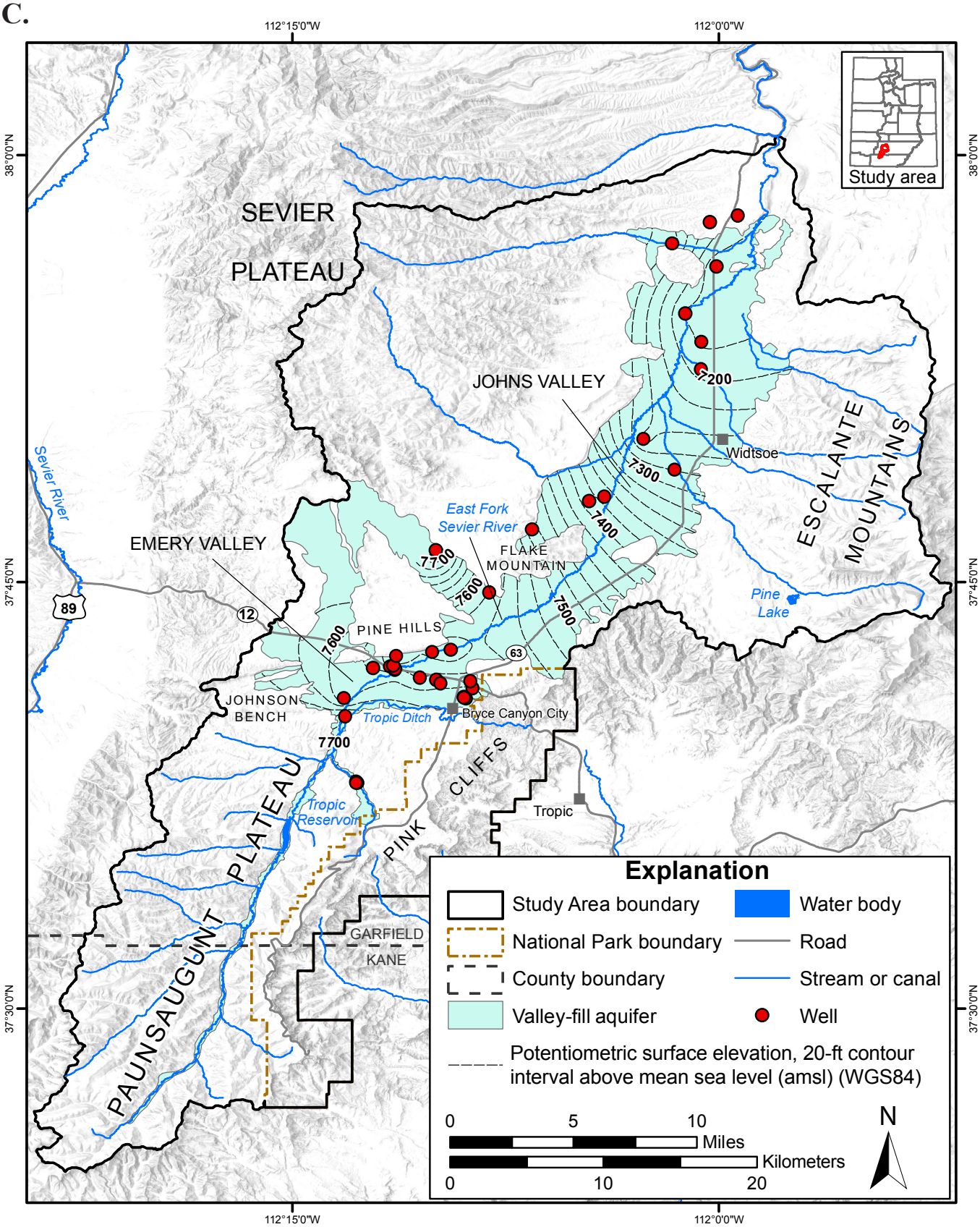

Figure 12. Continued. *Potentiometric surface maps of water levels from wells. Overall direction of groundwater flow is north-northeast.* ***C)*** *Spring 2022 water levels.*

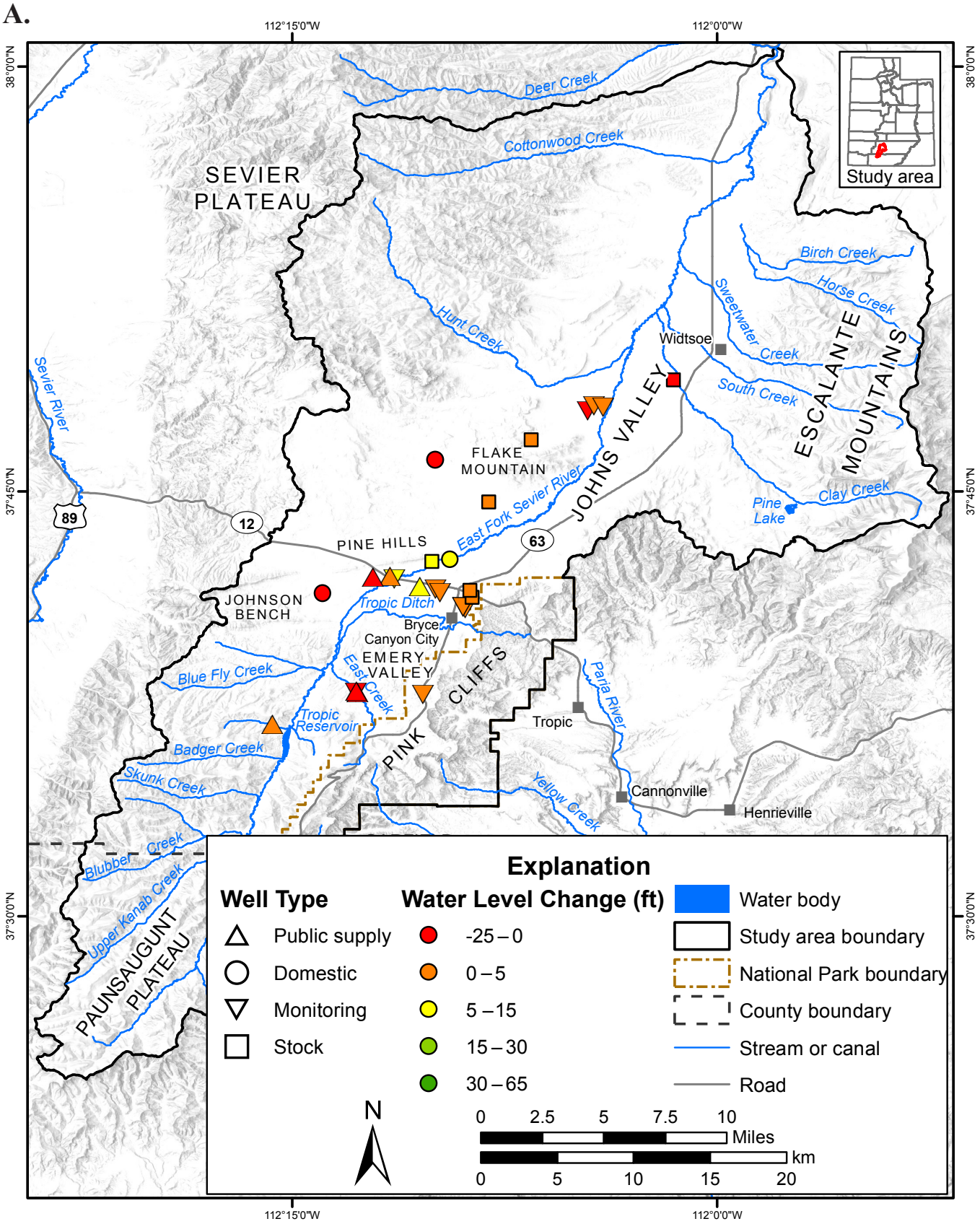

Figure 13. *Change in water-level elevation in wells.* ***A)*** *Autumn 2019 to spring 2020.*

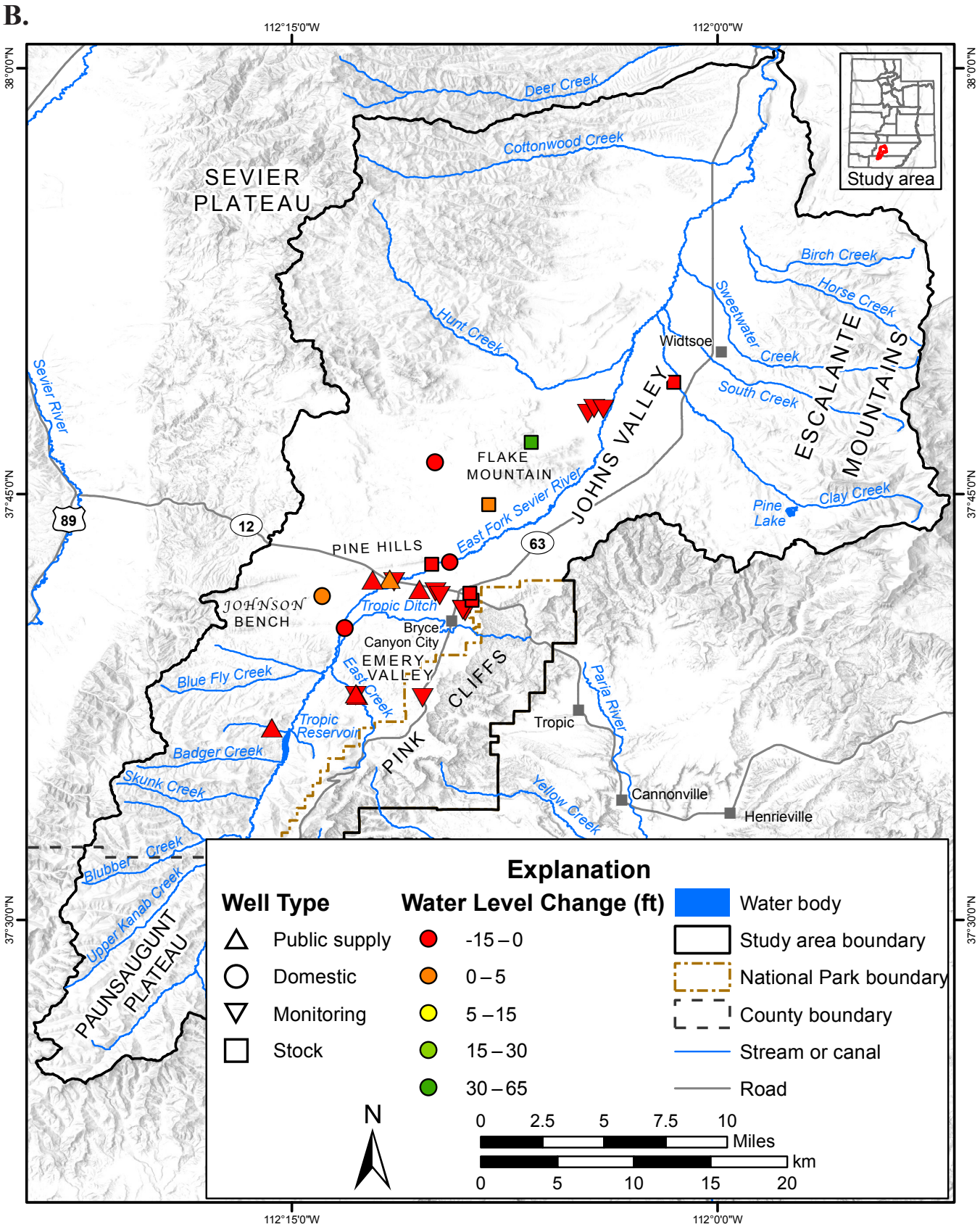

Figure 13. Continued. *Change in water-level elevation in wells.* ***B)*** *Spring 2020 to autumn 2020.*

C.

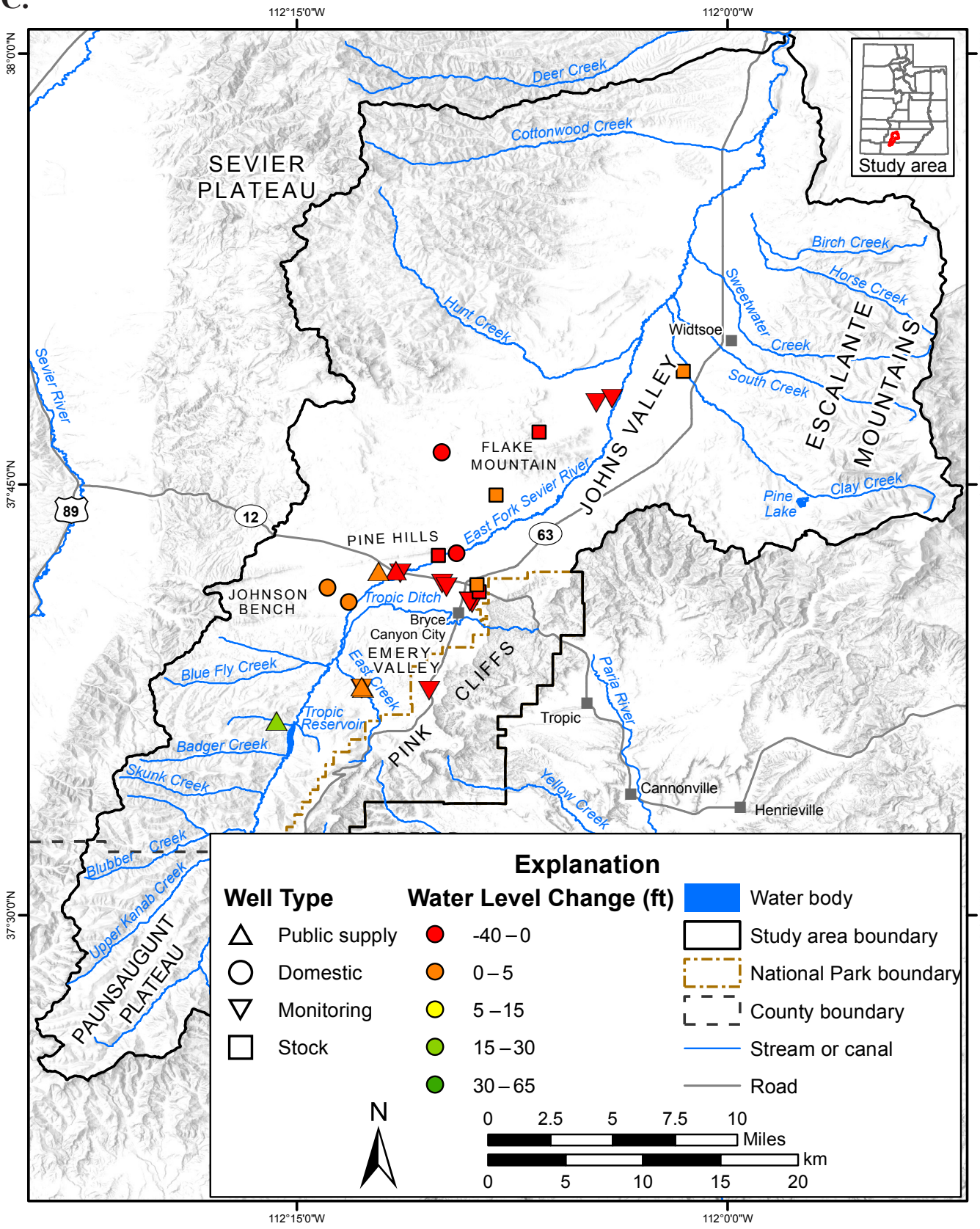

Figure 13. Continued. *Change in water-level elevation in wells.* ***C)*** *Autumn 2020 to spring 2021.*

D.

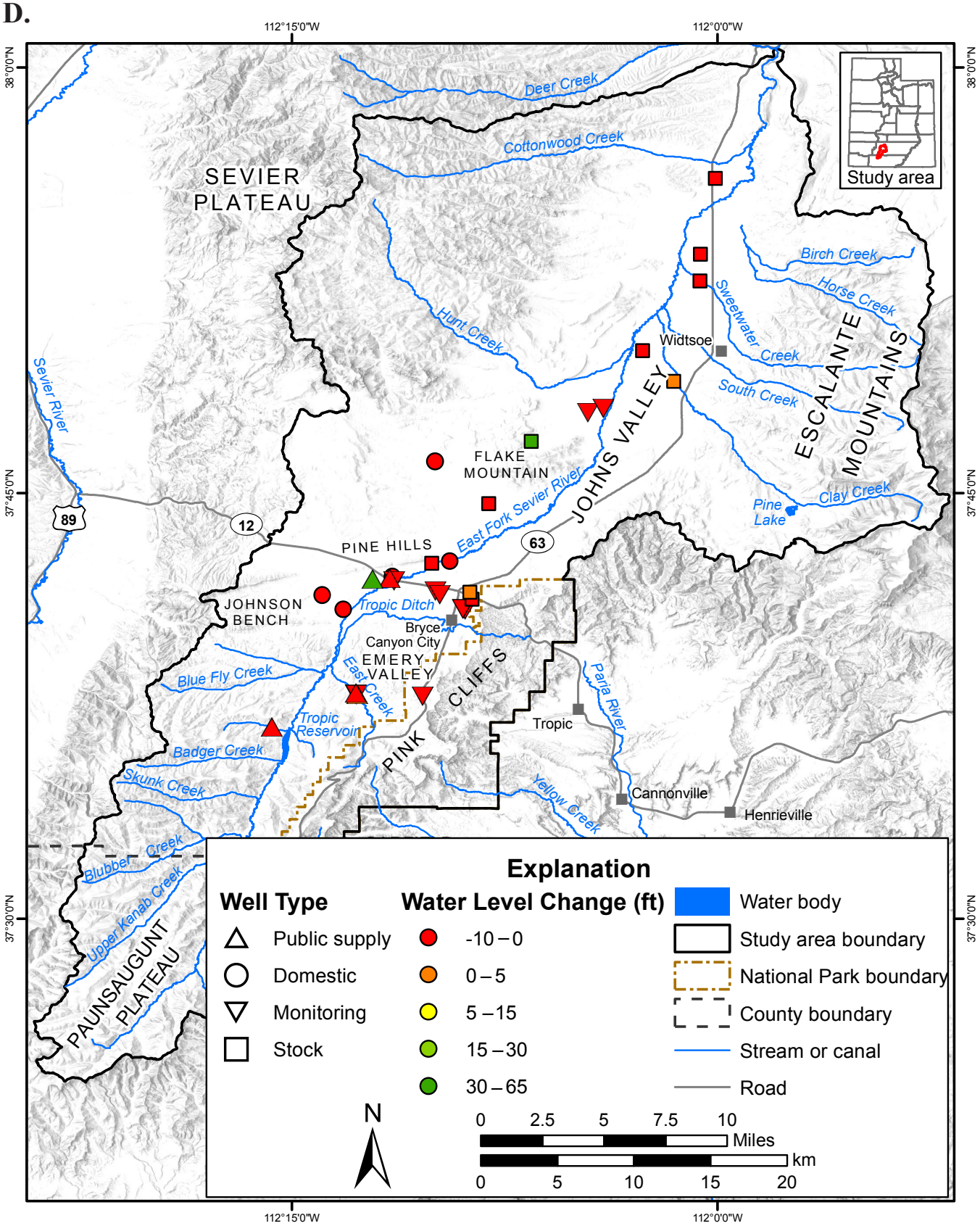

Figure 13. Continued. *Change in water-level elevation in wells.* ***D)*** *Spring 2021 to autumn 2021.*

E.

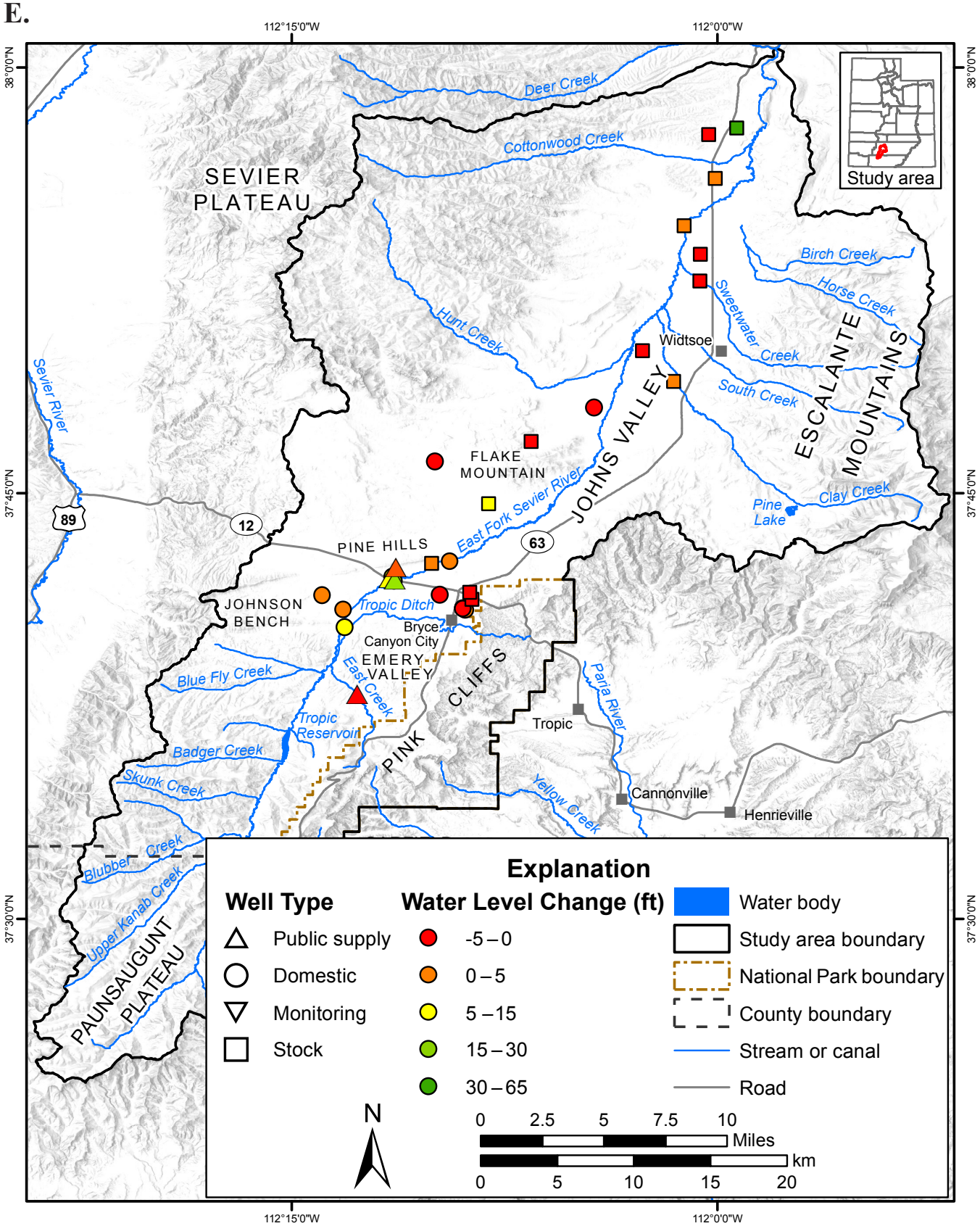

Figure 13. Continued. *Change in water-level elevation in wells.* ***E)*** *Autumn 2021 to spring 2022.*

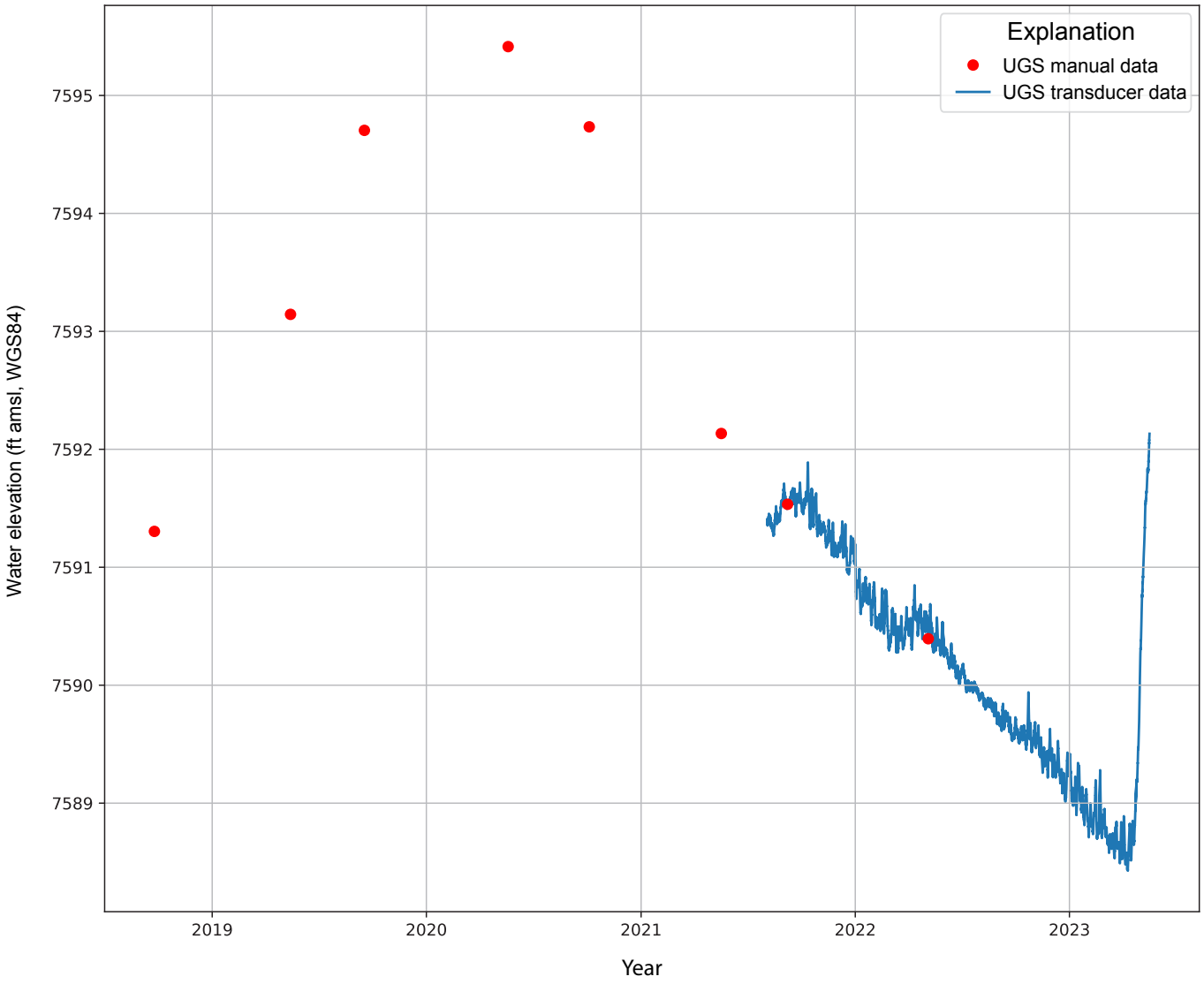

Figure 14. *Water-level data for monitoring well BC23.*

Table 1. *Water-level data during spring 2022 and spring 2023 for a subset of valley-fill aquifer (VFA) and bedrock wells. Water levels rose during 2023 due to high winter precipitation in VFA monitoring wells and not in bedrock wells.*

Well ID[1]	Date	Water level (ft bgs)[2]	Date	Water level (ft bgs)	Aquifer
BC23	5/5/22	28.33	5/17/23	26.51	VFA
BC24	5/5/22	19.53	5/17/25	16.15	VFA
BC13	5/9/22	187.51	5/17/23	186.1	bedrock
BC96	5/9/22	46.85	5/17/23	48	bedrock
BC122	5/5/22	25.57	5/17/23	25.56	bedrock

[1] See Appendix D Tables D-1 and D-2 for site information and older water-level data.
[2] bgs = below ground surface

Well USGS ID 374205112091501 (Bryce Airport well) is located in Emery Valley at the Bryce Canyon Airport and is completed through valley fill and the John Henry Member of the Straight Cliffs Formation. Although water levels have been measured at this well since 1947, it was used as a water-supply well until 1990 when it was replaced. Therefore, we only used data from 1990 to the present for analysis. Well USGS ID 374845112031001 (a.k.a. the Johns Valley well) is located in southern Johns Valley, northeast of the Garfield County landfill, and is completed in the valley-fill aquifer. The overall trend of the Bryce Airport well since 1990 is +0.03 feet (+0.009 m) per year, with depth to water hovering at ~30 feet (9 m) (Figure 15). Despite a few multi-year variations exceeding 10 feet (3 m), the overall trend appears stable. The overall trend of the Johns Valley well since 1963 is +0.2 feet (+0.06 m) per year (Figure 15). Yearly and multi-year variations in this well occasionally exceed 30 feet (9 m), but on average, water levels in this well have been slowly increasing, including over the past three decades. Based on the stability present in these water-level records, we conclude that long-term change in storage in the valley-fill aquifer is negligible.

Discharge Measurements

We measured discharge (flow) at 32 unique stream locations and 29 unique spring locations from 2018 to 2022 (Figure 11). We measured discharge to (1) determine groundwater–surface-water interaction and quantify the amount of water gained or lost from streamflow, and (2) quantify the amount of groundwater discharge from springs when feasible. We used a Hach FH950 electromagnetic current velocity meter or a Marsh-McBirney electromagnetic current velocity meter and the 0.6 depth method to measure velocity across a stream transect and compute the cross-sectional area. At springs and smaller channels and culverts with lower flow, we measured discharge using a portable v-notch weir, the neutral buoyant object method, or a graduated measuring device (e.g., a 5-gallon bucket, 1-gallon bucket, or a pint-size bucket) and a stopwatch. Discharge measurement site information is given in Appendix D Tables D-1, D-3, and D-4.

We observed streamflow on the East Fork Sevier River ranging from 0.17 to 43.79 cubic feet per second (cfs) (0.005–1.24 m^3/s) during our study. The East Fork Sevier River had the highest flows in spring 2019. Spring flow measurements ranged from 0.001 cfs (0.00003 m^3/s) at many smaller springs to 2.13 cfs (0.06 m^3/s) for BC128 (Figure 16) located in northern Johns Valley. Tropic Ditch discharge ranged from a low of 0.52 cfs (0.015 m^3/s) during autumn 2021 to a high of 19.1 cfs (0.54 m^3/s) during spring 2019. Stream and spring discharge measurements are detailed in Appendix D Tables D-3 and D-4.

We used our periodic discharge measurements at repeat locations to create stage-discharge relationships to quantify streamflow as part of the water budget. The methodology and results of that technique are discussed in the Streamflow subsection of the Water Budget Development section below. Time-specific discharge measurements are the basis of our seepage runs.

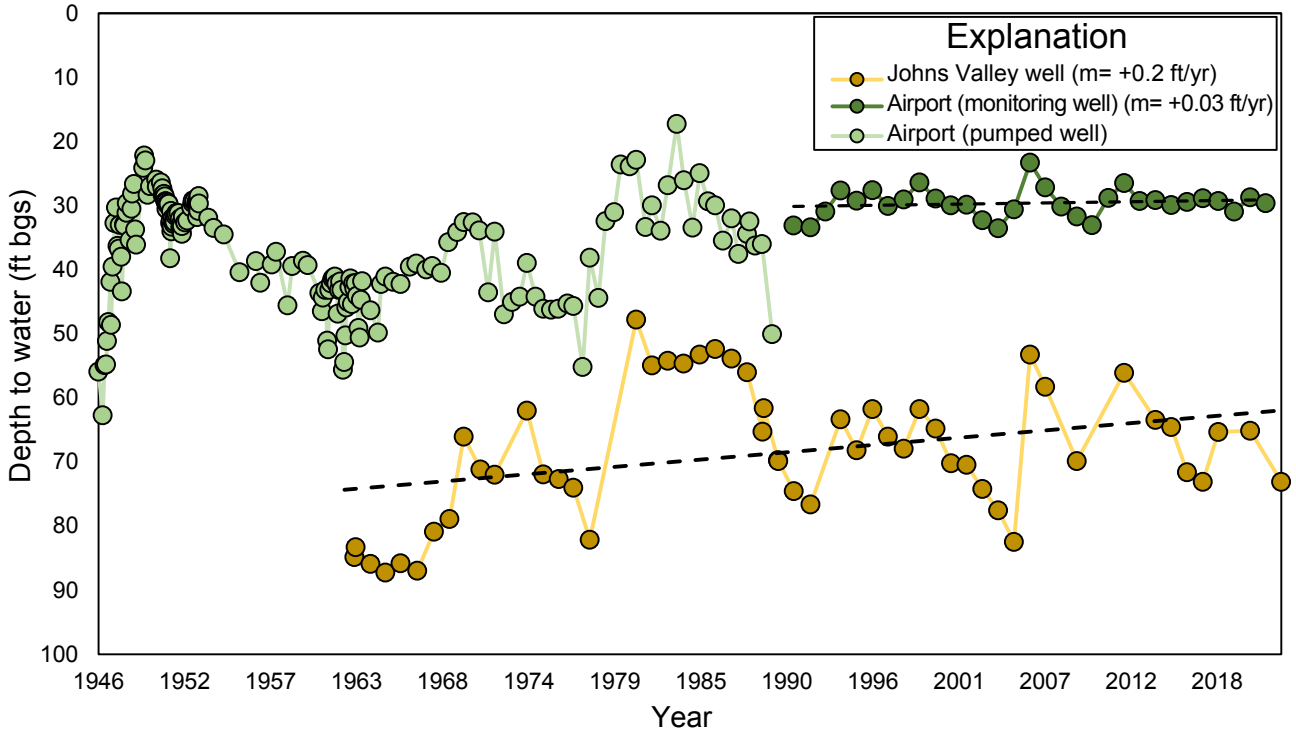

Figure 15. *Long-term monitoring records of groundwater levels (depth below ground surface [bgs]) measured at Johns Valley well (USGS ID 374845112031001) and airport well (USGS ID 374205112091501). The airport well record reflects active pumping until replacement in 1991, at which point it became a monitoring well.*

A.

B.

Figure 16. A) *Unnamed spring BC128S issues from alluvium near Osiris Tuff outcrop; flow discharge averaged 1.95 cfs from 2021 to 2022.* ***B)*** *View northeast of a ditch fed by unnamed spring BC128S flowing north and feeding the adjacent ~100-acre wetland in northern Johns Valley.*

Stream Seepage Studies

Gaining an understanding of the extent of groundwater–surface-water interaction in Johns and Emery Valleys is a key goal of this study. Streams interact with groundwater in three basic ways: streams gain water from inflow of groundwater through the streambed when the water table is higher than the streambed or the depth of water in the stream; streams lose water to groundwater by outflow through the streambed when the water table is below the bottom of the streambed; or they do both, gaining in some reaches and losing in other reaches (Winter et al., 1998). If the water table rises or falls through time, losing sections can become gaining sections and vice versa.

Methods

Seepage studies using discharge measurements, coupled with geochemistry and environmental tracer analysis, form the basis of our understanding of the degree of interaction between surface water and groundwater. Seepage runs involve measuring streamflow on multiple sections of a watercourse, ideally in as short a time span as possible.

During 2018, 2019, and 2020, we performed a total of four seepage runs on the East Fork Sevier River and Tropic Ditch along seven segments that span from a point 1.2 miles (1.9 km) above Tropic Reservoir dam to either the main Tropic Ditch diversion (4.4 miles [7 km] below Tropic Reservoir dam) or to the northern extent of the study area (~4 miles [6.4 km] northeast of Flake Mountain) (Appendix E Figures E-1 and E-2). The East Fork Sevier River flows from its headwaters at the south end of the Paunsaugunt Plateau over thin stream alluvium overlying the Wahweap Formation to about 0.5 miles (0.8 km) south of Tropic Reservoir dam, where the underlying bedrock is the Claron Formation. Where the East Fork Sevier River enters Emery Valley, it crosses thicker valley-fill deposits. The Tropic Ditch seepage runs were performed from the main Tropic Ditch diversion to the point where the Tropic Ditch crosses Highway 12 in Bryce Canyon National Park. From just below the confluence of East Creek and East Fork Sevier River, the Tropic Ditch is piped underground in valley-fill sediments until it daylights east of Bryce Canyon City in Water Canyon above Mossy Cave Springs. It then flows across the Claron Formation within Bryce Canyon National Park. Only during the spring 2019 seepage run was a measurable amount of water flowing in the East Fork Sevier River past the Tropic Ditch diversion point. We report results from 2018 to 2020 here but focus on results from 2021 to 2022 to emphasize the entire study area.

We expanded the study area to include all of Johns Valley to the north and performed seepage runs in October 2021 and May 2022. These runs included the original seepage run sampling locations, but were expanded to the northern study area boundary in Black Canyon to include additional sites along the East Fork Sevier River and its tributaries (Figure 17). Each of these runs was performed by three teams measuring streamflow simultaneously on a given stream segment. We took additional flow measurements in October 2022 at three reaches of the East Fork Sevier River before its confluence with Deer Creek in Black Canyon.

Prior to seepage runs, we inventoried all diversions (canals, ditches) or tributaries (natural or irrigation return ditches) to or from the stream segments using high-resolution aerial imagery, ground survey, and interviews with irrigation users before the seepage runs. Autumn runs were conducted during base flow conditions and spring runs during the late part of spring runoff.

We calculated gains and losses for discrete reaches of the East Fork Sevier River and Tropic Ditch as the difference between the flow measured at each location and the flow measured at the location immediately upstream of that location, plus any tributary flow and minus any diversions:

$$\textit{Gain or loss} = \textit{downstream flow} - (\textit{upstream flow} + \textit{tributary} - \textit{diversion}) \quad (1)$$

Negative values indicate the stream channel lost flow between the upstream and downstream locations and positive values indicate the stream gained water from its banks between the locations. Error in the gain/loss calculation is the sum of the error values of all measurements in that calculation and is likely an overestimate of the error associated with each calculation.

Seepage Study Results

Flow in October 2018 ranged from 0 cfs in the central reaches to 9.1 cfs (0.26 m^3/s) above Tropic Reservoir (Appendix E Figures E-1 and E-2). The East Fork Sevier River was losing from above the reservoir to the Tropic Ditch diversion (reaches 1 and 2) and was dry from the ditch diversion to Tom Best Road (reaches 3–5). Tropic Ditch gained, within error, from the ditch diversion to the top of Water Canyon (reach 6). Flow in Tropic Ditch at the top of Water Canyon was 7.9 cfs (0.22 m^3/s) (Table 2; Appendix D Table D-3).

In June 2019, after a winter with above-average precipitation, the East Fork Sevier River was gaining from above the reservoir to Tropic Ditch (reaches 1 and 2) and was losing from there to Tom Best Road (Appendix E Figures E-1 and E-2). Flows ranged from 6.3 cfs (0.18 m^3/s) at Tom Best Road to 43.8 cfs (1.2 m^3/s) above the ditch diversion. The upper reaches had notable gains, as the thin alluvium was likely saturated during the runoff season. This seepage run was the only one during which the East Fork Sevier River flowed beyond the ditch diversion into Emery Valley. The Tropic Ditch is permitted to divert up to 20 cfs (0.57 m^3/s) from April 1 to June 1 and up to 15 cfs (0.42 m^3/s) from June 1 to October 15. Due to the above-average snowpack, up to 60% of the East Fork Sevier River's flow continued past the diversion point. As the

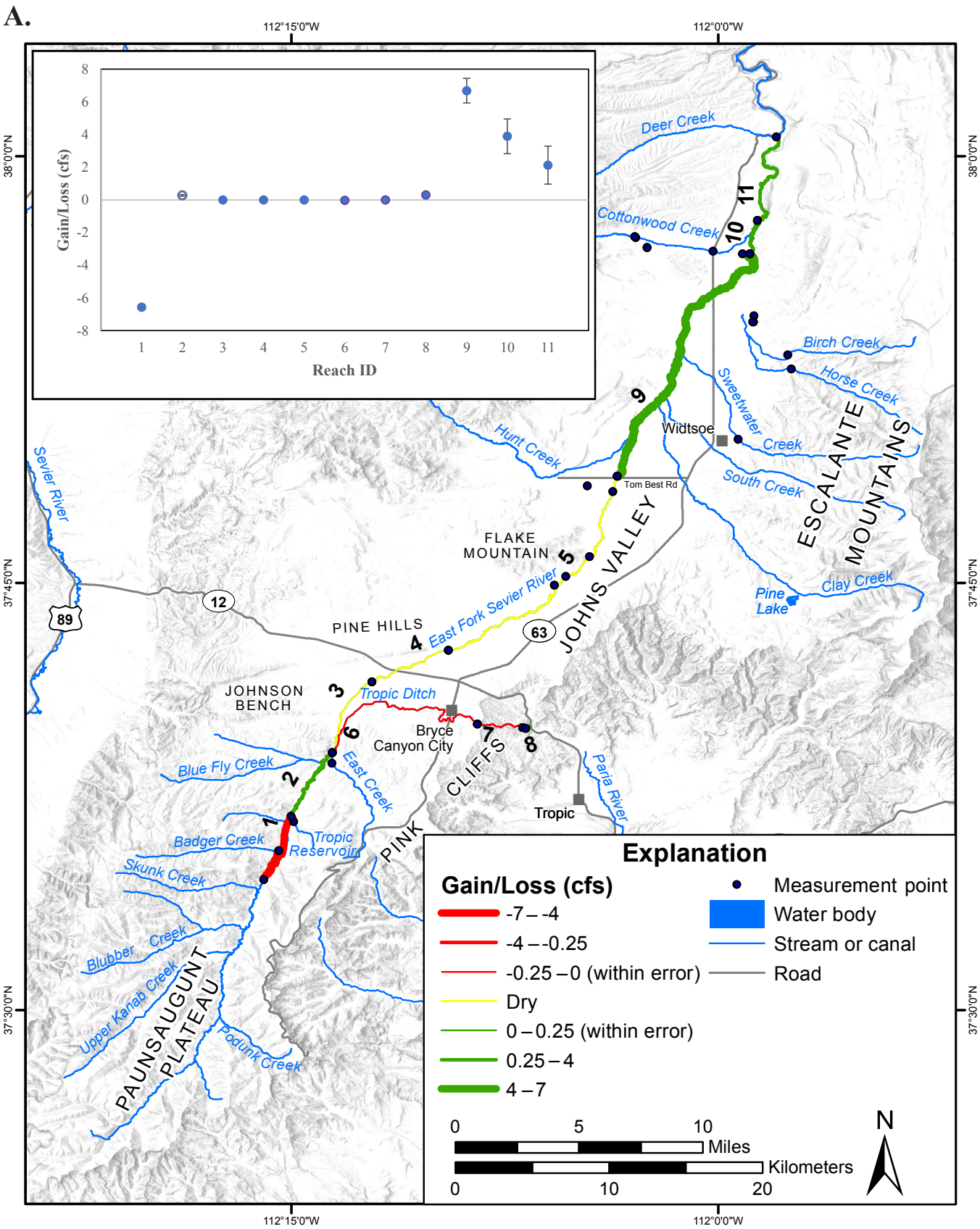

Figure 17. *Gaining and losing reaches of the East Fork Sevier River and Tropic Ditch. **A)** Fall 2021.*

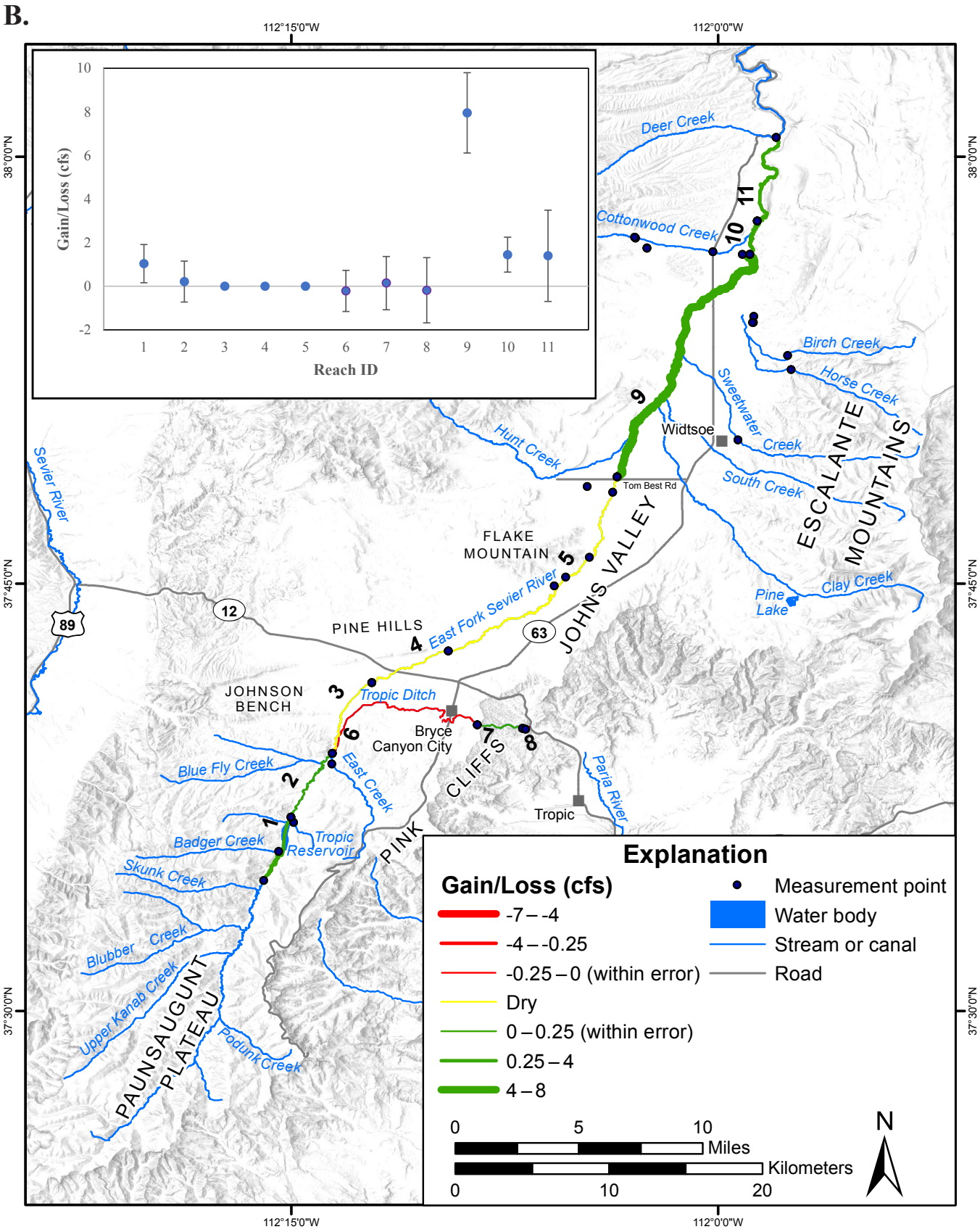

Figure 17. Continued. *Gaining and losing reaches of the East Fork Sevier River and Tropic Ditch.* ***B)*** *Spring 2022.*

Table 2. *Gains, losses, and reach status for seepage runs on the East Fork Sevier River and Tropic Ditch.*

		October 2018 Seepage Run				June 2019 Seepage Run				September 2019 Seepage Run				May 2020 Seepage Run				October 2021 Seepage Run				May 2022 Seepage Run			
Reach ID	**Reach Description**	**Gain/ loss (cfs)**	**Cumulative measurement error (cfs)**	**% of flow gained/ lost**	**Reach status**	**Gain/ loss (cfs)**	**Cumulative measurement error (cfs)**	**% of flow gained/ lost**	**Reach status**	**Gain/ loss (cfs)**	**Cumulative measurement error (cfs)**	**% of flow gained/ lost**	**Reach status**	**Gain/ loss (cfs)**	**Cumulative measurement error (cfs)**	**% of flow gained/ lost**	**Reach status**	**Gain/ loss (cfs)**	**Cumulative measurement error (cfs)**	**% of flow gained/ lost**	**Reach status**	**Gain/ loss (cfs)**	**Cumulative measurement error (cfs)**	**% of flow gained/ lost**	**Reach status**
1	East Fork above Tropic Reservoir to below Tropic Reservoir dam	-0.65	0.60	-7	losing	5.1	4.75	15	gaining	6.86	1.76	91	gaining	-0.9	1.56	-7	losing (within error)	-6.56	0.14	-98	losing	1.04	0.88	13	gaining
2	East Fork below Tropic Reservoir Dam to Tropic Ditch diversion	-1.09	1.15	-13	losing (within error)	3.4	5.54	9	gaining (within error)	1.51	2.42	10	gaining (within error)	1.43	1.61	12	gaining (within error)	0.28	0.05	168	gaining	0.22	0.94	2	gaining (within error)
3	East Fork above Tropic Ditch diversion to E Fork Rd bridge	0	0	0	dry	-1.0	4.75	-2	losing (within error)	0	0	0	dry	0	0	0	dry	0	0	0	dry	0	0	0	dry
4	East Fork at E Fork Rd bridge to airport bridge	0	0	0	dry	-3.1	2.35	-12	losing	0	0	0	dry	0	0	0	dry	0	0	0	dry	0	0	0	dry
5	East Fork at airport bridge to Tom Best Spring Rd	0	0	0	dry	-15.7	1.41	-72	losing	0	0	0	dry	0	0	0	dry	0	0	0	dry	0	0	0	dry
6	East Fork Tropic Ditch diversion to Tropic Ditch above Bryce Canyon rim	0.56	1.12	8	gaining (within error)	-1.0	4.34	-2	losing (within error)	0.57	2.59	4	gaining (within error)	-0.22	2.05	-2	losing (within error)	-0.04	0.06	-6	losing (within error)	-0.21	0.94	-2	losing (within error)
7	Tropic Ditch above Bryce Canyon rim to below Tropic Ditch falls	-	-	-	-	-1.3	1.61	-7	losing (within error)	0.35	2.66	2	gaining (within error)	2.82	2.26	22	gaining	-0.02	0.06	-3	losing (within error)	0.15	1.22	2	gaining (within error)
8	Tropic Ditch below falls to below Mossy Cave outflow	-	-	-	-	3.5	1.73	23	gaining	-0.44	2.66	-3	gaining (within error)	-1.37	2.65	-9	losing (within error)	0.30	0.07	58	gaining	-0.18	1.50	-2	losing (within error)
9	Tom Best Spring Rd to East Fork Near Osiris and Gleaves spring	-	-	-	-	-	-	-	-	-	-	-	-	-	-	-	-	6.68	0.75	-	gaining	7.95	1.84	-	gaining
10	East Fork Near Osiris and Gleaves Spring to East Fork at Flying V Ranch	-	-	-	-	-	-	-	-	-	-	-	-	-	-	-	-	3.89	1.06	58	gaining	1.45	0.80	18	gaining
11	East Fork at Flying V Ranch to East Fork above Deer Creek con-fluence	-	-	-	-	-	-	-	-	-	-	-	-	-	-	-	-	2.12	1.16	20	gaining	1.40	1.29	15	gaining

river flowed over deep permeable valley-fill deposits, approximately 75% of the flow was lost to groundwater by the time it reached the farthest downstream measurement point, 30 stream miles (48 km) away. The Tropic Ditch was losing, within error, from the diversion to Water Canyon Falls (reach 6) and gaining from there to below the Mossy Cave outflow (reaches 7 and 8). Flow in the Tropic Ditch ranged from 15.5 to 16.8 cfs (0.44–0.48 m^3/s) (Table 2; Appendix D Table D-3).

In September 2019, the area above the ditch diversion (reaches 1 and 2) was still gaining, but less than in the spring. The East Fork Sevier River below the ditch diversion was dry (reaches 3–5). Flows ranged from 0 to 15.9 cfs (0–0.45 m^3/s) in the East Fork Sevier River, with the highest flow measured above the ditch diversion (BCEF3). The Tropic Ditch was gaining, within error, from the ditch diversion to below the Mossy Cave outflow (reaches 6–8). Flow in the ditch ranged from 16.4 to 16.8 cfs (0.46–0.48 m^3/s) (Table 2; Appendix D Table D-3).

In May 2020, the East Fork was slightly losing above the reservoir (reaches 1 and 2) and slightly losing between the reservoir and the ditch diversion (reaches 3–5). The East Fork Sevier River below the ditch diversion was dry, as the diversion captured the entirety of the river flows. Flows ranged from 0 to 12.9 cfs (0–0.37 m^3/s), with the highest flow measured above the ditch diversion (BCEF3). Tropic Ditch was losing slightly from the diversion to the rim of Water Canyon (reach 6), gaining from the rim to Water Canyon Falls (reach 7), and losing slightly again from the falls to below the Mossy Cave outflow (reach 8). Both losing reaches were within error. Flow in the Tropic Ditch ranged from 12.7 to 15.5 cfs (0.36–0.44 m^3/s) (Table 2; Appendix D Table D-3).

From 2021 on, we extended the seepage runs to include all of Johns Valley up to the northern study area boundary in Black Canyon. During the October 2021 seepage run, the East Fork Sevier River was losing above Tropic Reservoir (reach 1) and gaining between Tropic Reservoir and the Tropic Ditch diversion (reach 2; Figure 17A). There was no net flow between the ditch diversion and Tom Best Road (reaches 3–5). The East Fork was gaining through all reaches north of Tom Best Road (reaches 9–11), though the stream did not start to gain until well north of Tom Best Road, in the middle of reach 9. Flows ranged from 0 to 12.7 cfs (0–0.36 m^3/s), with the highest flow recorded above the confluence with Deer Creek (end of reach 11). Tropic Ditch was losing slightly, within error, from the diversion to Water Canyon Falls (reach 6) and gaining from the falls to below the Mossy Cave outflow (reaches 7 and 8). Flow in Tropic Ditch was 0.5 to 0.8 cfs (0.01–0.2 m^3/s) when East Fork Sevier River flow was not being diverted.

In May 2022, the East Fork Sevier River was gaining above the ditch diversion (reaches 1 and 2; Figure 17B). There was no net flow in the central portion of the study area (reaches 3–5). The East Fork Sevier River was gaining again north of Tom Best Road to the Black Canyon (reaches 9–11). Once again, flow was not observed directly at Tom Best Road, but rather farther north into reach 9. Flows ranged from 0 to 10.8 cfs (0–0.31 m^3/s), with the highest flow measured above the confluence with Deer Creek. The Tropic Ditch was losing slightly from the diversion to the rim of Water Canyon (reach 6), gaining from the rim to Water Canyon Falls (reach 7), and losing slightly again from the falls to below the Mossy Cave outflow (reach 8), all within error (Table 2). Flow in Tropic Ditch ranged from 9.3 to 9.5 cfs (0.26–0.27 m^3/s) (Appendix D Table D-3).

In October 2022 in only the northern part of Johns Valley, flow on the East Fork Sevier River ranged from 0 to 9.6 cfs (0–0.27 m^3/s) at the East Fork Sevier River crossing at Johns Highway Road and the East Fork Sevier River before the confluence with Deer Creek, respectively (Appendix D Table D-3). East Fork Sevier River flow near an unnamed spring (Figure 16, BC128S) was 4.7 cfs (0.13 m^3/s) and increased markedly downstream (7.5 cfs [0.21 m^3/s]) as measured at the bridge near Flying V ranch (BC131EF) (Appendix D Table D-3). An extensive perennial wetland area (~100 acres) exists between the unnamed spring (Figure 16, BC128S) and the East Fork Sevier River. The source of this water is likely valley-fill aquifer groundwater based on our potentiometric surface maps and groundwater chemistry.

CHEMISTRY OF GROUNDWATER AND SURFACE WATER

The type of geologic materials in a drainage basin and the length of time groundwater is in contact with those materials are fundamental controls on water chemistry (Winter et al., 1998). Groundwater and surface water chemistry can indicate the quality of available water, as well as help us understand the conceptual groundwater system. The water chemistry from wells, springs, and streams in different locations and at different well depths, when viewed with other physical data, can help us infer flow paths of groundwater and interactions with surface water.

We sampled 62 sites from 2018 to 2022, focusing on characterizing the major solute chemistry of water from 32 wells, 29 springs (15 springs have only field parameters and total dissolved solids [TDS] derived from converted specific conductance data), and 3 surface water sites (Figure 18). We also analyzed water quality for a subset of 27 wells and 16 springs, including nutrients (nitrate plus nitrite, ammonia, phosphate) and iron. All samples were analyzed by the Utah Department of Health, Chemical and Environmental Services Division of the Utah Public Health Laboratory (Appendix D Tables D-1 and D-5).

Methods

We collected water samples using standard field sampling practices (Utah Division of Water Quality, 2014). At each

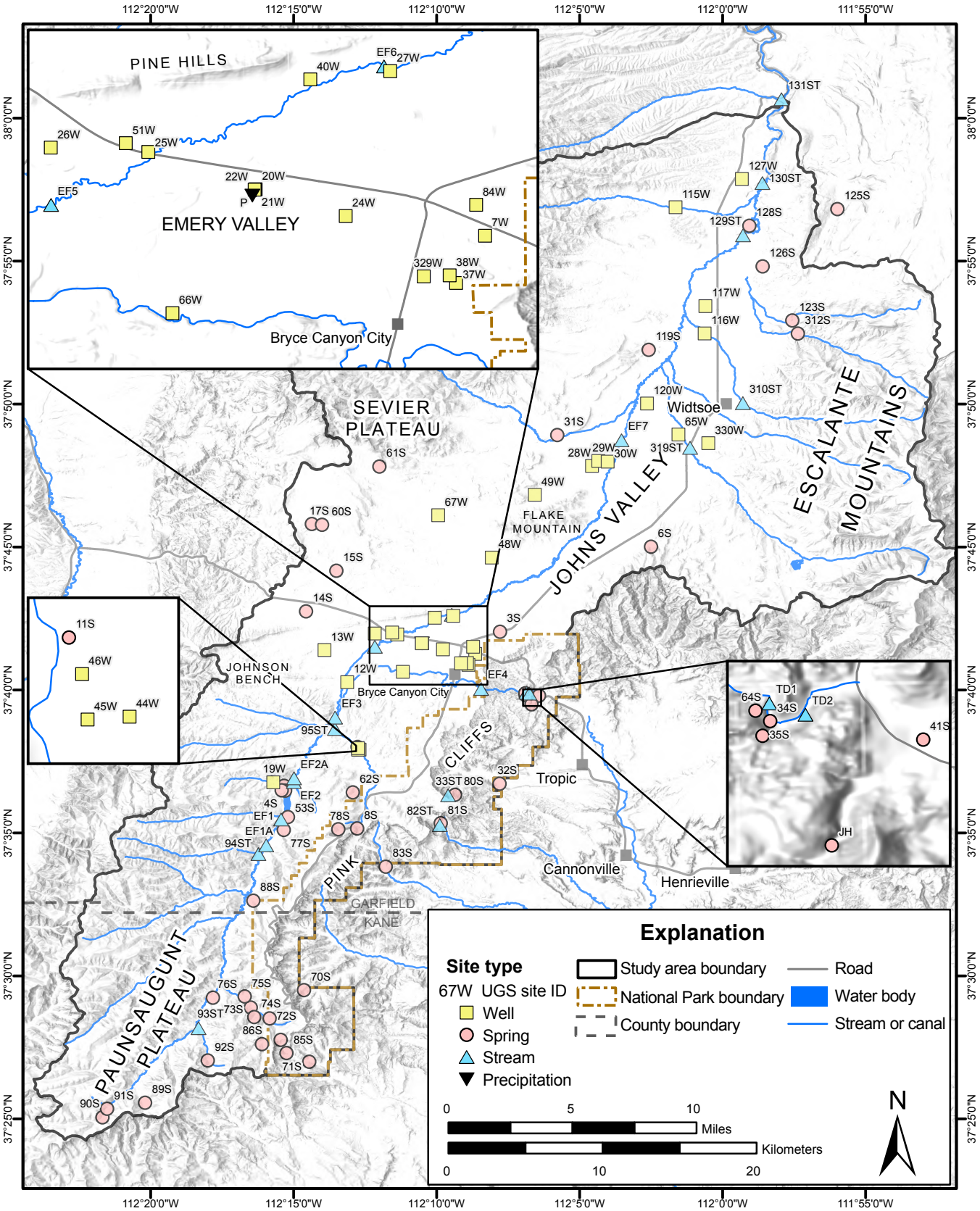

Figure 18. *Well, spring, stream, and precipitation sample locations.*

location, we measured field chemistry parameters: pH, specific conductance, and temperature. Most wells had been in use on the day of sampling and the well was run at least 15 minutes to allow stabilization of field parameters within 0.1 pH units, 0.1°C, and 5 microSiemens per centimeter (µs/cm) specific conductance. Dissolved metals samples were field filtered within 15 minutes of collection time. Samples were collected in lab-provided bottles and stored on ice until proper laboratory delivery.

Chemistry of Groundwater and Surface Water

Total Dissolved Solids and Major Solutes

Water quality based on TDS is generally excellent throughout the study area (Figure 19). Measured TDS concentrations range from 178 to 716 mg/L (Appendix D Table D-1); the average TDS concentration in the study area is 295 mg/L. The average TDS concentration in the valley-fill aquifer is 276 mg/L (n = 28), whereas the average TDS concentration in bedrock aquifers is 311 mg/L (n = 33). TDS concentrations for groundwater samples from all but four sites are below 500 mg/L. TDS concentration in surface water averaged 289 mg/L from three sites.

Major solute composition in the study area is predominantly calcium-magnesium-bicarbonate type, as shown in a Piper diagram illustrated using a color scheme after Peeters (2014) (Figure 20). Calcium and magnesium are the dominant cations, apart from one sample having significant sodium from a likely fault-controlled spring flowing from the Cretaceous Grand Castle Formation on the northeastern margin of Johns Valley. Bicarbonate is the dominant anion, apart from one sample with significant chloride from a well screened in Cretaceous bedrock at the east end of Emery Valley. The somewhat uniform composition and lack of major spatial variation of major solutes reflects the dominant rocks and corresponding mineralogic composition of valley-fill sediments derived from them.

Lower quality water, in terms of elevated TDS, mostly occurs within the Cretaceous sandstone aquifer. The higher quality water in the valley-fill material is likely due to recharge directly from precipitation in the higher elevations and from surface infiltration. The lower quality water in the bedrock aquifers may be from longer residence times of groundwater reaching the bedrock aquifer.

Nutrients and Iron

Nitrate plus nitrite concentrations range from <0.1 to 1.47 mg/L (Figure 21). All sampled sites had ammonia concentrations of <0.05 mg/L, except for one well that measured 0.164 mg/L. The background nitrate concentration is 0.35 mg/L and geometric mean nitrate concentration in the principal valley-fill aquifer is 0.23 mg/L. Total phosphate ranges from <0.003 to 0.159 mg/L. Iron concentrations were analyzed in 13 wells and had a range of <30 micrograms per liter (µg/L) to 192 µg/L, with the majority below detection levels. We discuss water quality in greater detail in the Septic-Tank Density section below.

Groundwater Quality Classification

We submitted a petition on behalf of Garfield County to the Utah Department of Environmental Quality (DEQ) Water Quality Board to formally classify the principal valley-fill aquifer in Johns and Emery Valleys as Class IA—Pristine groundwater (Wallace and Schlossnagle, 2021). Class IA groundwater is defined by the Water Quality Board as having TDS concentrations less than 500 mg/L (Utah Division of Water Quality, 1998). The classification is based on groundwater quality data supporting the proposed classification, for which we used TDS data from 32 wells and 22 springs (Appendix D Table D-1). Where insufficient data exist, we extrapolated groundwater quality conditions based on local geologic characteristics. The Johns and Emery Valleys valley-fill aquifer was formally classified by the DEQ Water Quality Board in January 2021.

To facilitate groundwater-quality classification, we used data collected from 28 wells and 21 springs during autumn 2018, spring 2019, and autumn 2019. Data utilized included specific conductance from 27 wells and 20 springs, general chemistry from 26 wells and 16 springs, and nutrients from 27 wells and 16 springs (Appendix D; Appendix F Plate F-1). We augmented our data with dissolved metals and pesticides values from 14 sites recorded in the USGS National Water Information System (NWIS) and Utah Department of Agriculture and Food (UDAF) databases. Select solutes reported in these databases include aluminum, arsenic, boron, barium, bromide, copper, lead, selenium, iron, manganese, fluoride, zinc, lithium, silicon, and uranium.

Specific conductance for the 47 wells and springs measured ranges from 297 to 884 µS/cm. We computed TDS concentrations from specific conductance measurements using a conversion factor of 0.61. This conversion factor was calculated by comparing TDS and specific conductance data collected in this study (Appendix F Figure F-1). Using this conversion factor, we calculated TDS values for one well and five springs sampled for this study. The converted TDS values range from 307 to 364 mg/L; all but one of these samples are below 500 mg/L and classified as Pristine water quality as defined by the Utah Water Quality Board.

In addition to groundwater quality data, we also documented potential contaminant sources in Johns and Emery Valleys (Appendix F Plate F-2 and Table F-1). We mapped potential groundwater contaminant sources including facilities related to mining, manufacturing, agricultural practices,

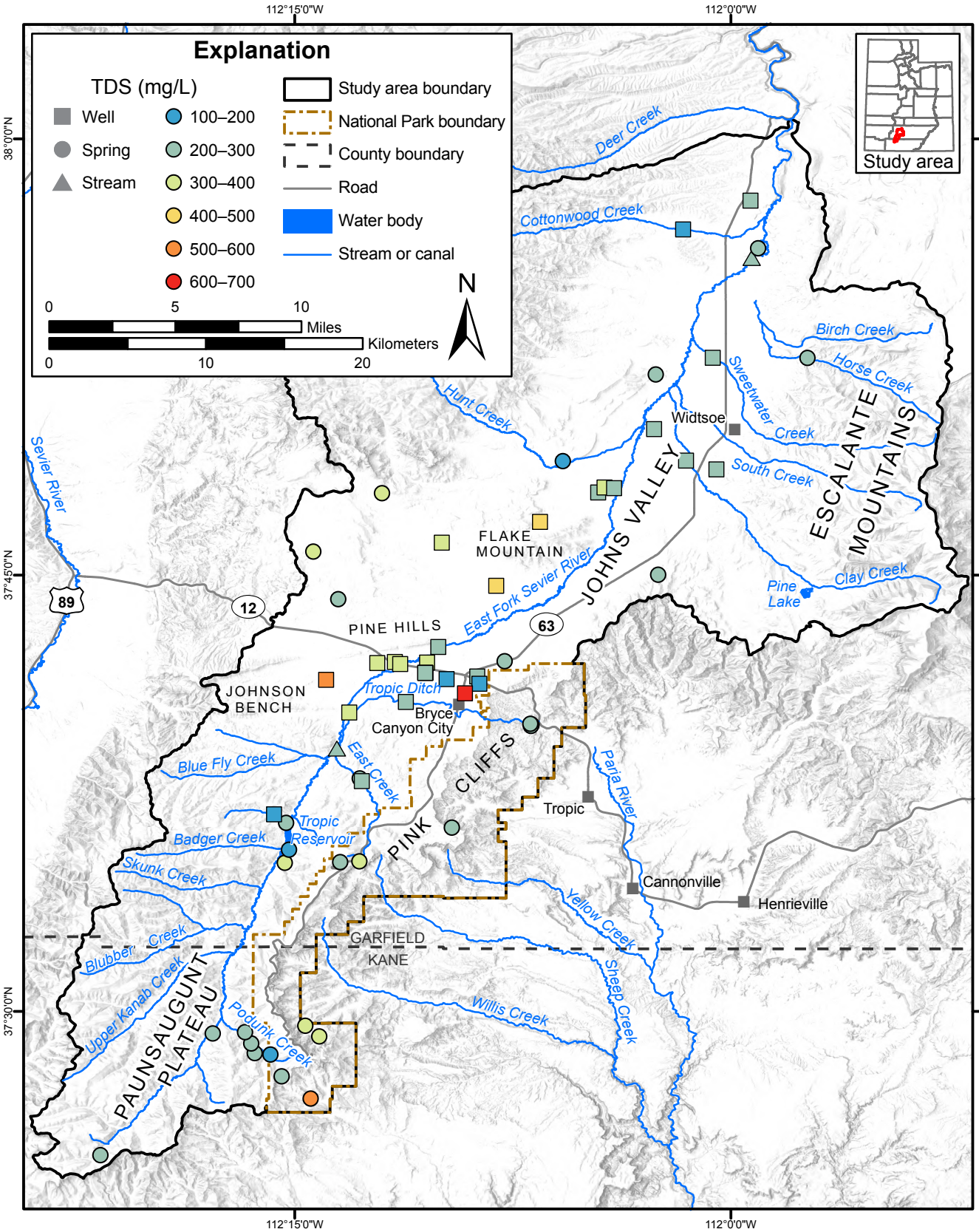

Figure 19. *Total-dissolved-solids concentration map for wells, springs, and streams within Johns and Emery Valleys.*

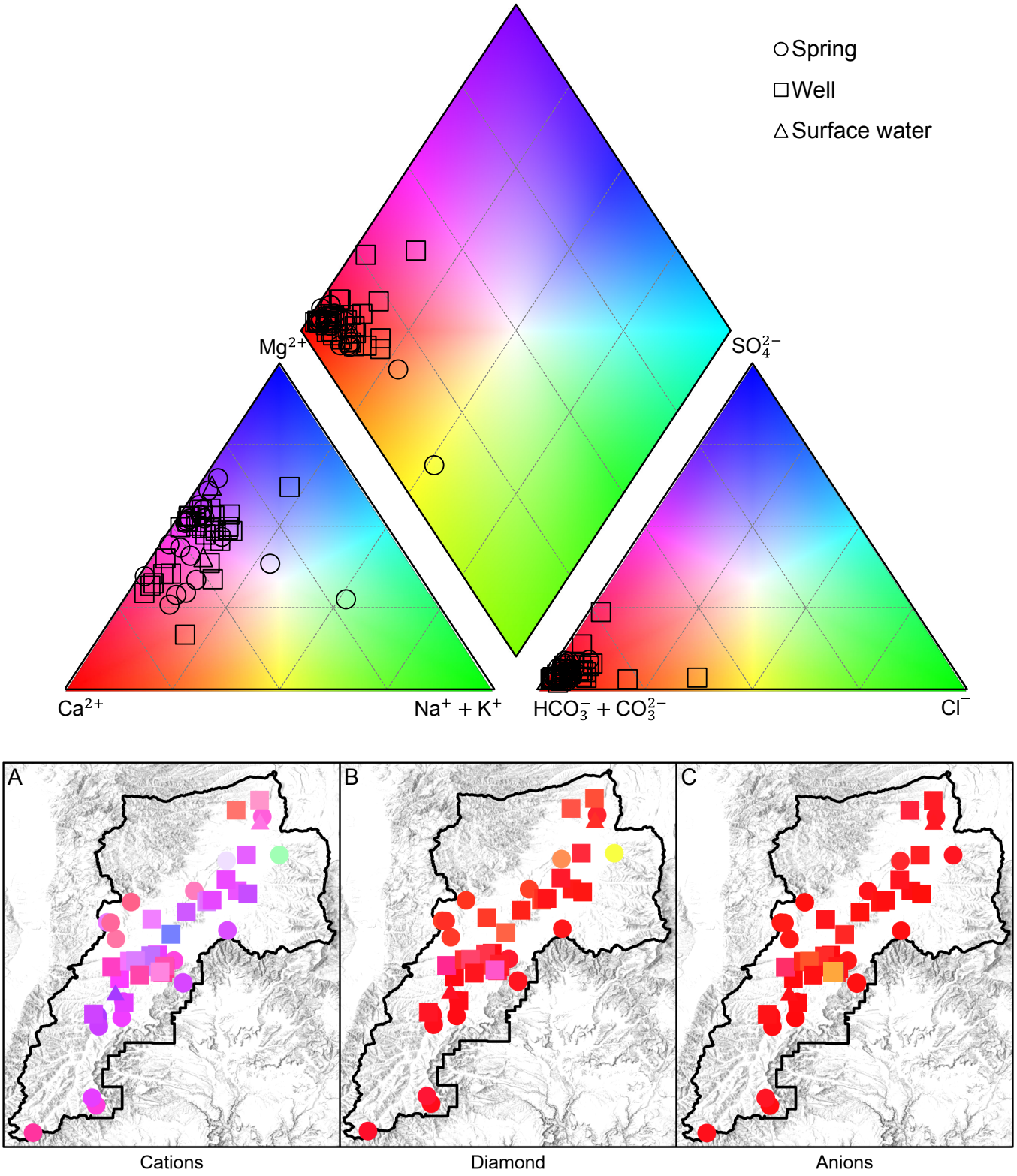

Figure 20. *General chemistry characterized by an overall calcium-magnesium bicarbonate type for all sample sites in the study area by well, spring, and surface;* ***A)*** *all sites as cations;* ***B)*** *all sites as diamonds; and* ***C)*** *all sites as anions.*

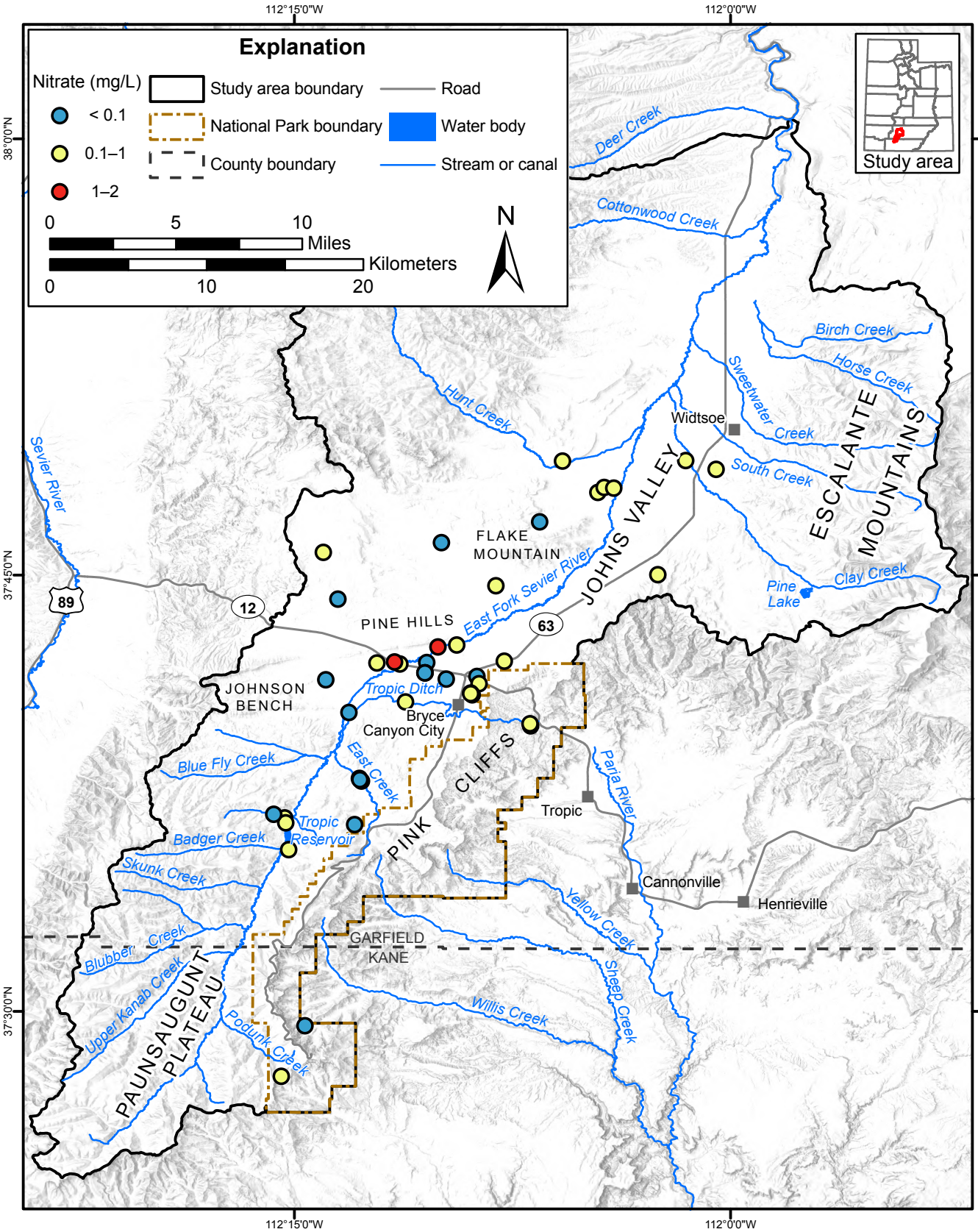

Figure 21. *Nitrate concentration for wells and springs in the study area.*

and wastewater-treatment facilities. Eighty-four potential contaminant sources in the following categories were mapped in Johns and Emery Valleys:

(1) mining, which includes abandoned and active gravel mining operations and borrow pits that potentially contribute metals, solvents, and petroleum products;

(2) agricultural practices, which consist of irrigated and non-irrigated crops, active and abandoned animal feedlots, corrals, and stables/barnyards that potentially contribute nitrate;

(3) industrial facilities that potentially contribute pesticides, metals, solvents, petroleum products, and polychlorinated biphenyl (PCB) spills associated with a variety of sources such as transportation facilities, salt storage facilities, transformer (power) stations, and cell towers;

(4) small businesses, such as hotels, restaurants, retail shops, and commercial shooting ranges, some of which may contribute pollutants such as metals and solvents;

(5) large lawns, including parks and cemeteries, that may contribute fertilizer and pesticides;

(6) service stations including auto shops and gas stations that may contribute petroleum products, antifreeze, and solvents, and junkyard/salvage operations that may contribute pollutants such as metals and solvents; and

(7) waste-disposal sites that may contribute pollutants such as solvents, metals, and nitrate.

In addition to the above-described potential contaminants, septic tank soil-absorption systems are also present in Johns and Emery Valleys. Since 1978, 36 wastewater permits have been issued or are in process in the study area (Jeremy Roberts, Southeastern Utah Public Health Department, verbal/written communication, August 15, 2019). Outside of towns and cities, septic-tank systems in Garfield County, until recently, have been widely spaced. Within Bryce Canyon National Park, a few septic tanks still exist (Moyle Johnson, verbal communication, November, 2020) but were likely more prevalent historically within the Bryce community.

ENVIRONMENTAL TRACERS

Environmental tracers are naturally occurring or anthropogenic chemicals or isotopes that can indicate water sources and flow processes such as recharge, flow rate, geologic subsurface interactions, residence times, and mixing between sources (Kendall and Caldwell, 1998). Ideal tracers have well-defined input sources and input histories, are inert (no reactions) or geochemically conservative (limited reactions), have transport mechanisms identical to water, and are detected precisely and economically. The use of multiple tracers provides a more comprehensive understanding of the groundwater system. We analyzed water samples from wells and springs for tritium and radiocarbon concentrations, and from precipitation, streams, wells, and springs for stable isotope composition.

Methods and Theory

Stable Isotopes of Water

Oxygen-18 (^{18}O) and deuterium (^{2}H) are naturally occurring stable isotopes of oxygen and hydrogen. Water molecules containing the lighter isotopes (i.e., $^{1}H_2{}^{16}O$) and heavier isotopes (i.e., $^{2}H^{1}HO$ and $H_2{}^{18}O$) fractionate preferentially during phase changes such as evaporation and condensation. Values for ^{18}O and ^{2}H are expressed as ratios in delta notation (δ) per mill (‰) relative to a reference standard:

$$\delta x = (Rx/Rstandard - 1) \times 1000 \quad (2)$$

where:

δx = delta notation of the sample x (in per mill, ‰)

Rx = isotopic ratio of $^{2}H/^{1}H$ or $^{18}O/^{16}O$ in the sample (no units)

$Rstandard$ = isotopic ratio of $^{2}H/^{1}H$ or $^{18}O/^{16}O$ in the standard (no units)

The reference standard for ^{18}O and ^{2}H is Vienna Standard Mean Ocean Water (VSMOW) (Gonfiantini, 1978). The global meteoric water line (GMWL) represents approximate isotopic composition for $\delta^{18}O$ and $\delta^{2}H$ of precipitation (Craig, 1961; Rozanski et al., 1993; Clark and Fritz, 1997) (Figure 22):

$$\delta^2H = 8(\delta^{18}O) + 10 \quad (3)$$

Higher fractions of heavier isotopes are considered "enriched" (less negative) and lower fractions of heavier isotopes are considered "depleted" (more negative). Precipitation can be enriched or depleted depending on origin, distance inland, elevation, form of precipitation, and event intensity. Precipitation at high elevation, inland areas, and snow is more depleted relative to precipitation at low elevation, coastal areas, and rain (Clark and Fritz, 1997). Regionally, precipitation generally plots along a local meteoric water line (LMWL), which typically differs slightly from the GMWL (Clark and Fritz, 1997). During evaporation of groundwater or surface water, $\delta^{18}O$ is enriched more than $\delta^{2}H$, so samples that have been partially evaporated deviate from the LWML.

We collected stable isotope samples of precipitation, streams, wells, and springs. Precipitation samples were collected approximately every two months for a total of 11 samples. The precipitation collection site was chosen for its central location within the study area and accessibility. Our precipitation sampler consists of a 2.5-gallon HDPE carboy, containing

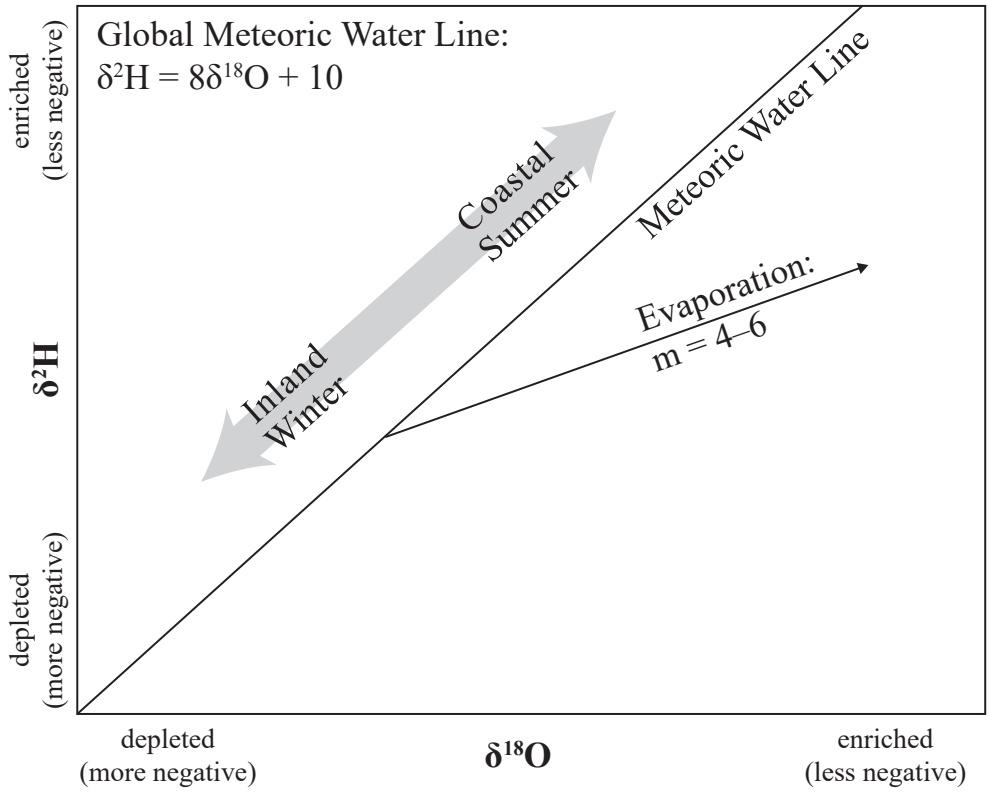

Figure 22. *Relation of oxygen-18 to deuterium in waters, including some factors that affect depletion and enrichment.*

approximately 16 ounces of mineral oil to prevent evaporation, connected to a funnel and housed in a 30-gallon garbage can with the lid inverted to aid in the collection of rain and snow (modified from those described by Ingraham and Taylor [1991] and Scholl et al. [1996]) (Figure 23). Precipitation collection began December 2018 and concluded September 2021.

Stream samples were collected from 19 sites along the East Fork Sevier River and its tributaries, the Tropic Ditch, and Yellow Creek at the south end of Bryce Canyon National Park. Sampling occurred from October 2018 to August 2021. Seven sites were sampled more than once.

Groundwater samples were collected from 34 wells and 47 springs. Repeat sampling was performed at 25 wells and 23 springs. Sampling occurred between September 2018 and July 2022.

All stable isotope samples were field-filtered with disposable 0.45-µm disc filters into 10 mL snap-cap or crimp-cap vials with no head space. Isotopic analysis of $\delta^{18}O$ and δ^2H was performed by cavity ring-down spectrometry at the University of Utah Stable Isotope Ratio Facility for Environmental Research (SIRFER).

Figure 23. *Precipitation collector for the study area.*

Tritium

Tritium (^3H) provides a qualitative age of groundwater for determining the relative time when water entered the groundwater system (Clark and Fritz, 1997). Tritium is an

unstable isotope of hydrogen with a half-life of 12.32 years, therefore tritium concentration in groundwater isolated from other water will decrease by one-half after 12.32 years. Tritium is produced naturally in the upper atmosphere in small quantities, but above-ground thermonuclear testing from 1952 to the late 1970s added tritium to the atmosphere in amounts that far exceed the natural production rates, and, as a result, tritium concentrations in precipitation also increased. The amount of tritium in the atmosphere from weapons testing peaked in the early to mid-1960s and has been declining since atmospheric nuclear testing ceased. Tritium concentrations in water are reported in tritium units (TU). One TU represents one tritiated water molecule per 10^{18} non-tritiated water molecules (Clark and Fritz, 1997). In Utah, concentrations in precipitation measured since 1953 ranged from background levels of 3 to 13 TU to over 8000 TU in 1963 (Lindsey et al., 2019). Tritium in the atmosphere is incorporated into water molecules and enters the groundwater system as recharge from precipitation. Because tritium is part of the water molecule, it is not affected by chemical reactions other than radioactive decay, and thus can be used as a tracer of groundwater on a time scale of less than 10 to about 67 years before present. Water that entered the groundwater system before 1952 and has remained isolated from younger water contains negligible tritium. Therefore, tritium can be used to distinguish between water that entered an aquifer before 1952 and water that entered the aquifer after 1952. Location-specific thresholds for a groundwater sample can be calculated for defining modern and premodern groundwater, using measured or estimated time-series records of tritium for a given location (Lindsey et al., 2019). Using the tritium record in precipitation for a grid cell defined by 37°–39° N. latitude and 110°–115° W. longitude and groundwater samples collected in 2019 and 2022, we define premodern thresholds as 0.19 TU and 0.16 TU, and modern thresholds as 1.7 TU and 1.4 TU, respectively. Samples falling within this range between premodern and modern are considered mixed. A mixture of water having different tritium ages complicates interpretation. We sampled 13 wells and five springs for tritium analysis (Table 3). Samples were collected in two 0.5 L HDPE bottles and sealed with minimal head space. Tritium concentration was measured at the University of Utah Department of Geology and Geophysics Dissolved and Noble Gas Laboratory in Salt Lake City, Utah, via the tritium-^{3}He ingrowth method (Solomon and Cook, 2000), which measures the concentration of ^{3}He, a radioactive decay product of tritium.

Radiocarbon

Carbon-14 (^{14}C) is a naturally occurring radioactive isotope of carbon that has a half-life of about 5730 years, which allows the determination of groundwater residence times of up to 40,000 years (Kalin, 2000). Carbon-14 data are expressed as percent modern carbon (pmC) relative to A.D. 1950 levels, based on the National Bureau of Standards oxalic acid standard. Carbon-13 (^{13}C) is a naturally occurring stable isotope of carbon that is used to evaluate chemical reactions involving carbon (Clark and Fritz, 1997). Carbon-13 is expressed as an isotopic ratio (^{13}C/^{12}C), reported as delta (δ) values in units of parts per thousand (per mill or ‰) relative to the Vienna Pee Dee Belemnite (VPDB) standard. The δ^{13}C ratio in groundwater depends upon numerous factors, which include the type of vegetation in the recharge area, whether carbonate (and the δ^{13}C compositions of those minerals) is dissolved or precipitated during recharge, and whether the system is open or closed. We sampled 12 wells and four springs for carbon isotope analysis (Table 3). Samples were collected in 1 L HDPE bottles sealed with minimal head space and analyzed by accelerator mass spectrometer at the University of Georgia Center for Applied Isotope Studies in Athens, Georgia.

Carbon-14 is produced naturally in the upper atmosphere by a cosmic ray reaction with nitrogen. Atmospheric testing of nuclear weapons also produced elevated ^{14}C concentrations, so in some instances values greater than 100 pmC can occur in groundwater. Carbon-14 is not part of the water molecule, so ^{14}C activities are affected by chemical reactions between the aquifer material and the dissolved constituents in the water. Chemical reactions can either add or remove carbon; therefore, knowledge of chemical reactions that occur during recharge and transport through the aquifer are necessary for estimating the initial activity (Ao) of ^{14}C. Age calculations require estimates of some chemical parameters during recharge and model calculations of reactions during groundwater transport.

Ao is the initial, non-decayed ^{14}C composition of the groundwater and must be determined to calculate ^{14}C ages. In the absence of subsurface reactions, Ao is assumed to be 100 pmC. However, this assumption is rarely valid due to the common presence of carbonate minerals and elevated CO_2 concentrations in the soil. Many models account for geochemical reactions and gas exchanges to determine Ao (Ingerson and Pearson, 1964; Mook, 1972; Tamers, 1975; Fontes and Garnier, 1979; Han and Plummer, 2013). We calculated Ao using the revised Fontes and Garnier model of Han and Plummer (2013), which models isotopic exchange controlled by soil gas CO_2 in the unsaturated zone and carbonate minerals in the saturated zone. We assumed end members of radiocarbon activity and δ^{13}C ratios to be 100 pmC and -21.8 ± 1.4‰, respectively for soil gas CO_2 (Hart, 2009), and 0 pmC and 0‰ for carbonate minerals, respectively.

Groundwater age is calculated by:

$$t = \tau \ln (Ao/A) \quad (4)$$

where:

t = groundwater age (years)

τ = 8267, a constant equal to ^{14}C half-life (5730 yrs) ÷ ln 2

Ao = calculated initial ^{14}C activity (pmC)

A = measured ^{14}C activity (pmC)

Table 3. *Tritium and radiocarbon concentrations, carbon isotope ratios, and radiocarbon model age results.*

				Tritium		Carbon-14				
UGS Site ID	**Site type**	**Sample date**	**Aquifer**	**Concentration (TU)**	**Qualitative age**	**Concentration (pmC)**	**d13C (‰)**	**Uncorrected age (yr B.P.)**	**Fontes and Garnier correction age (yr B.P.)**	**Revised Fontes and Garnier correction age (yr B.P.)**
BC6S	Spring	5/15/19	Claron	1.56	Modern	73.3	-9.38	2563	--*	--*
BC35S	Spring	6/11/19	Claron	1.95	Modern	55.1	-7.87	4929	--	--
BC31S	Spring	6/11/19	Claron	5.60	Modern	85.7	-11.21	1277	--	--
BC68S	Spring	6/18/19	Claron	3.79	Modern	100.3	-10.58	--*	--	--
BC128S	Spring	7/19/22	Alluvium	1.83	Modern	--	--	--	--	--
BC142W	Well	5/15/19	Alluvium	--	--	96.4	-10.81	307	--	--
BC40W	Well	5/16/19	Alluvium	0.40	Mixed	80.0	-8.17	1845	--	--
BC21W	Well	5/14/19	Alluvium	2.80	Modern	98.0	-10.49	165	--	--
BC44W	Well	5/15/19	Alluvium	3.50	Modern	96.5	-11.52	294	--	--
BC66W	Well	6/12/19	Alluvium	2.88	Modern	99.0	-9.19	79	--	--
BC28W	Well	6/11/19	Alluvium	1.39	Mixed	73.5	-10.13	2550	--	--
BC30W	Well	6/11/19	Alluvium	2.83	Modern	--	--	--	--	--
BC48W	Well	5/15/19	Claron	3.71	Modern	105.6	-12.02	--	--	--
BC13W	Well	5/13/19	Cretaceous	0.01	Pre-modern	16.2	-6.88	15,036	6700	4800
BC19W	Well	6/10/19	Cretaceous	0.12	Pre-modern	12.0	-7.96	17,508	10,200	8600
BC329W	Well	7/19/22	Cretaceous	1.11	Mixed	93.4	-11.15	567	--	--
BC127W	Well	7/19/22	Alluvium	1.24	Mixed	--	--	--	--	--
BC120W	Well	7/19/22	Alluvium	1.27	Mixed	92.7	-10.40	628	--	--
BC330W	Well	7/20/22	Claron	0.31	Mixed	48.3	-10.03	6013	--	--

* Null value indicates a given model resulted in a negative age

If A is greater than Ao, the sample likely contains ^{14}C produced from nuclear testing and indicates the sample has at least some component of modern water, which can be verified using tritium data.

Results

Stable Isotopes of Water

Stable isotope ratios from precipitation, surface water, and groundwater range from -126‰ to -24.7‰ for δ^2H and -16.7‰ to -3.4‰ for $\delta^{18}O$ (Appendix D Table D-6). Ninety-five percent of samples fall within the range of -109‰ to -87‰ for δ^2H and -15‰ to -10‰ for $\delta^{18}O$. Differences in sample ratios are apparent when differentiated by sample type (Figure 24).

Precipitation: The mean δ^2H and $\delta^{18}O$ ratios in precipitation are -88.7 ± 34‰ and -12.2 ± 4.5‰, respectively (Figure 24). Winter precipitation is much more depleted than non-winter precipitation (Figure 25). Precipitation origin is likely the cause of this difference. During winter, the polar jet stream brings storm systems from the Pacific Ocean, whereas during summer, monsoonal flow brings limited amounts of precipitation originating from the Gulf of California, Gulf of Mexico, and Pacific Ocean (Gillies and Ramsey, 2009).

The slope of a linear regression line using all precipitation is 7.6. Global and local meteoric water lines typically have slopes near 8 (Clark and Fritz, 1997). Due to what is likely evaporation of summer precipitation, either during rainfall or within the precipitation collector, the slope of a LMWL based on our samples is slightly underestimated.

Surface water: Surface water samples consist of the East Fork Sevier River and tributaries, the Tropic Ditch, and Yellow Creek, an ephemeral stream on the east side of Bryce Canyon National Park (Figure 26). The mean ratios of δ^2H and $\delta^{18}O$ in surface water are -93.9 ± 4.5‰ and -12.1 ± 1‰, respectively (Figure 24). The data fall along a local evaporation line (LEL) based on a linear regression ($R^2 = 0.84$) of surface water data with a slope of 4.2, which is consistent with evaporative fractionation of surface water found elsewhere (Clark and Fritz, 1997). The most enriched surface water sample was an autumn season sample from Skunk Creek, a headwaters tributary to the East Fork Sevier River (Figure 25).

We assessed temporal and along-reach trends for the spring 2019 and autumn 2019 sampling events for the East Fork Sevier River and Tropic Ditch. In both spring and autumn, we observed isotopic enrichment due to evaporation from upstream to downstream of Tropic Reservoir (Figure 27). Downstream of Tropic Reservoir we observed isotopic depletion, likely from small tributaries or groundwater input, until the Tropic Ditch diversion (Figure 27). In spring 2019, after the heavy snowpack, the East Fork Sevier River was still flowing beyond the Tropic Ditch diversion point. The stable isotope composition remained constant until

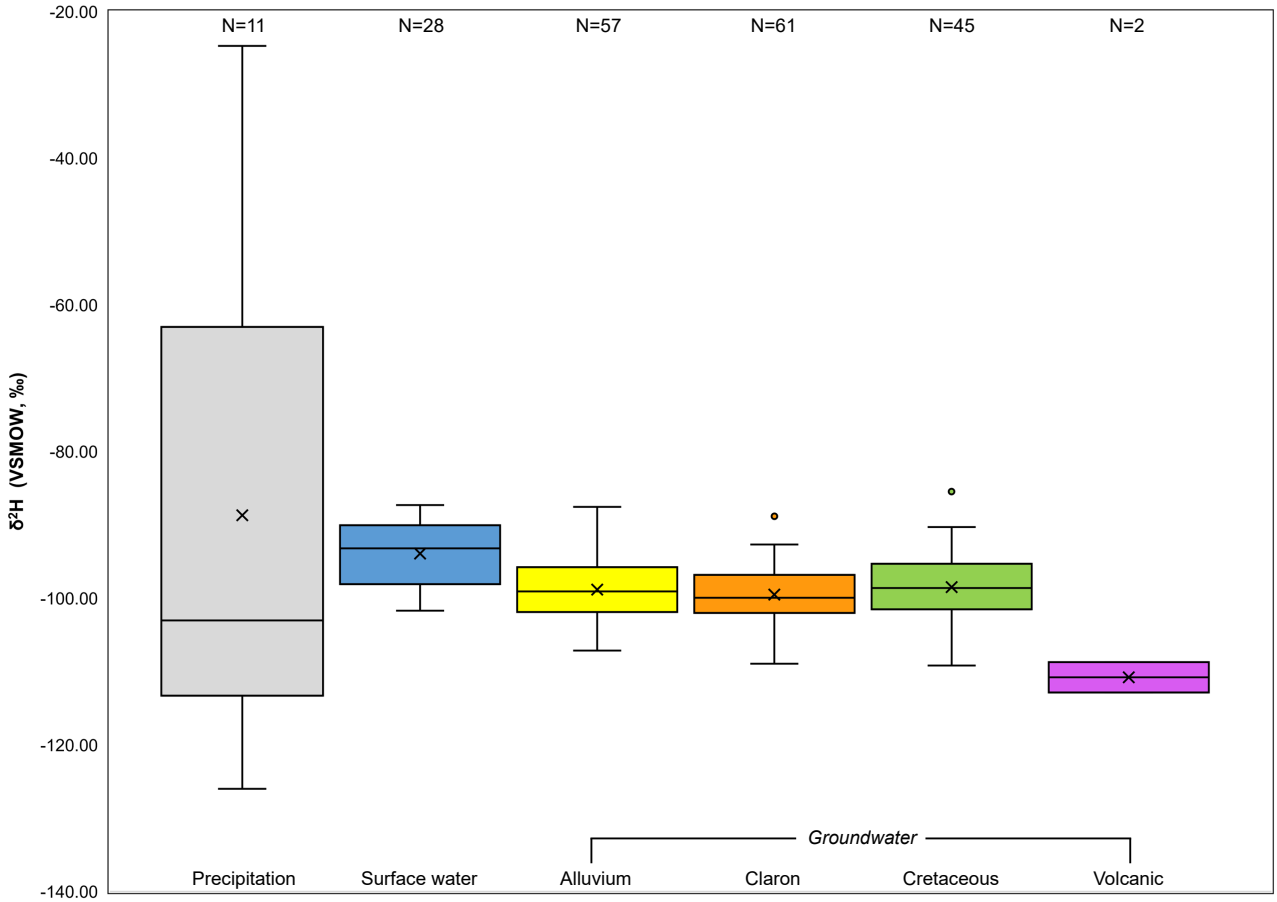

Figure 24. *Statistical comparison of δ^2H in study area waters. VSMOW = Vienna Standard Mean Ocean Water.*

the river entered Emery Valley, at which point it became a losing reach and we observed evaporative enrichment. In spring 2019, the river composition was within or near the range of valley-fill aquifer compositions until the enrichment over the losing reach. However, the autumn 2019 river composition started closer to the mean valley-fill aquifer composition but was then enriched heavily via evaporation within Tropic Reservoir.

The isotopic composition of the Tropic Ditch was enriched in spring 2019 from the diversion point to the rim of Water Canyon, despite being piped below ground. We observed depletion as the Tropic Ditch flows through Water Canyon, possibly due to groundwater input from the springs and seeps of the Claron Formation. However, the composition enriched slightly beyond the input from Mossy Cave springs (Figure 27A). In autumn 2019, we observed completely opposite changes in isotope composition in the Tropic Ditch: depletion from the diversion point to the start of Water Canyon, followed by enrichment within Water Canyon. This change may reflect increased evaporation and a seasonal decrease in groundwater input, although the composition depletes with the addition of Mossy Cave springs outflow (Figure 27B). The dominant factor controlling autumn isotope composition of the East Fork Sevier River and Tropic Ditch appears to be long residence time of water within Tropic Reservoir, allowing heavy evaporative enrichment.

Springs and wells: The mean ratio of δ^2H in wells is -99 ± 4.4‰ (Figure 26). Enrichment of heavier isotopes (less negative isotopic signatures) in groundwater in the western United States has been attributed to paleoclimate effects (White and Chuma, 1987) such as arid conditions, and to extensive evaporation prior to recharge. Evaporation prior to recharge occurs in both surface water and soil water and can yield evaporation line slopes ranging from 2.5 in soils to greater than 6 in large water bodies (Gibson et al., 2008). Evaporative enrichment is evident in wells screened in each of the main study area aquifers (Figure 28). This evaporative signal may be from evaporation of surface water prior to recharge in losing sections of streams, or from evaporation prior to infiltration of in situ snowmelt on the valley floor. The mean ratio of δ^2H in springs is -99.3 ± 4.7‰ (Figure 26). Evaporative enrichment is also apparent in spring samples, most notably from springs issuing from the Claron and Cretaceous aquifers. Evaporative enrichment in these aquifers may be from evaporation during direct recharge, or from evaporation-influenced alluvial groundwater seeping into the underlying formations. Some of these samples may have experienced evaporation from the time of discharge to sample collection. Stable isotope ratios of groundwater

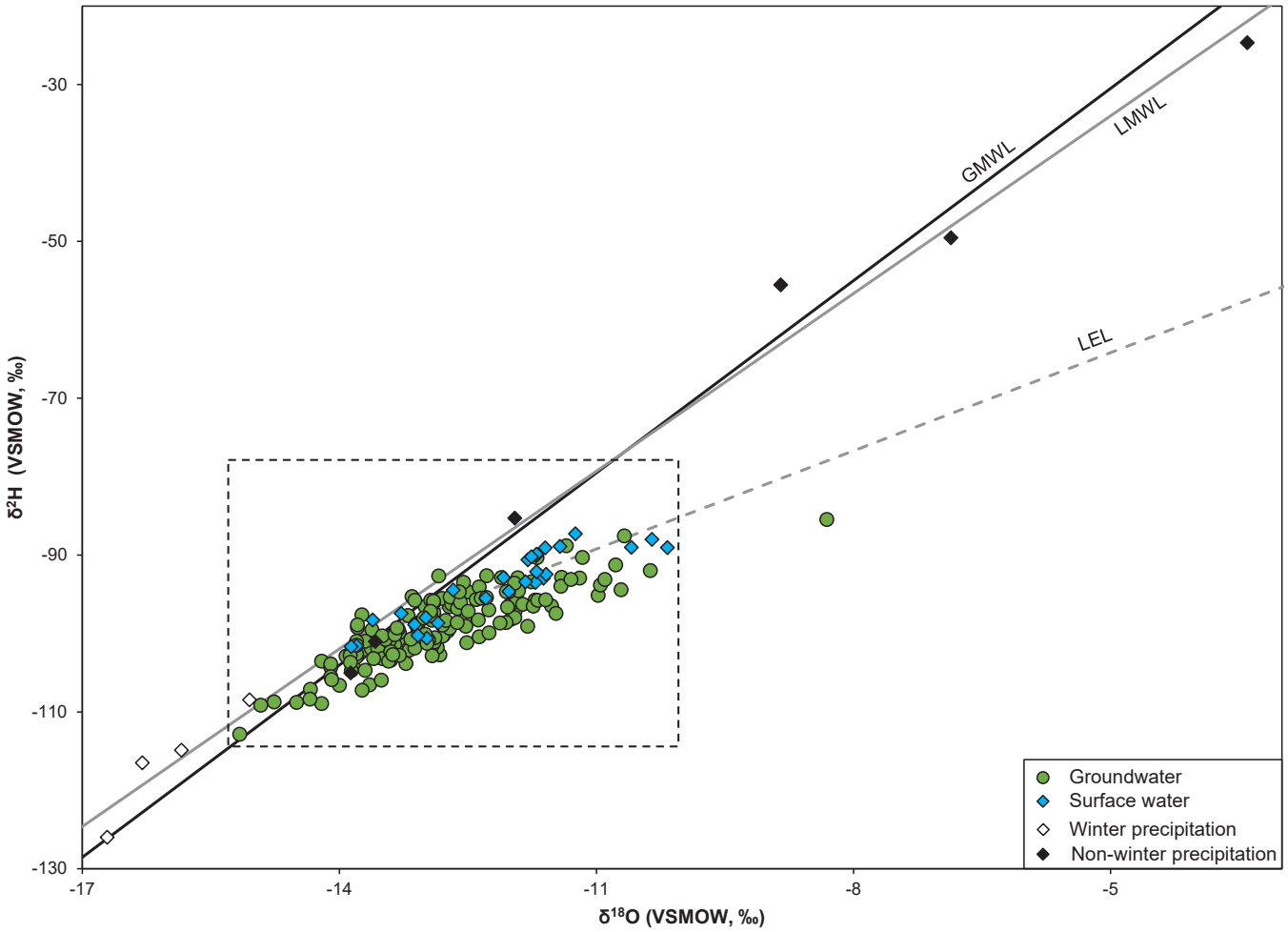

Figure 25. *Stable isotope ratios in precipitation, groundwater, and surface water. The dashed box shows the extent of Figure 28, which gives a detailed plot of groundwater and surface water ratios. GMWL = global meteoric water line, LMWL = local metoric water line, LEL = local evaporation line, VSMOW = Vienna standard mean ocean water.*

throughout the study area indicate that recharge is a mixture of winter and non-winter precipitation, predominantly weighted toward winter precipitation (Figure 25). Spring samples issuing from volcanic deposits on the eastern margin of northern Johns Valley are the most depleted ratios in the study area, excluding precipitation. These springs may be recharged entirely from winter snowpack, rather than a mix of winter- and non-winter precipitation like most springs and wells indicate.

Tritium

We collected water samples for tritium analysis from 13 wells and five springs in the study area (Figure 29, Table 3). Tritium concentrations measured in groundwater range from 0.01 to 5.60 TU with a mean of 2.04 TU and a mean measurement uncertainty of 0.23 TU. Samples BC13W and BC19W have tritium concentrations less than the premodern threshold and are considered premodern. Ten samples have tritium concentrations greater than the modern threshold and are considered modern, whereas the remaining six samples have concentrations between the thresholds and are considered mixed (Table 3). The two premodern samples are from wells screened in the Cretaceous bedrock aquifer at relatively deep depths of 285 and 420 feet (86.9 to 128 m) below ground surface (bgs). Modern and mixed samples come from the alluvial, Claron, and Cretaceous aquifers. Modern and mixed samples from the Cretaceous aquifer are from wells screened across the alluvium-bedrock interface at relatively shallow depths.

Radiocarbon

We collected water samples for radiocarbon analysis from 12 wells and four springs in the study area (Figure 29, Table 3). We also include data from three wells collected by Loughlin Water Associates (Bill Loughlin, written communication, 2023). Carbon-14 activities ranged from 12.0 to 105.6 pmC (Table 3). The mean measurement uncertainty is 0.22 pmC, excluding samples from BC13W and BC19W, which had uncertainties of 0.064 and 0.066 pmC, respectively. Sample $\delta^{13}C$ ratios ranged from -12.0‰ to -6.9‰ (Table 3). Bomb-peak ^{14}C is present in most of the samples, as indicated by a measured ^{14}C activity greater than the Ao value calculated using the revised Fontes and Garnier model (Han and Plummer,

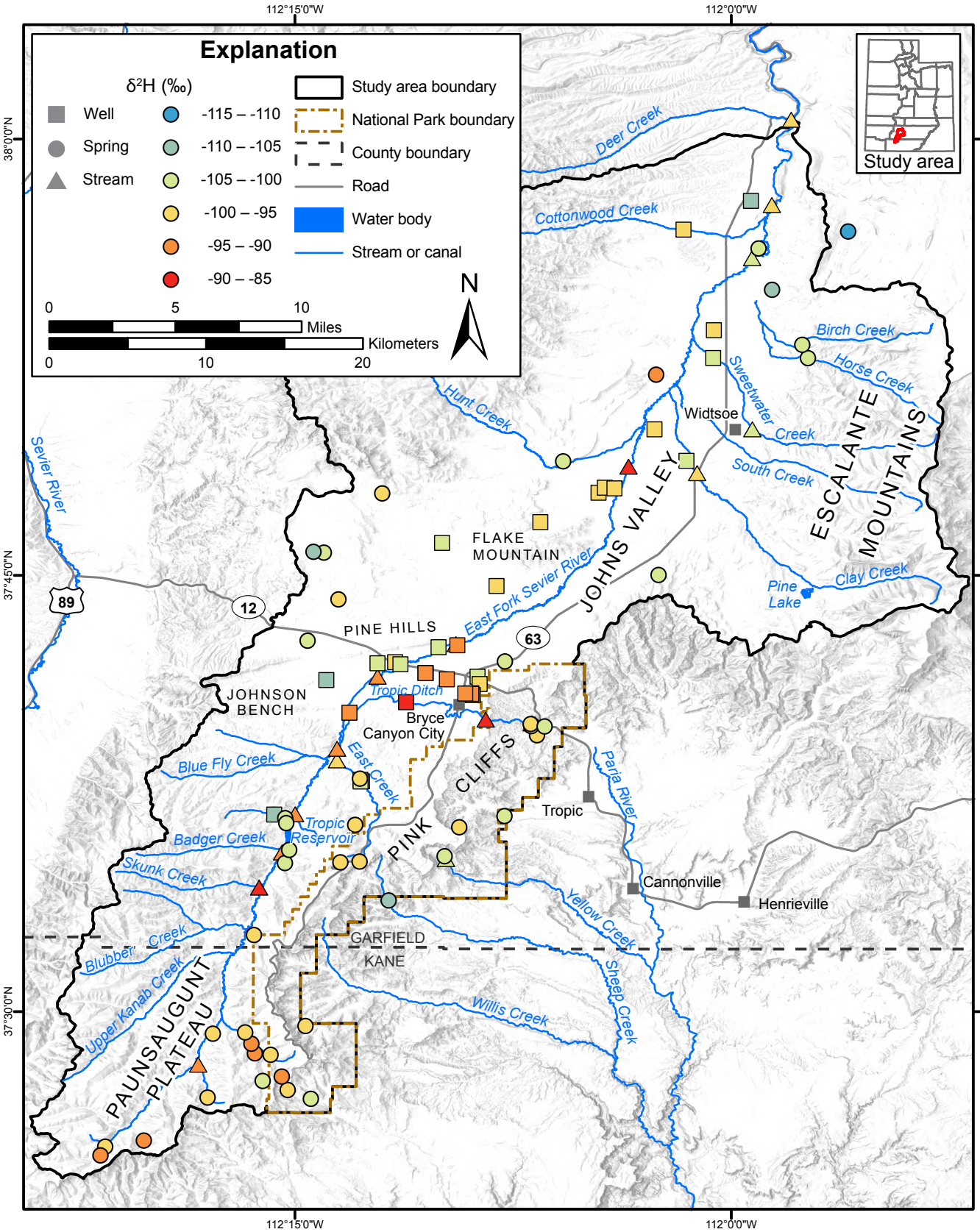

Figure 26. *Map of δ^2H in study area wells, springs, and streams.*

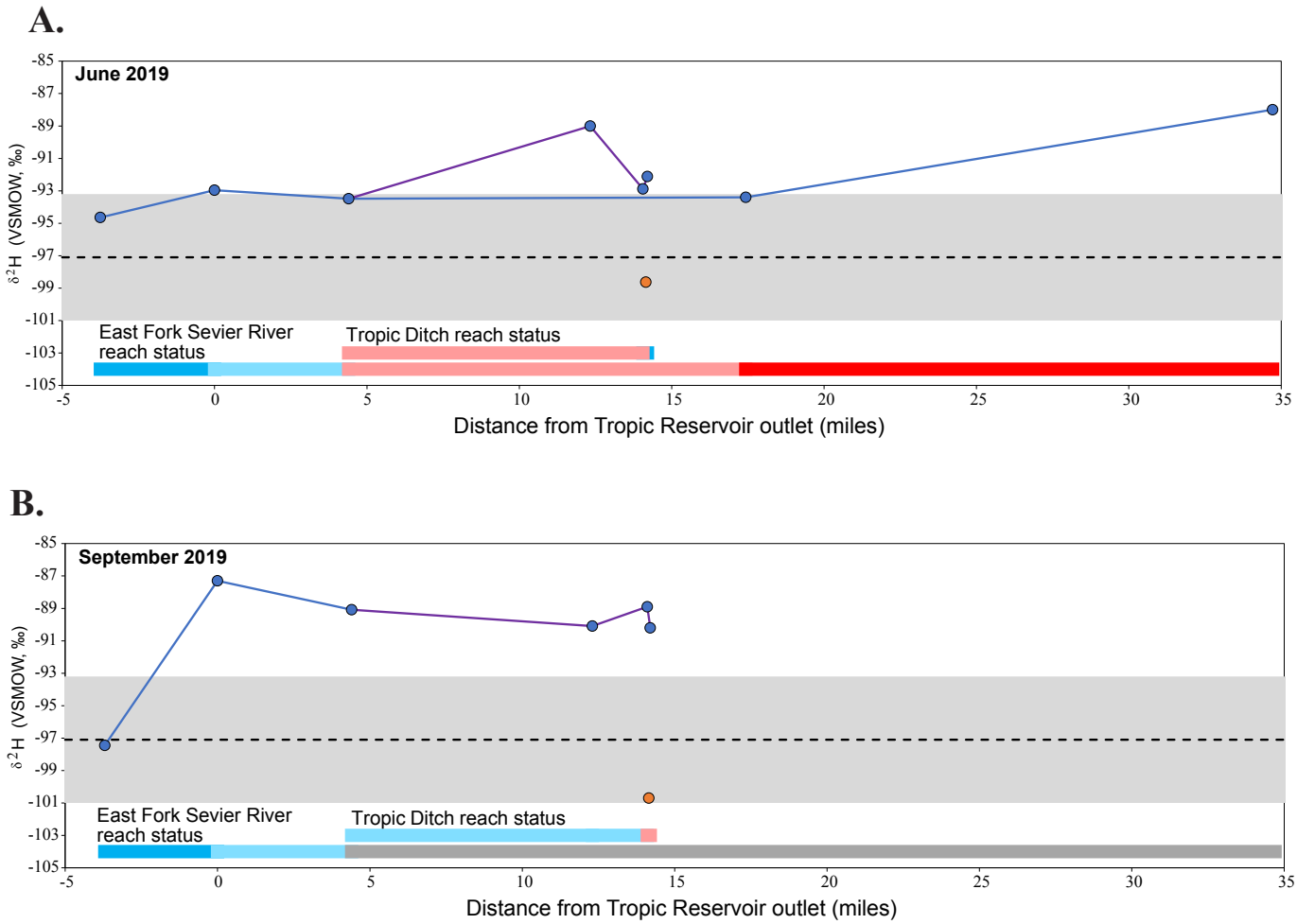

Figure 27. *δ^2H and gaining or losing status in stream reaches versus distance from Tropic Reservoir.* ***A)*** *δ^2H and reach status in June 2019.* ***B)*** *δ^2H and reach status in September 2019. Blue line is East Fork Sevier River, purple line is Tropic Ditch; orange circle is Mossy Cave spring; black dashed line and gray box are valley-fill aquifer average and standard deviation, respectively. Reach status: red = losing, light red = losing within measurement error, blue = gaining, light blue = gaining within measurement error. VSMOW = Vienna standard mean ocean water.*

2013). Bomb-peak ^{14}C is also evident by comparing $\delta^{13}C$ ratios to ^{14}C activities. Samples with bomb-peak ^{14}C plot above and right of the mixing line between soil gas and carbonate minerals (Figure 30).

We calculated ^{14}C ages using the revised Fontes and Garnier model (Han and Plummer, 2013) for the two samples with measured ^{14}C activities less than the calculated Ao values. The ^{14}C ages for samples BC13W and BC19W are 4800 ± 500 and 8600 ± 500 ^{14}C yr before present (BP), respectively. The age uncertainty is derived from the uncertainty in soil gas CO_2 $\delta^{13}C$ ratios (Hart, 2009). These samples are from wells screened in the Cretaceous bedrock aquifer at relatively deep depths of 285 and 420 feet (86.9 to 128 m) below ground surface, respectively. These ages suggest a much slower groundwater flow rate, or much longer groundwater flow path, than the valley-fill aquifer. Samples BC329W and BC1 are also screened in the Cretaceous bedrock aquifer, but across the alluvium-bedrock interface at depths of 45 feet (13.7 m) below ground surface, which could explain the modern ^{14}C activity. Sample BC330W, from a well screened in the Claron Formation and underlying Cretaceous Grand Castle Formation, has a moderate ^{14}C activity of 48.3 pmC and a mixed tritium age, suggesting a mixed source of modern and premodern recharge.

DISCUSSION

Conceptual Groundwater Flow Model

The study area boundary, most of which is the surface drainage divide for the East Fork Sevier River, provides a good approximation of the limits of the groundwater basin. We recognize, however, that some localized sections of the study area boundary may not represent the true groundwater divide. The underlying Cretaceous aquifer, part of the regionally extensive Mesaverde aquifer group, extends northward below the surface drainage divide.

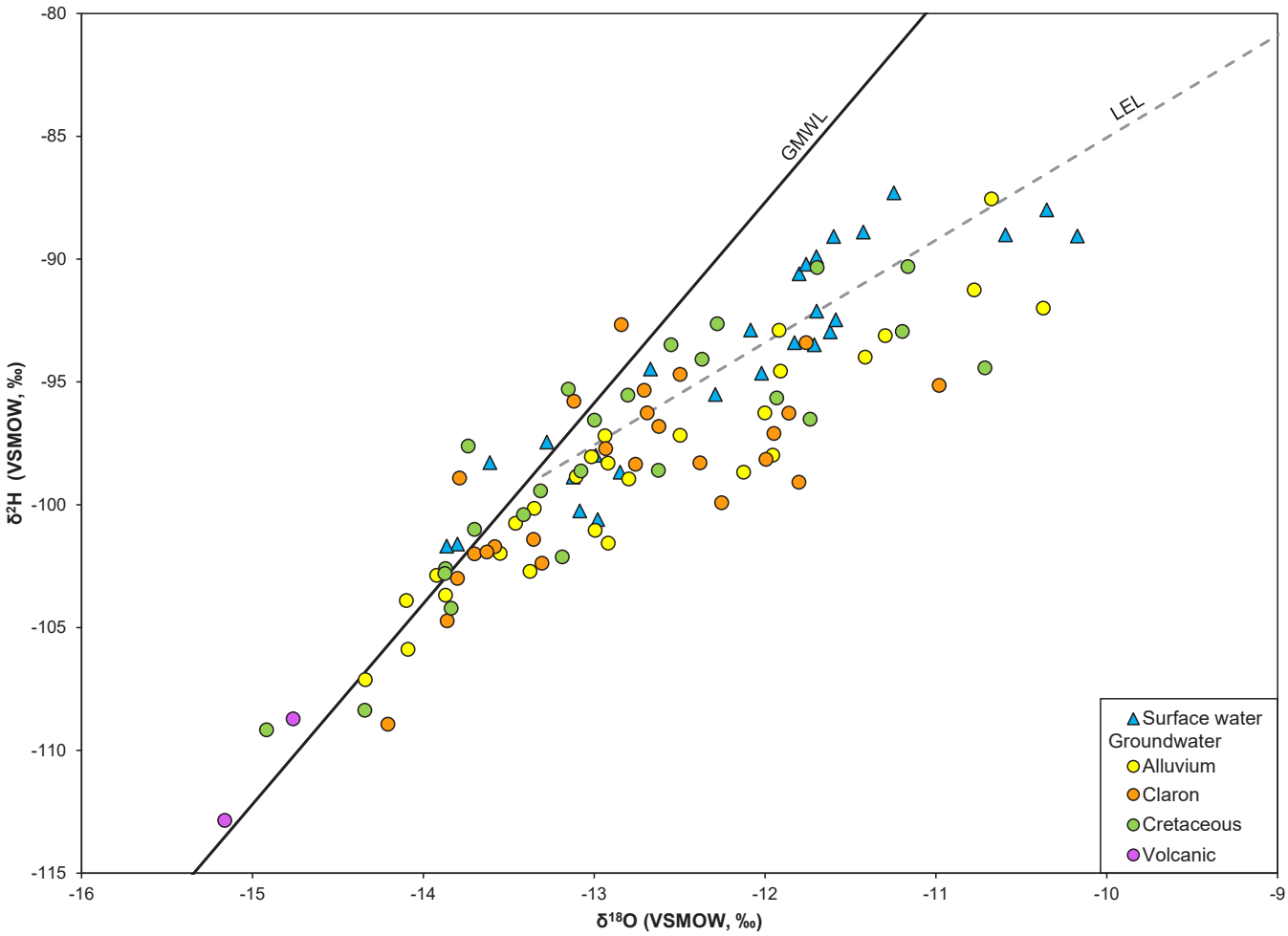

Figure 28. *Stable isotope ratios in groundwater and surface water. GMWL = global meteoric water line, LEL = local evaporation line, VSMOW = Vienna standard mean ocean water.*

Valley-Fill Aquifer

The valley-fill aquifer receives recharge from in situ infiltration of snowmelt and precipitation on the valley floor, seepage from streams (primarily the East Fork Sevier River) as they enter the valley, and unconsumed irrigation water applied to the land surface. Septic-tank leachate also provides a small quantity of local recharge to the valley-fill aquifer. The occurrence and amount of subsurface inflow from adjacent bedrock aquifers is unknown. Groundwater in the valley-fill aquifer flows from the valley margins (i.e., the Paunsaugunt Plateau, Sevier Plateau, and Escalante Mountains) toward Tropic Reservoir and the East Fork Sevier River, approximately perpendicular to potentiometric contours assuming no major anisotropy in the horizontal component of hydraulic conductivity. Valley-fill groundwater discharges to pumping wells in Emery and Johns Valleys, and to the East Fork Sevier River and wetlands near the north boundary of the study area (Figure 31).

Valley-fill aquifer thickness varies from less than 50 to 350 feet (<15–107 m) (Figure 8). Valley-fill deposits along the valley margins are less than 50 feet (<15 m) thick, and well logs provide no evidence of thickening adjacent to valley-bounding faults. The spatial distribution of valley-fill thickness is poorly constrained but is highly variable in western Emery Valley; valley fill is as much as 200 feet (61 m) thick in central Emery Valley and as much as 350 feet (107 m) thick in Johns Valley. These sediments are the principal reservoir for groundwater; however, groundwater storage in the valley fill is relatively limited based on its thickness. Most groundwater in the valley-fill aquifer has experienced some evaporation and contains some tritium. This is consistent with groundwater in the valley-fill aquifer: originating as surface water experiencing evaporation in Tropic Reservoir and/or along the East Fork Sevier River prior to infiltration; as recharge into the Claron aquifer and discharging to surface water before infiltrating into the valley-fill aquifer; or from evaporation prior to infiltration of in situ snowmelt on the valley floor.

Water levels in most valley-fill wells fluctuate depending on winter precipitation, indicating storage is limited. The potentiometric surface in the valley-fill aquifer generally increases in the spring and declines in the fall. Water levels in wells completed in bedrock aquifers were less variable than wells completed in valley fill, with some water levels declining and others rising during different seasons and years, weather independent.

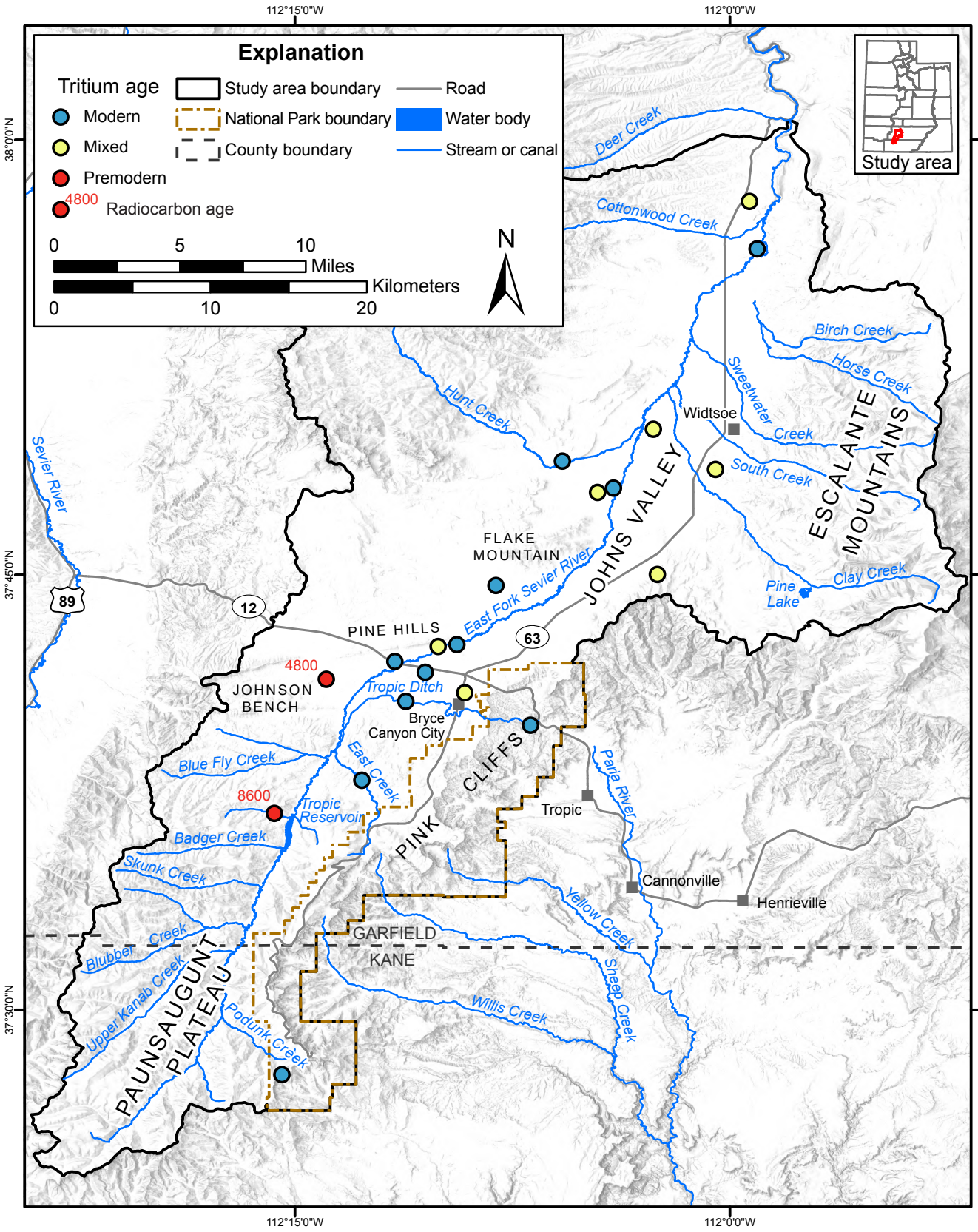

Figure 29. *Environmental tracer map showing tritium and select radiocarbon model ages.*

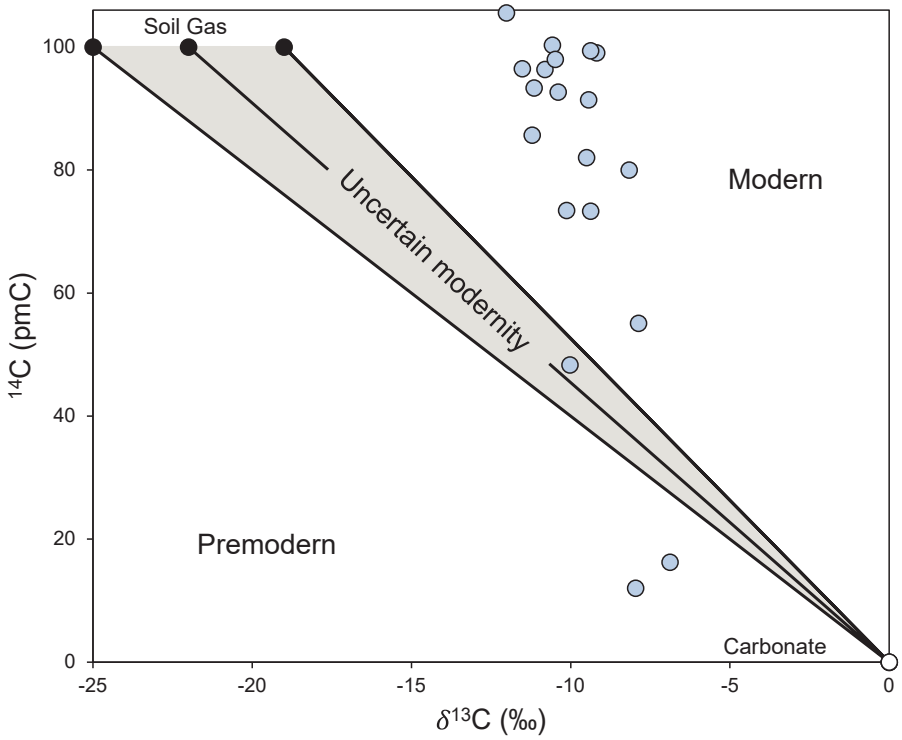

Figure 30. *Carbon isotopes in groundwater samples and simple mixing lines.*

Water-level increases in valley-fill wells after heavier winter snowpack indicates the valley-fill aquifer is more sensitive to precipitation via surface water runoff and direct infiltration than the bedrock aquifers (Appendix G Figure G-1). Groundwater pumping also likely contributes to water-level fluctuations in the valley-fill aquifer, particularly along the more densely developed Highway 12 corridor. However, scant long-term water level data show no evidence of decline in the period of record.

Bedrock Aquifers

Recharge from precipitation to the bedrock aquifers flows either toward springs and streams to become surface flow, or through the bedrock below Johns and Emery Valleys. The Claron Formation is the highest stratigraphic layer of the Pink Cliffs within Bryce Canyon National Park; springs situated along the rim likely receive recharge directly from precipitation in the higher elevation areas of the rim on the escarpment of the Paunsaugunt Plateau. The lower elevation springs that emanate from the Cretaceous formations may receive recharge from the overlying stratigraphy or directly from precipitation on Cretaceous bedrock outcrop exposures.

The isotopic signature of water from the Cretaceous aquifers shows little evidence of evaporation or connection to surface water. Radiometric dating using carbon and tritium isotopes indicates that two distinct aquifer zones may be within the Cretaceous bedrock: an upper zone near the valley-fill aquifer with a mixture of modern and premodern recharge, and a deeper zone with radiocarbon ages of approximately 4800 to 8600 years before present.

The hydraulic properties of the Paunsaugunt fault zone and various thrust faults in the study area may influence regional groundwater flow patterns and potential capture of spring flow and groundwater by future development in Emery and Johns Valleys. Further work is needed to understand whether these faults act as groundwater flow barriers, conduits, or a combination.

Seepage between Bedrock and Valley-Fill Aquifers

Our chemistry and environmental tracer results show that surface water, precipitation, and water in the valley-fill and Claron aquifers have similar chemistry. However, environmental tracers indicate that water from wells screened deep in the Cretaceous aquifers is older than water in the overlying Claron and valley-fill aquifers. Loughlin Water Associates (2022) shows water levels in a currently non-producing well completed in the upper Cretaceous sandstone just below valley fill (BC122W) declines from about May through February and rises from about March through April in response to seasonal fluctuations in recharge. Groundwater levels in the well have fallen overall since the well was drilled in October 2020 in response to the regional drought. However, water levels in the bedrock well do not appear to be affected by the pumping of other nearby wells completed in alluvium, including nearby public-supply wells (BC20W, BC21W, and BC22W). Loughlin Water Associates (2022) also observed a decline of 2 to 3 feet (0.3–0.6 m) when a nearby public-supply well (BC51W), also completed in the upper zone of Cretaceous sandstone, was pumped continuously at ~80 gallons per minute for one to three days. This observation aligns with previous research

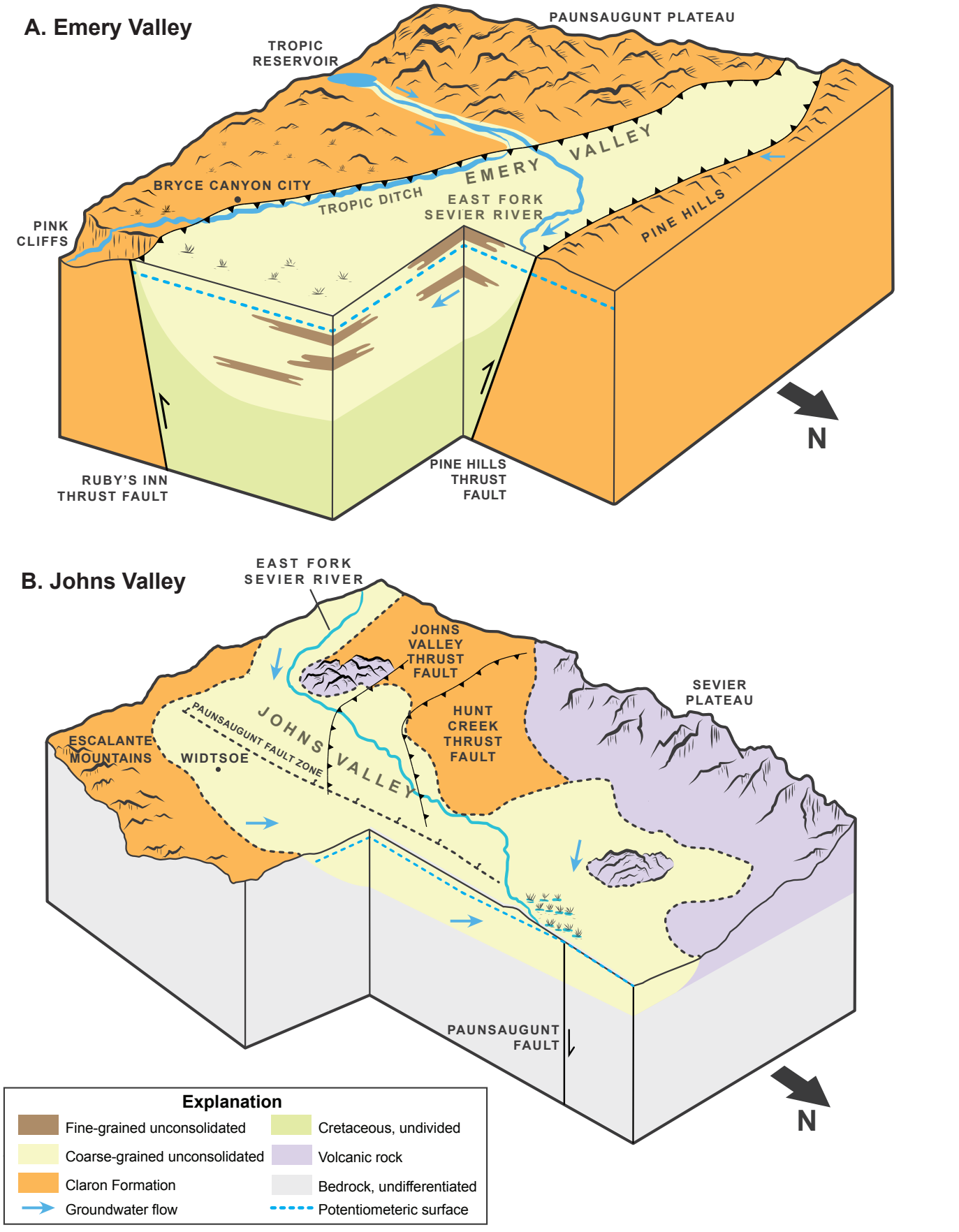

Figure 31. *Simplified block diagram of the hydrogeologic systems of* ***A)*** *Emery Valley and* ***B)*** *Johns Valley showing groundwater flow direction, major faults, and geologic units.*

that assumed that vertical flow between aquifers is minimal (Carpenter et al., 1967).

Thiros and Brothers (1993) calculated vertical hydraulic conductivity as 0.01% to 1% of horizontal hydraulic conductivity in the alluvial aquifer of the main stem of the Sevier River. We conclude that lateral homogeneity and vertical heterogeneity in the valley-fill and bedrock aquifers of the East Fork Sevier River drainage will lead to similarly preferred horizontal flow rather than vertical flow. We assume that the portion of precipitation that infiltrates this region moves dominantly horizontally from the lower-conductivity bedrock to the higher-conductivity valley fill.

Further research is needed to determine the exact relationship between the bedrock and valley-fill aquifers. The installation of nested piezometers, completed in valley fill and bedrock, combined with pump tests would increase our understanding of vertical flow.

Groundwater–Surface-Water Interaction

Surface water plays a key role in the groundwater system of Johns and Emery Valleys. Losing streams and tributaries recharge the valley-fill aquifer when and where the water table is below the bottom of the streambed, especially during low-flow conditions. Conversely, streams are gaining in areas having shallow water tables, especially during runoff season when the aquifer is receiving in-place recharge on the valley floor. This interchange of groundwater and surface water is apparent in the environmental isotope data. Our results show an evaporative signal in the alluvial aquifer, and considerable overlap between the isotopic signatures of surface water and the valley-fill aquifer, suggesting recharge from streams.

The interchange between surface water and the valley-fill aquifer between Tropic Reservoir and Emery Valley is net gaining to surface water but can transition to net gaining to groundwater in autumn depending on the snowpack and releases controlled by Tropic Reservoir. Based on our observations from spring data, the valley-fill aquifer in Johns and Emery Valleys is net gaining to groundwater when surface water is actively flowing through the valleys and the East Fork Sevier River is not fully diverted by the Tropic Ditch. This dynamic transitions to net gaining to surface water at the northern end of Johns Valley where the water table essentially intersects the land surface and perennial wetlands are supported.

WATER BUDGET

Water Budget Development

We estimated a water budget for the drainage basin for water years 2017 to 2021 (water year October 1 to September 30) using the USGS Soil-Water-Balance (SWB) model (Westenbroek et al., 2018) and by quantifying annual inflow and outflow. The primary inflow component of the water balance is precipitation and the main known outflow components are evapotranspiration, loss to the Tropic Ditch, and loss to the East Fork Sevier River at the northern boundary of the study area.

Soil Water Balance Model

The SWB model calculates spatial and temporal variations of net infiltration, which is a good approximation of groundwater recharge. The SWB model is a modified Thornthwaite-Mather soil-water-balance model, computed on daily time step.

The spatial data input requirements of the SWB model include Daymet climate data (Thornton et al., 2021), a digital elevation model (DEM) for calculating water flow direction, a descriptive soils layer, and land cover data. All spatial data were projected into an Albers equal area projection (EPSG:5070) and clipped to a rectangular area that encapsulated the study area, plus a 2-kilometer (1.2 mi) buffer. All spatial data used in the model were raster data in ASCII format.

Soil properties used in the SWB model are taken from the U.S. Department of Agriculture Soil Survey Geographic Database (SSURGO) dataset (Natural Resources Conservation Service, 2022). From the SSURGO dataset, we used the Soil Hydrologic Group and Available Water Storage 0–150 centimeter (0–59 inch) layers served by ESRI ArcGIS Living Atlas. Available water storage indicates the amount of water a soil can hold that is available to plants. The soil hydrologic groups are created based on physical properties of the soil which dictate whether precipitation will predominantly run off or infiltrate. These soil properties were tied to a lookup table for the model that designated curve numbers according to the soil group. The SWB model uses the Natural Resources Conservation Service curve number rainfall-runoff method (U.S. Department of Agriculture, 1986) to help determine the amount of surface water (precipitation and runoff) that is infiltrated as it passes over a cell in the model. We used curve number values from Tillman (2015), because that research covered the Upper Colorado River basin which has similar geology and topography to the study area.

The SWB model uses the Hargreaves-Samani (1985) method to produce spatially variable estimates of potential evapotranspiration (PET) from spatially varying minimum and maximum air temperature data for each daily time step. The air temperature data are from Daymet grids that were downloaded programmatically from the Thredds server.

For the land use spatial input, we used 2019 National Land Cover Database (NLCD) data from the Multi-Resolution Land Characteristics Consortium (https://www.mrlc.gov/data/nlcd-2019-land-cover-conus). These data have a format that is acceptable and easy to augment for input into the SWB model. Like soil, land use is tied to a lookup table that dictates runoff versus recharge for the SWB model.

To generate a flow direction raster, which is used by the SWB model to determine runoff direction, we used 30-meter-resolution (98 ft) elevation data from the Utah Geospatial Resource Center (UGRC) created by the USGS. To determine flow direction from elevation, major "sinks" (low points) are filled and then an eight-direction flow tool is applied to the sink-filled elevation data.

We applied the model to daily data from calendar years 2016 to 2021, using 2016 as a model "warm up" year. We summarized the results by water year. The resulting rasters were averaged to determine the monthly and yearly average soil water, actual evapotranspiration, runoff, and recharge.

Remotely Sensed Data

We divided the study area using two different methods for remote analysis: (1) above and below the Tropic Ditch diversion and (2) between the bedrock and valley-fill aquifers, with the bedrock subdivided into the part south of the valley-fill aquifer and the part east/west of the valley-fill aquifer. We also mapped phreatophytes, crops, and areas of open water to determine groundwater sources of evapotranspiration (ET).

We used the Open-ET SSEBop (Operational Simplified Surface Energy Balance Model; https://github.com/Open-ET/openet-ssebop) model configuration to estimate ET. SSEBop, developed by Senay et al. (2013, 2017), uses Landsat and Daymet data to calculate ET. For reference ET, we used The University of Idaho Gridded Surface Meteorological Dataset (gridMET; Abatzoglou, 2012). We used this model to calculate ET over the entire basin and to calculate ET specific to phreatophytes, crops, and open water.

To calibrate the SWB model outputs, we analyzed PRISM (Parameter-elevation Regressions on Independent Slopes Model; Daly et al., 2008, 2015) and Daymet V4 (Thornton et al., 2021) datasets. We compared these precipitation data to the SWB model outputs and found good agreement ($r^2 > 0.90$).

Streamflow

We relied on the SWB model to estimate streamflow due to a lack of available data. We verified the SWB model using transducers placed along the main stem of the East Fork Sevier from August 2021 to October 2022. We also used historical data from two decommissioned USGS gage stations to confirm relationships between precipitation (PRISM) and runoff. Streamflow leaves the basin via the Tropic Ditch and the East Fork Sevier River at the northern boundary of the study area.

USGS Gage Data: No gages exist within the study area, but two sites existed previously. The East Fork Sevier River gage near Ruby's Inn (10183900) collected data at variable frequencies from October 1, 1961, to October 1, 2015, and the East Fork Sevier River gage near Antimony, Utah (10184450) has data available from July 1, 1961, to September 9, 1966. Although these dates are well outside of our study period, we were able to analyze and compare them to our values for base flow conditions.

We examined the relationship between the measured flow at the USGS site 10183900 and precipitation of the upstream watershed area from PRISM precipitation data. We matched a best-fit function to the data to estimate current water year flows from the East Fork Sevier River based on the amount of precipitation in a given water year. We found that from 1962 to 1995, runoff averaged 11% of precipitation and ranged from 6% to 20% of precipitation. The SWB model suggests runoff is closer to 2% of precipitation. Transducer data and hand measurements recorded in 2021 and 2022 suggest runoff is about 3% of precipitation. Therefore, we accept the SWB model runoff values, but assume the results represent a minimum. Alternatively, the SWB model results may represent a change in management practices, with more surface water being diverted for agricultural use after 1995, resulting in a smaller ratio of runoff to precipitation.

Transducer data: We attempted to estimate streamflow of the East Fork Sevier River by monitoring the water level in the stream channel at 60-minute intervals at locations along its course during water year 2022, targeting areas of change such as above and below Tropic Reservoir and the Tropic Ditch diversion. Due to the short observation period and other issues, such as the transducers freezing, these data are of limited use and the results function only as extreme bounds to compare with modeled flow.

We processed the stream transducer data to estimate the hourly discharge of the East Fork Sevier River. We used Solinst Levelogger vented pressure transducers that do not require a correction for barometric pressure. We also deployed non-vented pressure transducers in Tropic Reservoir and at the discharge measurement point below the Tropic Ditch diversion. We corrected these transducer data for barometric pressure using atmospheric pressure recorded on a Solinst barometric pressure logger located at BLM well (BC23W) in the approximate center of the study area. We used a linear regression between the raw water pressure and barometric data to correct for atmospheric pressure. After removing barometric pressure, the adjusted measurements indicate water pressure above the transducer.

Transducer measurements for the East Fork Sevier River started on August 3, 2021, and continued to October 25, 2022, allowing for summary statistics and aggregate calculations over water year 2022 (Appendix G Figures G-6 through G-8).

We collected absolute manual measurements of the stream stage. These data only represent the "relative stage" of the stream (relative changes of the water level in the stream). The relative stage measurements in the transducers have obvious

jumps or "tares" when the transducers were moved to download data. The obvious jumps were visible in the data as sudden offsets of more than 0.25 feet (0.076 m) between hourly measurements. We manually adjusted and removed these offsets from the data, re-aligning the data where the obvious jumps occurred. We also removed data from both vented and non-vented transducers in cases where streamflow decreased and the transducer froze during the winter months. These periods were identified as times when temperature was below 0°C and pressure values ceased to fluctuate normally, instead holding at a steady value.

We matched the manual discharge measurement to the closest-in-time relative stage measurement, then plotted the manual discharge values against the relative stage measurements in a scatter plot and fit a power function to the points. The power function (Braca, 2008) is in the form of:

$$Q = C(x+A)^B \quad (5)$$

where:

Q = stream discharge

A, B, C = fitting coefficients

x = absolute stage of the stream

This equation assumes steady, uniform flow in a rectangular channel and does not accommodate for hysteresis. However, we chose this equation because of limited manual data and the ease of its application. Once we fit the power equation to the streamflow data, we applied the equation to the relative stage data from the transducers to produce hourly estimates of stream discharge. We calculated r^2 values of 1.0 at a site directly above the Tropic Ditch diversion using two manual measurements, 1.0 at Flying V Ranch bridge using two manual measurements, and 0.37 at the north boundary site using four manual measurements. However, values for r^2 will always equate to 1.0 when only two manual measurements are collected. Due to the paucity of measurements, these numbers are not a reliable measure of how well the simplified equation is representing streamflow. We were not able to calculate flow at the site below the Tropic Ditch diversion due to a lack of manual measurements.

East Fork Sevier River Seepage Runs: Seepage runs are one way to quantify the amount of streamflow lost to or gained from the groundwater system at one point in time. We used the results of our spring and autumn seepage runs on the stream system to estimate the volume of water gained or lost by streams and then used those data to estimate gains and losses throughout the year. Seepage run methods and results are described in the Stream Seepage Studies section above.

Tributaries and springs: We collected flow data from springs and tributaries from 2018 to 2022. We measured flow using a Hach FH950 electromagnetic current velocity meter, a Marsh-McBirney electromagnetic current velocity meter, weir plates, buckets, neutral buoyant objects, and Parshall flumes.

Well and Spring Water Usage

We tabulated annual water use data from 2017 to 2021 using data supplied voluntarily by public water suppliers through the Utah Water Use Program (Utah Division of Water Rights, 2022). The Utah Division of Water Resources conducts detailed studies every four years on municipal and industrial water use by community water systems that detail the type of use (potable, secondary, indoor, outdoor, and others) (Utah Division of Water Resources, 2019). The municipal and industrial use studies provide a framework to interpret and verify the annual Water Use Program data. We also tabulated water rights for domestic use, which summed to slightly less than 50 acre-feet/yr (Table 4). Water use amounts based on water rights are assumed to be maximum estimates of actual water use. We summed municipal, industrial, and domestic water use for total water consumption.

Infiltration of Unconsumed Irrigation

All water applied to crops during our study period was diverted from springs and tributaries. We measured flow from these source areas and noted that they infiltrated the ground surface fully, whether in their natural channels or on the fields, minus evapotranspired water. We used SWB model runoff from the bedrock areas adjacent to the valley-fill aquifer to calculate the total water flowing onto the aquifer, which is also the total volume of runoff lost to the aquifer. Water used for irrigation is a portion of this value but was not partitioned from total adjacent runoff. The SWB model was used to calculate infiltration over bedrock adjacent to the valley-fill aquifer. A portion of this water flows through the subsurface directly to the aquifer, whereas some daylights at springs along the margins of the valley. This spring water is lost to the groundwater in the channel or diverted to fields, where it also infiltrates the ground surface or is consumed by ET. Similar to runoff, we did not partition the portion of spring water used for irrigation but considered its loss to the aquifer included in water infiltrating adjacent bedrock. Our methods for calculating loss to ET are summarized in the Remotely Sensed Data section of this report.

Septic-Tank Drain-Field Seepage

We estimated the volume of groundwater recharge from septic-tank drain-field leachate by multiplying the population using septic tanks by per capita indoor water use. The Bryce area has high seasonal population variability because it is a tourist destination with resort lodging used on a part-time basis. We obtained the number of septic-tank systems based on data provided by the Southwestern Health Department and Garfield County. Aerial imagery was used to identify structures served by these systems (Southwestern Utah Health Department, Jeremy Roberts, written communication, September 15, 2019; Kaden

Figgins, Garfield County Economic Development Director, written communication, November 19, 2019). We identified 36 septic systems and three large underground wastewater disposal systems (LUWDS); three additional LUWDS are approved for construction. Each LUWDS discharges the equivalent of about 170 septic systems. To calculate recharge from the domestic septic tanks, we used 2.56 people per household and an average use of 151 gallons of water per person per day (Utah Division of Water Resources, 2010; see the Septic-Tank-Density Analysis section below). Sewage lagoons exist in the central part of the study area, but these are well designed and therefore not considered in the water budget.

Table 4. *Domestic water rights listed in the Utah Division of Water Rights Database associated with the Johns and Emery Valleys valley-fill aquifer.*

Water Right No.	CFS	Acre-feet
61-1857	0.009	1.988
61-1464	-	2.996
61-2916	-	0.84
61-2403	-	1
61-96	-	0.552
61-2693	-	0.168
61-100	-	0.03
61-133	-	0.013
61-147	-	0.02
61-3213	-	1
61-1466	0.081	18.15
61-126	0.007	1.6
61-299	0.018	4
61-3213	-	1
61-480	0.015	0.45
61-2896	0.01	2.1
61-1767	0.015	1.368
61-2952	-	0.25
61-2936	-	0.25
61-2890	-	0.25
61-2636	-	0.25
61-2412	-	1
61-1907	-	1
61-1908	-	0.982
61-1945	-	1
61-1815	0.012	1.101
61-2915	0.007	0.84
61-1601	-	1.09
61-2752	-	0.25
61-289	0.067	missing value
61-801	0.111	missing value
61-388	0.015	missing value
61-481	0.044	missing value
61-549	0.015	missing value
	TOTAL	**46**

Water Budget Results for Johns and Emery Valleys

The main components of the water budget for the groundwater system in the Johns and Emery Valleys drainage basin for water years 2019 through 2021 are summarized in Table 5. We followed Thiros and Brothers (1993) in assuming that the surface-water drainage boundary is a groundwater divide and any possible interbasin flow reaching the valley-fill would be insignificant compared to other sources of recharge. Therefore, precipitation is the only primary input to the system. Water can leave the system by three primary means: evapotranspiration, discharge to the Tropic Ditch, and discharge from East Fork Sevier River (Figure 32 and see Appendix G Figures G-2 through G-5 for SWB model raster results).

Recharge/Precipitation

The SWB model calculated an average of 382,965 acre-feet/yr of precipitation from 2017 to 2021. Of this amount, 0.33% (2018) to 4.09% (2019) of precipitation becomes infiltration, which is less than Thiros and Brothers' (1993) estimated value of 5% for the entire East Fork Sevier River basin. The SWB model uses Daymet data for precipitation. We compared Daymet data with PRISM precipitation data and found them to be similar for this region, confirming our use of SWB model outputs for precipitation (Table 5).

Discharge

Evapotranspiration: We calculated ET using the SSEBop method and the SWB model. SSEBop calculated ET values 10% to 85% higher than those calculated by the SWB model. It also calculated ET as up to 200% of precipitation. SSEBop and SWB ET results are more similar near the valley floor and less similar in the upland areas of the watershed. We believe that the ponderosa and pinyon-juniper forests may be the source of error in the SSEBop method. Other sources of error could come from clouds and shadows in the remotely sensed data. The SWB model suggests ET is on average 98% of net precipitation (2017–2021).

We elected to use SWB values for ET to apply a single model, and also because of the difference between precipitation and SSEBop ET. The SWB model suggests an average ET of 19 acre-feet/yr for Tropic Reservoir (2017–2021) (Table 7). ET represents 97% of water leaving the study area (SWB model 2017–2021 average). In general, ET and precipitation have a direct relationship and vary together over time.

We calculated ET specific to phreatophytes, wetlands, and riparian areas in the basin. Total ET from these groundwater sources averages 5055 acre-feet/yr, which is 1.4% of total ET (Table 6).

Table 5. *Recharge and discharge estimates showing gains from precipitation and losses from evapotranspiration (ET) and runoff for the study area (in acre-feet per year).*

	2019			2020			2021			2017-2021 Average
Inputs	Above Diversion	Below Diversion	Basin Total	Above Diversion	Below Diversion	Basin Total	Above Diversion	Below Diversion	Basin Total	
Precipitation	140,411	394,242	**534,653**	76,654	233,262	**309,916**	92,405	285,277	**377,682**	**382,965**
Total Input			**534,653**			**309,916**			**377,682**	**382,965**
Outputs	Above Diversion	Below Diversion	Basin Total	Above Diversion	Below Diversion	Basin Total	Above Diversion	Below Diversion	Basin Total	
Evapotranspiration Total	119,984	360,914	**480,898**	71,815	226,162	**297,977**	85,189	266,906	**352,095**	**372,435**
ET from open water	-	-	39	-	-	25	-	-	27	30
ET from agriculture	-	-	2435	-	-	1770	-	-	1777	1940
ET from riparian	-	-	2057	-	-	1223	-	-	1385	1535
ET from wetlands	-	-	2162	-	-	1281	-	-	1474	1580
Other ET	-	-	474,206	-	-	293,679	-	-	347,433	367,350
Surface flow out Total			**16,736**			**4305**			**11,121**	**8017**
Tropic Ditch	5760	-	5760	940	-	940	3686	-	3686	2656
North Boundary	-	10,976	10,976	-	3365	3365	-	7435	7435	5361
Total Output	125,744	371,890	**497,634**	72,755	229,527	**302,282**	88,875	274,342	**363,216**	**380,452**
Storage Change			**37,018**			**7634**			**14,466**	**2513**

Surface water discharge: We attempted to use transducers to calculate flow for water year 2022. The transducer data ratings curve is of limited use because we only have two or three manual measurements to constrain the continuous flow record. Rough jumps in the transducer record of the northern boundary flow site are likely caused by changes in the stilling well and transducer height at that location. Freezing likely caused an increase in pressure at the downstream and upstream transducers near the Tropic Ditch diversion because the thermometers in the transducers reported temperatures near or below 0°C that are coincident with the pressure increases. In addition, water year 2022 may not be representative of other water years in the study area. For example, the Tropic Reservoir gate was left open during the winter months of 2022 (Kirk Forbush, Utah Division of Water Rights, written communication, March 2022), preventing the reservoir from filling and the water managers from performing controlled releases of water to Johns and Emery Valleys.

Due to the limitations of our collected transducer data, we chose to use SWB model runoff for our water budget calculations. The Tropic Ditch is permitted to divert up to 20 cfs (0.57 m^3/s) from April 1 to June 1 and up to 15 cfs (0.42 m^3/s) from June 1 to October 15. We reviewed available transducer data and calculated a rough estimate of total acre-feet flowing below the Tropic Reservoir dam and above the diversion for water year 2022. We used the same dataset to estimate the total acre-feet that exceeded 15 cfs (0.42 m^3/s) in water year 2022, or the water that would be bypassing the diversion and flowing to Johns and Emery Valleys. We found that about 3% of the total flow was above the diversion, meaning that surface water discharge to Tropic Ditch was 97% of runoff from the basin upstream of it. We therefore consider that 97% of runoff from above the diversion ditch, as calculated by the SWB model, represents water lost to the Tropic Ditch. Using these ratios, we calculated that 266 to 5760 acre-feet/yr is diverted to the Tropic Ditch and 8 to 178 acre-feet/yr flows beyond the diversion. These values, with an average of 2656 ac-ft/yr, are in the range of those reported by Carpenter et al. (1967) who found that 2610 acre-feet/yr was diverted to the Tropic Ditch. We assume that all water flowing beyond the diversion was lost to groundwater during our period of study. Changes in management could significantly alter the 3% value we are reporting. For example, we observed that the ditch was still open on October 21, 2021, preventing water from flowing into the East Fork Sevier River.

We used runoff from the watershed below the Tropic Ditch diversion to model surface water runoff at the northern boundary of the study area. We estimated a range of 537 to 10,976 acre-feet/yr, with an average of 5361 acre-feet/yr (2017–2021). These numbers agreed well with the available transducer data, which indicated a baseflow of 7617 acre-feet/yr at the northern boundary of the study area during the 2022 water year. The SWB model values also agreed well with our flow measurements in the northern part of the study area in 2021 and 2022, which suggested a baseflow of about 8000 acre-feet/yr.

Change in Storage

We calculated groundwater and soil-water change in storage on two time-scales: the period of record (1947–2022) and seasonal fluctuations. Change in storage for the valley-wide water balance is the difference between input and output.

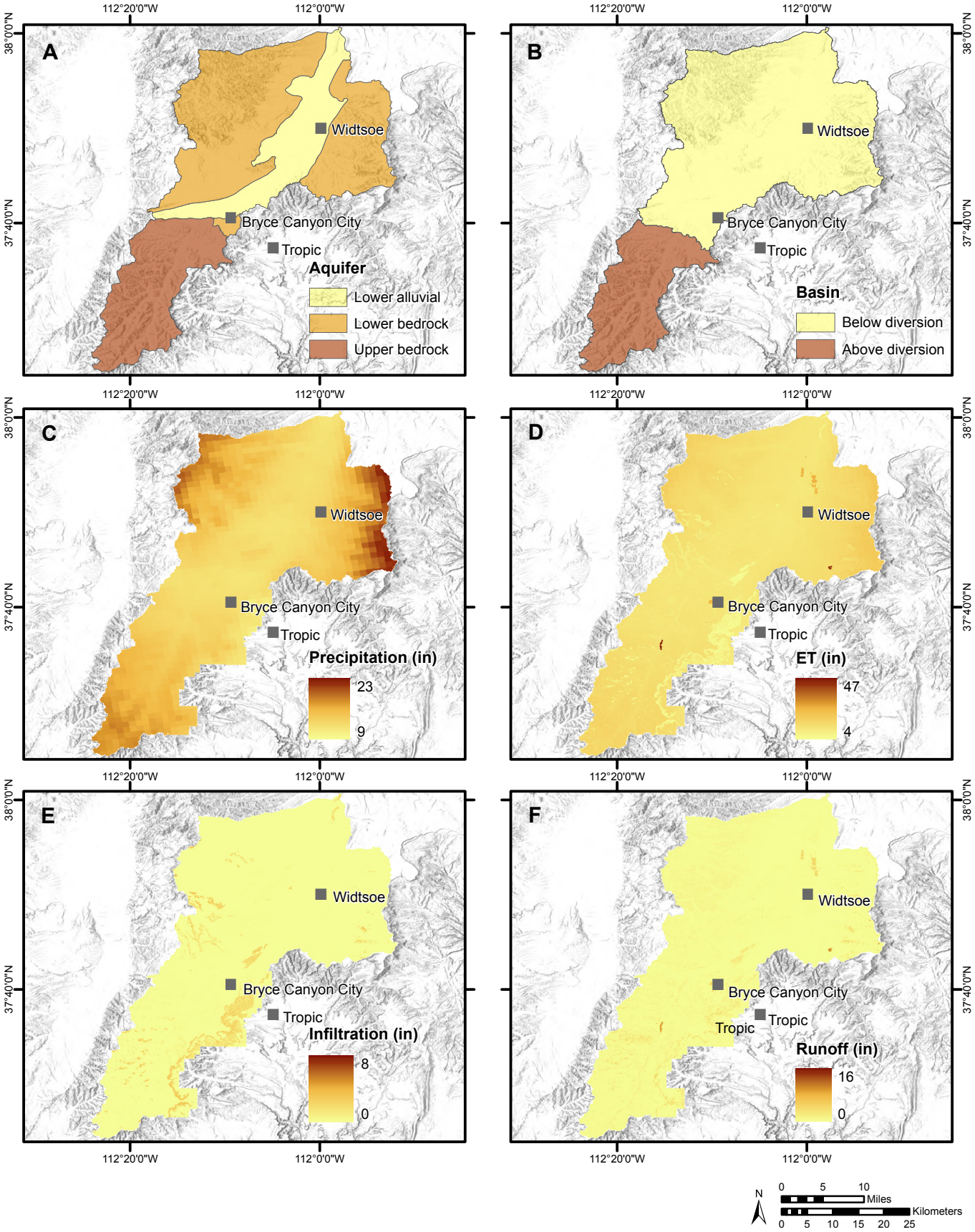

Figure 32. *Maps showing the two ways that the Bryce study area was divided for analysis in the SWB model and example SWB model output rasters.* ***A)*** *Lower alluvial, lower bedrock, and upper bedrock boundaries used for analysis in the SWB model and water budget calculations.* ***B)*** *Areas above and below the Tropic Ditch diversion used for analysis in the SWB model and water budget calculations. Output rasters from the SWB model of water year 2021 showing:* ***C)*** *precipitation,* ***D)*** *evapotranspiration,* ***E)*** *infiltration, and* ***F)*** *runoff.*

Table 6. *The valley-fill aquifer (VFA) water budget (in acre-feet per year).*

Recharge	2017	2018	2019	2020	2021	Averages	Source/Notes
Precipitation infiltration	678	191	2748	497	308	**884**	SWB[1] model
Recharge from septic tanks	62	62	62	62	62	**62**	36 domestic tanks and 3 large underground disposals
Recharge from surrounding runoff	3312	413	7054	2503	5549	**3766**	SWB model
Recharge from upper East Fork	81	8	178	29	114	**82**	SWB model[2]
Interflow from above diversion that recharges VFA	-	0	16	6	0	**6**	Seepage runs and darcy equation range of 6-16 ac-ft/yr
Groundwater recharge from adjacent mountain bedrock	4005	400	12,465	3664	1035	**4391**	SWB model[3]
Total Recharge	**8138**	**1074**	**22,523**	**6761**	**7068**	**9190**	
Discharge	**2017**	**2018**	**2019**	**2020**	**2021**	**Averages**	**Source**
Total phreatophyte evapotranspiration	6060	3654	6653	4274	4635	**5055**	
Wetlands	*1918*	*1066*	*2162*	*1281*	*1474*	*1580*	SWB model
Riparian	*1929*	*1080*	*2057*	*1223*	*1385*	*1535*	SWB model
Agriculture	*2213*	*1508*	*2435*	*1770*	*1777*	*1940*	SWB model
Pumping Total	346	361	375	342	369	**358**	
Public	*296*	*311*	*325*	*292*	*319*	*308*	Estimated from water rights
Domestic	*50*	*50*	*50*	*50*	*50*	*50*	Estimated from water rights
Groundwater Discharge to East Fork at North Boundary	4489	537	10,976	3365	7435	**5578**	SWB
Total Discharge	**10,895**	**4553**	**18,005**	**7981**	**12,440**	**10,992**	
Net Groundwater Change	**-2757**	**-3479**	**4518**	**-1220**	**-5372**	**-1801**	

[1] SWB = soil water balance

[2] Assumes 3% runoff from south basin makes it past the diversion

[3] Assumes 100% of infiltration to bedrock adjacent to the VFA recharges the VFA eventually, as well as 9.5% upper bedrock area recharge.

Table 7. *Tropic Reservoir water budget (in acre-feet per year).*

		Acre-feet per water year			Source/Notes
Component		**2019**	**2020**	**average**	
Inputs	Flow into Tropic Reservoir	15,782	7240	9479	Seepage runs water years 2019, 2020, 2022
	Precipitation into Tropic Reservoir	362	193	278	Daymet, assumes Tropic Reservoir area is 180 acres
	Total	**16,144**	**7433**	**9757**	
Outputs	Evaporation from Tropic Reservoir	23	18	19	SWB model average 2018-2021
	Flow out of dam	15,803	9339	9520	Seepage runs
	Total	**15,825**	**9357**	**9540**	
	Water year input - water year output	**319**	**-1925**	**217**	Possible loss/gain to groundwater, missed surface flow, or reservoir recharge/drawdown
	Reservoir storage change (+ increase)			0	Assumed no net change over multi-year period

Considering the long-term record, we reviewed existing well data from well USGS ID 374205112091501 (Bryce Airport well) at the Bryce Canyon Airport to examine long-term trends for the valley. This well is finished in the upper parts of the Cretaceous bedrock aquifer, but is chemically similar to the valley-fill aquifer (see Chemistry of Groundwater and Surface Water section) and the longest record that we have available in the area. The depth to water fluctuates but maintains an average around 30 feet (9.14 m) (Figure 15). We interpret this to mean that net storage change over the period of record is close to zero.

We examined groundwater levels to form hypotheses about seasonal fluctuations in storage. Conditions during autumn 2018 were drier than normal, with water levels lower in most wells than any other year or season measured. After a heavy snowpack in 2019 (116% of the 30-year median) water levels rose in alluvial wells, and after below-average snowpack in 2020 (70% of the 30-year median) water levels declined in alluvial wells (Appendix D Figure D-2). Water levels in wells completed in bedrock were less variable than alluvial wells, with some water levels declining and others rising during different seasons and years, weather independent (Appendix D Figure D-2). This demonstrates the connection between precipitation and change in groundwater storage, where wetter periods of time yielded higher groundwater levels or an increase in storage. Conversely, drier periods yielded lower groundwater levels or decreased storage. These findings suggest that extended periods of above-average precipitation could increase storage and extended periods of drought could decrease storage in the valley-fill aquifer, even though the long-term trend in storage change has been close to zero.

Valley-Fill Aquifer Water Budget

We estimated the 2017–2021 water year components of input and output from the valley-fill aquifer to conceptualize the interchange of water between groundwater and surface water (Table 6) and to see how a change in one component may influence other components. To constrain the components we used the SWB model, seepage runs, and compilation of available data.

Recharge to the Valley-Fill Aquifer

Precipitation: Precipitation directly over the valley-fill aquifer averaged 36,255 acre-feet/yr from 2017 to 2021 based on the SWB model. Infiltration from precipitation ranged from 191 (2018) to 2748 acre-feet/yr (2019). Average infiltration was 884 acre-feet/yr (2017–2021) (Table 6). We calculated precipitation using the SWB model (Daymet) and confirmed these data using PRISM.

Losing streams: During the study period, all of the East Fork Sevier River flow bypassing the Tropic Ditch diversion was lost to the valley-fill aquifer. Water users are permitted to divert up to 20 cfs (0.57 m^3/s) through the Tropic Ditch from April 1 to June 1 and up to 15 cfs (0.42 m^3/s) from June 1 to October 15. We used transducer data to determine periods when flow above the diversion was in excess of 15 cfs (0.42 m^3/s). In 2022, this was about 3% of the total runoff recorded by our transducer. Therefore, we took 3% of runoff calculated for the area above the diversion by the SWB model to be the total groundwater contribution from the watershed above the Tropic Ditch diversion. Runoff passing the diversion ranged from 8 to 178 acre-feet/yr and averaged 82 acre-feet/yr.

All flow from runoff in tributaries to the East Fork, adjacent to the valley-fill aquifer, fully infiltrates the alluvium. We used SWB runoff calculated for the adjacent uplands to estimate tributary recharge. Runoff from these areas ranged from 413 to 7054 acre-feet/yr and averaged 3766 acre-feet/yr from 2017 to 2021. We compared these values to average point flow measurements for each tributary collected between 2018 and 2022. These hand measurements totaled to an average of 3518 acre-feet/yr, which confirms the SWB model calculations.

Unused irrigation seepage and septic-tank drain-field seepage: As discussed above, Johns and Emery Valleys rely on stream and spring water for irrigation. The SWB model allowed us to calculate total values for water entering the valley-fill aquifer, all of which eventually recharges the aquifer, whether in channel or on the fields, less ET.

Groundwater recharge by septic-system leachate, both domestic and LUWDS, was about 62 acre-feet/yr for water years 2018–2021.

Throughflow from above the Tropic Ditch diversion: We used a simple Darcy flux calculation to approximate flow in the valley-fill aquifer past the Tropic Ditch diversion. A gradient of 0.007 exists near the diversion, where the valley bottom is approximately 1320 feet (400 m) wide and we estimate about 10 feet (3 m) of alluvial fill across the valley bottom. Thiros and Brothers (1993) determined that hydraulic conductivity of alluvial fill in this area ranged from 6 to 20 ft/day (1.8–6 m/day), similar to our calculated geometric mean hydraulic conductivity of 12 ft/day (3.7 m/day) (Appendix C Table C-2). Using these inputs we calculate a range of flow from 6 to 16 acre-feet/yr. The years 2018 and 2021 were exceptionally low precipitation years, limiting water availability, so we determined that there was no throughflow during these water years. The year 2019 had above-average precipitation, so we used the upper end of the range at 16 acre-feet/yr. The year 2020 had below-average precipitation, so we used a lower approximation of 6 acre-feet/yr.

Mountain-block recharge: For this study, we assume precipitation that infiltrates bedrock adjacent to the valley-fill aquifer moves primarily horizontally, eventually charging small alluvial channels, fans, or the aquifer directly as the water moves from the lower-hydraulic-conductivity bedrock

to higher-hydraulic-conductivity valley fill. We delineated infiltration in the bedrock adjacent to the aquifer and used the SWB infiltration output to estimate recharge. We determined mountain-block recharge was 400 to 12,465 acre-feet/yr, with an average of 4391 acre-feet/yr (2017–2021).

Discharge from the Valley-Fill Aquifer

Evapotranspiration from the groundwater system: Evapotranspiration directly from groundwater (as opposed to the surface or vadose zone) occurs through plants transpiring water from the water table or capillary fringe. Evaporation from bare ground occurs if the water table or capillary fringe is near the surface. This ET occurs primarily in areas of wetland vegetation, including riparian areas, where the groundwater table is shallow and within the reach of plant roots. Studies in the western U.S. have shown that phreatophytes, especially greasewood, can utilize groundwater from a water table as deep as 30 feet (9 m) below surface when precipitation does not meet plant needs (Moreo et al., 2007).

We delineated areas of wetland, riparian, and irrigated vegetation. We then summarized SWB model output rasters of actual ET by these boundaries. ET from phreatophytes ranged from 3654 to 6653 acre-feet/yr, with an average total of 5055 acre-feet/yr.

Gaining stream: The East Fork Sevier River is losing or dry through most of its course, with no flow through the center of the valley. The river gains abruptly in the northern part of the study area, due to groundwater discharge. Using runoff values from the SWB model, we estimated flow in the East Fork Sevier River to be 537 to 10,976 acre-feet/yr and an average of 5578 acre-feet/yr (2017–2021). For water year 2022, we estimated a total flow of 7617 acre-feet at the northern end of the study area using our transducer data. Hand measurements taken during 2021 and 2022 suggest a total flow at the northern boundary of approximately 8000 acre-feet/yr.

Well and spring discharge: The largest sources of well discharge from the groundwater system are public supply wells (PSWs): Ruby's Inn, Bristlecone, Bryce Canyon Pines, and Bryce Canyon National Park. Water pumped from PSWs has increased with increased development. The Bristlecone well had records from 2015 to 2021, with one year calculated as average water use and the remainder as metered water use. The range of use for Bristlecone is 18.08 to 36.70 acre-feet/yr, with an average use of 30.33 acre-feet/yr. Two Ruby's Inn water supply wells have data beginning in 1981, but we used the same data range as the Bristlecone well to provide average annual use. For the years 2015 to 2021, average combined use for the PSWs was 233.38 acre-feet/yr, read from a metered unit. The Bryce Canyon Pines well provides data for only 2020 and 2021, with an average use of 16.75 acre-feet/yr. Two PSWs serving Bryce Canyon National Park combined for an average use of 59.69 acre-feet/yr from 2015 to 2021. We estimate the total average discharge from PSWs to be about 308 acre-feet/yr.

We estimated discharge from domestic wells and wells not reported to the Water Use Program (Utah Division of Water Rights, 2022) by applying either the full water right for small domestic water rights or a fraction of the water right for larger rights. These private wells use a total of approximately 50 acre-feet/yr, with individual rights ranging from 0.29 to 18.15 acre-feet/yr.

Another way to estimate water use is by per capita use. Garfield County residents used an estimated 151 gallons of water per person per day in 2015 (Utah Division of Water Resources, 2019). The 2020 population estimate for Bryce Canyon City is 336 (U.S. Census Bureau, 2021). Therefore, total groundwater use is about 57 acre-feet/yr. For our calculations, we used the 50 acre-feet/yr estimated by examining water rights in the valley. Irrigation wells rely on surface water, not groundwater.

Groundwater outflow exiting the basin: We estimated that flow in the alluvium through Black Canyon is insignificant due to the small cross-sectional area of the alluvium. Carpenter et al. (1967) also determined that net groundwater flow into and out of the valley was negligible.

Tropic Reservoir Budget

Recharge

Tropic Reservoir receives recharge primarily from direct precipitation and streamflow from the East Fork Sevier River, and Henderson and Badger Creeks. Groundwater inflow may be another small component. Surface flow into the reservoir ranged from 5417 to 15,782 acre-feet/yr and averaged 9479 acre-feet/yr.

Discharge

Discharge from Tropic Reservoir is primarily from evapotranspiration and releases of water to the East Fork Sevier River drainage. Groundwater outflow may be another small, poorly constrained component. SWB evapotranspiration values for Tropic Reservoir ranged from 17 to 22 acre-feet/yr and averaged 19 acre-feet/yr from 2018 to 2021. Flow out of the dam was measured by hand during seepage runs during the 2019, 2020, and 2022 water years. Flow ranged from 3419 to 15,803 acre-feet/yr and averaged 9520 acre-feet/yr.

Storage Change

Overall, net storage change in the reservoir during the study period is close to zero, but seasonal changes and management

practices create annual changes in water storage. Total average recharge is 9740 acre-feet/yr and total average discharge is 9540 acre-feet/yr. It is possible that water seeps from the reservoir, but more data are required to confirm this value.

Water Supply

Historical well records and previous water budgets show that the valley watershed has been in a generally balanced state since the 1960s. Long-term monitoring records indicate that wet years in which water is put into storage in the groundwater reservoir balance dry years (Figure 15). However, there are few long-term data records to support this idea, making several of the water budget components difficult to quantify. Therefore, we recommend continuous monitoring of select sites. The valley-fill and Claron aquifers appear sensitive to increases or decreases in precipitation, with water levels in wells increasing or decreasing directly in response to heavy or light snowpack years (Figure 14). Similarly, continued drought could offset the observed balance in the aquifers and result in net depletion of the groundwater. The immediate response of these aquifers to snowpack indicates that the response to prolonged drought may also be instantaneous and directly related.

SEPTIC-TANK DENSITY ANALYSIS

Introduction

Groundwater resource development and increased applications for water rights and large underground wastewater disposal systems (LUWDS) prompted part of this study to understand groundwater quality and quantity in the study area. Most new development is expected to be on valley-fill deposits of the unconsolidated alluvial aquifer. We performed a nutrient analysis (discussed earlier) and septic-tank density study of the area to understand the impact of future growth due to an increase in LUWDS (mostly from hotels). We characterized the water chemistry of the Emery Valley and southwestern Johns Valley drainage basin as it pertains to the valley-fill aquifer thickness and land-use practices with emphasis on nitrate. Coupled with the nutrient data, we provide a mass-balance analysis based on septic-tank systems and groundwater flow available for mixing and background nitrate concentrations and conducted a potential contaminant source inventory to determine a correlation between land use and nitrate concentrations.

Land-use planners have long used soil maps and septic-tank suitability maps to determine where septic-tank systems will likely percolate within an acceptable range. However, studies show that percolation alone does not remediate many constituents found in wastewater, such as nitrate. Under aerobic conditions, ammonium from septic-tank effluent can convert to nitrate, contaminating groundwater and posing potential health risks to humans (primarily very young infants; Comley, 1945; Fan et al., 1987; Bouchard et al., 1992). Studies involving lab rats ingesting a combination of nitrate and heptamethyleneimine in drinking water reported an increase in tumor occurrence (Taylor and Lijinsky, 1975). However, epidemiological investigations involving human beings have shown conflicting evidence. Stomach cancer in humans associated with nitrate from drinking water was reported in Colombia and Denmark (Cuello et al., 1976; Fraser et al., 1980). Conversely, investigations in the United Kingdom and other countries indicate no correlation exists between nitrate levels and cancer incidence (Forman, 1985; Al-Dabbagh et al., 1986; Croll and Hayes, 1988; Taneja et al., 2017). The U.S. Environmental Protection Agency (EPA) maximum contaminant level for drinking water (and Utah groundwater quality standard) for nitrate as nitrogen is 10 mg/L (U.S. EPA, 2022). Mass-balance calculations of nitrate in groundwater have been used to evaluate the potential impact of septic-tank systems on groundwater quality in Utah (Hansen, Allen, and Luce, Inc., 1994; Zhan and McKay, 1998; Wallace and Lowe, 1999; Lowe and Wallace, 1999; Lowe et al., 2000, 2002, 2003; Bishop et al., 2007a, 2007b; Jordan et al., 2019; Schlossnagle et al., 2022).

The purpose of septic-tank density mapping conducted in this study is to provide recommended septic-tank densities for the Bryce Canyon City area, including Emery Valley and southern Johns Valley, using the mass-balance approach to evaluate potential water-quality degradation. We estimated groundwater hydraulic conductivity from aquifer tests and specific capacity data to estimate flow. For the study area, we determined subdomain area acreage, groundwater flow volume, number of existing septic-tank systems, and present-day nitrate concentrations. Then, using the appropriate amount of wastewater and accompanying nitrogen load introduced per septic-tank system and large-scale wastewater disposal systems from hotels, we projected nitrogen loadings based on increasing numbers of septic tank soil-absorption systems. By limiting allowable degradation of groundwater nitrate concentration to 1 mg/L (the amount of water-quality degradation acceptable by government officials in previous septic-tank density studies), we were then able to derive septic-tank density recommendations valley-wide.

With continued human population growth and installation of septic tank soil-absorption systems in new developments, the potential for contamination from septic systems will increase. At the time we conducted this study, the estimated 2019 population of Bryce Canyon City was 222 with an average of 3.3 people per household (pph), so we extrapolated the average population estimate of 3.3 pph in the Bryce area and applied it to the 36 septic systems outside of Bryce Canyon City to calculate effluent per day for a domestic home. We applied a mass-balance calculation to evaluate the potential impact of septic-tank systems on groundwater quality in Johns and Emery Valleys, allowing planners to help designate appropriate average septic-system densities in their community. The current minimum lot size in Garfield County for septic systems is one

acre per system. We used nitrate as a proxy for dispersion and dilution of most common septic-tank effluent constituents because it is soluble, mobile, and less expensive to test than other constituents. We used this analysis as a gross model for evaluating the possible impact of proposed developments using septic-tank systems for wastewater disposal on groundwater quality.

The Mass-Balance Approach

General Methods

We use a mass-balance approach for water-quality degradation assessments because it is a practical method to apply under time, budget, and data availability/acquisition constraints, and it provides a quantitative basis for land-use planning decisions. In the mass-balance approach to compute projected nitrate concentrations, the average nitrogen mass expected from projected new septic tanks is added to the existing mass of nitrogen in groundwater and then diluted with the estimated groundwater flow available for mixing, plus water that is added to the system by septic tanks and LUWDS. We used an estimated discharge of 198 gallons (749 L) of effluent per day for a domestic home based on a per capita indoor usage of 60 gallons (227 L) per day (Utah Division of Water Resources, 2010) by an average 3.3-person household (U.S. Census Bureau, 2017). We used an estimated nitrogen loading of 64 mg/L of effluent per domestic septic tank based on (1) an average 3.3 people per household, (2) an average nitrogen loading of 17 g nitrogen per capita per day (Kaplan, 1988), (3) 227 L per capita per day water use, and (4) an assumed retention of 15% of the nitrogen in the septic tank (to be later removed during pumping) (Andreoli et al., 1979); this estimated nitrogen loading is close to Bauman and Schafer's (1985) nitrogen concentration in septic-tank effluent of 62 ± 21 mg/L based on the averaged means from 20 previous studies. We determined groundwater flow available for mixing, the major control on nitrate concentration in aquifers when using the mass-balance approach (Wallace and Lowe, 1999), using aquifer test data compiled from drinking water source protection documents on six wells in the study area, along with specific capacity data from well logs (Appendix C Table C-1).

We obtained the number of septic-tank systems based on data provided by the Southwest Utah Public Health Department, Garfield County, and aerial imagery to identify structures served by a septic-tank system (Southwest Utah Public Health Department, Jeremy Roberts, written communication, September 15, 2019; Kaden Figgins, Garfield County Economic Development Director, written communication, November 19, 2019).

For the analysis, we used 36 septic systems and six LUWDS (three existing and three proposed but not yet operating) in the study area (Figure 33). Ambient nitrate concentration is 0.35 mg/L. For our mass-balance calculations, we allowed a 1 mg/L degradation above current background levels of nitrate (a value adopted by other Utah counties as an acceptable level of degradation to be protective of water quality [Hansen, Allen, and Luce, Inc., 1994]) as a reference point to evaluate the potential impact of increased numbers of septic-tank systems. Local government officials may choose a different nitrate concentration as an acceptable level of degradation, but we recommend a maximum of 5 mg/L nitrate concentration under special circumstances (for example, if background nitrate concentrations are uncommonly high) to be protective of water quality.

In our mass-balance approach, the nitrogen mass from the projected additional septic systems and LUWDS was added to the current nitrogen mass and then diluted with the amount of groundwater flow available for mixing plus the water added by the septic-tank systems and LUWDS themselves. We used the following equation to determine the projected nitrate concentration resulting from additional septic systems, and thus to determine how many septic-tank systems can be added before exceeding a designated target nitrate concentration:

$$N_P = \frac{[(ST_T - ST_C)Q_{ST}] * N_{ST} + [N_A(Q_{GW} + [ST_T * Q_{ST}])] + [N_{ST} * Q_{UW}]}{[ST_T * Q_{ST}] + Q_{GW} + Q_{UW}} \quad (6)$$

where:

N_P = projected nitrate concentration (mg/L),

N_A = ambient (background) nitrate concentration for the domain (mg/L)

N_{ST} = estimated average nitrate concentration from septic tanks (mg/L)

ST_T = total number of septic tanks in the domain (variable, unitless)

ST_C = current number of septic tanks (constant, unitless)

Q_{ST} = flow from each septic tank in liters per second (L/s)

Q_{UW} = flow from LUWDS (L/s)

Q_{GW} = groundwater flow derived from transmissivity data (L/s)

To determine a recommended septic-system density, we divided the domain area acreage by the total number of septic tanks (ST_T) that existed at the projected nitrate concentration (N_P).

Groundwater Flow Calculations

We calculated groundwater flow available for mixing using the Darcy flow equation as:

$$Q = KbLi \quad (7)$$

where:

Q = volume of discharge (ft^3/sec)

K = hydraulic conductivity (ft/sec)

b = vertical mixing zone thickness (ft)

L = width of cross section (ft) where flow occurs

i = hydraulic gradient (ft/ft)

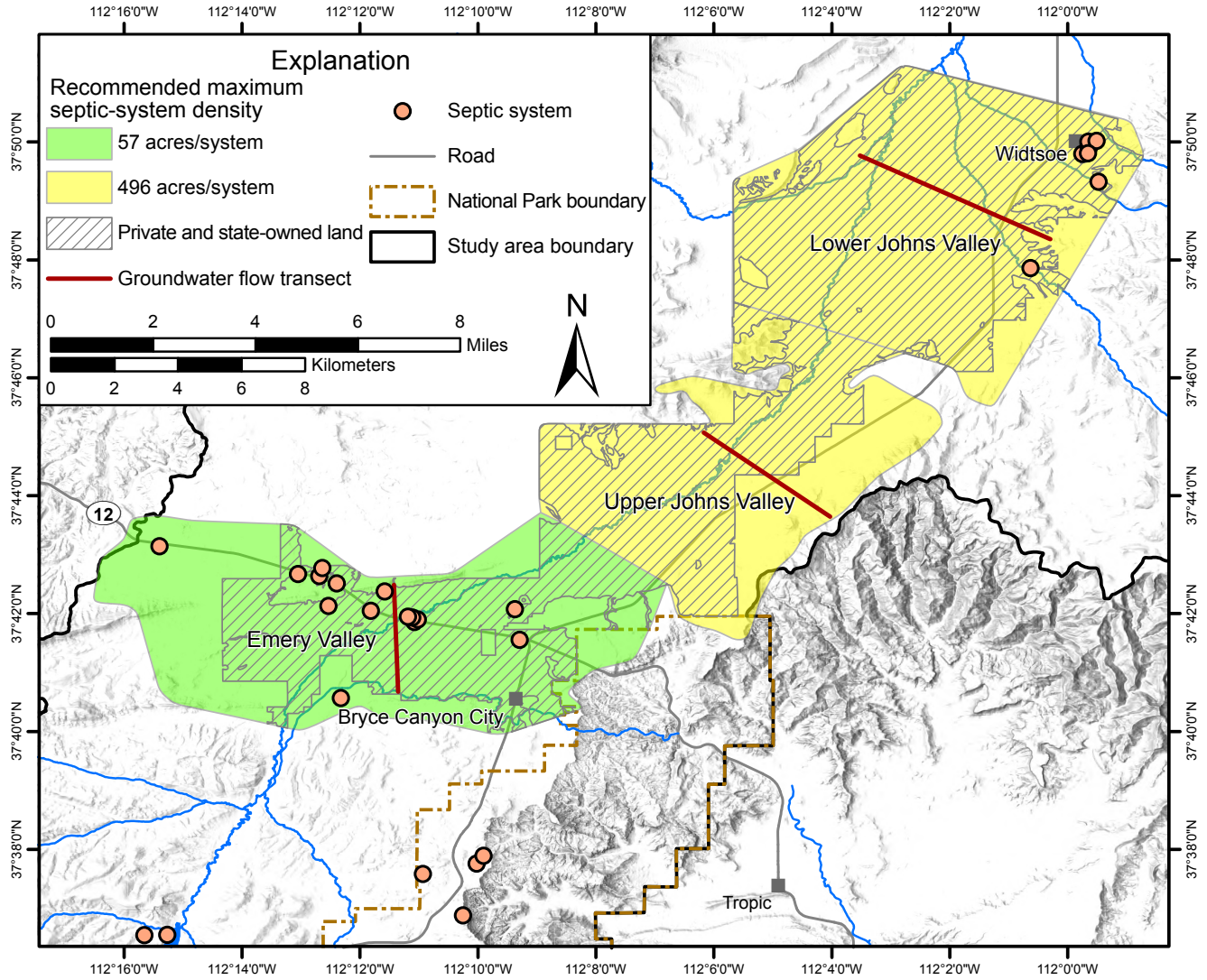

Figure 33. *Location of septic systems and subdomains in the study area.*

We used data from aquifer tests compiled from drinking water source protection documents (Diedre Beck, Utah Division of Drinking Water, written communication, February 2, 2019) and well logs to estimate groundwater flow for our mass-balance approach assessment (Appendix C Table C-1). We used well water levels measured during autumn 2018 to determine groundwater flow direction and generate a potentiometric surface map. In the study area, we interpreted the mixing zone as represented by up to 150 feet of alluvium based on valley-fill aquifer thickness (Figure 8) and depth to water; we assumed uniform and complete mixing/dilution of septic-tank effluent occurs within this layer. The upper part of the aquifer is where nitrate associated with septic-tank systems is most likely to degrade water quality. Bauman and Schafer (1985) found that mixing zone thickness has minimal impact on nitrate concentrations in aquifers having low groundwater velocities like those commonly found in Utah. This offsets the potential of the high ratio of horizontal to vertical hydraulic conductivity to limit the depth of the mixing zone. Aquifer parameters used to quantify groundwater flow are detailed in Table 8.

We used discharge data from the Utah Division of Water Quality for LUWDS (Robert Beers, written communication, April 23, 2020) to augment the amount of effluent discharged from domestic septic tanks. At the time of this analysis, three LUWDS discharged from larger facilities along Highway 12: Bryce Canyon Pines (11,779 gallons per day [gpd]), Bryce Canyon Resort and Shuttle Terminal (22,000 gpd), and Bryce Point Lodge (7565 gpd). Other LUWDS proposals have been approved by the Utah Division of Water Quality for two hotels north of Bryce Point Lodge (29,500 gpd total) and additional recreational vehicle pads at Bryce Canyon Pines (4375 gpd). Because these latter facilities have been approved and are expected to discharge water into the aquifer, we take these numbers into account in our mass-balance calculations.

Region-Specific Septic-System Density Evaluations

We partitioned the study area into three subdomains in Emery Valley and southern Johns Valley using region-specific

Table 8. *Aquifer parameters used to compute groundwater flow available for mixing.*

Parameter	Emery Valley	Lower Johns Valley	Upper Johns Valley
Hydraulic conductivity (K)	28.8 ft/day	2.43 ft/day	2.43 - 28.8 ft/day*
Thickness of mixing zone (b)	100 ft	150 ft	100 - 150 ft*
Width of cross section (L)	10,990 ft	17,780 ft	13,460 ft
Hydraulic gradient (I)	0.00624	0.00521	0.00521 - 0.00624*
Volume of water available for mixing (Q)	2.29 ft^3/sec	0.39 ft^3/sec	0.2 - 4.2 ft^3/sec

*Based on values used in Emery Valley and lower Johns Valley calculations

groundwater flow available for mixing to aid in determining recommended septic-system density and lot size (Figure 33). Reported acreages and septic-system densities are based only on land where future development is feasible (e.g., private and State-owned land). One subdomain is Emery Valley, which has the most development, the highest existing septic-system density of the study area, and all currently operating and proposed LUWDS. A second subdomain is referred to as lower Johns Valley, which includes the unincorporated community of Widtsoe, and has some development and existing septic systems. The third subdomain is referred to as upper Johns Valley, the southernmost part of Johns Valley between Emery Valley and lower Johns Valley. This area currently has little to no development and no existing septic systems.

Emery Valley

Groundwater flow direction is generally to the east in Emery Valley. Based on water-level data collected in autumn 2018 and spring 2019, the average horizontal hydraulic gradient in the valley ranges from 0.0051 to 0.0062. Based on specific capacity data from wells in the valley fill, transmissivities in the Emery Valley subdomain range from 72 to 10,680 ft^2/day. From transmissivity we calculate hydraulic conductivities ranging from 3 to 557 ft/day. Using the average hydraulic gradient, hydraulic conductivities, and a mixing zone thickness of 100 feet (30.5 m), we estimated groundwater flow available for mixing through a 2.1-mile (3.4 km) transect (Figure 33) is 2.29 ft^3/sec (Table 8). Of the 36 septic systems in the study area, 28 are in or immediately upgradient of Emery Valley (Figure 33). Emery Valley is approximately 8700 acres, so the current average septic-system density is about 310 acres/system. The three existing and three proposed but not operating LUWDS are also located within Emery Valley.

Figure 34A shows a plot of projected nitrate concentration in the Emery Valley area versus number of septic systems and septic-system density. For Emery Valley to maintain an overall nitrate concentration of 1.35 mg/L (allowing 1 mg/L of degradation as described above), the total number of septic systems should not exceed 152 based on the estimated nitrogen load of 64 mg/L per septic system. The increase in nitrogen concentration corresponds to an increase of 124 new septic systems and an average septic-system density of 57 acres/system (Figure 34A). However, the maximum discharge from the approved but not yet operating LUWDS is equivalent to approximately 171 additional septic systems, exceeding the recommendation. The additional nitrate loading from LUWDS would raise the overall nitrate concentration to 4.68 mg/L. We can assume that discharge from LUWDS in Emery Valley is coupled with high tourism season (March through early October). Groundwater pumping for culinary use would also peak during this time, increasing the potential for movement of septic-tank effluent toward water-supply wells. If we reduce new LUWDS discharge to 60% of maximum to better estimate the likely flow of LUWDS used at capacity only part of the year, the resultant discharge is equivalent to 103 additional septic systems and an overall nitrate concentration of 3.15 mg/L. If the allowable nitrate degradation concentration is increased to 5 mg/L, then between 440 and 508 additional septic systems could be added, depending on discharge from the additional LUWDS. The corresponding septic-system density is 14 acres/system (Appendix F Table F-2).

Lower Johns Valley

Groundwater flow direction is generally to the north-northeast in lower Johns Valley. Based on water-level data collected in autumn 2018 and spring 2019, the average hydraulic gradient in lower Johns Valley is 0.0052. Based on estimates from limited specific capacity data, transmissivities in the lower Johns Valley subdomain range from 25 to 355 ft^2/day. From transmissivity, we calculated hydraulic conductivities ranging from 0.26 to 59 ft/day. Using the average hydraulic gradient given above, hydraulic conductivities, and a mixing zone thickness of 150 feet (45.72 m), estimated groundwater flow available for mixing through a 3.37-mile (5.42 km) transect (Figure 33) is 0.39 ft^3/sec. Of the 36 septic systems in the study area, eight are in lower Johns Valley. Lower Johns Valley is approximately 14,200 acres, so the current average septic-system density is about 1775 acres/system. In 2019, there were no LUWDS in lower Johns Valley.

Figure 34B shows a plot of projected nitrate concentration in the lower Johns Valley area versus the number of septic systems and septic-system density. For lower Johns Valley to maintain an overall nitrate concentration of 1.35 mg/L (allowing 1 mg/L of degradation as described above), the total

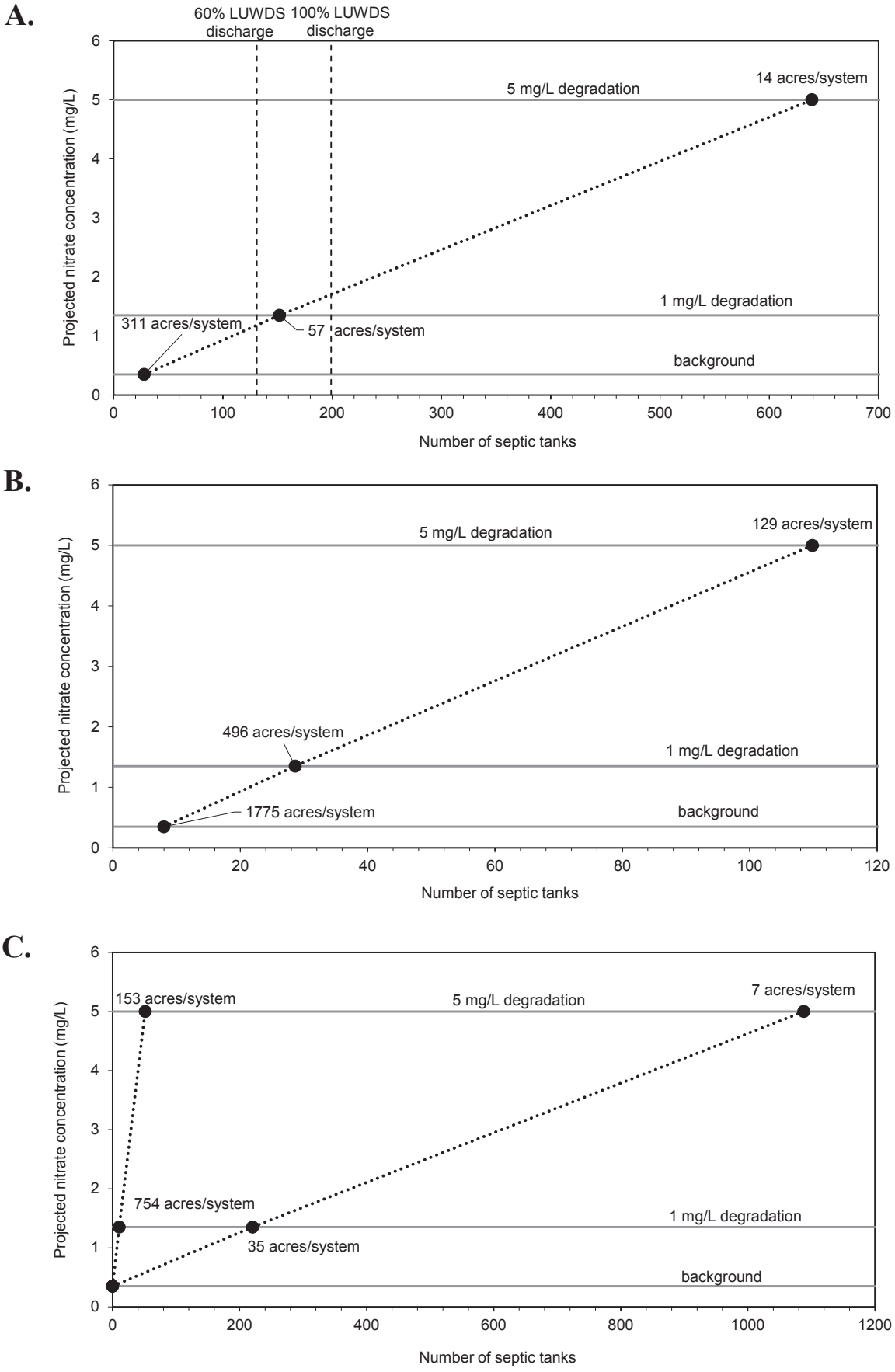

Figure 34. *Projected nitrate concentration versus septic-system density. LUWDS = large underground wastewater disposal system.* ***A)*** *Emery Valley subdomain.* ***B)*** *Lower Johns Valley subdomain.* ***C)*** *Upper Johns Valley subdomain.*

number of septic systems should not exceed 29 based on the estimated nitrogen load of 64 mg/L per septic system. This total corresponds to an increase of 21 new septic systems and an average septic-system density of about 496 acres/system (Figure 34B). If the allowable nitrate degradation concentration is increased to 5 mg/L, 102 additional septic systems could be added, resulting in a septic-system density of 129 acres/system (Appendix F Table F-2).

Upper Johns Valley

Groundwater flow direction is generally to the northeast in upper Johns Valley, which is about 7800 acres. There are no wells in this subdomain from which to derive transmissivity, hydraulic conductivity, or hydraulic-gradient data from estimates. Using the wide range of hydraulic gradient and hydraulic conductivity values from Emery Valley and lower Johns Valley and a mixing zone thickness ranging from 100 to 150 feet (30.5 to 45.7 m), maximum estimated groundwater flow available for mixing through a 2.55-mile (4.10 km) transect (Figure 33) ranges from 0.2 to 4.2 ft^3/sec (Table 8). There are no septic systems or LUWDS in upper Johns Valley.

Figure 34C shows a plot of projected nitrate concentration in the upper Johns Valley area versus number of septic systems and septic-system density. For upper Johns Valley to maintain an overall nitrate concentration of 1.35 mg/L (allowing 1 mg/L of degradation as described above), the total number of septic systems should not exceed between 10 and 220, based on the estimated nitrogen load of 64 mg/L per septic system and the range of groundwater flow estimates. This total corresponds to an increase of 10 to 220 new septic systems and an average septic-system density of about 35 to 754 acres/system (Figure 34C). If the allowable degradation level of nitrate concentration is increased to 5 mg/L, between 51 and 1088 septic systems could be added, depending on groundwater flow calculations. The corresponding septic-system density would be 7 to 153 acres/system (Appendix F Table F-2).

Discussion

For our analysis, we only considered housing units built within the limits of the valley-fill aquifer and ignored housing units in Bryce Canyon City and Bryce Canyon National Park that are serviced by two separate sewage lagoons. Furthermore, we only considered groundwater that flows in the valley-fill aquifer, not the sandstone or limestone aquifers, as we consider it to be the primary path for groundwater in the shallow subsurface where septic leachate is focused. In addition, our approach assumes uniform spatial distribution of septic systems and temporally consistent production of effluent. Tourism-related development is likely to be concentrated along the current corridor of development and both effluent production and groundwater pumping for culinary supply are likely to be higher during the peak tourism season.

Figure 34 shows plots of projected nitrate concentration versus number of septic-tank systems located in the valley fill in the study area in three different subdomains. The present-day ambient (background) nitrate concentration for the valley-fill aquifer is 0.35 mg/L nitrate as nitrogen. The valley-fill aquifer (excluding Tropic Reservoir and non-developable lands) has a collective surface area of approximately 63,700 acres, so the existing average septic-system density is 1770 acres per system. If we only consider land where future development is feasible (e.g., private and State-owned), the surface area is 30,700 acres and existing septic-system density is 853 acres per system. Based on our analyses, maximum estimated groundwater flow available for mixing in the valley-fill aquifer ranges from 0.39 ft^3/sec in the lower Johns Valley subdomain to 2.29 ft^3/sec in the Emery Valley subdomain. Given the higher uncertainty in the upper Johns Valley subdomain, groundwater flow available for mixing ranges from 0.2 to 4.2 ft^3/sec. Higher septic-system discharge is expected to be coupled with future population growth, which is included in the equation. The scenarios we present allow 1 mg/L of degradation over the 2019 mean concentration. Allowable water-quality degradation of 1 mg/L nitrate in the scenarios presented above is for discussion only; our data can be used to make land-use decisions for any level of water-quality degradation.

We did not consider agricultural contributions to groundwater nitrate in our approach, and new septic input may be partially negated by a decrease in agricultural nitrate input as land use changes from agriculture to residential. Nitrate contribution to groundwater from future development could also be lessened by a requirement that new systems use advanced nitrogen removal technology. Advanced systems may decrease the amount of total nitrogen in effluent by more than 50% compared to the 64 mg/L value we used in our analysis (Lancellotti et al., 2017).

The 2019 geometric mean nitrate concentration in the principal valley-fill aquifer is 0.23 mg/L, and, because nitrate concentrations in wells are log-normally distributed, there is a 95% certainty that a well's nitrate concentration will not exceed 0.91 mg/L under current conditions. As mean concentration increases with the addition of septic tanks and LUWDS, the probability of encountering high nitrate concentrations also increases.

Recommendations

Our analyses of nitrate concentrations/water-quality degradation provide the least conservative (best case) first approximation of long-term groundwater pollution from septic-tank systems. The plots of projected nitrate concentration versus number of septic-tank systems (Figure 34) show recommended septic-tank density based on the parameters described above. For land-use planning purposes, we consider two categories of recommended maximum septic-tank system densities for development using septic tank soil-absorption

systems for wastewater disposal: 57 acres per system in Emery Valley and 496 acres per system in southern Johns Valley (Figure 34, Appendix F Table F-2). We recommend applying the more conservative septic-system density calculated for the lower Johns Valley subdomain to the upper Johns Valley subdomain given the groundwater flux uncertainty in the upper Johns Valley mass-balance analysis. Our lot-size recommendations apply to development using septic systems for wastewater disposal, and are not relevant to development using well-engineered, well-constructed sewage lagoon systems or advanced onsite wastewater treatment systems. However, poorly engineered and constructed sewage lagoon systems could have a greater negative impact on groundwater quality than septic-tank systems.

FUTURE WATER RESOURCE IMPACTS AND DEVELOPMENT

Water Supply

The water supply for Johns and Emery Valleys is primarily modern groundwater from the valley-fill aquifer. The widespread presence of modern groundwater in the valley-fill and Claron Formation aquifers suggests these aquifers are actively recharged with relatively short flow paths and thus sensitive to fluctuations in snowpack levels and climate change and are susceptible to surface-based contamination sources.

Shallow groundwater systems such as the Johns and Emery Valleys valley-fill aquifer that are dominated by modern water are indicative of active in situ recharge and are typically highly responsive to climate variability on short time scales (Kundzewicz and Doell, 2009). If, in the future, climate change results in reduced snow water equivalent and soil moisture and increased extreme precipitation events and consumptive water use due to higher potential evapotranspiration as predicted for central Utah (USGCRP, 2018), in situ recharge to the valley-fill aquifer may decline.

Shallow, young groundwater systems lacking major areas of valley-floor discharge (i.e., upward vertical hydraulic gradient) and laterally continuous confining layers above the aquifer, as is present in Johns and Emery Valleys, are highly susceptible to contamination from nearby sources. The most likely new sources of potential groundwater contamination will come from tourism-related development.

Increased future water use in the Johns and Emery Valleys will likely be related to tourism-based development. Future development of groundwater resources in the valley-fill aquifer may result in a reduction of groundwater discharge to the East Fork Sevier River, an already scarce surface water resource. Shallow water in the valley-fill aquifer is generally recharged locally and is sensitive to climatic changes (Figure 14). An increase in groundwater withdrawal from the valley-fill aquifer can affect the water table, potentially reducing the hydraulic gradient toward northern Johns Valley, and thus recharge, to the valley.

Effect of Adding LUWDS and Septic Systems

Eight LUWDS projects are currently planned for the area north of Highway 12 as of June 2023, with potential flow of 140,850 gallons per day (gpd). Each of these is required to treat the wastewater per the Utah Division of Water Quality's requirements so that the treated effluent has no more than 2.5 mg/L total inorganic nitrogen upon discharge (Robert Beers, written communication, DWQ, November 15, 2022). The installation of these LUWDS will nearly double the amount of effluent currently discharged in Emery Valley.

New development using septic tanks as wastewater disposal will mostly return to the groundwater system, though as poorer quality groundwater recharge. New development using existing sewage lagoons could potentially discharge as surface water, but with likely negligible evaporation in this high-desert cold climate.

Need for Increased Monitoring of Tropic Reservoir, Tropic Ditch Diversion, and East Fork Sevier River Flow

This study concludes that the valley-fill aquifer is recharged by precipitation and surface water, responding readily to fluctuations in climate. Wetter-than-average years result in increased groundwater levels, whereas drier-than-average years result in decreased water levels. In recent times, all water flowing beyond the Tropic Ditch diversion into Emery Valley has been lost to groundwater, highlighting the aquifer's reliance on the East Fork Sevier River and its tributaries. This study demonstrates that groundwater discharge in northern Johns Valley supports an extensive wetlands system and streamflow in the East Fork Sevier River. Some of this groundwater likely recharges in the mountains in the northern part of the valley, far from currently proposed development, but some is derived from the valley-fill aquifer in the Emery–southern Johns Valley area. Extensive groundwater development in Emery Valley and southern Johns Valley would cause the potentiometric surface in the valley-fill aquifer there to decline, reducing the hydraulic gradient to the north and thereby capturing some of the groundwater discharge in northern Johns Valley. Reduced groundwater discharge would potentially affect the groundwater-dependent ecosystem represented by the wetlands and decrease streamflow out of the valley. The Sevier River basin suffered the greatest reduction in streamflow and reservoir storage in Utah during the 2021–2022 extreme drought (https://www.nrcs.usda.gov/wps/portal/wcc/home/quicklinks/states/utah/water/). Due to the close link between groundwater and surface water in Emery and Johns Valleys and limited groundwater storage in the valley-fill aquifer, reduction of the potentiometric surface may impact streamflow in an already vulnerable system. The exception is the northernmost reach

in Johns Valley, where groundwater recharges the East Fork Sevier River as it exits the basin. The scant long-term water-level data indicate groundwater levels have fluctuated around a steady average, but extended drought could easily alter this balanced pattern and result in decreased water availability. The relatively recent period of drought has increased the percentage of total recharge coming from the East Fork Sevier River, which depends on how Tropic Reservoir and Tropic Ditch are managed. We suggest continued monitoring of this drainage at points above and below Tropic Reservoir, in the Tropic Ditch, and of the East Fork Sevier River as it exits northern Johns Valley, especially if the drought persists.

The interaction between the valley-fill aquifer and bedrock aquifers is poorly understood. In general, groundwater levels increase or decrease in valley-fill aquifer wells in response to the amount of winter precipitation and resulting recharge compared to bedrock wells, which show little or no response to fluctuations in precipitation events. It would be beneficial to construct nested piezometers completed in both aquifers so that pump tests could be conducted to better understand the vertical gradient between aquifers and the amount and location of groundwater–surface-water exchange between the East Fork Sevier River and the valley-fill aquifer. Monitoring wells could also enable evaluation of the hydrogeologic influence of local faults.

SUMMARY

Groundwater resource development and the threat of future drought in Garfield County in the area including Bryce Canyon City in Emery Valley and adjoining Johns Valley to the north prompted this study. Water quality and quantity and the potential for water-quality degradation are critical elements determining the extent and nature of future development in the valleys. Most development in the area centers along the east-west corridor of Highway 12 that borders Bryce Canyon City and the gateway to Bryce Canyon National Park. Tourism is the major draw to the area where millions of people visit, thereby acting as a temporary population who enjoy seasonal and recreational opportunities. Because of the potential increase in growth from tourism-related development and an increased demand on water resources, this study was warranted to aid with careful land-use planning and resource management to preserve Johns and Emery Valleys' surface and groundwater resources.

The primary goals of this study were to (1) characterize the hydrogeology of the Johns and Emery Valleys drainage basin as it pertains to the occurrence and flow of groundwater, with emphasis on delineating the valley-fill aquifer thickness and lithology and determining the water-yielding characteristics of unconsolidated and fractured-rock aquifers in the study area; (2) characterize groundwater levels, chemistry, flow paths, and connection to surface water; (3) develop a water budget for the drainage basin; and (4) develop septic-system density recommendations and an aquifer classification map.

New data collected for this study includes 124 gravity measurements; water levels in 45 wells; discharge measurements at 32 streams and canals and 29 springs; general chemistry from 62 wells, springs, and surface water sites; water quality from 43 wells and springs; stable isotopes from 101 wells, springs, surface water, and precipitation; and radiometric isotopes from 19 wells and springs.

Groups of geologic units having similar hydrogeologic properties are classified as either aquifers (unconsolidated valley fill, Tertiary conglomerate, Cretaceous sandstone/conglomerate), confining units (Tertiary tuff and volcaniclastic mudstone/siltstone, Cretaceous shale), or having mixed hydrogeologic properties (Tertiary brecciated volcaniclastics and tuff, Tertiary mudstone/limestone/siltstone/sandstone, and Cretaceous sandstone/siltstone/mudstone). The principal aquifer in Johns and Emery Valleys is the unconsolidated valley-fill aquifer, which is mostly unconfined, except locally. Despite the classification of the Claron Formation as a mixed hydrogeologic unit, it is one of the primary bedrock aquifers of the region.

Johns and Emery Valleys have complex structural components of faults and folds that likely affect groundwater movement. The north-south-trending Paunsaugunt normal fault runs the length of the study area bordering Johns Valley on the east and extends south along the eastern margin of Bryce Canyon National Park. The Pine Hills and Rubys Inn thrust faults, which strike east-west and form the northern and southern boundaries, respectively, of Emery Valley, and the Johns Valley and Hunt Creek thrust faults northwest of Flake Mountain, which strike northeast through central and northern Johns Valley, respectively, may play a role in the movement of groundwater from bedrock aquifers to the valley-fill aquifer. The role of faults on the groundwater system needs additional research.

Most supply wells in the study area are completed in the valley-fill aquifer, the upper unconfined zone of the Cretaceous aquifer, or across the valley-fill–Cretaceous interface. Geometric mean transmissivities for the valley-fill aquifer and bedrock aquifers (Cretaceous and Claron Formation) are 316 and 69 ft^2/day, respectively. High-quality aquifer test data are generally limited to the Highway 12 corridor through Emery Valley and the thin alluvial drainages on the Paunsaugunt Plateau. Our understanding of valley-fill transmissivity in much of Johns Valley is based on limited specific capacity data from domestic and stock wells, so we may be underestimating transmissivity in this region of greatest aquifer thickness.

Our potentiometric surface maps typically show a slight groundwater depression within Emery Valley, which we attribute to localized pumping of public-supply wells. Potentiometric surface maps and water level change maps

generally show decreasing water levels from spring to autumn, especially following years with below-average snowpack and/or precipitation. Water levels in spring 2022 continued decreasing from the prior year due to an exceptionally poor snowpack. Bedrock wells are less sensitive to climatic variation; wells completed in bedrock show lesser variability in water level measurements and trends do not reflect seasonal or annual variation as in the valley-fill aquifer. Additionally, though long-term monitoring records are sparse, they indicate that groundwater levels in Johns and Emery Valleys are relatively stable.

Stream discharge on the East Fork Sevier River ranged from 0.17 to 43.79 cfs. Our seepage studies show that the East Fork Sevier River on average gains water from groundwater in the Paunsaugunt Plateau, but when it is allowed to flow into Emery Valley over deep valley-fill deposits, begins to lose water to groundwater. The Tropic Ditch plays a key role in this dynamic, as most or all of the river's flow is diverted away from Emery Valley during the growing season. At the northern end of Johns Valley, the East Fork Sevier River becomes a gaining stream again as it encounters the high water table associated with groundwater discharge and extensive wetlands.

Groundwater and surface water is of uniform excellent quality, with a few exceptions. TDS concentrations are low, averaging 295 mg/L, and no sample constituents exceeded primary or secondary water quality standards. TDS concentrations are lower in the valley fill (276 mg/L) than the bedrock aquifers (311 mg/L). Groundwater chemistry throughout the study area aquifers is classified as calcium-magnesium-bicarbonate type water. These consistent data indicate relatively short travel distances where water does not have sufficient time to incorporate additional ions, or the aquifers through which water flows have similar geologic chemical composition, yielding indistinguishable soluble constituents. Overall groundwater quality for the valley-fill aquifer is formally classified as Pristine water quality according to the Utah Division of Water Quality Board.

Environmental tracer analysis allowed us to make several distinctions regarding the aquifers and surface water in Johns and Emery Valleys. Stable isotope ratios of groundwater throughout the study area indicate that recharge is a mixture of winter and summer precipitation, predominantly weighted toward winter precipitation. Stable isotope composition of the East Fork Sevier River falls along an evaporation line consistent with evaporative fractionation of surface water elsewhere, and appears to be controlled by residence time in Tropic Reservoir. Stable isotope ratios from wells and springs show signs of evaporative enrichment as well, due to either evaporation of surface water prior to recharge in losing sections of streams, or from evaporation prior to infiltration of in situ snowmelt. Tritium and radiocarbon data indicate that most wells and springs sampled have a modern recharge source, including wells and springs located in the valley-fill aquifer, Claron Formation, and upper zone of the Cretaceous bedrock aquifer. Tritium and radiocarbon data for two wells screened in the lower zone of the Cretaceous bedrock aquifer at relatively deep depths indicate premodern recharge, with radiocarbon ages ranging from 4800 to 8600 years.

We estimated a water budget for the drainage basin for water years 2017 to 2021 (water year October 1 to September 30) by quantifying annual inflow and outflow. Precipitation is the primary inflow component, and evapotranspiration, loss to the Tropic Ditch, and loss to the East Fork Sevier River at the northern study area boundary are the main outflow components. Our study found that all water flowing past the Tropic Ditch diversion northward in the East Fork Sevier channel is lost to groundwater. All tributary streams were also losing to groundwater through the central part of the study area, which highlights the aquifer's reliance on water from the East Fork Sevier River and its tributaries. The East Fork Sevier River gains in the northernmost reach in Johns Valley, near Black Canyon, where groundwater is discharging to the surface.

A basin-wide soil-water balance for the watershed study area shows that for the valley-fill aquifer, the greatest source of recharge was from adjacent mountain bedrock and surrounding runoff followed by precipitation; discharge for the valley-fill aquifer is dominantly from groundwater seepage to the East Fork Sevier River at the northern boundary followed by evapotranspiration and well water withdrawals. The soil-water balance indicated an average recharge to the valley-fill aquifer of about 9200 acre-feet/yr and average net loss of about 11,000 acre-feet/yr from 2017 to 2021, a time period characterized by drought. Although the long-term change in storage has been close to zero, we recommend careful water resource management for future development given the observed quick response of groundwater levels to climate conditions on shorter timescales.

Tropic Reservoir receives recharge primarily from streamflow from the East Fork Sevier River and small tributaries and direct precipitation; recharge from groundwater is possible but unquantified. Surface flow into the reservoir ranged from 5417 to 15,782 acre-feet/yr and averaged 9479 acre-feet/yr. Discharge from Tropic Reservoir is primarily from evapotranspiration and releases of water to the East Fork Sevier River. Groundwater outflow may be another small, poorly constrained component. SWB model evapotranspiration values for Tropic Reservoir ranged from 17 to 22 acre-feet/yr and averaged 19 acre-feet/yr from 2018 to 2021.

We performed a septic-tank density mass-balance analysis to produce maximum septic-system density recommendations. The mass-balance approach for the valley-fill aquifer in Johns and Emery Valleys indicates that two categories of recommended maximum septic-tank system densities are appropriate for development using septic tank soil-absorption systems for wastewater disposal: 57 acres per system in Emery Valley and 496 acres per system in Johns Valley.

These recommended maximum septic-tank system densities are based on an increase in mean nitrate concentration of 1 mg/L. If the allowable nitrate degradation concentration is increased from 1 to 5 mg/L, maximum septic-tank system density recommendations in Emery and Johns Valley change to 14 acres per system and 129 acres per system, respectively. Allowing this level of nitrate degradation will increase the probability that nitrate concentrations in individual wells could rise above the EPA maximum contaminant level.

Johns and Emery Valleys and the Bryce Canyon City area are sparsely inhabited, though pressures to accommodate tourism-related development have resulted in increased demand on water resources. Future water supply in the valleys will depend on precipitation because the valley-fill aquifer is sensitive to changes in climate. An increased reliance on large-scale underground septic systems may impact the Pristine water quality of the aquifer. Careful water management planning is recommended to preserve the high quality of water resources in the area.

ACKNOWLEDGMENTS

This study was funded by the Utah Division of Water Rights, the National Park Service, the Utah Division of Water Quality, and the Utah Geological Survey. We thank Wayne Sawyer, William Jones, and Moyle Johnson (NPS) for accompanying us in the field at Bryce Canyon National Park. We thank Fred Syrett for allowing access to Ruby's Inn water supply and monitoring wells. Special thanks to Daryl Spencer, Kevin Poe, Tye Ramsay, and Levi Holms for granting access to private property and in some cases, accompanying us to their wells and providing historical information regarding land use and irrigation. We thank Kaden Figgins of Garfield County for providing critical county-wide comment and insight. We thank the landowners for allowing us to access their property and sample their wells. We thank Bill Loughlin (Loughlin Water Associates) for providing data and thoughtful discussions related to this study. We thank Lucy Jordan, Claire Spangenberg, Elisabeth Stimmel, Torri Duncan (UGS), Will Hurlbut, and Emily McDermott (formerly of UGS) for valuable contributions to fieldwork for this study. We thank Lucy Jordan, Stephanie Carney, and Mike Hylland (UGS); Keyvan Asgar and David Jones (Utah Division of Water Rights); Tyler Gilkerson and Jeff Hughes (National Park Service); and Danielle Lenz (Utah Division of Water Quality) for providing comments to the report.

REFERENCES

Abatzoglou J.T., 2011, Development of gridded surface meteorological data for ecological applications and modelling: International Journal of Climatology, v. 33, no. 1, p. 121–131, https://doi.org/10.1002/joc.3413.

Al-Dabbagh, S., Forman, D., Bryson, D., Stratton, I., and Doll, R., 1986, Mortality of nitrate fertilizer workers: British Journal of Industrial Medicine, v. 43, 507 p.

Andreoli, A., Bartilucci, N., Forgione, R., and Reynolds, R., 1979, Nitrogen removal in a subsurface disposal system: Journal (Water Pollution Control Federation), p. 841–854.

Bauman, B.J., and Schafer, W.M., 1985, Estimating groundwater quality impacts from on-site sewage treatment systems, *in* Proceedings of the Fourth National Symposium on Individual and Small Community Sewage Systems, Dec. 10–11, 1984, New Orleans, Louisiana: American Society of Agricultural Engineers Publication 07-85, p. 285–295.

Biek, B., Rowley, P.D., Anderson, J.J., Maldanado, F., Moore, D.W., Hacker, D.B., Eaton, J.G., Hereford, R., Sable, E.G., Filkhorn, H.F., and Matyjasik, B., 2015, Geologic map of the Panguitch 30 x 60 quadrangle, Garfield, Iron, and Kane Counties, Utah: Utah Geological Survey Map M-270dm, scale 1:62,500, https://doi.org/10.34191/M-270DM.

Bishop, C.E., Wallace, J., and Lowe, M., 2007a, Recommended septic tank soil-absorption-system densities for the principal valley-fill aquifer, Sanpete Valley, Sanpete County, Utah: Utah Geological Survey Report of Investigation 259, 36 p., https://doi.org/10.34191/RI-259.

Bishop, C.E., Wallace, J., and Lowe, M., 2007b, Recommended septic tank soil-absorption-system densities for the shallow unconfined aquifer in Cache Valley, Cache County, Utah: Utah Geological Survey Report of Investigation 257, 35 p., https://doi.org/10.34191/RI-257.

Bouchard, D.C., Williams, M.K., and Surampalli, R.Y., 1992, Nitrate contamination of groundwater—sources and potential health effects: American Water Works Association Journal, v. 84, no. 9, p. 85–90.

Bowers, W.E., 1991, Geologic map of Bryce Canyon National Park and vicinity, southwestern Utah: U.S. Geological Survey Miscellaneous Investigations Series Map I-2108, 15 p., 1 plate, scale 1:24,000.

Bown, T.M., Hasiotis, S.T., Genise, J.F., Maldonado, F., and Bowers, E.M., 1997, Trace fossils of Hymenoptera and other insects, and paleoenvironments of the Claron Formation (Paleocene and Eocene), southwestern Utah, *in* Maldonado, F., and Nealey, L.D., editors, Geologic studies in the Basin and Range-Colorado Plateau transition in southeastern Nevada, southwestern Utah, and northwestern Arizona, 1995: U.S. Geological Survey Bulletin 2153, p. 43–58.

Braca, G., 2008, Stage-discharge relationships in open channels—practices and problems: FORALPS Technical Report 11, University of Trento, Italy, Department of Civil and Environmental Engineering, 24 p.

Bradbury, K.R., and Rothschild, E.R., 1985, A computerized technique for estimating the hydraulic conductivity of

aquifers from specific capacity data: Groundwater, v. 23, no. 2, p. 240–246.

Carpenter, C.H., Robinson, G.B. Jr., and Bjorklund, L.J., 1967, Ground-water conditions and geologic reconnaissance of the upper Sevier River basin, Utah: U.S. Geological Survey Water Supply Paper 1836, 98 p.

Clark, I., and Fritz, P., 1997, Environmental isotopes in hydrogeology: Boca Raton, CRC Press, 328 p.

Comley, H.H., 1945, Cyanosis in infants caused by nitrates in well water: Journal of the American Medical Association, v. 129, p. 112.

Cooper, H.H., and Jacob, C.E., 1946, A generalized graphical method for evaluating formation constants and summarizing wellfield history: EOS, Transactions American Geophysical Union, v. 27, no. 4, p. 526–534.

Craig, H., 1961, Isotopic variations in meteoric waters: Science, v. 133, no. 3465, p. 1702–1703.

Croll, B.T., and Hayes, C.R., 1988, Nitrate and water supplies in the UK: Environmental Pollution, v. 50, no. 1-2, p. 163–187.

Cuello, C., Correa, P., Haenszel, W., Gordillo, G., Brown, C., Archer, M., and Tannenbaum, S., 1976, Gastric cancer in Colombia—cancer risk and suspect environmental agents: Journal of the National Cancer Institute, v. 57, p. 1015–1020.

Daly, C., Halbleib, M., Smith, J.I., Gibson, W.P., Doggett, M.K., Taylor, G.H., Curtis, J., and Pasteris, P.A., 2008, Physiographically-sensitive mapping of temperature and precipitation across the conterminous United States: International Journal of Climatology, v. 28, p. 2031–2064.

Daly, C., Smith, J.I., and Olson, K.V., 2015, Mapping atmospheric moisture climatologies across the conterminous United States: PloS ONE, v. 10, no. 10, doi:10.1371/journal.pone.0141140.

Davis, G.H., and Pollock, G.L., 2010, Geology of Bryce Canyon National Park, Utah, *in* Anderson, P.B., Chidsey, T.C., Jr., and Sprinkel, D.A., editors, Geology of Utah's Parks and Monuments: Utah Geological Association Publication 28, p. 37–59.

Doelling, H.H., 2008, Geologic map of the Kanab 30 x 60 quadrangle, Kane and Washington Counties, Utah, and Coconino and Mohave Counties, Arizona: Utah Geological Survey Map MP-08-2dm, scale 1:100,000, https://doi.org/10.34191/MP-08-2DM.

Doelling, H.H. and Willis, G.C., 2018, Interim geologic map of the Escalante 30 x 60 quadrangle, Garfield and Kane Counties, Utah: Utah Geological Survey OFR-690dm, scale 1:100,000, https://doi.org/10.34191/OFR-690DM.

Domenico, P.A., 1972, Concepts and models in groundwater hydrology: New York, McGraw Hill, 416 p.

Doremus, L., and Kreamer, D., 2000, Groundwater movement and water chemistry at Bryce Canyon National Park: Water Resources in Arizona and the Southwest—Proceedings of the 2000 Meetings of the Hydrology Section Arizona-Nevada Academy of Science, p. 81–94.

Dutton, C. E., 1880, Geology of the high plateaus of Utah: U.S. Geographical and Geological Survey of the Rocky Mountain Region: Washington, Government Printing Office, 307 p.

Fan, A.M., Willhite, C.C., and Book, S.A., 1987, Evaluation of the nitrate drinking water standard with reference to infant methemoglobinemia and potential reproductive toxicology: Regulatory Toxicologic Pharmacology, v. 7, no. 2, p. 135–148.

Fontes, J.C., and Garnier, J.M., 1979, Determination of the initial ^{14}C activity of the total dissolved carbon—a review of the existing models and a new approach: Water Resources Research, v. 15, p. 399–413.

Forman, D., 1985, Nitrates, nitrites and gastric cancer in Great Britain: Nature, v. 313, p. 620–625.

Fraser, P., Chilvers, C., Beral, V., and Hill, M.J., 1980, Nitrate and human cancer, a review: International Journal of Epidemiology, v. 9, p. 3–11.

Gettings, P., Chapman, D.S., and Allis, R., 2008, Techniques, analysis, and noise in a Salt Lake Valley 4D gravity experiment: Geophysics, v. 73, no. 6, p. WA71–WA82.

Gibson, J.J., Birks, S.J., and Edwards, T.W.D., 2008, Global prediction of δ_A and δ^2H-$\delta^{18}O$ evaporation slopes for lakes and soil water accounting for seasonality: Global Biogeochemical Cycles, v. 22, no. 2, p. GB2031.

Gillies, R.R., and Ramsey, R.D., 2009, Climate of Utah, *in* McGinty, E.I.L., editor, Rangeland resources of Utah: Logan, Utah State University Cooperative Extension Service, p. 39–45.

Gonfiantini, R., 1978, Standards for stable isotope measurements in natural compounds: Nature, v. 271, no. 5645, p. 534–536.

Goldstrand, P.M., 1994, Tectonic development of Upper Cretaceous to Eocene strata of southwestern Utah: Geological Society of America Bulletin, v. 106, p. 145–154.

Goldstrand P.M., and Mullet, D.J., 1997, The Paleocene Grand Castle Formation—a new formation on the Markagunt Plateau of southwestern Utah, *in* Maldonado, Florian, and Nealey, D.L., editors., Geologic studies in the Basin-and-Range–Colorado Plateau transition in southeastern Nevada, southwestern Utah, and northwestern Arizona, 1995: U.S. Geological Survey Bulletin 2153, p. 59–77.

Gregory, H.E., 1944, The geology and geography of the Paunsaugunt region: U.S. Geological Survey Professional Paper 226, 116 p., 4 plates, scale 1:62,500.

Han, L.F., and Plummer, L.N., 2013, Revision of Fontes & Garnier's model for the initial ^{14}C content of dissolved inorganic carbon used in groundwater dating: Chemical Geology, v. 351, p. 105–114.

Hansen, Allen, and Luce, Inc., 1994, Hydrogeologic/water quality study, Wasatch County, Utah: Salt Lake City, unpublished consultant's report, p. III-1–III-18.

Hart, R., 2009, Isotopic evaluation of carbon dioxide in soil gas in Utah for a more accurate input variable in groundwater age models: Provo, Utah, Brigham Young University, M.S. thesis, 62 p.

Hargreaves, G.H., and Samani, Z.A., 1985, Reference crop evapotranspiration from temperature: Applied Engineering in Agriculture, v. 1, no. 2, p. 96–99, doi: 10.13031/2013.26773.

Hem, J.D., 1985, Study and interpretation of the chemical characteristics of natural water: U.S. Geological Survey Water-Supply Paper 2254, 263 p.

Hintze, W.J., Aiken, C., Brozena, J., Coakley, B., Dater, D., Flanagan, G., Forsberg, R., Hildenbrand, T., Keller, G.R., Kellogg, J., Kucks, R., Li, X., Mainville, A., Morin, R., Pilkington, M., Plouff, D., Ravat, D., Roman, D., Urrutia-Fucugauchi, J., Veronneau, M., Webring, M., and Winester, D., 2005, New standards for reducing gravity data—the North American gravity database: Geophysics, v. 70, no. 4, p. J25–J32.

Ingerson, E., and Pearson, F.J., 1964, Estimation of age and rate of motion of ground water by the ^{14}C method, *in* Miyake, Y., and Koyama, T., editors, Recent researches in the fields of hydrosphere, atmosphere and nuclear chemistry: Editorial Committee for Sugawara Volume, Water Research Laboratory, Nagoya University, Tokyo, p. 263–283.

Ingraham, N.L., and Taylor, B.E., 1991, Light stable isotope systematics of large-scale hydrologic regimes in California and Nevada: Water Resources Research, v. 27, no. 1, p. 77–90.

Johnson, A.I., 1967, Specific yield—compilation of specific yield for various materials: U.S. Geological Survey Water-Supply Paper 1662-D, 74 p.

Jordan, J.L., Smith, S.D., Inkenbrandt, P.C., Lowe, M., Hardwick, C., Wallace, J., Kirby, S.M., King, J.K., and Payne, E.E., 2019, Characterization of the groundwater system in Ogden Valley, Weber County, Utah, with emphasis on groundwater–surface-water interaction and the groundwater budget: Utah Geological Survey Special Study 165, 222 p., 3 plates, https://doi.org/10.34191/SS-165.

Kalin, R.M., 2000, Radiocarbon dating of groundwater systems, *in* Cook, P.G., and Herczeg, A.L., editors, Environmental tracers in subsurface hydrology: Boston, Springer, p. 111–144.

Kaplan, O.B., 1988, Septic systems handbook: Chelsea, Lewis Publishers, Inc., 290 p.

Kendall, C., and Caldwell, E.A., 1998, Fundamentals of isotope geochemistry, *in* Kendall, C., and McDonnell, J.J. editors, Isotope tracers in catchment hydrology: Amsterdam, Elsevier Science, p. 51–86.

Knudsen, T.R., Biek, R.F., and Eaton, J.G., *in preparation*, Geologic map of Bryce Canyon National Park and vicinity: Utah Geological Survey Map, 2 plates, scale 1:24,000.

Kundzewicz, Z., and Doell, P., 2009, Will groundwater ease freshwater stress under climate change?: Hydrological Sciences Journal, v. 54, p. 665–675.

Lancellotti, B.V., Loomis, G.W., Hoyt, K.P., Avizinis, E., and Amador, J.A., 2017, Evaluation of nitrogen concentration in final effluent of advanced nitrogen-removal onsite wastewater treatment systems (OWTS): Water, Air, & Soil Pollution, v. 228, no. 10, p. 383.

Lawton, T.F., Pollock, S.L., and Robinson, R.A.J., 2003, Integrating sandstone petrology and nonmarine sequence stratigraphy—application to the Late Cretaceous fluvial systems of southwestern Utah, U.S.A.: Journal of Sedimentary Research, v. 73, no. 3, p. 389–406.

Lindsey, B.D., Jurgens, B.C., and Belitz, K., 2019, Tritium as an indicator of modern, mixed, and premodern groundwater age: U.S. Geological Survey Scientific Investigations Report 2019–5090, 18 p., https://doi.org/10.3133/sir20195090.

Loughlin Water Associates, LLC, 2022, Expert report—Ruby's Inn vs. Teresa Wilhelmsen et al.—Case No. 200600028, 107 p.

Lowe, M., and Wallace, J., 1999, The hydrogeology of Ogden Valley, Weber County, Utah, and recommended wastewater management practices to protect groundwater quality, *in* Spangler, L.E., and Allen, C.J., editors, Geology of northern Utah and vicinity: Utah Geological Association Publication 27, p. 313–336.

Lowe, M., Wallace, J., and Bishop, C.E., 2000, Analysis of septic-tank density for three areas in Cedar Valley, Iron County, Utah—a case study for evaluations of proposed subdivisions in Cedar Valley: Utah Geological Survey Water Resource Bulletin 27, 66 p., https://doi.org/10.34191/WRB-27.

Lowe, M., Wallace, J., and Bishop, C.E., 2002, Water-quality assessment and mapping for the principal valley-fill aquifer in Sanpete Valley, Sanpete County, Utah: Utah Geological Survey Special Study 102, 91 p., 13 plates, https://doi.org/10.34191/SS-102.

Lowe, M., Wallace, J., and Bishop, C.E., 2003, Ground-water quality classification and recommended septic tank soil absorption-system density maps, Cache Valley, Cache County, Utah: Utah Geological Survey Special Study 101, 31 p., 10 plates, https://doi.org/10.34191/SS-101.

Mackin, J.H., and Rowley, P.D., 1976, Geologic map of the Three Peaks quadrangle, Iron County, Utah: U.S. Geological Survey Geologic Quadrangle Map GQ-1297, scale 1:24,000.

Maldonado, F., and Moore, R.C., 1995, Geologic map of the Parowan quadrangle, Iron County, Utah: U.S. Geologi-

cal Survey Geologic Quadrangle Map 1762, 1 plate, scale 1:24,000.

Maldonado, F., and Williams, V.S., 1993a, Geologic map of the Parowan Gap quadrangle, Iron County, Utah: U.S. Geological Survey Geologic Quadrangle Map 1712, 1 plate, scale 1:24,000.

Maldonado, F., and Williams, V.S., 1993b, Geologic map of the Paragonah quadrangle, Iron County, Utah: U.S. Geological Survey Geologic Quadrangle Map 1713, 1 plate, scale 1:24,000.

Marine, W.I., 1963, Ground-water resources of the Bryce Canyon National Park Area, Utah with a section on the drilling of a test well: U.S. Geological Survey Water-Supply Paper 1475-M, p. 441–486.

Mook, W.G., 1972, On the reconstruction of the initial ^{14}C content of groundwater from the chemical and isotopic composition, *in* Eighth International Conference on Radiocarbon Dating: Royal Society of New Zealand, p. 342–352.

Moreo, M.T., Laczniak, R.J., and Stannard, D.I., 2007, Evapotranspiration rate measurements of vegetation typical of ground-water discharge areas in the Basin and Range carbonate-rock aquifer system, White Pine County, Nevada, and adjacent areas in Nevada and Utah, September 2005–August 2006: U.S. Geological Survey Scientific Investigations Report 2007–5078, 37 p.

Mullet, D.J., 1989, Interpreting the early Tertiary Claron Formation of southern Utah: Geological Society of America Abstracts with Programs, v. 21, p. 120.

Natural Resources Conservation Service, 2021, National Water and Climate Center, Online, Agua Canyon Utah SNOTEL site annual water year data: https://wcc.sc.egov.usda.gov/reportGenerator/view/customMultiTimeSeriesGroupByStationReport/annual_water_year/end_of_period/, accessed April 26, 2021.

Natural Resources Conservation Service, 2022, Soil survey geographic (SSURGO) database: United States Department of Agriculture, Online: https://sdmdataaccess.sc.egov.usda.gov, accessed December 2022.

National Park Service, 2020, Bryce Canyon NP annual recreation visitation 1929–last calendar year: Online, https://irma.nps.gov/STATS/SSRSReports/Park%20Specific%20Reports/Annual%20Park%20Recreation%20Visitation%20(1904%20-%20Last%20Calendar%20Year)?Park=BRCA, accessed January 2023.

Ott, A.L., 1999, Detailed stratigraphy and stable isotope analysis of the Claron Formation, Bryce Canyon National Park: Pullman, Washington State University, M.S. thesis, 129 p.

Pan-American Center for Earth and Environmental Studies (PACES), 2012, Gravity database of the US: University of Texas, El Paso, Online, http://research.utep.edu/paces, accessed June 2021.

Peeters, L., 2014, A background color scheme for Piper plots to spatially visualize hydrochemical patterns: Groundwater, v. 52, no. 1, p. 2–6.

Roberts, E.M., 2007, Facies architecture and depositional environments of the Upper Cretaceous Kaiparowits Formation, southern Utah: Sedimentary Geology, v. 197, p. 207–233.

Rowley, P.D., Mehnert, H.H., Naeser, C.W., Snee, L.W., Cunningham, C.G., Steven, T.A., Anderson, J.J., Sable, E.G., and Anderson, R.E., 1994, Isotopic ages and stratigraphy of Cenozoic rocks of the Marysvale volcanic field and adjacent areas, west-central Utah: U.S. Geological Survey Bulletin 2071, 35 p.

Rowley, P.D., Biek, R.F., Sable, E.G., Boswell, J.T., Vice, G.S., Hatfield, S.C., Maxwell, D.J., and Anderson, J.J., 2013, Geologic map of the Brian Head quadrangle, Iron County, Utah: Utah Geological Survey Map 263DM, 38 p., 2 plates, scale 1:24,000.

Rozanski, K., Araguás-Araguás, L., and Gonfiantini, R., 1993, Isotopic patterns in modern global precipitation, *in* Swart, P.K., Lohmann, K.C., McKenzie, J., and Savin, S., editors, Climate change in continental isotopic records: American Geophysical Union, Geophysical Monograph Series, v. 78, p. 1–36, https://doi.org/10.1029/GM078p0001.

Schlossnagle, T.H., Wallace J., and Payne, N., 2022, Analysis of septic-tank density for four communities in Iron County, Utah—Newcastle, Kanarraville, Summit, and Paragonah: Utah Geological Survey Report of Investigation 284, 27 p., https://doi.org/10.34191/RI-284.

Scholl, M.A., Ingebritsen, S.E., Janik, C.J., and Kauahikaua, J.P., 1996, Use of precipitation and groundwater isotopes to interpret regional hydrology on a tropical volcanic island—Kilauea volcano area, Hawaii: Water Resources Research, v. 32, no. 12, p. 3525–3537.

Senay, G., Bohms, S., Singh, R., Gowda, P., Velpuri, N., Alemu, H., Verdin, J., 2013, Operational evapotranspiration mapping using remote sensing and weather datasets—A new parameterization for the SSEB approach: Journal of the American Water Resources Association, v. 49, https://doi.org/10.1111/jawr.12057.

Senay, G., Schauer, M., Friedrichs, M., Manohar, V., Singh, R., 2017, Satellite-based water use dynamics using historical Landsat data (1984–2014) in the southwestern United States: Remote Sensing of Environment, v. 202, https://doi.org/10.1016/j.rse.2017.05.005.

Solomon, D.K., and Cook, P.G., 2000, ^{3}H and ^{3}He, *in* Cook, P., and Herczeg, A.L., editors, Environmental tracers in subsurface hydrology: Boston, Kluwer Academic Publishers, p. 397–424.

Tamers, M.A., 1975, Validity of radiocarbon dates on groundwater: Geophysical Surveys, v. 2, no. 2, p. 217–239.

Taneja, P., Labhasetwar, P., Nagarnaik, P., and Ensink, J.H.H., 2017, The risk of cancer as a result of elevated levels of

nitrate in drinking water and vegetables in Central India: Journal of Water & Health, v. 15, p. 602–614.

Taylor, H.W., and Lijinsky, W., 1975, Tumor induction in rats by feeding heptamethyleneimine and nitrite in water: Cancer Research, v. 35, p. 505–812.

Tillman, F.D., 2015, Documentation of input datasets for the soil-water balance groundwater recharge model of the Upper Colorado River Basin: U.S. Geological Survey Open-File Report 2015–1160, 26 p., https://doi.org/10.3133/ofr20151160.

Theis, C.V., 1935, The relation between the lowering of the piezometric surface and the rate and duration of discharge of a well using ground-water storage: EOS, Transactions American Geophysical Union, v. 16, no. 2, p. 519–524.

Thiros, S.A., and Brothers, W.C., 1993, Ground-water hydrology of the upper Sevier River Basin, south-central Utah, and simulation of ground-water flow in the valley-fill aquifer in Panguitch Valley: Utah Department of Natural Resources Technical Publication 102, 121 p.

Thornton, M.M., Shrestha, R., Wei, Y., Thornton, P.E., Kao, S., and Wilson, B.E., 2021, Daymet– daily surface weather data on a 1-km grid for North America, version 4: ORNL DAAC, Oak Ridge, Tennessee.

U.S. Census Bureau, 2017, 2012–2016 American community survey 5-year estimates: Online, https://factfinder2.census.gov, accessed June 2020.

U.S. Census Bureau, 2021, 2020 Census data, Online, https://data.census.gov/cedsci/, accessed January 2023.

U.S. Department of Agriculture, 1986, Urban hydrology for small watersheds: Natural Resources Conservation Service Technical Release 55 (TR-55), 164 p.

U.S. Environmental Protection Agency, 2022, Current drinking water standards: Online, https://www.epa.gov/ground-water-and-drinking-water/national-primary-drinking-water-regulations, accessed March 3, 2022.

U.S. Global Change Research Program, 2018, Impacts, risks, and adaptation in the United States—Fourth National Climate Assessment, Volume II: Washington, D.C. , 1515 p., doi: 10.7930/NCA4.2018.

Utah Division of Water Quality, 1998, Aquifer classification guidance document: Salt Lake City, unpublished Utah Division of Water Quality report, 9 p.

Utah Division of Water Quality, 2014, Standard operating procedure for collection of water chemistry samples: Salt Lake City, Utah Division of Water Quality unpublished report, 25 p.

Utah Division of Water Resources, 2010, 2009 residential water use—survey results and analysis of residential water use for seventeen communities in Utah: Salt Lake City, Utah Department of Natural Resources, 37 p.

Utah Division of Water Resources, 2019, 2015 Municipal and industrial water use data—2019 version 2: Salt Lake City, Utah Department of Natural Resources, 267 p.

Utah Division of Water Resources, 2022, Online: Water related land use: Online, https://utahdnr.maps.arcgis.com/apps/webappviewer/index.html?id=a77c7bcf67fc4c60bb745bff5d1818bd, accessed September 15, 2022.

Utah Division of Water Rights, 2018, Online: Well information-map server: Online, https://maps.waterrights.utah.gov/EsriMap/map.asp?layersToAdd=wellsearch, accessed throughout the entire study 2018 to 2023.

Utah Division of Water Rights, 2022, Utah water use program: Online, https://waterrights.utah.gov/asp_apps/generalWaterUse/WaterUseList.asp, accessed September 15, 2022.

Wallace, J., and Lowe, M., 1999, A mass-balance approach for recommending septic tank–soil-absorption system density/lot-size requirements based on potential water quality degradation due to nitrate examples from three Utah valleys, *in* Spangler, L.E., and Allen, C.J., editors, Geology of northern Utah and vicinity: Utah Geological Association Publication 27, p. 267–274.

Wallace, J., and Schlossnagle, T.H., 2021, Petition for groundwater quality classification, Bryce Canyon area, Garfield County, Utah: Utah Division of Water Quality unpublished Aquifer Classification Petition Document, 46 p.

Wallace, J., Schlossnagle, T.H., Hurlow, H.H., Payne, N., and Hardwick, C., 2021, Hydrogeologic study of the Bryce Canyon City area, including Johns and Emery Valleys, Garfield, County, Utah: Utah Geological Survey Open File Report 733, 69 p., https://doi.org/10.34191/OFR-733.

Westenbroek, S.M., Engott, J.A., Kelson, V.A., and Hunt, R.J., 2018, SWB Version 2.0—a soil-water-balance code for estimating net infiltration and other water-budget components: U.S. Geological Survey USGS Numbered Series 6-A59, https://doi.org/10.3133/tm6A59.

White, D.E., and Chuma, N.J., 1987, Carbon and isotopic mass balance models of Oasis Valley–Forty-Nine Mile Canyon ground water basin, southern Nevada: Water Resources Research v. 23, no. 4, p. 571–582.

Williams, P.L., and Hackman, R.J., 1971, Geology, structure, and uranium deposits of the Salina quadrangle, Utah: U.S. Geological Survey Miscellaneous Geology Investigations Map 1-591, scale 1:250,000.

Winter, T.C., Harvey, J.W., Franke, O.L., and Alley, W.M., 1998, Ground water and surface water—a single resource: U.S. Geological Survey Circular 1139, 79 p.

Zhan, H., and McKay, W.A., 1998, An assessment of nitrate occurrence and transport in Washoe Valley, Nevada: Environmental and Engineering Geoscience, v. 4, no. 4, p. 479–489.

APPENDICES

APPENDIX A

Percentage Log of Well Cuttings

UTAH GEOLOGICAL SURVEY

Well Name: 1 Bryce Well Owner: Lion/Monsanto API #: 4301710662
Location: 37.69264, -112.217187 (WGS84); 990FNL 990FWL Section 10 T36S R04W (PLSS)
Geologist: Hugh Hurlow

Depth Range (feet)		PERCENTAGES						COMMENTS
		Unconsolidated/Disaggregated[A] Categories are lithologic types; see descriptions below						
		Sandstone[1]	Limestone[2]	Tuff[3]	Quartzite[4]	Crystalline quartz & calcite[5]	Siltstone[6]	
0	30	50					0	Sandstone particles are variably weathered.
30	40	50	45	2	0	3	0	" "
40	50	50	45	3	0	2	0	" "
50	60	85	0	5	0	5	5	Sandstone is disaggregated
60	70	60	30	8	0	2	0	Sandstone particles are variably weathered.
70	80	60	30	8	0	2	0	" "
80	90	75	20	4	0	1	0	" "
90	100	85	20	2	0	3	0	" "
100	110	60	35	3	0	2	0	" "
110	120	30	60	5	5	0	0	" "
120	130	5	45	5	45	0	0	" "
130	140	5	45	5	45	0	0	" "
140	150	60	30	4	3	3	0	" "
150	160	70	24	0	2	2	2	" "
160	170	45	50	0	3	0	2	" "
170	180	30	39	30	0	1	0	" "
180	190	45	45	2	5	1	2	" "
190	200	75	20	3	1	1	0	" "
200	270	-	-	-	-	-	-	No cuttings. See note B.
270	280	95	2	1	1	0	1	See note C.
280	290	98	1	1	0	0	0	" "

Notes

A. Cuttings from 0 to 200 feet depth consist of rock fragments of sand to pebble size, and disaggregated minerals. The wide variety of rock types and ages and presence of some rounded, weathered boundaries on pebble-sized fragments in the cuttings indicate that these are unconsolidated basin-fill deposits. The basin-fill deposits may be entirely gravel and sand, or finer-grained material may have been washed away during drilling and/or sample collection.

B. The basin fill-bedrock contact is interpreted to be between 200 and 270 feet deep.

C. Sandstone is fresh, unlike in cuttings from shallower depths. Non-sandstone fragments may be derived from well bore above. Interpreted as John Henry Member of the Straight Cliffs Formation in this interval and below.

Lithologic Type Descriptions – Basin Fill

1. Gray to pale-brown, fine- to coarse-grained quartz-lithic sandstone, well- to moderately sorted, calcite cement.
2. Orange, pink, and white micrite to microcrystalline limestone, interpreted as Claron Formation (Eocene).
3. White to pale-gray quartz-phyric tuff, microcrystalline groundmass, thin quartz veins. Phenocrysts are 1–2 mm diameter.
4. Dark gray to black, fine-grained quartzite grading to siltstone, noncalcareous cement.
5. Crystalline calcite and quartz, translucent to milky-opaque. May include vein quartz and calcite and detrital quartz grains derived from sandstone.
6. Pale to dark-gray siltstone, calcareous or noncalcareous, laminations visible in some pebble-size fragments.

Consolidated Rock

Depth Range (feet)		**PERCENTAGES** Consolidated[2] See descriptions below.			**COMMENTS**
		Sandstone	Siltstone	Igneous	
290	300	98	2	0	Fresh sandstone. A few limestone & tuff fragments.
300	310	98	2	0	Fresh sandstone. A few limestone & tuff fragments.
310	320	96	4	0	Fresh sandstone. A few limestone & tuff fragments.
320	330	98	2	0	Fresh sandstone. A few limestone & tuff fragments.
330	340	78	22	0	Fresh sandstone & siltstone.
340	350	50	50	0	Siltstone is white, tan & gray.
350	360	30	70	0	Siltstone is white to gray. Sandstone is fine grained.
360	370	0	100	0	Siltstone is white to gray; calcareous cement.
370	380	4	96	0	Siltstone is medium to dark gray, grading to very fine sandstone.
380	390	0	100	0	Siltstone is gray to tan-gray.
390	400	25	75	0	Sandstone is fine grained; calcareous cement.
400	410	0	100	0	Siltstone is gray to tan-gray.
410	420	0	100	0	Siltstone is gray to tan-gray.
420	430	5	95	0	" "
430	440	50	50	0	" "
440	450	95	4	1	" "
450	460	50	50	0	" "
460	470	5	95	0	" "
470	480	100	0	0	Sandstone is fine to medium grained, well sorted.
480	490	95	4	1	" "
490	500	80	20	0	" "
500	510	95	5	0	Cuttings at 100-foot intervals examined below.
600	610	50	50	0	Sandstone is fine grained.
700	710	70	30	1	Sandstone is fine to medium grained.
800	810	100	0	0	Sandstone is medium to coarse grained, lithic.
900	910	100	0	0	Sandstone is medium to coarse grained, lithic.
1000	1010	90	10	0	" "
1100	1110	50	50	0	" "
1200	1210	90	10	0	Sandstone is fine to medium grained.

Lithologic Type Descriptions – Bedrock

John Henry Member of the Straight Cliffs Formation

Sandstone: Gray to pale brown, fine to coarse grained quartz-lithic sandstone, well to moderately sorted, calcite cement.

Siltstone: Pale gray to pale brown siltstone, calcite or silica cement, easily disaggregated, planar laminations visible in some larger fragments.

Igneous Rocks

Igneous-rock fragments are (1) black and gray, striated devitrified tuff or glass, and (2) andesitic(?) flow or intrusive rock having small phenocrysts of quartz and plagioclase, and gray to black, dense, microcrystalline groundmass. Fragments of these rocks occur in small amounts in several intervals. The igneous rocks may be derived from caving of the borehole, where a deposit of Mount Dutton Formation may have been encountered below the basin-fill deposits and above the Straight Cliff Formation in the interval from which no cuttings were recovered; or may be small intrusive masses.

APPENDIX B

Gravity Data

Link to supplemental data:

https://ugspub.nr.utah.gov/publications/special_studies/ss-172/ss-172b.xlsx

APPENDIX C

Reference list of Utah Division of Drinking Water Source Protection Documents and Aquifer Test Methods Cited on Table C-1.

Bowen Collin & Associates, Inc., 2018, Drinking water source protection plan for Bryce Canyon Pines well no. 3, Public Water System No. 09027, Source ID WS003: Draper, Utah, unpublished consultant's report for Bryce Canyon Pines, 92 p.

Bulloch Brothers Engineering, Inc., 2001, Drinking water source protection plan, Bristlecone well #1, Foster's Bryce Canyon Area Parcels Bristlecone Development, Garfield County, Utah: Cedar City, Utah, unpublished consultant's report for Foster's Bryce Canyon Area Parcels Bristlecone Development, 54 p.

Cascade Water Resources, 2022, Drinking water source protection plan for the Under Canvas Bryce Canyon Well 1, Garfield County, Utah: Park City, Utah, unpublished consultant's report for Under Canvas, 53 p.

Cooper, H.H., and Jacob, C.E., 1946, A generalized graphical method for evaluating formation constants and summarizing well field history: American Geophysical Union Transactions, v. 27, p. 526-534.

Dixie National Forest, 2012, Source protection plan for King Creek Campground well, Public Drinking Water System No. 09052, Source No. 02, Dixie National Forest: Cedar City, Utah, unpublished drinking water source protection report, 38 p.

Hantush, M.S., and Jacob, C.E., 1955, Non-steady radial flow in an infinite leaky aquifer, Am. Geophys. Union Trans., vol. 36, no. 1, pp. 95-100.

Leslie & Associates, Inc., 2009, Updated drinking water source protection plan for Ruby's Inn Resort: Cedar City, Utah, unpublished consultant's report for Ruby's Inn, 138 p.

Loughlin Water Associates, LLC, 2022, Expert Report: Ruby's Inn vs Teresa Wilhelmsen et al—Case No. 200600028, 107 p.

Moench, A.F., 1993, Computation of type curves for flow to partially penetrating wells in water-table aquifers: Groundwater, v. 31, p. 966-971.

National Park Service Water Resources Division, 1998, Drinking water source protection plan, East Creek well field, Bryce Canyon National Park: Fort Collins, Colorado, unpublished drinking water source protection report, 45 p.

Theis, C.V., 1935, The relation between the lowering of the piezometric surface and the rate and duration of discharge of a well using groundwater storage: American Geophysical Union Transactions, v. 16, p. 519-524.

Table C-1. *Aquifer characteristics compiled from Utah Division of Drinking Water source protection documents.*

UGS Site ID	Hydro ID[1]	WIN[2]	Source Name	System Name	Well Depth (feet)	Geologic Description	Test Method[3]	T (feet squared per day)	Reference[3]
BC20W	1050	3595	Well #2	Ruby's Inn	153	Valley fill	Theis, 1935	51,600	Leslie & Associates, Inc., 2009
-	1048	431484	Well #1	Ruby's Inn	140	Valley fill	Theis, 1935	60,700	Leslie & Associates, Inc., 2009
BC19W	1019	433375	Well #2	King Creek Campground	440	Wahweap Sandstone	Theis, 1935	65	Dixie National Forest, 2012
-	1002	441545	Well No. 3	Bryce Canyon Pines	155	Claron Formation	Theis, 1935	600	Bowen Collins & Associates, 2018
BC46W	1025	-	Well #2	Bryce Canyon National Park	52	Valley fill	Moench, 1993	8900	NPS Water Resources Division, 1998
BC51W	1011	16592	Bristlecone Well #1	Bristlecone Development	133	Valley fill	Cooper-Jacob, 1946	709	Bulloch Brothers Engineering, Inc., 2001
BC122W	1081	44069	MD Bryce Well	-	187	Straight Cliffs Sandstone	Cooper-Jacob, 1946	706	Loughlin Water Associates, LLC, 2022
BC330W	1085	445895	Under Canvas Bryce Canyon Well #1	Under Canvas, Inc.	700	Pine Hollow/ Grand Castle Formations	Hantush-Jacob, 1955	1350	Cascade Water Resources, 2022

[1] Hydro ID is the unique site identifier used in generating cross sections
[2] WIN is the unique well identifier used by the Utah Division of Water Rights
[3] See appendix C reference list

Table C-2. *Aquifer properties determined from water well log specific capacity data.*

UGS Site ID	Hydro ID[1]	WIN[2]	Aquifer	Transmissivity (ft^2/day)	Hydraulic Conductivity (ft/day)	Screen Length (ft)	Yield (gpm)	Pump Duration (hr)	Well Diam. (in)	Well Depth (ft)
-	1001	33124	bedrock	517	3.83	135	30	0.5	6	150
-	1002	441545	bedrock	157	3.14	50	40	14	8	240
BC22W	1004	431483	valley fill	10680	427	25	275	24	12	172
BC27W	1007	8318	valley fill	72	3.14	23	20	1	6	63
BC40W	1010	35339	valley fill	277	11.08	25	25	1	6	91
BC51W	1011	16592	valley fill	539	6.13	88	100	5	8	136
-	1013	33693	bedrock	36	0.13	284	15	1.5	6.625	300
BC25W	1014	427430	valley fill	167	8.33	20	60	3	8	125
-	1020	27631	bedrock	33	0.82	40	30	4	8	420
BC12W	1021	433455	valley fill	5574	557.45	10	290	8	10	51
BC46W	1025	-	valley fill	2455	65.46	37.5	160	24	8	52
-	1027	32773	valley fill	342	11.41	30	30	1	6	106
BC67W	1030	430599	valley fill	10	0.51	20	5	4	6	60
BC49W	1032	432734	bedrock	21	0.52	40	24	4	6.625	353
BC48W	1033	434148	bedrock	56	0.31	181	10	2.5	5	200
BC66W	1034	15622	valley fill	210	21.04	10	30	4	4	50
BC120W	1036	432247	valley fill	75	0.94	80	150	4	5	250
BC65W	1037	434225	valley fill	25	0.26	99	9	2	6	240
-	1038	-	bedrock	8	0.07	117	1.5	6	6	205
-	1048	431484	valley fill	213	17.78	12	50	4	6	140
BC21W	1049	3607	valley fill	686	34.28	20	100	4	8	114
BC20W	1050	3595	valley fill	735	38.68	19	100	4	6	153
-	1051	-	bedrock	189	18.89	10	20	4	6	216
-	1052	-	bedrock	1116	18.61	60	60	1	8	125
BC328W	1059	-	bedrock	49	0.70	70	30	4	4	195
BC329W	1060	-	bedrock	38	0.31	120	17	4	4	165
BC38W	1061	-	bedrock	70	0.70	100	30	4	4	145
BC37W	1062	-	bedrock	116	1.01	115	60	4	4	145
BC39W	1063	-	bedrock	35	0.33	108	20	4	4	145
-	1066	-	valley fill	355	59.11	6	8	1	6	176
-	1068	16034	bedrock	177	2.73	65	15	2	6	181
BC118W	1069	16066	valley fill	378	9.45	40	30	2	6	87
BC116W	1070	16068	valley fill	378	10.49	36	30	2	6	107
-	1071	23999	bedrock	37	0.25	147	15	2	5	267
-	1073	29478	bedrock	40	0.34	119	25	2	5	297
-	1074	34106	bedrock	13	0.13	103	7	4	5	273
-	1075	427600	bedrock	27	0.67	40	5	2	4	330
-	1076	429785	bedrock	11	0.27	40	5	4	5	290
BC117W	1078	432226	valley fill	173	2.88	60	125	2	5	250
-	1079	442668	bedrock	39	0.48	80	50	36	8.625	350
BC96W	1080	443888	bedrock	11	0.14	80	10	24	8	340
BC122W	1081	444069	bedrock	647	16.17	40	100	24	8	187
BC133W	1083	445090	bedrock	70	0.70	100	90	4	5	340
-	1084	445126	bedrock	165	1.65	100	120	4	5	300
BC330W	1085	445895	bedrock	1252	4.82	260	97	24	6	795
-	1087	446861	bedrock	13	0.12	103	7	4	6.625	243
BC115W	1090	-	valley fill	473	5.38	88	50	2	6.625	128

[1] Hydro ID is the unique site identifier used in generating cross sections

[2] WIN is the unique well identifier used by the Utah Division of Water Rights

APPENDIX D

Water Level, Discharge, and Water Chemistry Data

Link to supplemental data:

https://ugspub.nr.utah.gov/publications/special_studies/ss-172/ss-172d.xlsx

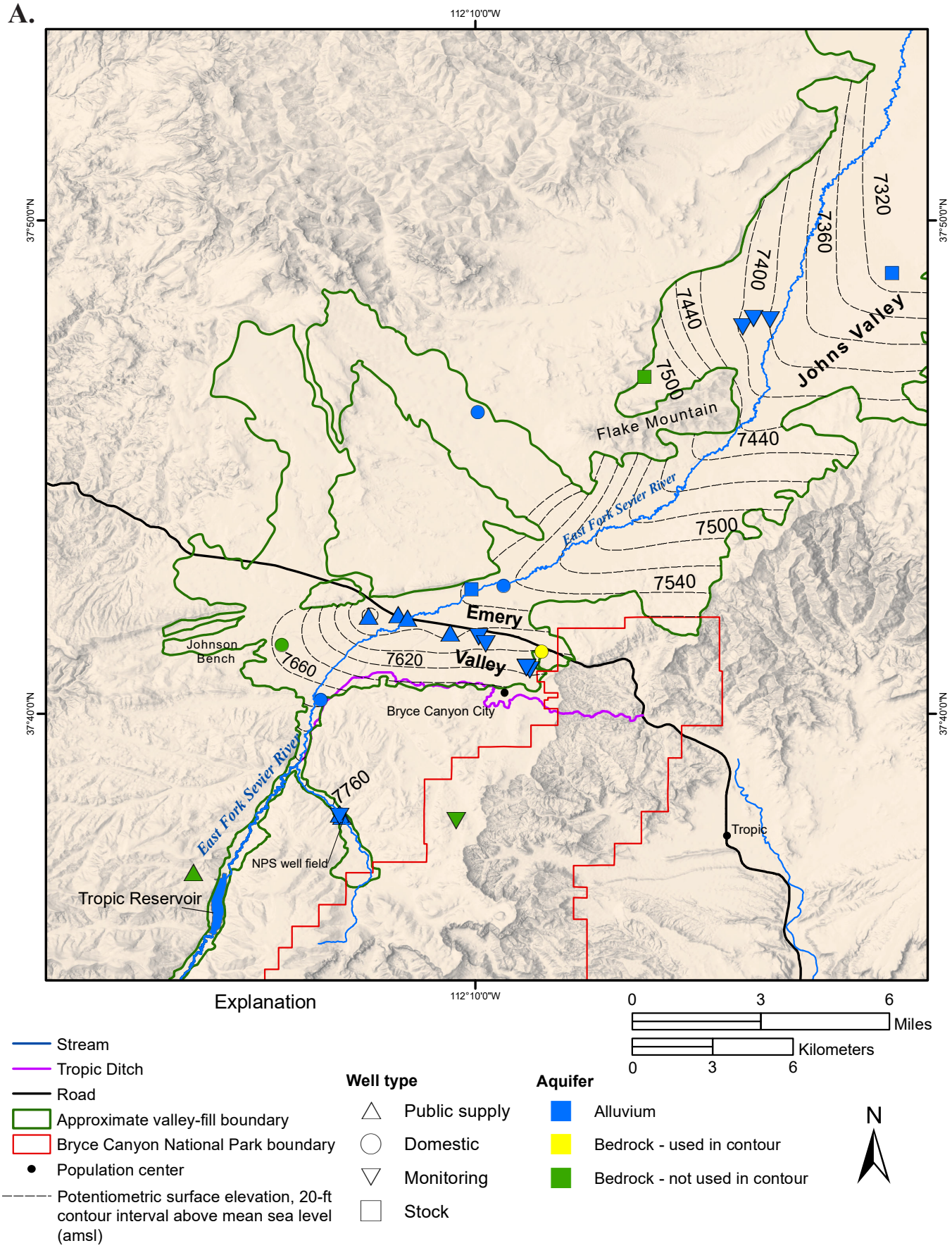

Figure D-1. *Potentiometric surface maps of water levels from wells. Overall direction of groundwater flow is north-northeast. Adapted from Wallace et al. (2021).* ***A)*** *Autumn 2018 water levels, 20-ft contour interval above mean sea level (amsl).*

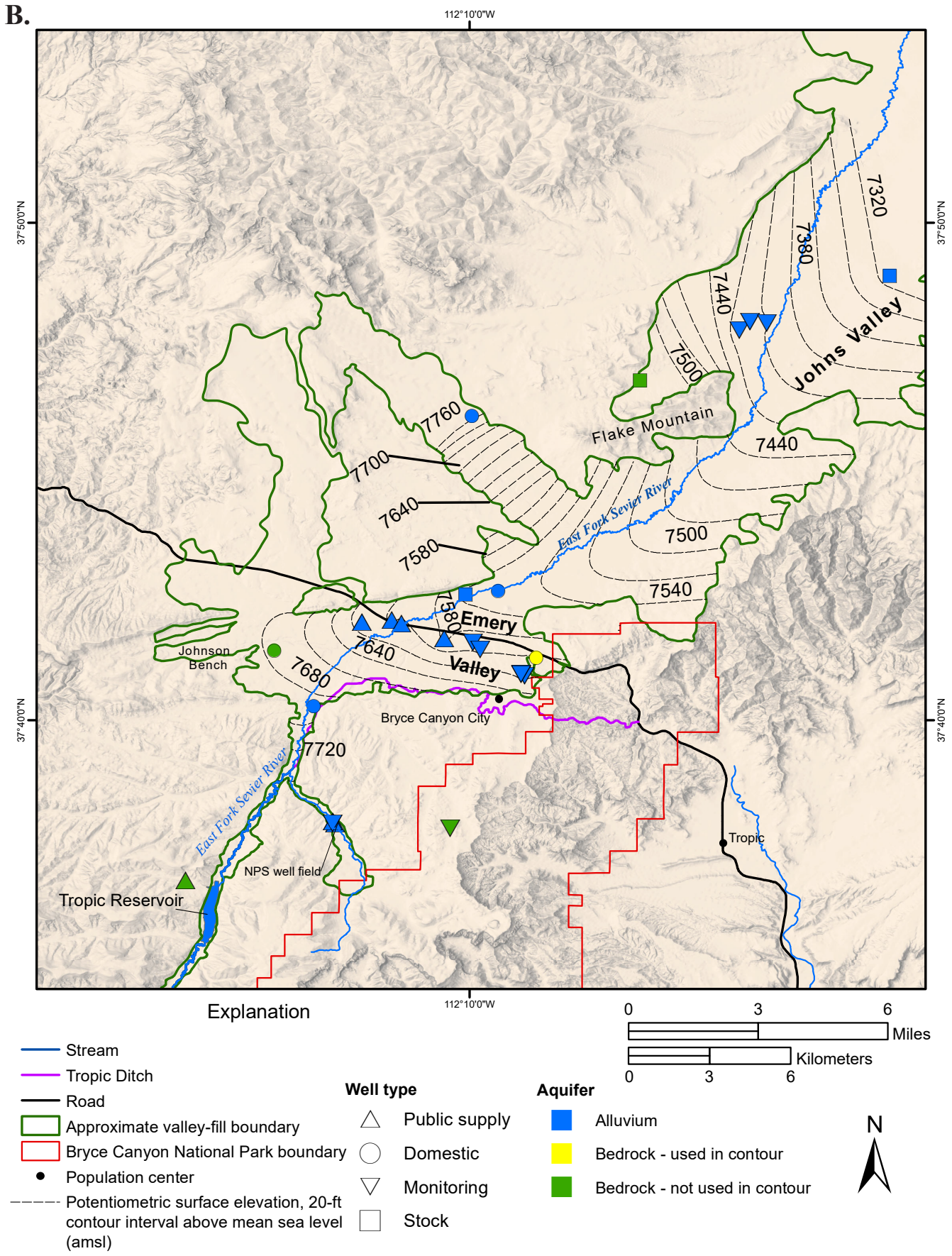

Figure D-1. Continued. *Potentiometric surface maps of water levels from wells. Overall direction of groundwater flow is north-northeast. Adapted from Wallace et al. (2021).* ***B)*** *Spring 2019 water levels, 20-ft contour interval amsl.*

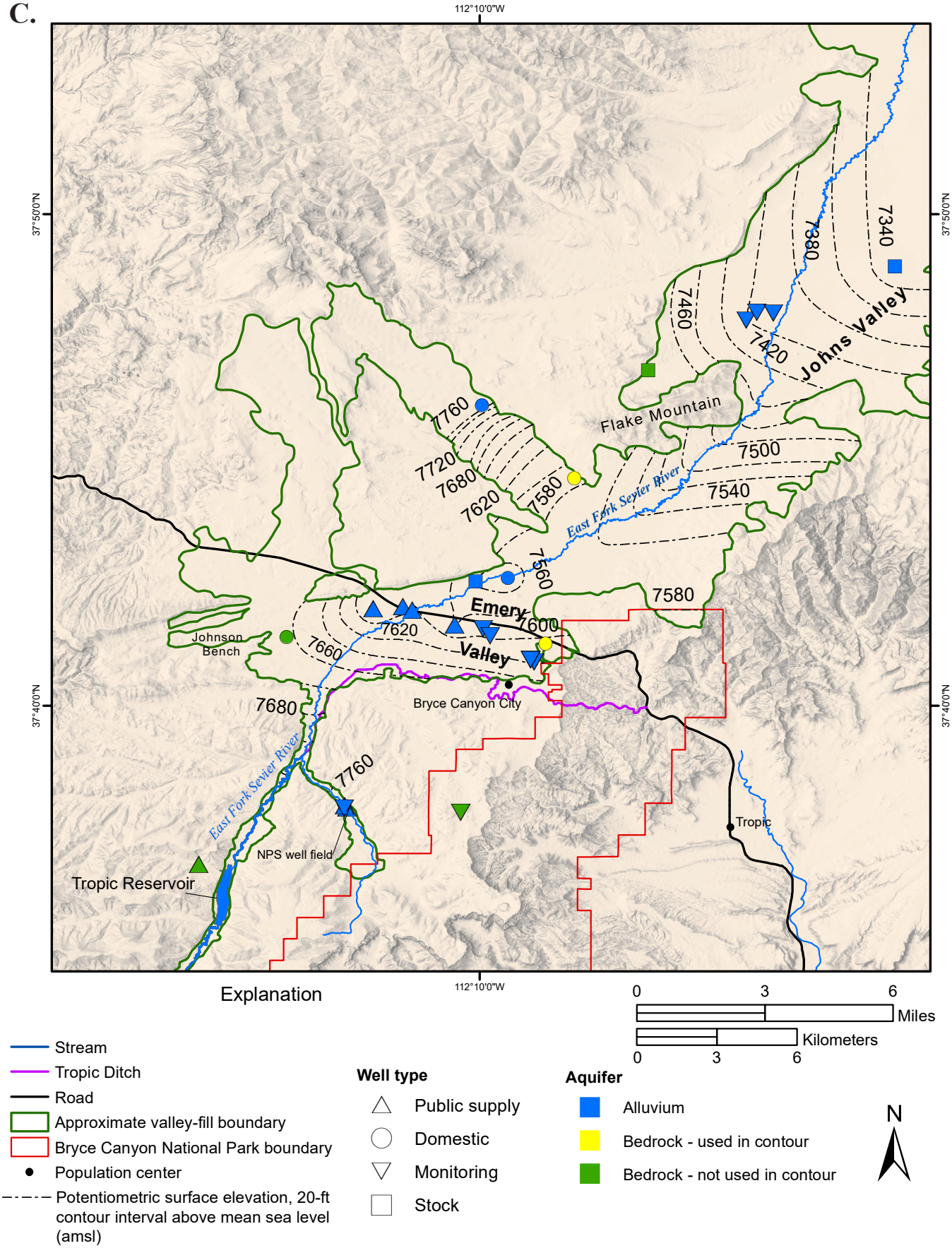

Figure D-1. Continued. *Potentiometric surface maps of water levels from wells. Overall direction of groundwater flow is north-northeast. Adapted from Wallace et al. (2021).* ***C)*** *Autumn 2019 water levels, 20-ft contour interval amsl.*

D.

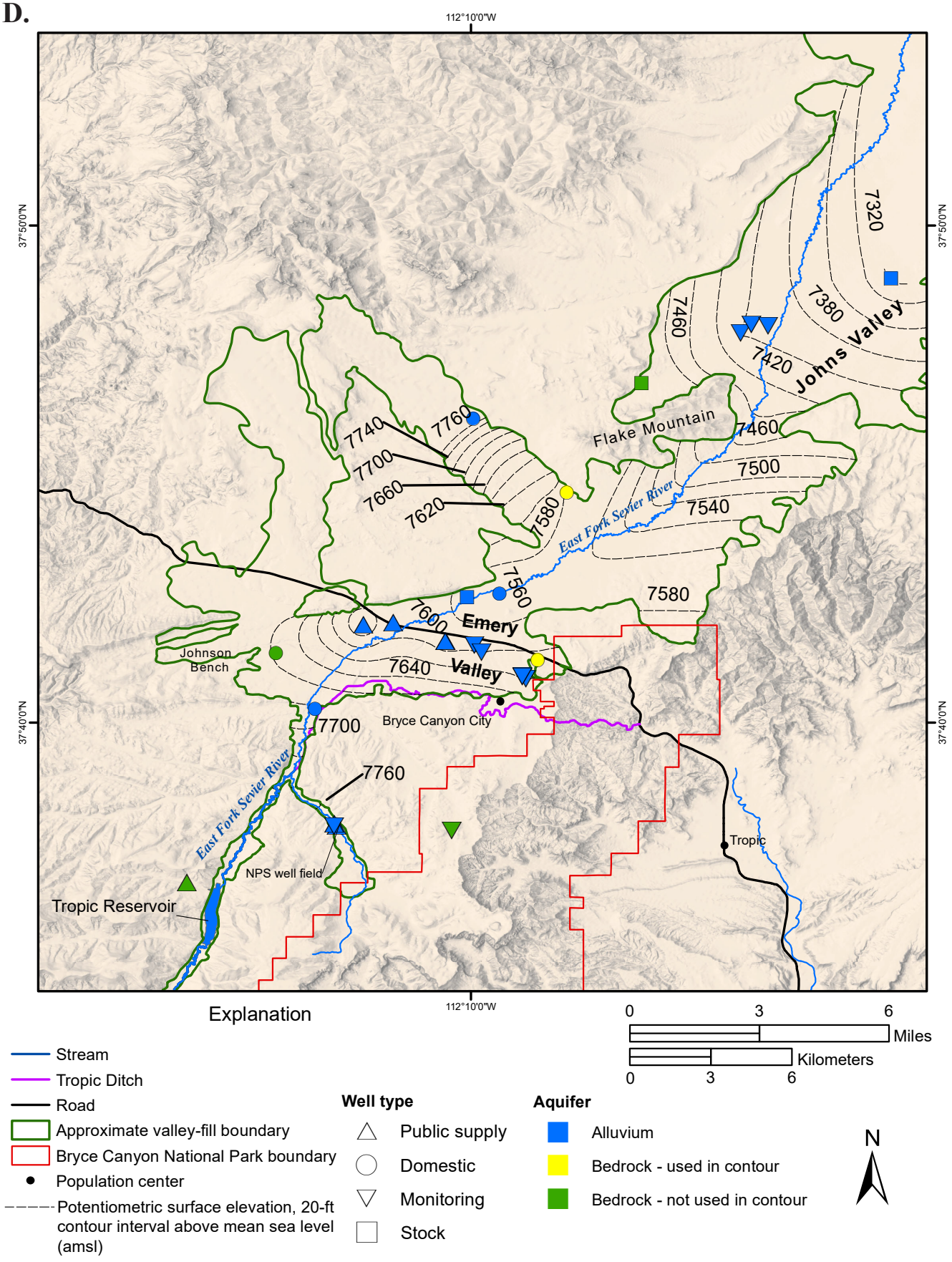

Figure D-1. Continued. *Potentiometric surface maps of water levels from wells. Overall direction of groundwater flow is north-northeast. Adapted from Wallace et al. (2021).* ***D)*** *Spring 2020 water levels, 20-ft contour interval amsl.*

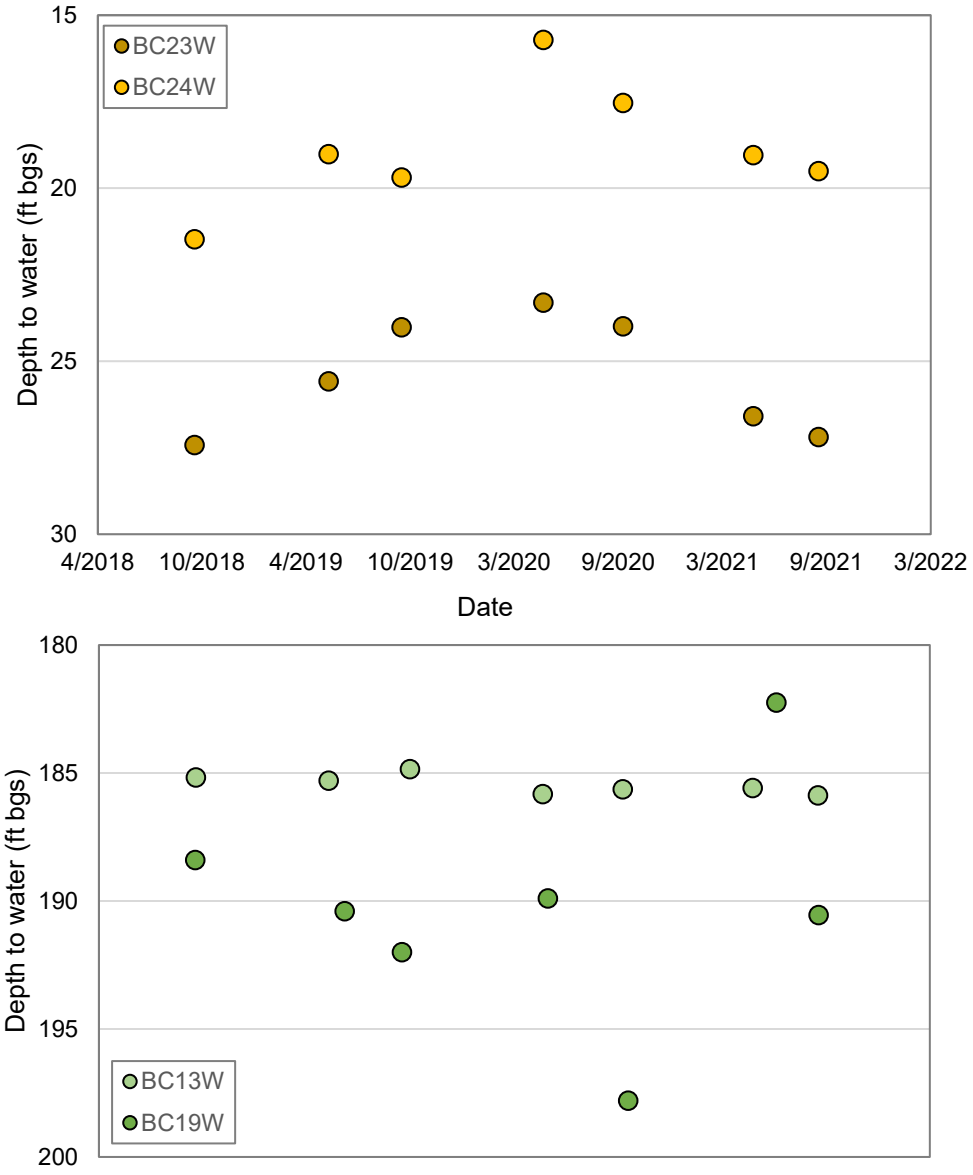

Figure D-2. *Short-term monitoring records of valley-fill aquifer monitoring wells (BC23W, BC24W) and Cretaceous aquifer wells (BC13W, BC19W).*

APPENDIX E

Seepage Run Data

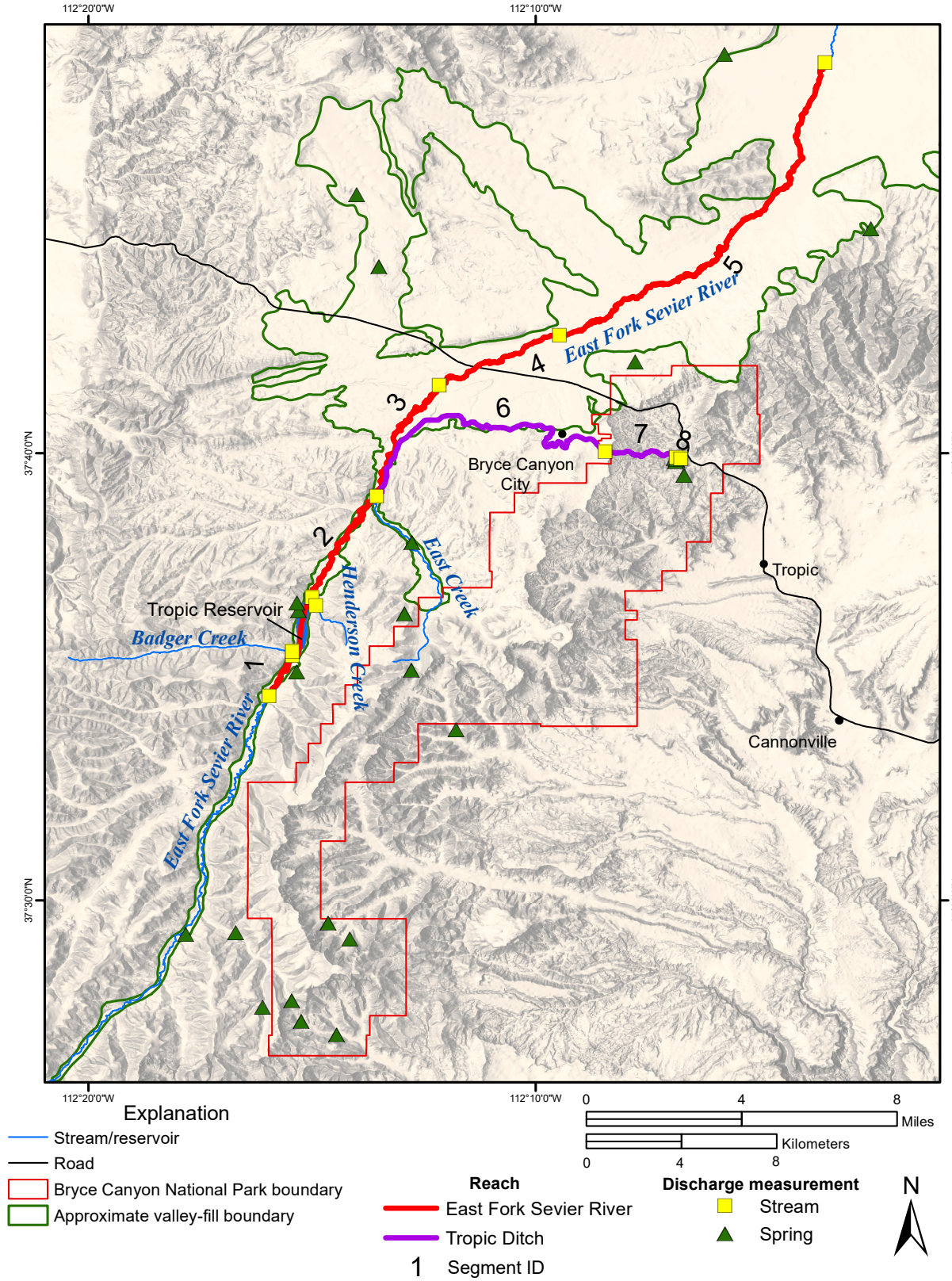

Figure E-1. *Location of seepage run reaches, and stream and spring discharge measurements from 2018 to 2020.*

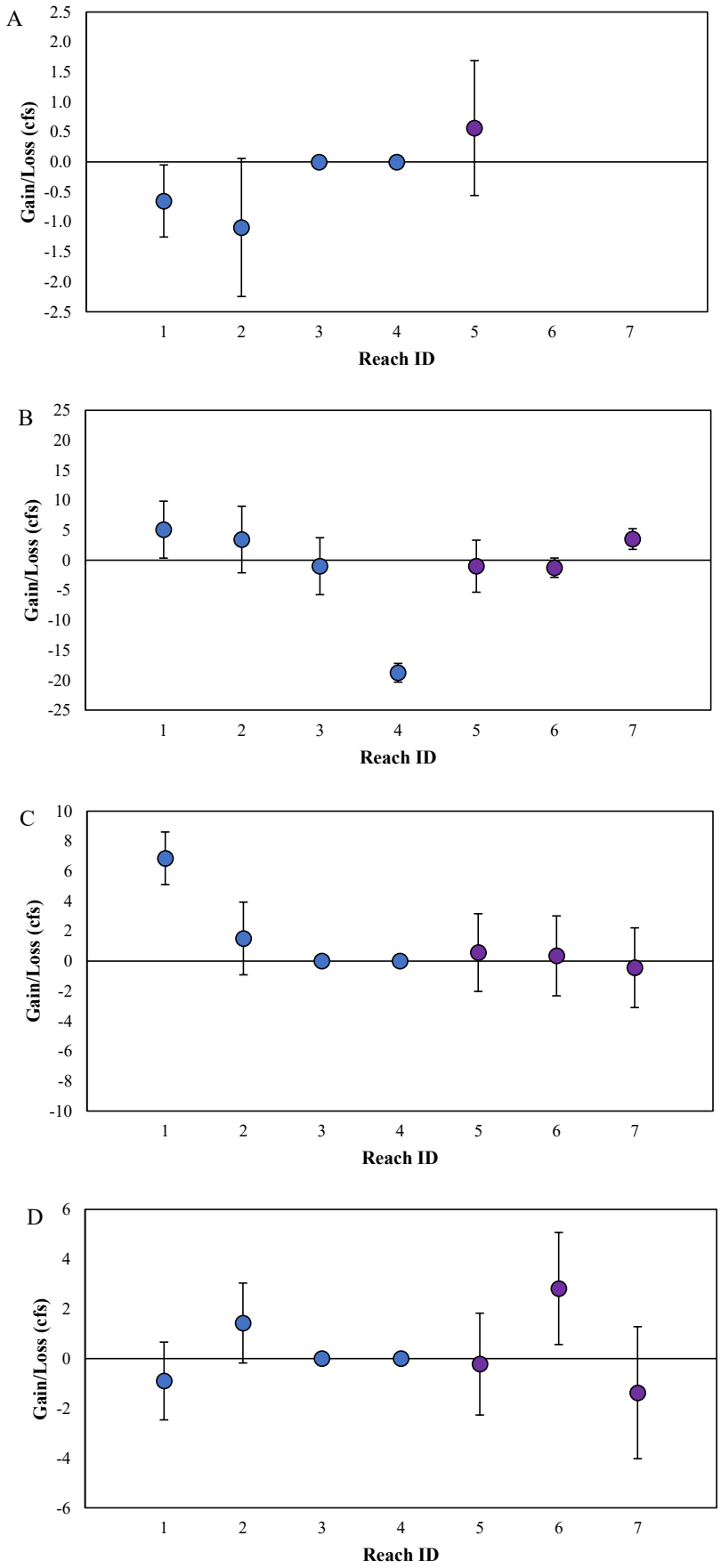

Figure E-2. *Gaining and losing reaches of the East Fork Sevier River (blue symbols) and Tropic Ditch (purple symbols) from* ***A)*** *autumn 2018,* ***B)*** *spring 2019,* ***C)*** *autumn 2019,* ***D)*** *spring 2020. See Table 2 for reach IDs.*

APPENDIX F

Potential Contaminant Inventory, Septic-Tank Density Recommendations, and Groundwater Quality Classification

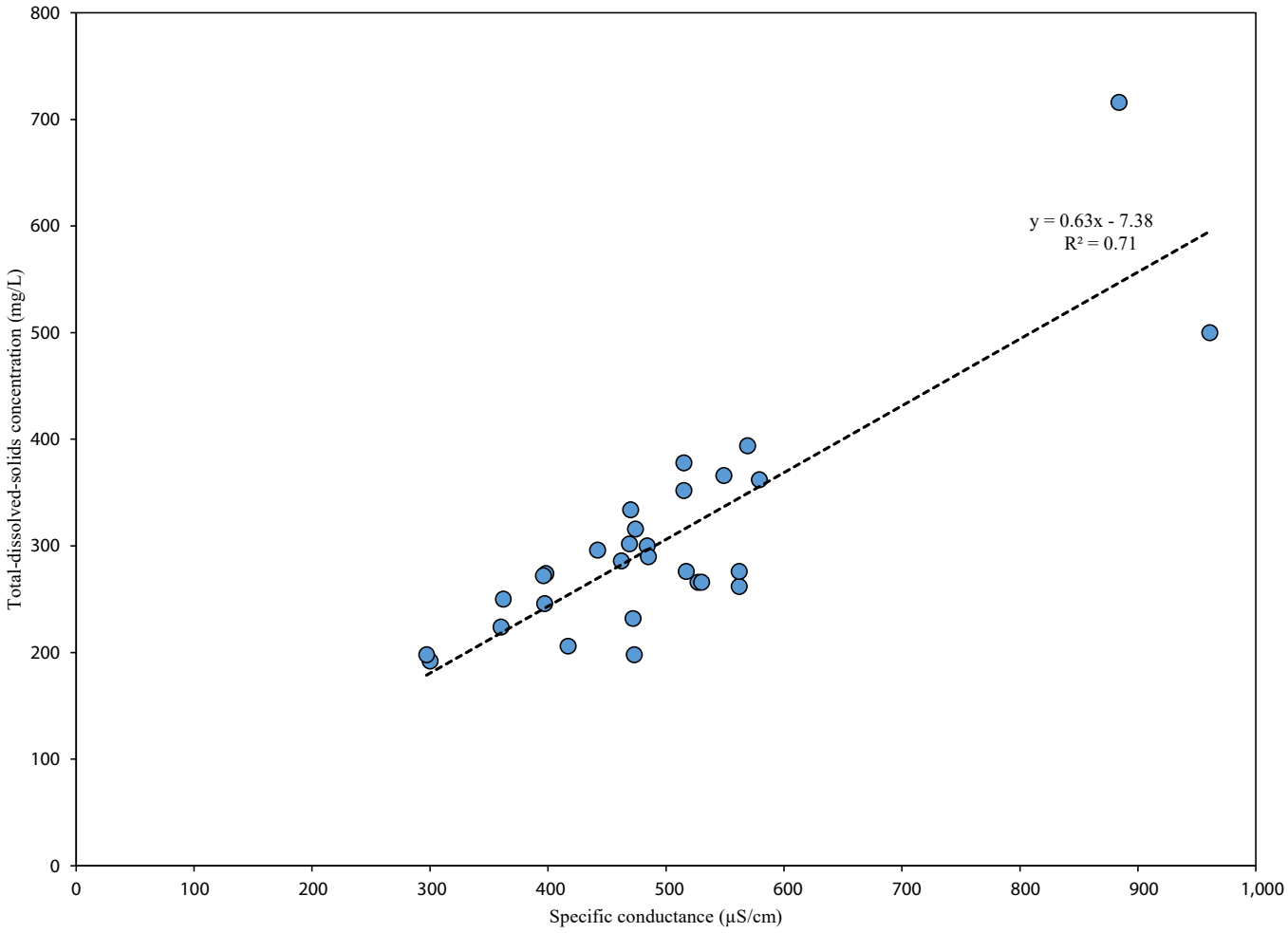

Figure F-1. *Total-dissolved-solids (TDS) concentration versus specific conductance for 29 wells in Johns and Emery Valleys. Based on Hem's (1985) equation for estimating TDS from specific conductance: KA=S, where K=specific conductance, S=TDS, A ranges from 0.4 to 0.8 with an average A=0.63 (slope) used as the conversion factor to compute TDS in the study area.*

Table F-1. *Potential contaminant inventory for Johns and Emery Valleys, Garfield County, Utah.*

FIELD ID	TYPE	Description of potential contaminant	Pollutant
1	AFO[1]	equestrian campground	fertilizers, manure, nitrates
2	Waste Disposal	RV dump station	metals, solvents, nitrates
3	AFO	horse corral	fertilizers, manure, nitrates
4	Former AFO	abandoned corral	fertilizers, manure, nitrates
5	AFO	corral	fertilizers, manure, nitrates
6	Service station	service station	solvents, petroleum
7	Business	RV park	metals, solvents, nitrates
8	AFO	horse corral	fertilizers, manure, nitrates
9	Junk Yard/Salvage	junk site	metals, solvents, petroleum
10	AFO	corral	fertilizers, manure, nitrates
11	Business	hotel, restaurant	solvents
12	AFO	horse corral, rodeo arena	fertilizers, manure, nitrates
13	AFO	corral	fertilizers, manure, nitrates
14	AFO	corral	fertilizers, manure, nitrates
15	Government	rest area	solvents, nitrates
16	Government	guard station	metals, solvents, petroleum
17	AFO	corral	fertilizers, manure, nitrates
18	Junk Yard/Salvage	personal junk yard	metals, solvents, petroleum
19	Former AFO	abandoned corral	fertilizers, manure, nitrates
20	Junk Yard/Salvage	junk site	metals, solvents, petroleum
21	Former AFO	abandoned corral	fertilizers, manure, nitrates
22	Mining	inactive borrow pit	metals, solvents, petroleum
23	Former AFO	abandoned corral	fertilizers, manure, nitrates
24	Business, AFO	wildlife museum, ATV storage, exotic animal corral	fertilizers, manure, nitrates
25	Mining	inactive borrow pit	metals, solvents, petroleum
26	Mining	inactive borrow pit	metals, solvents, petroleum
27	Business	hotel, restaurant	solvents
28	AFO	mule/horse corral	fertilizers, manure, nitrates
29	Former AFO	abandoned corral	fertilizers, manure, nitrates
30	Government	waste disposal, automotive storage/scrap yard	metals, solvents, petroleum
31	Junk Yard/Salvage	junk site	metals, solvents, petroleum
32	Mining	gravel pit	metals, solvents, petroleum
33	Government	maintenance yard, paint shop, automotive repair	metals, solvents, petroleum
34	Mining	inactive borrow pit	metals, solvents, petroleum
35	Waste Disposal	sewage lagoons	metals, solvents, nitrates
36	Government	radio towers	metals, solvents
37	Industry	power sub station	PCBs
38	Former AFO	abandoned corral	fertilizers, manure, nitrates
39	Junk Yard/Salvage	junk site	metals, solvents, petroleum
40	AFO	coral	fertilizers, manure, nitrates
41	Business	hotel, restaurant	solvents
42	Service station	abandoned service station	metals, solvents, petroleum
43	AFO	elk preserve	fertilizers, manure, nitrates
44	Waste Disposal	RV dump station	metals, solvents, nitrates
45	Mining	inactive borrow pit	metals, solvents, petroleum
46	AFO	horse corral	fertilizers, manure, nitrates
47	AFO	corral	fertilizers, manure, nitrates
48	Mining	inactive borrow pit	metals, solvents, petroleum

Table F-1. Continued. *Potential contaminant inventory for Johns and Emery Valleys, Garfield County, Utah.*

FIELD ID	TYPE	Description of potential contaminant	Pollutant
49	Junk Yard/Salvage	auto scrap yard/storage	metals, solvents, petroleum
50	AFO	horse corrals	fertilizers, manure, nitrates
51	Business	RV park	metals, solvents, nitrates
52	Waste Disposal	RV dump station	metals, solvents, nitrates
53	Waste Disposal	sewage lagoons	metals, solvents, nitrates
54	Business, Large Lawn	hotel, large lawns	pesticides, fertilizer
55	Mining	inactive borrow pit	metals, solvents, petroleum
56	Government	fire station	metals, solvents, petroleum
57	Business	maintenance yard, automotive repair	metals, solvents, petroleum
58	Business	restaurants	solvents
59	Service station	service station	solvents, petroleum
60	Large Lawn	park	pesticides, fertilizer
61	Waste Disposal	RV dump station	metals, solvents, nitrates
62	Business	gift shop, restaurants	solvents
63	AFO	horse corral	fertilizers, manure, nitrates
64	Junk Yard/Salvage	personal junk yard	metals, solvents, petroleum
65	Industry	airport	metals, solvents, petroleum
66	Business	hotel, restaurants	solvents
67	Business, Large Lawn	restaurant, large lawn	pesticides, fertilizer
68	AFO	corral, rodeo grounds	fertilizers, manure, nitrates
69	Business, Large Lawn	hotel, large lawn	solvents, pesticides, fertilizers
70	Business	hotel	solvents
71	Industry	power sub station	PCBs
72	Business	abandoned restaurant	metals, solvents
73	Large Lawn	cemetary	pesticides, fertilizer
74	Business	RV park	metals, solvents, nitrates
75	Shooting range	shooting range	metals
76	Industry	cell tower	metals, solvents
77	AFO	corral	fertilizers, manure, nitrates
78	Junk Yard/Salvage	junk site	metals, solvents, petroleum
79	Former AFO	abandoned corral	fertilizers, manure, nitrates
80	Industry	cell tower	metals, solvents
81	Waste Disposal	landfill	metals, solvents, petroleum
82	Former AFO	abandoned corral	fertilizers, manure, nitrates
83	Junk Yard/Salvage	junk site	metals, solvents, petroleum
84	Former AFO	abandoned corral	fertilizers, manure, nitrates
85	Junk Yard/Salvage	junk site	metals, solvents, petroleum
86	Former AFO	abandoned corral	fertilizers, manure, nitrates
87	AFO	corral	fertilizers, manure, nitrates
88	AFO	corral	fertilizers, manure, nitrates
89	AFO	corral	fertilizers, manure, nitrates
90	Former AFO	abandoned corral	fertilizers, manure, nitrates
91	Mining	gravel pit	metals, solvents, petroleum
92	AFO	corral	fertilizers, manure, nitrates
93	AFO	corral	fertilizers, manure, nitrates
94	AFO	corral	fertilizers, manure, nitrates
95	AFO	corral	fertilizers, manure, nitrates
96	Former AFO	abandoned corral	fertilizers, manure, nitrates

Table F-1. Continued. *Potential contaminant inventory for Johns and Emery Valleys, Garfield County, Utah.*

FIELD ID	TYPE	Description of potential contaminant	Pollutant
97	AFO	corral	fertilizers, manure, nitrates
98	Former AFO	abandoned corral	fertilizers, manure, nitrates
99	Junk Yard/Salvage	personal junk yard	metals, solvents, petroleum
100	AFO	corral	fertilizers, manure, nitrates
101	AST[2]	above-ground storage tank	metals, solvents, petroleum
102	AST	above-ground storage tank	metals, solvents, petroleum
103	AST	above-ground storage tank	metals, solvents, petroleum
104	AST	above-ground storage tank	metals, solvents, petroleum

[1]Animal feed operation

[2] Above-ground storage tank

Table F-2. *Results of the mass-balance analysis using the best-estimate nitrogen loading of 64 mg/L N* for different groundwater flow domains and different nitrate concentration degradation level projections in Johns and Emery Valleys.*

Domain	Area (acres)	Current density (acres/system)	Projected total septic tanks[1]	Calculated density[2] (acres/system)	Projected total septic tanks (5 mg/L degradation)	Calculated density[3] (acres/system)
Emery Valley	8700	310	152	57	468[4]	14
					536	
Lower Johns Valley	14,200	1775	29	496	110	129
Upper Johns Valley	7800	--	10[5]	754[5]	51[5]	153[5]
			220	35	1088	7

* best-estimate calculation is based on a nitrogen load of 17 g N per capita per day (Kaplan, 1988) for a 3.3-person household and 198 gallons per household (Utah Division of Water Resources, 2010).

[1] Projected number of septic tanks based on 1 mg/L degradation of nitrate concentration.

[2] Calculated lot size based on 1 mg/L degradation of nitrate concentration above background concentration.

[3] Calculated lot size based on a degradation up to 5 mg/L nitrate concentration.

[4] Projected total septic tanks based on 100% LUWDS discharge (top) and 60% LUWDS discharge (bottom).

[5] Projected total septic tanks/calculated density based on minimum (top) and maximum (bottom) groundwater available for mixing.

UTAH GEOLOGICAL SURVEY
a division of
Utah Department of Natural Resources

Plate F-1
Groundwater Quality Classification, Johns and Emery Valleys, Garfield County, Utah

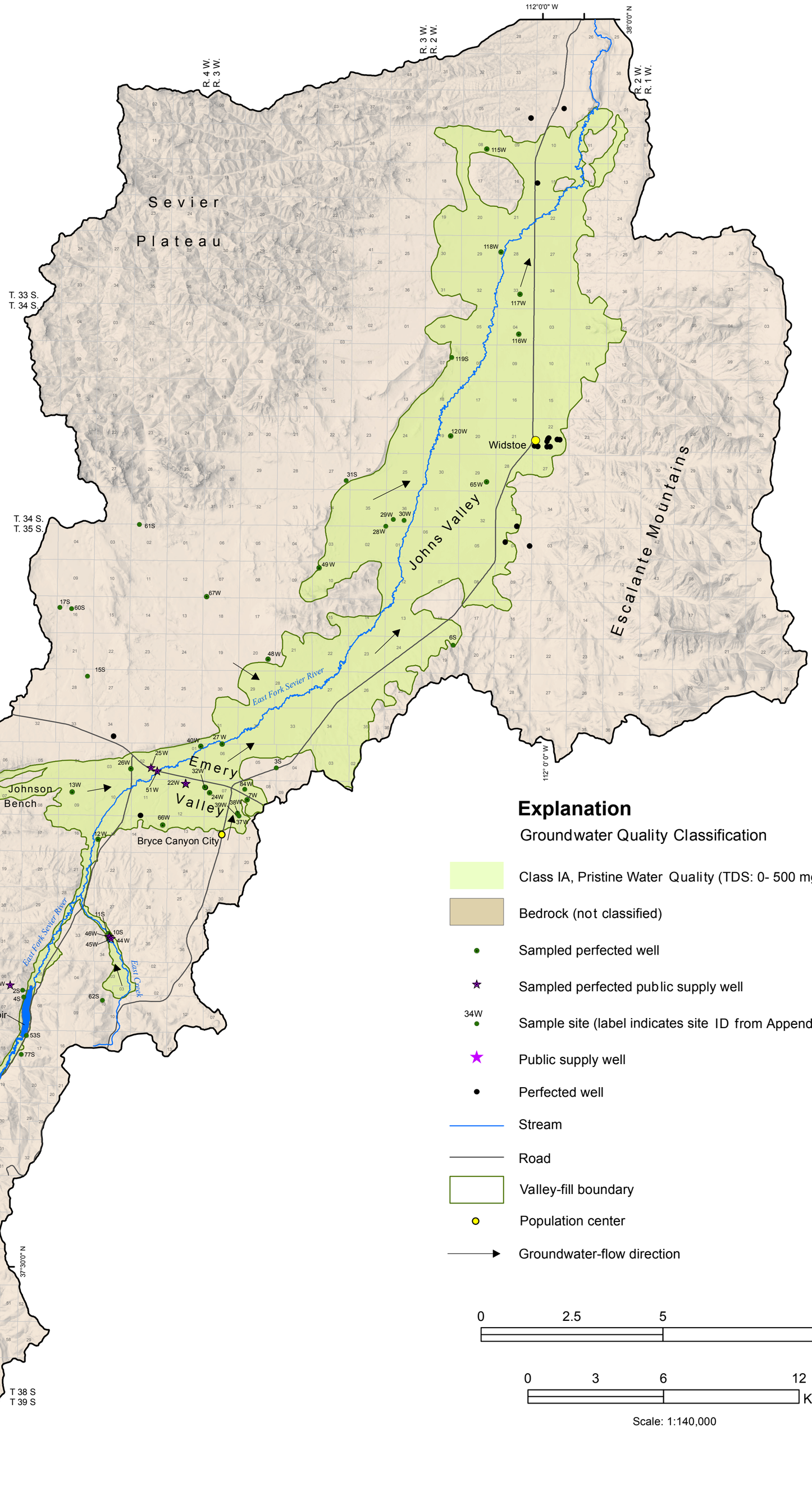

Explanation

Groundwater Quality Classification

- Class IA, Pristine Water Quality (TDS: 0- 500 mg/L)
- Bedrock (not classified)
- Sampled perfected well
- Sampled perfected public supply well
- 34W — Sample site (label indicates site ID from Appendix D)
- Public supply well
- Perfected well
- Stream
- Road
- Valley-fill boundary
- Population center
- Groundwater-flow direction

0 2.5 5 10 Miles

0 3 6 12 Kilometers

Scale: 1:140,000

This map was created from GIS files. Basemap constructed from features obtained from the UGRC.

Projection: UTM
Datum: NAD 83 Zone 12N
Cartography by Nathan Payne

UTAH GEOLOGICAL SURVEY
a division of
Utah Department of Natural Resources

Plate F-2
Potential Contaminant Sources,
Johns and Emery Valleys, Garfield County, Utah

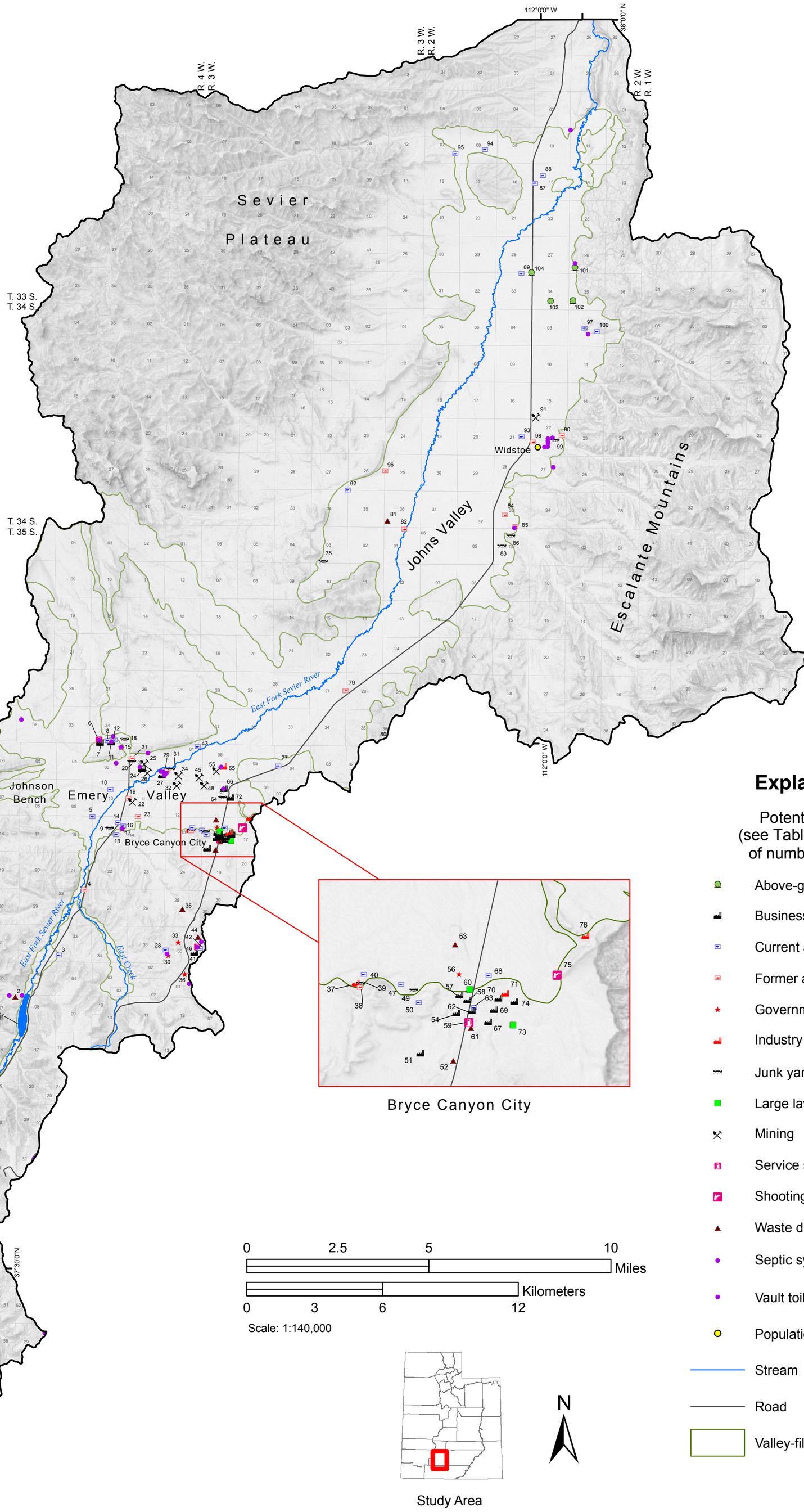

This map was created from GIS files. Basemap constructed from features obtained from the UGRC.

Projection: UTM
Datum: NAD 83 Zone 12N
Cartography by Nathan Payne

APPENDIX G

Water Budget Data

A

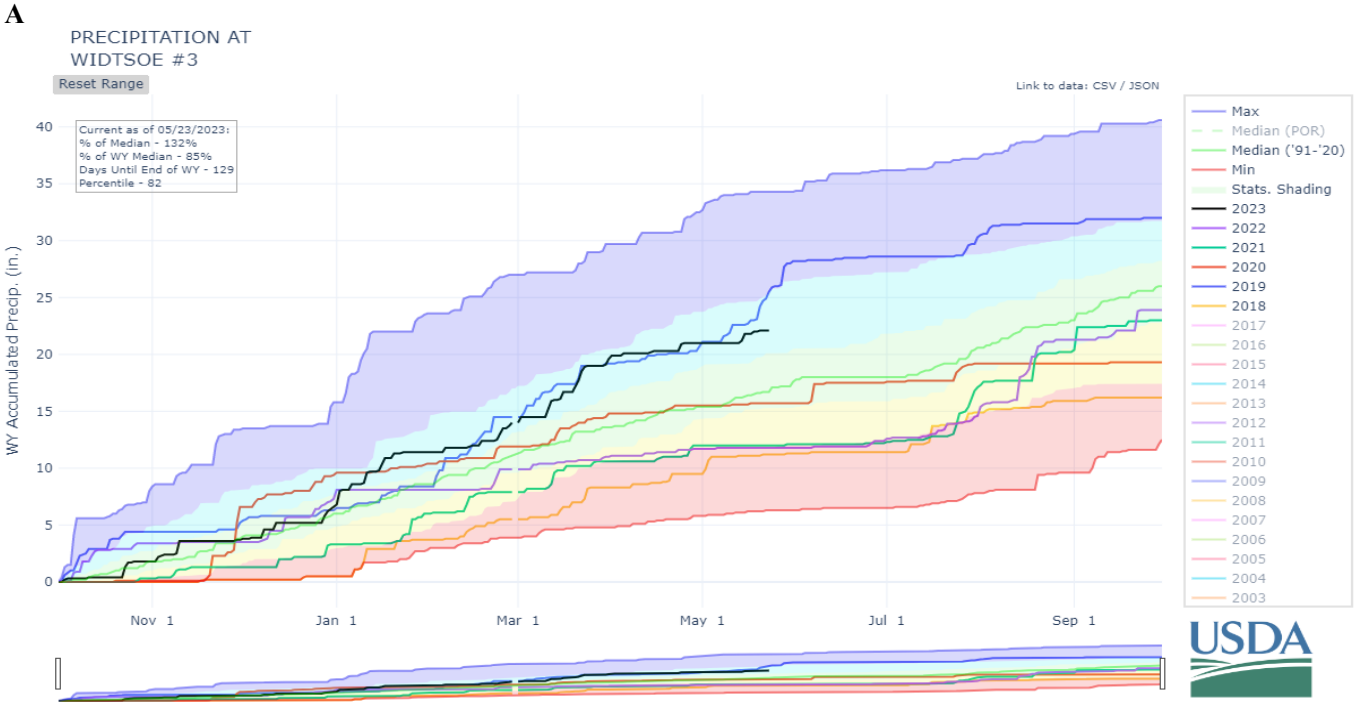

B

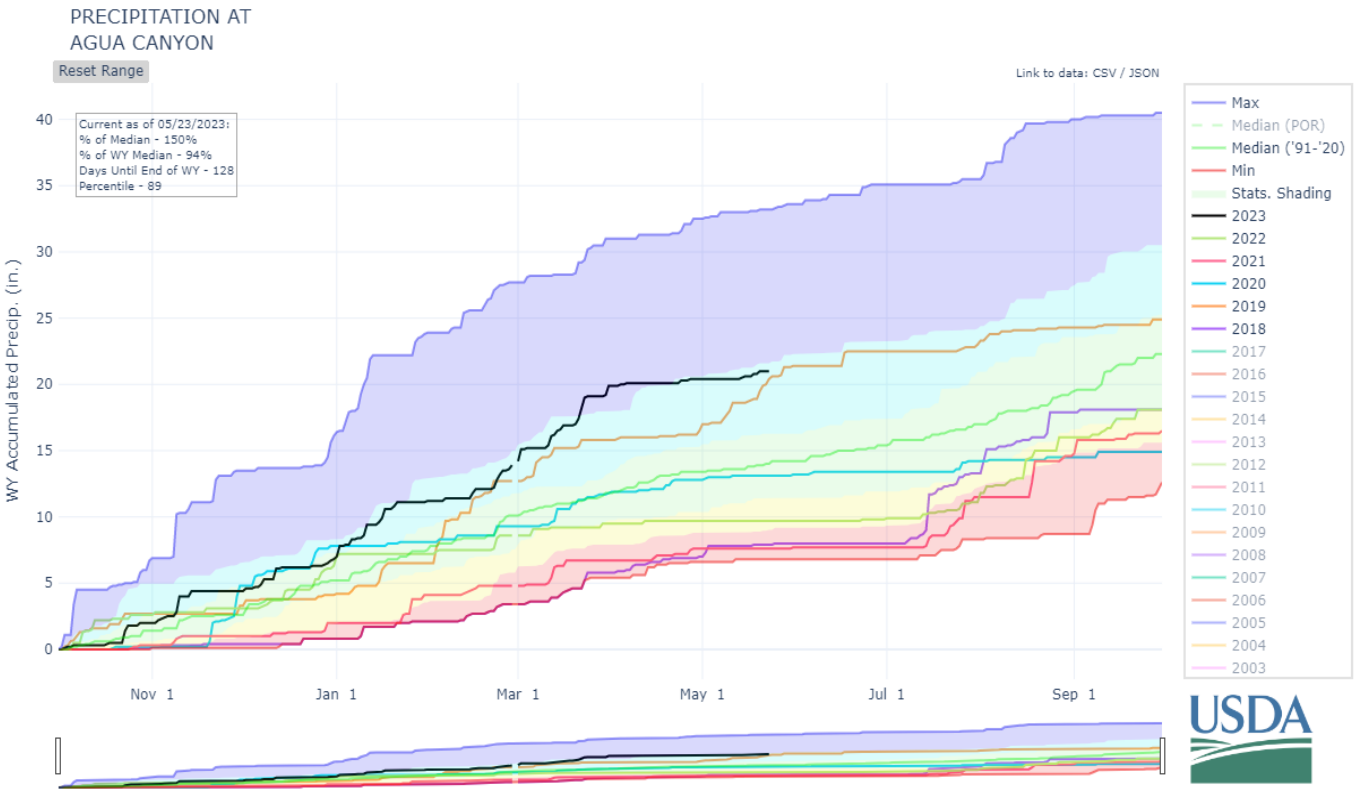

Figure G-1. *Snotel precipitation data for water years 2018 to 2023 at* ***A)*** *Widtsoe and* ***B)*** *Agua Canyon (from USDA website https://www.nrcs.usda.gov/wps/portal/wcc/home/quicklinks/states/utah/).*

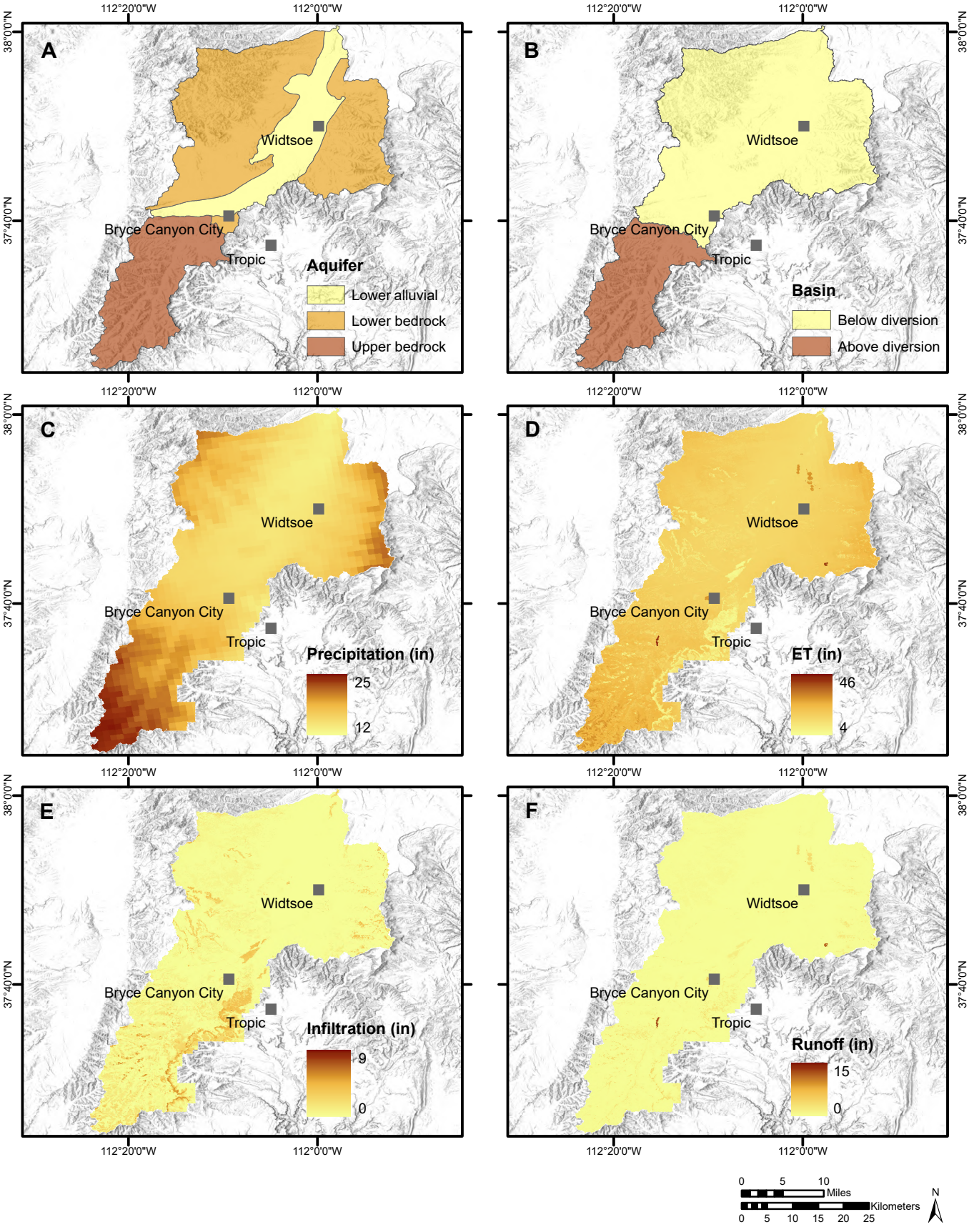

Figure G-2. A) *Lower alluvial, lower bedrock, and upper bedrock boundaries used for analysis in the SWB model and water budget calculations.* ***B)*** *Areas above and below the Tropic Ditch diversion used for analysis in the SWB model and water budget calculations. Output rasters from the SWB model of water year 2017 showing:* ***C)*** *precipitation,* ***D)*** *evapotranspiration (ET),* ***E)*** *infiltration, and* ***F)*** *runoff.*

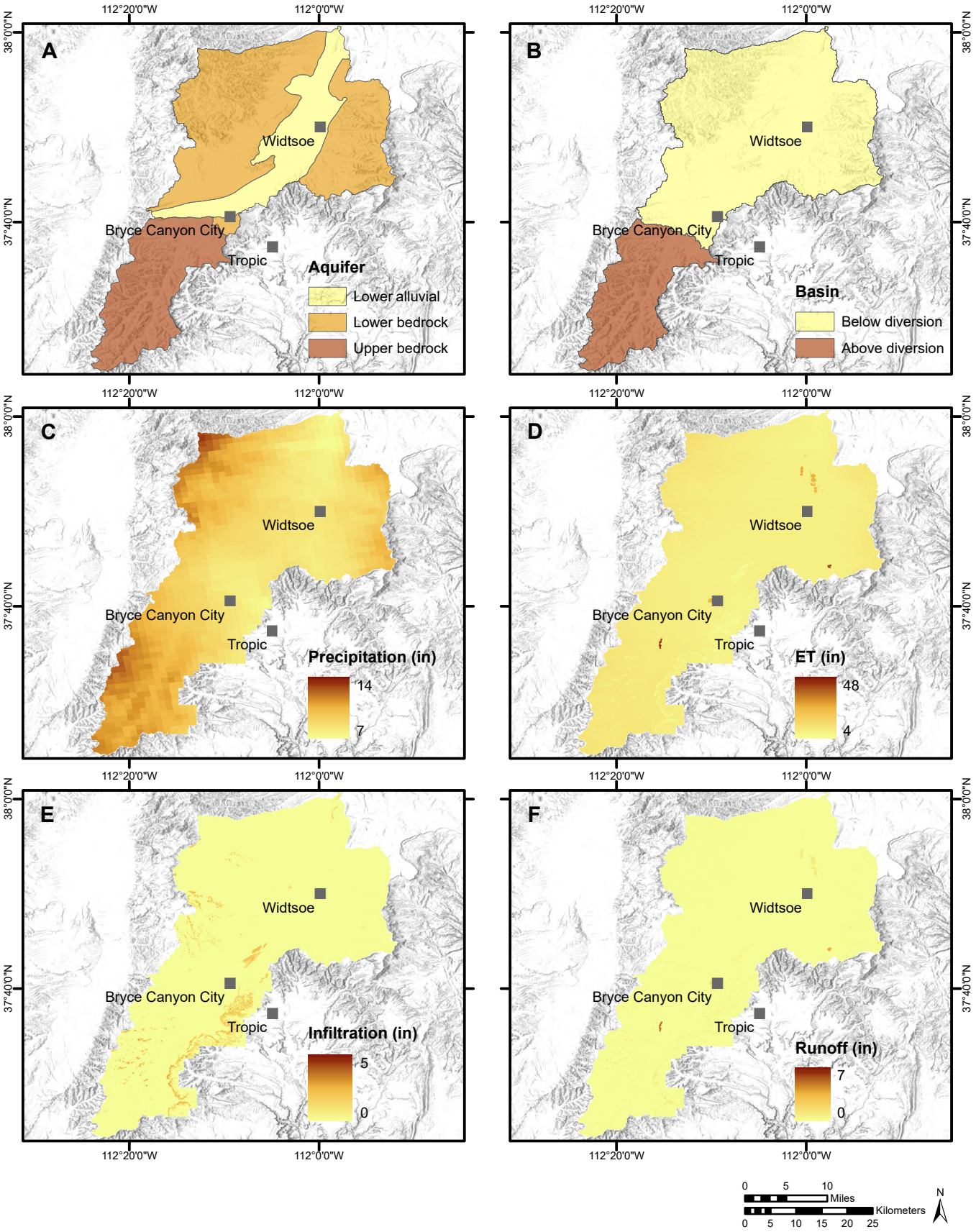

Figure G-3. A) *Lower alluvial, lower bedrock, and upper bedrock boundaries used for analysis in the SWB model and water budget calculations.* ***B)*** *Areas above and below the Tropic Ditch diversion used for analysis in the SWB model and water budget calculations. Output rasters from the SWB model of water year 2018 showing:* ***C)*** *precipitation,* ***D)*** *evapotranspiration (ET),* ***E)*** *infiltration, and* ***F)*** *runoff.*

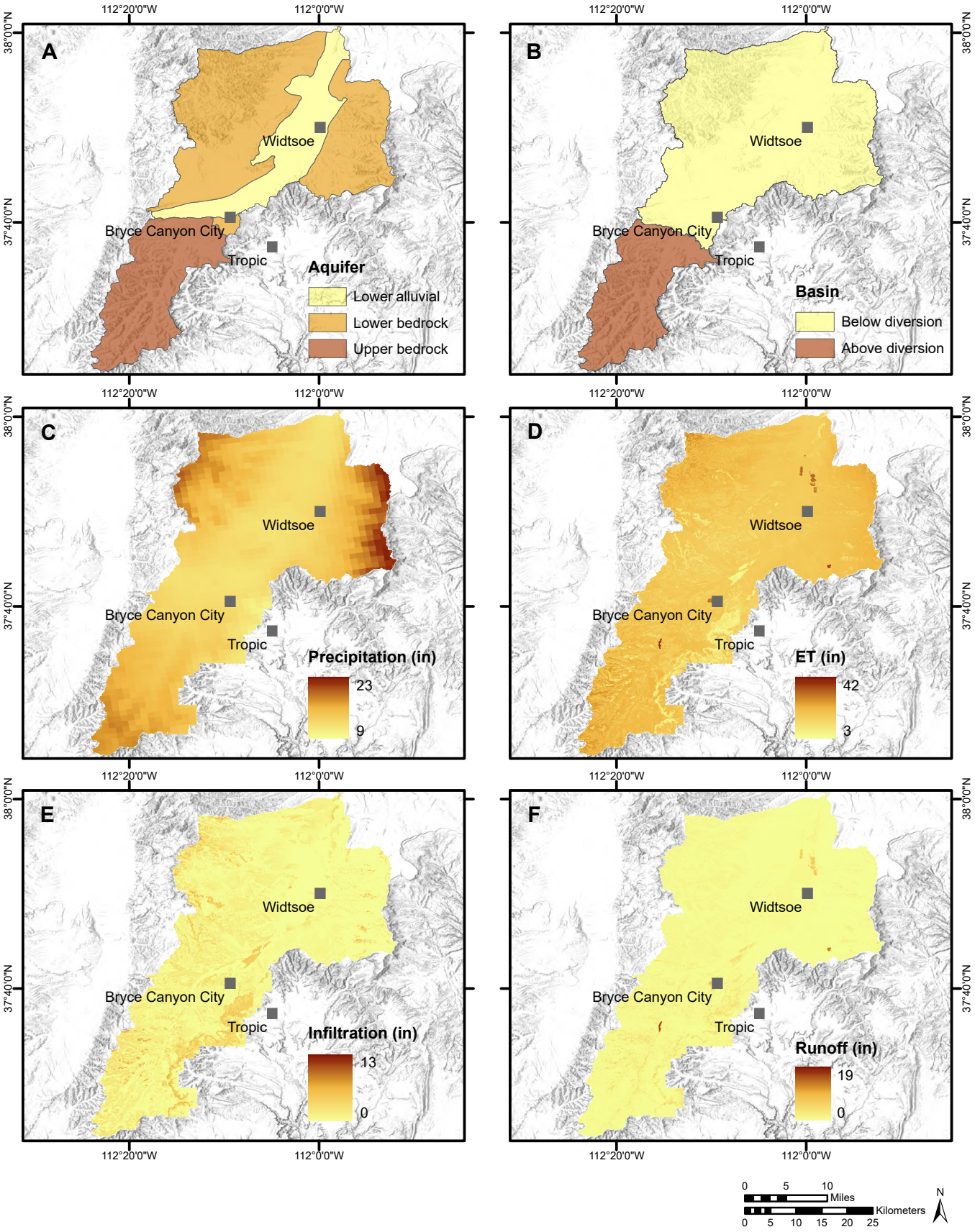

Figure G-4. A) *Lower alluvial, lower bedrock, and upper bedrock boundaries used for analysis in the SWB model and water budget calculations.* ***B)*** *Areas above and below the Tropic Ditch diversion used for analysis in the SWB model and water budget calculations. Output rasters from the SWB model of water year 2019 showing:* ***C)*** *precipitation,* ***D)*** *evapotranspiration (ET),* ***E)*** *infiltration, and* ***F)*** *runoff.*

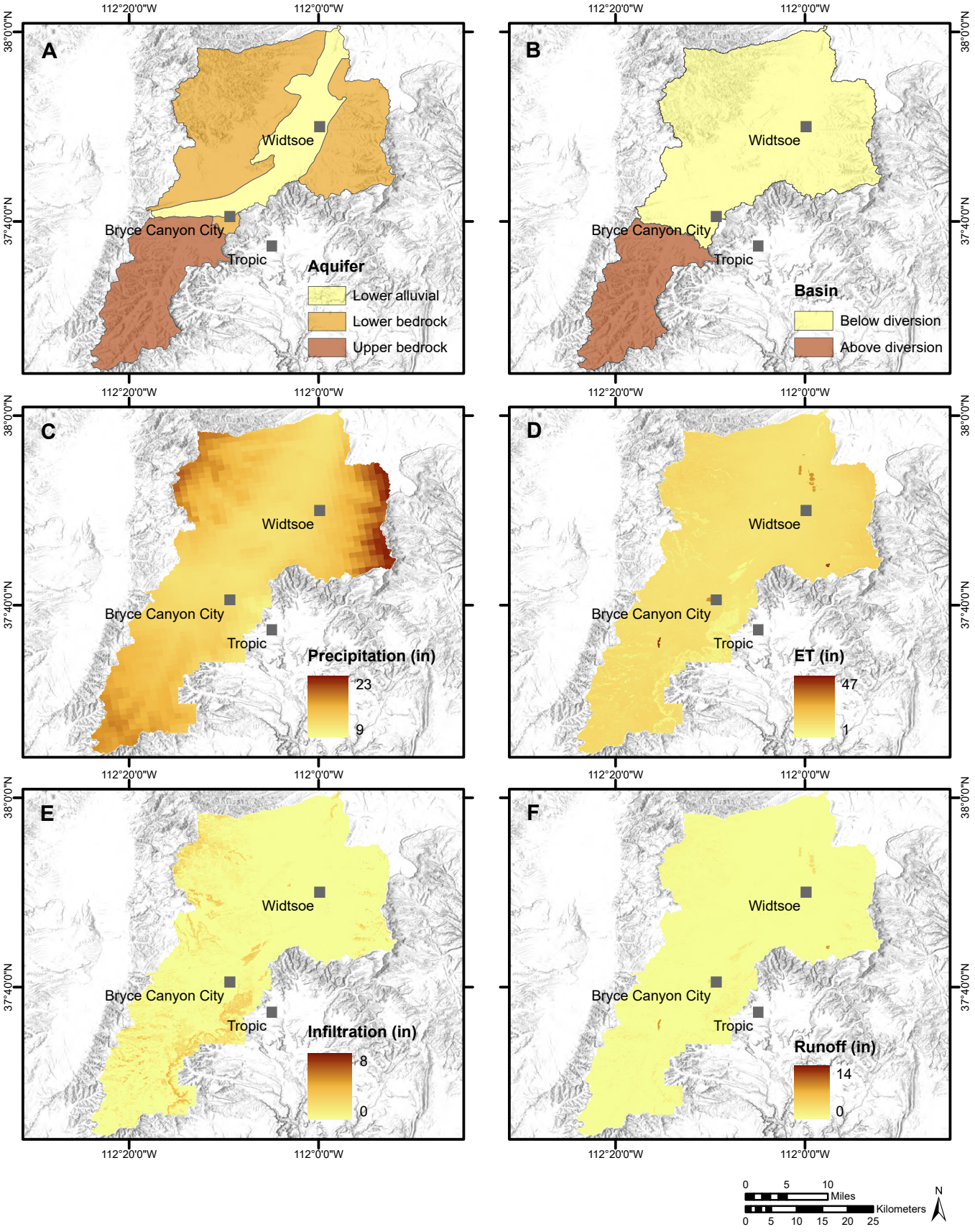

Figure G-5. A) *Lower alluvial, lower bedrock, and upper bedrock boundaries used for analysis in the SWB model and water budget calculations.* ***B)*** *Areas above and below the Tropic Ditch diversion used for analysis in the SWB model and water budget calculations. Output rasters from the SWB model of water year 2020 showing:* ***C)*** *precipitation,* ***D)*** *evapotranspiration (ET),* ***E)*** *infiltration, and* ***F)*** *runoff.*

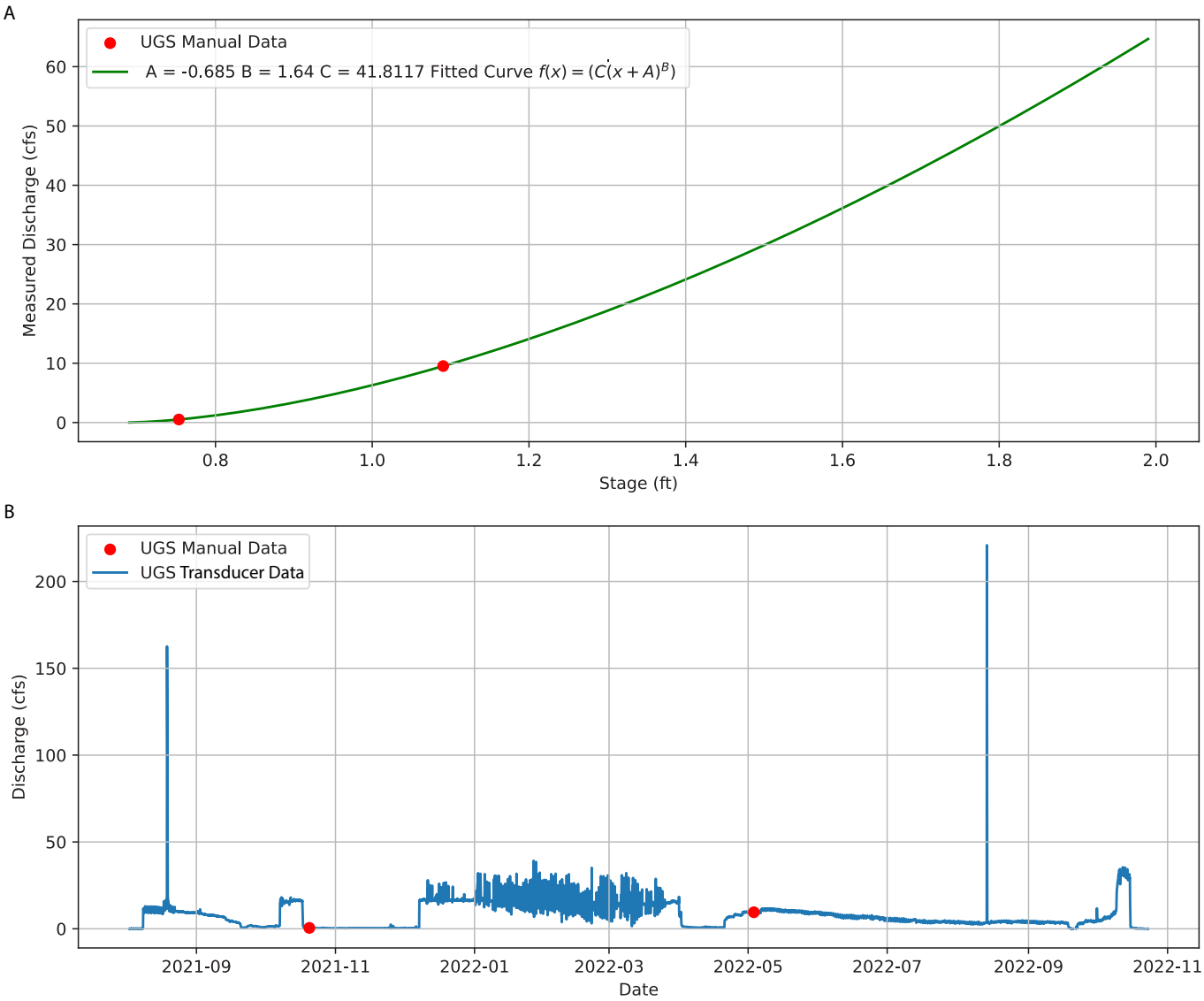

Figure G-6. A) *Ratings curve and* ***B)*** *resulting discharge measured on the East Fork Sevier River at site EF3, located just upstream of the Tropic Ditch diversion.*

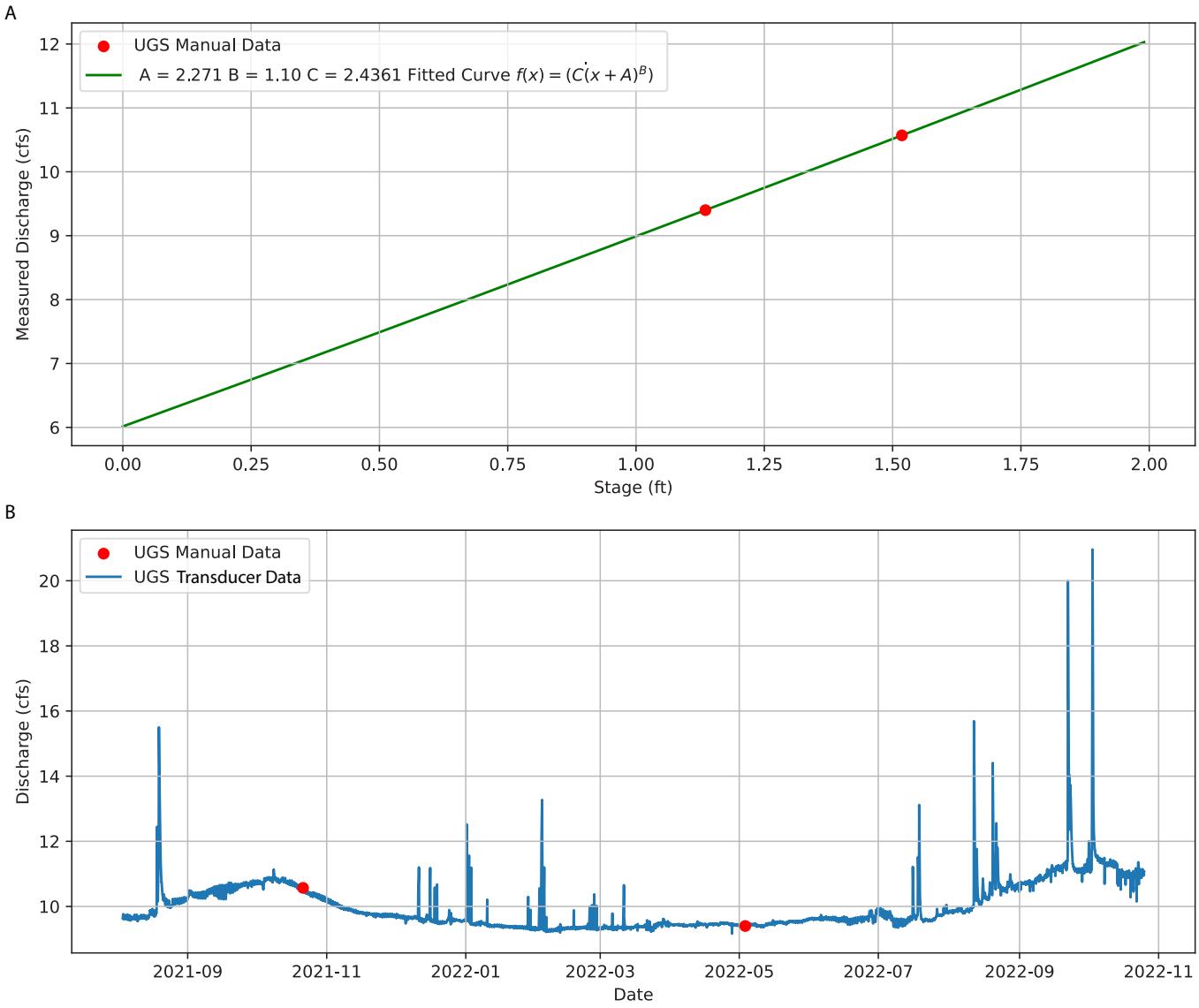

Figure G-7. A) *Ratings curve and* ***B)*** *resulting discharge measured on the East Fork Sevier River at site EF131, located on Flying V Ranch.*

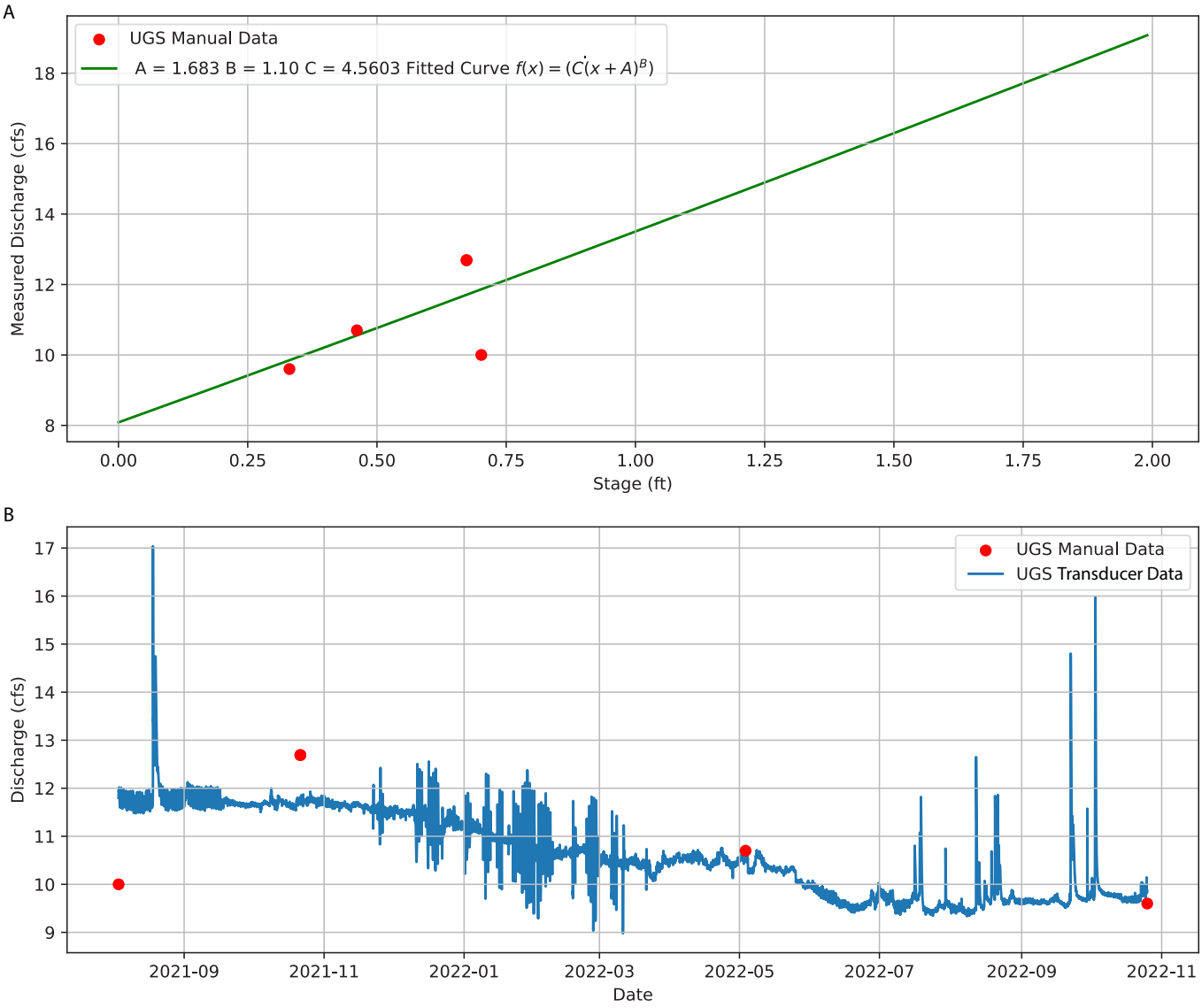

Figure G-8. A) *Ratings curve and* ***B)*** *resulting discharge measured on the East Fork Sevier River at site EF130, located at the northern end of the study area where the East Fork Sevier River flows into Black Canyon.*

Table G-1. *SWB variable outputs for years 2017-2021 with the study area divided into three subbasins: lower alluvial, upper bedrock, and lower bedrock. All values in acre-feet/year.*

	Gross_precipitation			Actual_ET			Interception			Rainfall		
Water Year	Lower Alluvial	Upper Bedrock	Lower Bedrock	Lower Alluvial	Upper Bedrock	Lower Bedrock	Lower Alluvial	Upper Bedrock	Lower Bedrock	Lower Alluvial	Upper Bedrock	Lower Bedrock
2017	75,347	135,984	238,196	82,012	139,943	255,221	4,944	31,156	45,543	46,777	61,596	122,237
2018	42,320	69,903	134,487	45,417	71,398	139,594	3,537	22,384	33,378	28,404	43,232	79,227
2019	92,620	152,311	292,955	86,571	129,181	267,109	5,940	37,116	56,080	46,617	58,309	117,137
2020	53,513	83,521	174,972	53,465	77,621	168,199	3,407	20,579	31,529	17,583	16,311	48,189
2021	63,973	100,205	216,249	60,377	91,687	201,744	3,622	19,996	35,965	41,897	62,922	132,177
	Reference_ETo			Irrigation			Net_infiltration			Rejected_net_infiltration		
Water Year	Lower Alluvial	Upper Bedrock	Lower Bedrock	Lower Alluvial	Upper Bedrock	Lower Bedrock	Lower Alluvial	Upper Bedrock	Lower Bedrock	Lower Alluvial	Upper Bedrock	Lower Bedrock
2017	228,735	254,935	575,062	1162	0	49	678	4931	3536	568	4511	2454
2018	240,029	270,525	604,798	1221	0	52	191	433	359	82	325	147
2019	212,078	237,962	534,203	1257	0	56	2748	7922	11,712	1175	9155	6738
2020	236,551	268,648	603,811	1370	0	64	497	2636	3414	521	2709	2207
2021	237,485	268,896	604,878	1103	0	50	308	789	960	419	1438	1459
	Runoff			Runon			Snowfall			Runoff_outside		
Water Year	Lower Alluvial	Upper Bedrock	Lower Bedrock	Lower Alluvial	Upper Bedrock	Lower Bedrock	Lower Alluvial	Upper Bedrock	Lower Bedrock	Lower Alluvial	Upper Bedrock	Lower Bedrock
2017	1046	3023	3312	0	0	0	28,570	74,388	115,959	1614	7534	5767
2018	118	326	413	0	0	0	13,917	26,670	55,260	201	651	560
2019	3378	6739	7054	0	0	0	46,003	94,002	175,818	4553	15,895	13,792
2020	807	1140	2503	0	0	0	35,930	67,211	126,783	1328	3849	4709
2021	1583	4303	5549	0	0	0	22,076	37,282	84,072	2002	5740	7008

Table G-2. *SWB variable outputs for years 2017-2021 with the study area divided into two subbasins: north and south of the Tropic Ditch diversion. All values in acre-feet/year.*

	Gross_precipitation		Actual_ET		Interception		Rainfall		Reference_ETo		Irrigation	
Water Year	**North**	**South**	**North**	**South**	**North**	**South**	**North**	**South**	**North**	**South**	**North**	**South**
2017	321,330	125,899	345,281	130,616	52,650	28,813	173,667	55,725	824,473	227,720	1211	0
2018	181,005	64,343	189,190	66,120	38,470	20,727	111,014	39,219	866,626	241,926	1272	0
2019	394,242	140,411	360,914	119,984	64,541	34,379	168,007	52,891	765,402	212,771	1313	0
2020	233,262	76,654	226,162	71,815	36,408	18,991	66,856	14,753	861,707	240,343	1433	0
2021	285,277	92,405	266,906	85,189	40,873	18,431	177,885	57,655	863,673	240,578	1153	0
	Net_infiltration		Rejected_net_ infiltration		Runoff		Runon		Snowfall		Runoff_outside	
Water Year	**North**	**South**	**North**	**South**	**North**	**South**	**North**	**South**	**North**	**South**	**North**	**South**
2017	4363	4368	3167	3854	4489	2710	0	0	147,663	70,174	7656	6564
2018	540	269	220	195	537	275	0	0	69,991	25,124	757	470
2019	14,763	7126	8535	8055	10,976	5938	0	0	226,235	87,520	19,511	13,993
2020	4003	2229	2797	2229	3365	969	0	0	166,406	61,901	6162	3198
2021	1285	518	1949	939	7435	3800	0	0	107,392	34,750	9384	4739